ADAPTIVE ALGORITHMS FOR IDENTIFICATION AND EQUALIZATION USING RECURSIVE FILTERS

Ph.D. Thesis

Author: Roberto López Valcarce
Advisor: Fernando Pérez González

2001

Escola Técnica Superior de
Enxeñeiros de Telecomunicación
Universidade de Vigo

Abstract

Adaptive filters play an important role in many control and signal processing applications such as system identification, echo and noise cancellation, adaptive equalization, etc. Although the potential advantage in terms of computational savings of adaptive IIR filters over their FIR counterparts has long been recognized, adaptive FIR filters are the most commonly used, due to their simplicity and robustness. Adaptive recursive filters present a series of drawbacks, which arise as a consequence of the nonlinear dependence of the filter output with the filter parameters due to the presence of feedback. Among these one finds problems such as multimodality of the cost function, ill-convergence in undermodeled cases, biased solutions, potential instability, etc.

In this thesis we analyze several issues arising in adaptive IIR filtering. Since in any practical application it is critical to ensure that the adaptive filter remains stable during operation, special attention is given to the normalized lattice structure which is known to provide the desired stability even when it becomes time-varying. To this end, an analysis of the convergence properties of previous adaptive lattice algorithms is developed, which reveals that these schemes may fail to converge even in ideal cases. To overcome this drawback, a systematic approach to the derivation of a lattice algorithm from a given direct form scheme is presented. The resulting implementation is fairly general and efficient, and it preserves the local convergence properties of the direct form algorithms in sufficient order settings, in contrast with previous approaches.

An analysis of several off-line system identification schemes, which serve as starting points to the development of on-line adaptive algorithms for IIR filters, is presented. This methods are iterative in nature and may break if the unknown system estimate at a given iteration is unstable. Conditions for the stability of equation error models which are the basis of these iterations are presented. Also, conditions on the input signal for the uniqueness of the fixed point of these iterations are given.

The convergence of one family of adaptive IIR filtering algorithms requires the satisfaction of a passivity condition involving the unknown system to be identified. One possibility to relax this requirement is the use of overparameterization. We investigate this issue, as well as the associated spectral richness conditions on the input signal, when the polyphase structure is adopted for the adaptive filter.

Recently, the potential of adaptive recursive filters for channel equalization in

digital communication systems has started to be recognized. We provide a thorough discussion of the problem and the theoretical framework for adaptive IIR filters in this application. The adaptation of the poles and the zeros of the filter can be carried out under different criteria. We investigate two different unsupervised algorithms for the adaptation of the recursive part of the equalizer: Output Variance Minimization (OVM) and a Pseudolinear Regression (PLR) method. In sufficient order cases both algorithms converge to the desired setting, in which the filter output becomes a white process. In undermodeled cases these algorithms do not necessarily converge to a Mean Squared Error minimum, but they generally provide acceptable performance. It is shown that under mild conditions PLR always admits a stationary point. Blind adaptation of the zeros of the equalizer can be done using schemes such as the constant modulus algorithm (CMA). A simple and efficient method for on-line reinitialization of CMA is presented, which exploits the fact that the recursive portion acts as a prewhitener. Given the interest of the topic, we give at the end some lines for further research in the area of adaptive recursive filtering applied to real problems such as those studied in the thesis.

Resumen

El filtrado adaptativo desempeña un papel importante en aplicaciones del procesado de señal tales como identificación de sistemas, cancelación de ruido y de eco, igualación adaptativa, etc. Aunque el potencial de los filtros IIR adaptativos para conseguir mejores prestaciones que los FIR ha sido reconocido desde hace tiempo, la simplicidad y robustez de los filtros FIR adaptativos ha hecho de éstos la solución preferida en la mayoría de los casos. Los filtros IIR adaptativos presentan una serie de problemas que son consecuencia de la dependencia no lineal de la señal de salida con los coeficientes del filtro, un producto de la presencia de realimentación. Entre estos problemas cabe mencionar la presencia de mínimos locales en la función de coste, convergencia lenta, sesgo en las soluciones en presencia de ruido, inestabilidad potencial, etc.

En esta tesis se analizan varios temas relacionados con el filtrado IIR adaptativo. Dado que en toda aplicación práctica de estos sistemas es preciso que el filtro adaptativo se mantenga estable, se presta especial atención a la estructura en celosía normalizada la cual es estable incluso cuando sus coeficientes varían a lo largo del tiempo. Para ello se realiza un análisis de las propiedades de convergencia de una serie de algoritmos para celosías propuestos anteriormente, del cual se desprende que estos esquemas pueden no converger incluso en situaciones ideales. Para paliar este problema se presenta una aproximación sistemática a la transformación de algoritmos en forma directa a celosía. Los esquemas en celosía resultantes son eficientes en cuanto a la potencia de cálculo requerida, y en casos de orden suficiente mantienen las propiedades de convergencia local de los algoritmos en forma directa originales.

Se presenta también un estudio de ciertos métodos de identificación de sistemas, los cuales sirven como puntos de partida para el desarrollo de algoritmos adaptativos para filtros IIR. Estos métodos son de naturaleza iterativa y pueden fallar si durante alguna iteración el estimador del sistema desconocido resulta ser inestable. Se presentan condiciones suficientes para garantizar la estabilidad del modelo obtenido por el método del error de ecuación, el cual sirve como base para estos esquemas iterativos. También se dan condiciones sobre la señal de entrada para garantizar la unicidad del punto fijo de estos métodos iterativos.

Una condición suficiente para la convergencia de cierta familia de algoritmos adaptativos es la verificación de cierta condición de pasividad sobre el sistema desconocido. Un método para relajar dicha condición es la sobreparametrización del

filtro adaptativo. Se investiga esta posibilidad en el caso de utilizar estructuras polifase, así como las condiciones asociadas de riqueza espectral sobre la señal de entrada.

Recientemente ha habido un renovado interés en la aplicación de filtros recursivos adaptativos al problema de igualación de canal en comunicaciones digitales. Se proporciona una presentación minuciosa del problema y el marco teórico del filtrado IIR adaptativo en esta configuración. La adaptación de los polos y los ceros del filtro puede realizarse usando criterios distintos. Para la adaptación de los polos se investigan dos criterios no supervisados: la minimización de la varianza de salida (OVM) y un esquema basado en regresión pseudolineal (PLR). En casos de orden suficiente, ambos algoritmos convergen al punto adecuado, en el que la señal de salida es blanqueada. En situaciones inframodeladas estos esquemas no convergen necesariamente a un mínimo del error cuadrático medio, aunque en general proporcionan soluciones válidas. Se demuestra la existencia de puntos estacionarios del algoritmo PLR en el caso inframodelado. La adaptación de los ceros del igualador puede realizarse mediante el algoritmo de módulo constante (CMA). Como consecuencia de que la parte recursiva del igualador blanquea la entrada a la parte no recursiva, es posible derivar un método sencillo para reinicializar el algoritmo CMA en su búsqueda del mínimo global del error cuadrático medio.

Finalmente se comentan las numerosas líneas de investigación que aparecen como consecuencia de nuestros resultados.

Notation

Acronyms

ADPCM	Adaptive Differential Pulse Code Modulation
ANC	Active Noise Control
ANF	Adaptive Notch Filter
AR	Autoregressive
ARMA	Autoregressive Moving Average
CMA	Constant Modulus Algorithm
DD	Decision Directed
DFE	Decision Feedback Equalizer
DSP	Digital Signal Processor
EE	Equation Error
EEL	Equation Error Lattice
FIR	Finite Impulse Response
GL	Gradient Lattice
HARF	Hyperstable Adaptive Recursive Filter
IIR	Infinite Impulse Response
ISI	Intersymbol Interference
IXN	Interpolation eXpanded Numerator
LE	Linear Equalizer
LMS	Least Mean Square
LSHARF	Lattice SHARF
LTI	Linear Time-Invariant
MA	Moving Average
MMSE	Minimum MSE
MSE	Mean Squared Error
ODE	Ordinary Differential Equation
OE	Output Error
OVM	Output Variance Minimization
PE	Persistently Exciting
PGL	Partial Gradient Lattice
PLR	Pseudo-linear Regression
psd	power spectral density
SHARF	Simplified Hyperstable Adaptive Recursive Filter
SM	Steiglitz-McBride
SML	Steiglitz-McBride Lattice
SM/XN	Steiglitz-McBride / eXpanded Numerator
SNR	Signal to Noise Ratio
SPGL	Simplified Partial Gradient Lattice
SPR	Strictly Positive Real
XN	eXpanded Numerator

Symbols

$E[\cdot]$	expectation operator
$\mathbb{R}$	real line
$\mathbb{C}$	complex plane
$\mathrm{Re}\{\cdot\}$	real part
$\mathrm{Im}\{\cdot\}$	imaginary part
$\langle f(z), g(z)\rangle_u$	weighted inner product
$[f(z)]_{0+}$	causal part of $f(z)$
$[f(z)]_+$	strictly causal part of $f(z)$
$\|\|\cdot\|\|$	norm
$\mathbf{0}$	zero matrix
z^*	conjugate of complex number z
$\mathbf{v}^T$	transpose of vector $\mathbf{v}$
$\mathbf{v}^\dagger$	conjugate transpose of vector $\mathbf{v}$

CONTENTS

Chapter 1

INTRODUCTION

1.1 Why adaptive IIR filters?

Adaptive filters are systems with the ability to change their operating characteristics in response to different conditions in the surrounding environment. This property is useful in settings in which the nature of such conditions is unknown, thus rendering the *a priori* design of an optimal, fixed filter impractical; or in situations where the statistical properties of the signals change with time, and the filter is required to track these variations. An adaptive filter consists of two conceptual blocks:

- A parametric structure performing the input-output (i.e. filtering) transformation.
- A procedure for updating the filter parameters as each new set of measurements is available (the *adaptive algorithm*).

The design of an adaptive filter includes the selection of an adequate structure and the update algorithm, a choice that is usually application dependent. Nevertheless, the most popular structure in adaptive signal processing is by far the linear finite impulse response (FIR) filter, usually implemented as a tapped delay line. Similarly, the most popular update mechanism for this structure is the Least Mean Square (LMS) algorithm, developed by Widrow and Hoff more than forty years ago [129], and its variants. Over the years LMS-based adaptive FIR filters have proved successful in many applications, lying at the core of adaptive signal processing [46, 130].

On the other hand there are certain situations in which the order of the adaptive filter must be relatively large in order to achieve a satisfactory level of performance. A large number of adaptive coefficients translates into heavier computational and memory loads as well as an increase in power consumption. Several approaches have been investigated in order to improve performance while keeping a reasonable number of adaptive parameters in the FIR structure, such as transform domain techniques [23, 115], subband adaptive filtering [41, 98], block processing [43], and

the use of sparse filters which adaptively allocate a reduced number of adjustable coefficients along the tapped delay line [47, 122].

Another possibility whose potential has long been recognized is the use of infinite impulse response (IIR) structures, which incorporate feedback in order to form the output as a linear combination of past values of both the input and output signals. This potential is attributed to the superior modeling abilities of pole-zero transfer functions, which can approximate long impulse responses with the same accuracy as an FIR (or all-zero) transfer function but with significantly fewer coefficients. For this reason there has been considerable interest in the problem of adapting recursive filters.

Several authors have considered the use of IIR structures with fixed poles, for which only the zeros of the transfer function are adapted [56, 99, 127, 132]. This technique can be very effective in situations in which some *a priori* knowledge is available regarding the filter operating environment, in order to choose the fixed poles of the filter. On the other hand, it is reasonable to expect fully adaptive IIR filters to provide better performance due to the added flexibility in the placement of the filter poles. This approach has received a great deal of attention by both the signal processing and the control communities [52, 105, 113]. However, while the area of adaptive FIR filtering has reached a considerable degree of maturity and the properties of adaptive FIR filters are reasonably well understood, a comparable theory for adaptive IIR structures is still lacking. Simply put, estimation of the optimum filter parameters becomes a nonlinear problem with the introduction of feedback in the filter structure. This raises a series of theoretical and practical issues that must be solved before the adaptive IIR filter replaces the widely used adaptive FIR filter. It is the goal of this thesis to further investigate some of these issues and to provide answers to several questions concerning adaptive IIR filtering. In order to motivate the problem, in the following sections we proceed to review several adaptive filtering applications for which the use of IIR structures has been explored, namely system modeling, echo cancellation, adaptive notch filtering, active noise control, predictive speech coding, and channel equalization.

1.1.1 Dynamical system modeling

Many concepts found in adaptive IIR filtering theory have their roots in the area of adaptive identification, developed by control researchers driven by the necessity of having a parameterization of the plant as a prerequisite for the design of suitable controllers. Assume the physical continuous-time process to be controlled admits a linear state-space description of the form

$$\dot{x}_c(t) = A_c x_c(t) + B_c u_c(t), \qquad y_c(t) = C_c x_c(t) + D_c u_c(t), \tag{1.1}$$

where u_c, y_c and x_c are respectively the continuous-time input, output, and state vectors. In data sampled systems the output signal is periodically sampled, and

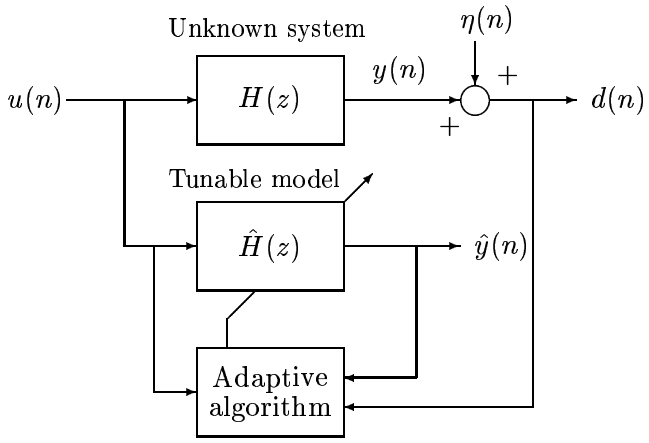

Figure 1.1: Adaptive filter in a system identification configuration.

the control signal u_c is specified at the sampling instants and held constant until the next cycle (this is often called zero-order hold digital to analog conversion). Defining $u(n) = u_c(nT)$, $y(n) = y_c(nT)$, $x(n) = x_c(nT)$ with T the sampling interval, the state-space representation of the corresponding discrete-time system obtained under these conditions is

$$x(n+1) = Ax(n) + Bu(n), \qquad y(n) = Cx(n) + Du(n), \tag{1.2}$$

where

$$A = \mathrm{e}^{A_c T}, \qquad B = \int_0^T \mathrm{e}^{A_c t}\mathrm{d}t \cdot B_c, \qquad C = C_c, \qquad D = D_c.$$

The objective of the control algorithm is to design $u(\cdot)$ according to some criterion [5], for which it is often necessary to have access to the transfer function from $u(\cdot)$ to $y(\cdot)$, given by

$$H(z) = C(zI - A)^{-1}B + D.$$

Observe that $H(z)$ has poles given by the eigenvalues of A, which are of the form $\lambda = \mathrm{e}^{\lambda_c T}$ with λ_c the eigenvalues of A_c. Hence in general $H(z)$ is an IIR transfer function, especially for fast sampling (small T) in which case its poles tend to cluster around the point $z = 1$ in the complex z plane. In that situation an FIR model for $H(z)$ would require a large number of coefficients to capture its dynamics; an IIR model is clearly preferred. In order to fit the parameters of the model, one could drive $H(z)$ with some input, record the corresponding output, and then run some off-line identification procedure [118]. Another approach is to perform identification in a recursive, on-line fashion, in which the coefficients are tuned recursively as each new input-output pair $\{u(n), y(n)\}$ becomes available [71]. This is especially appealing if the system parameters are slowly time-varying, as well as in adaptive control systems. The corresponding configuration is depicted in Figure 1.1. This system identification setting in which the goal of the adaptive

filter $\hat{H}(z)$ is to match an unknown plant $H(z)$ is a recurring theme in adaptive IIR filtering. Observe from Figure 1.1 that the plant output $y(n)$ is assumed to be corrupted by an additive disturbance $\eta(n)$ so that the measurable reference signal is $d(n) = y(n) + \eta(n)$. The so-called output error $d(n) - \hat{y}(n)$, where $\hat{y}(n)$ is the adaptive filter output, is often used as an indicator of the quality of the fit of $\hat{H}(z)$ to $H(z)$.

There are three possible situations for the system identification setting of Figure 1.1, depending on the relative orders of $H(z)$ and $\hat{H}(z)$. If $\deg \hat{H}(z) > \deg H(z)$, the adaptive filter is overparameterized. With IIR transfer functions this opens the possibility of pole-zero cancellations, such that there are infinitely many parameterizations of $\hat{H}(z)$ yielding the same desired transfer function $\hat{H}(z) = H(z)$. This may cause parameter drift during adaptation and slow down convergence, but in real world situations it is very unlikely that $\deg \hat{H}(z) > \deg H(z)$. When the degrees of the plant and the model coincide, one has the "matching order case" in which the parameterization of $\hat{H}(z)$ yielding $\hat{H}(z) = H(z)$ is unique (assuming , of course, that $H(z)$ itself is free of pole-zero cancellations). Finally, if $\deg \hat{H}(z) < \deg H(z)$, one has the "undermodeled case", for which it is impossible to achieve $\hat{H}(z) = H(z)$. Most of the available literature on system identification and adaptive IIR filtering focuses on the matching order case, for which the problem of algorithm design and analysis remains tractable. It is likely, however, that in a real world situation the physical process to be modeled via the filter $\hat{H}(z)$ does not admit a description in terms of a rational transfer function, and even if it does, its degree may be prohibitively large, and often unknown. Thus, undermodeled scenarios are of great practical importance, and unfortunately, they are also much harder to analyze [105].

1.1.2 Echo cancellation

Figure 1.2 shows a typical long distance telephone system loop, in which signals at each end are sent through a twisted pair to the local switching office. In the local office the twisted pair is connected to one port in a 4-port device known as a hybrid circuit which acts as a bridge between bidirectional and unidirectional lines. The fourth port of the hybrid is connected to a balancing impedance so that ideally signals coming in through the bidirectional line come out one of the unidirectional lines, while the signals arriving via the other unidirectional line come out the bidirectional line. However, design of the hybrids requires knowledge of the impedance characteristics at each port, and due to variations in the length, type and gauge of wire as well as the number of phone extensions, these values are not known precisely in practice. Imperfect impedance matching in the hybrid leads to signal leakage from the incoming unidirectional line to the outcoming one; this signal returns to the original transmitter as an echo. With speech signals, this echo creates an annoying effect if the total roundtrip delay of the connection exceeds 32 ms. Often compromise hybrids are deployed achieving an echo attenuation of 6 dB, but this is far from the attenuation levels specified by the recent ITU-T

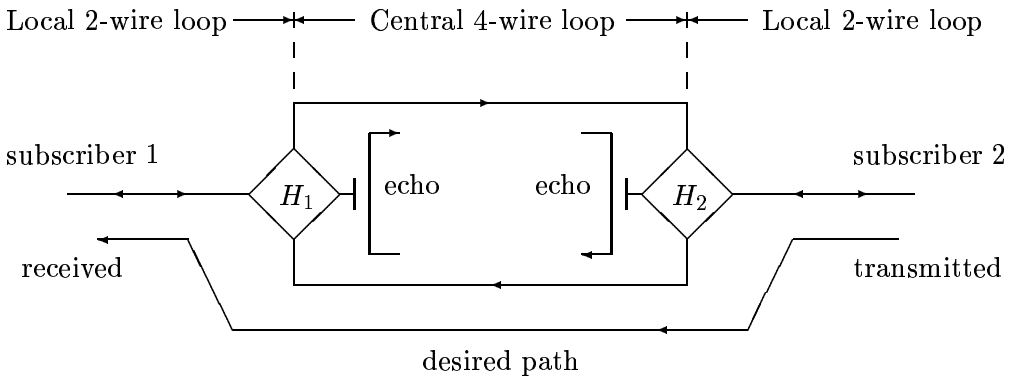

Figure 1.2: A 4-wire long distance telephone loop. H_1, H_2 denote the hybrid circuits.

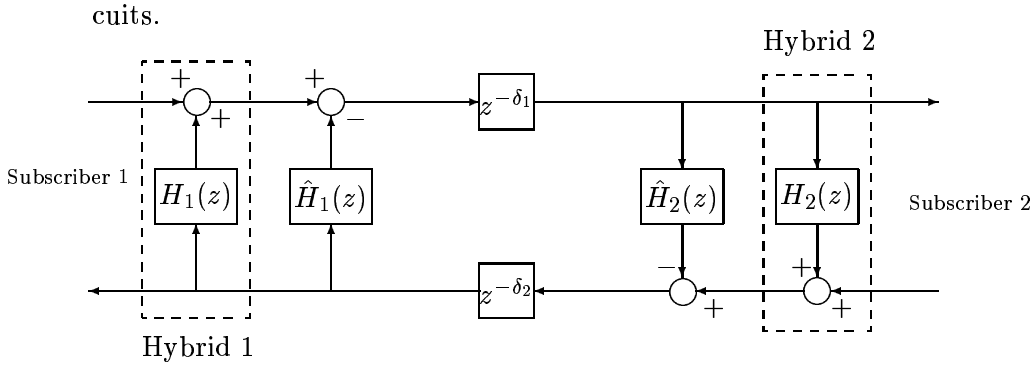

Figure 1.3: Echo cancellation in a telephone network.

Recommendation G.168 [35]. Additional echo suppressing devices, such as adaptive echo cancellers, are required in order to achieve these levels.

An echo canceller is a filter that sits inside the 4-wire loop across the hybrid with the purpose of substracting an estimate of the echo signal from the outgoing unidirectional line. This is depicted in Figure 1.3, where $H_1(z)$ and $H_2(z)$ represent the echo paths across the hybrids, and the blocks $z^{-\delta_1}$, $z^{-\delta_2}$ represent the transmission delays across each part of the 4-wire loop. The cancellers $\hat{H}_1(z)$, $\hat{H}_2(z)$ attempt to model the passthrough dynamics of the hybrids in order to remove the echo from the hybrids' outputs. Since the echo path transfer characteristics are not known beforehand, and moreover they may change during a call (for example as a result of a handoff in mobile telephone networks), the echo canceller is implemented by an adaptive filter.

Observe that each canceller in this configuration can be cast as in the system identification setting of Figure 1.1. For example, for the canceller $\hat{H}_1(z)$, the signal transmitted by Subscriber 1 plays the role of the additive disturbance $\eta(n)$ in Figure 1.1. This signal can overpower the echo (the output of $H_1(z)$) and make adaptation of $\hat{H}_1(z)$ difficult. Because of this, adaptive echo cancellers are usually implemented

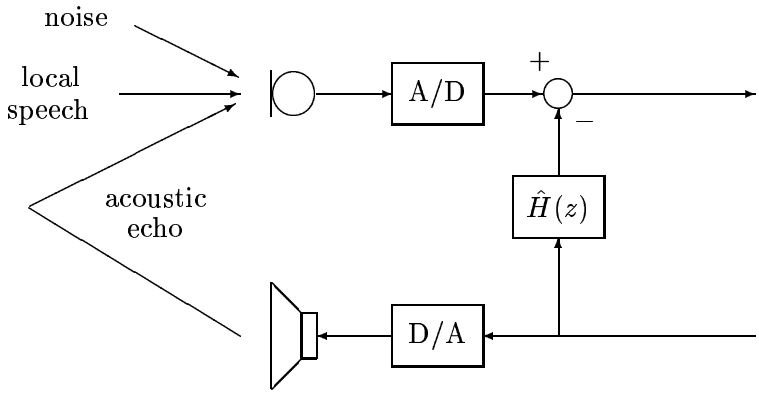

Figure 1.4: Acoustic echo cancellation

with double talk detection devices which inhibit adaptation whenever the near-end subscriber is active.

The typical effective time spans of echo paths in telephone networks are in the order of a few tens of milliseconds [88, 111], although state of the art cancellers handle echo path delays of up to 128 ms. With speech signals sampled at 8 kHz, FIR implementations of adaptive echo cancellers may require several hundreds of coefficients. In addition, voiceband data transmission applications, such as the full duplex data modem specified in CCITT Recommendation V.32, require echo cancelers to be placed at the line interface where hybrids connect the modem to the 2-wire line. These cancelers must achieve a considerably higher level of performance than in speech applications [13, 88].

The impulse response of the echo path is a linear combination of decaying exponentials, since the hybrid is an electronic circuit with discrete elements. Therefore the passthrough dynamics of the hybrid circuit is typically modeled by a transfer function with a few poles and several zeros. The inclusion of poles allows to model the echo tail that is related to the low frequecy time constants of the circuit [13]. This indicates that an IIR structure for the adaptive filter should be suitable for the echo cancellation task, as explored in [12, 31, 38, 40, 111].

Adaptive filtering also finds application in the area of *acoustic* echo cancellation. Acoustic echo arises in settings where a microphone and a loudspeaker are placed such that the microphone picks up part of the sound radiated by the loudspeaker and/or its reflections. The speech from the far-end terminal is then fed back to the far-end user who hears his or her own speech delayed by the roundtrip time of the connection. Adaptive echo cancellers can again be used, being now located between the loudspeaker input and the microphone output as shown in Figure 1.4. In conventional telephones, the design of the handpiece provides an adecuate attenuation level from the loudspeaker to the microphone. On the other hand, applications such as hands-free telephone systems, audio or video conference systems, hearing aids,

and voice control systems usually require adaptive cancellation of the acoustic echo in order to achieve satisfactory performance. In some cases, such as hearing aid systems, the impulse response of the acoustic echo path can be adequately modeled by an FIR filter with the order of 20 coefficients [133]. However, for hands-free and teleconference systems the large number of echo paths and reverberation effects in the enclosure (car, office, etc) may give rise to echo transfer functions with an effective duration of several hundreds of milliseconds. With a sampling rate of 8 kHz, an FIR filter may require thousands of coefficients to model these systems [8]. With such high filter orders an IIR structure for the canceller seems better suited at first glance; some arguments favoring IIR over FIR structures with the same number of free parameters were given in [83]. On the other hand, the results shown in [67] suggest that this is not the case. The main obstacle seems to be the nature of acoustic echo paths, whose energy spectra present many sharp peaks requiring a large number of coefficients for satisfactory modeling, irrespective of the type of model (FIR or IIR). Thus at this point the adequateness of IIR structures to the acoustic echo cancellation problem seems dubious.

1.1.3 Active noise control

Acoustic noise control has become ever more important in recent years as programs and policies are being established worldwide in order to reduce and control environmental noise produced by industrial equipment. Traditionally passive techniques such as barriers, enclosures, etc., have been used to attenuate the undesired acoustic noise. Although these passive silencers offer high attenuation over a wide range of frequencies, they tend to be expensive and bulky, and not very effective at low frequencies. An attractive alternative is active noise control (ANC), which is based on the superposition principle. The unwanted noise is canceled by an artificial noise signal of the same amplitude but opposite phase generated by an electroacoustic device (loudspeaker) driven by the ANC system [60]. Since the properties of the environment and the noise source may be time varying, ANC systems are usually adaptive in order to cope with these variations.

ANC systems can be classified as single-channel, which use a single loudspeaker to produce the canceling noise, or multichannel systems with several loudspeakers and sensors. Either of these can be based on a feedforward structure, in which the noise source is sensed before the canceling noise is produced, or feedback approaches lacking this noise reference input. Feedforward ANC systems can be either broadband or narrowband, depending on the spectral characteristics of the noise source. In narrowband ANC the fundamental frequency of the noise can be detected via nonacoustic sensors; this method, however, is not effective for nonperiodic noise since the fundamental driving frequency is the only reference available. Thus broadband applications must resort to acoustic sensors (microphones) to acquire the noise reference.

Figure 1.5 shows the schematics of a single-channel, broadband feedforward

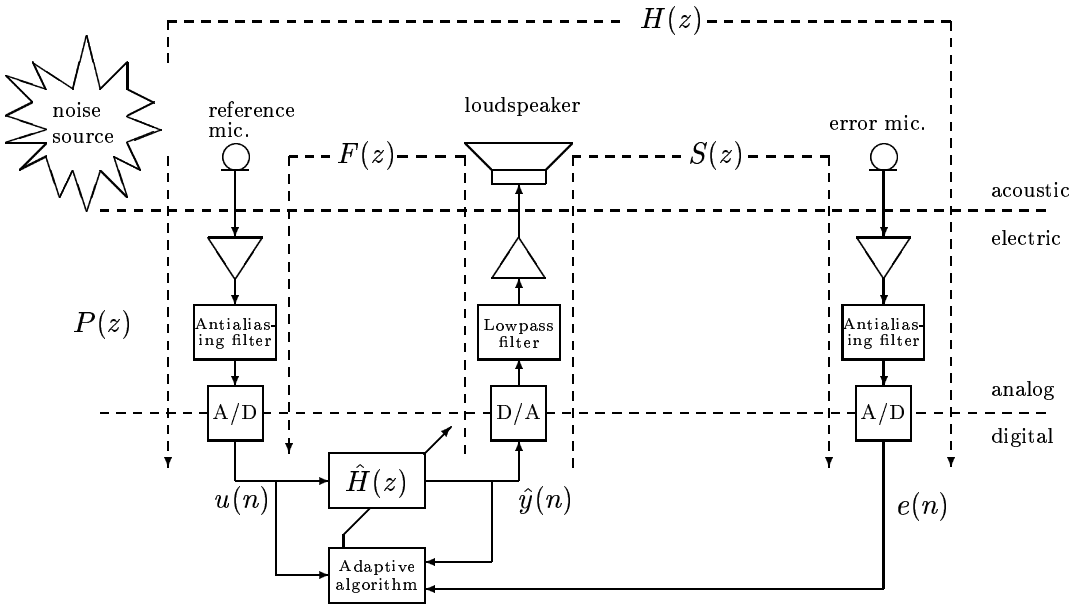

Figure 1.5: Single-channel, broadband feedforward active noise cancellation.

ANC system. The reference microphone picks up the noise signal which is sampled and processed by the adaptive filter $\hat{H}(z)$ to generate the signal that drives the loudspeaker. An error microphone located at the objective point provides a measure of the achieved noise reduction. Besides $\hat{H}(z)$, a number of transfer functions (acoustic paths) can be identified from Figure 1.5:

- $H(z)$, the path from the noise source to the sampled error signal $e(n)$;
- $P(z)$, the path from the noise source to the input $u(n)$ of the adaptive filter;
- $F(z)$, the path from the output $\hat{y}(n)$ to the input $u(n)$ of the adaptive filter, due to acoustic feedback from the loudspeaker to the reference microphone;
- $S(z)$, the path from the output $\hat{y}(n)$ of the adaptive filter to the sampled error signal $e(n)$.

The corresponding block diagram is represented in Figure 1.6. There are two paths through which the noise signal travels to reach the error microphone: the primary path $H(z)$ and the secondary path comprising $P(z)$, $\hat{H}(z)$, $F(z)$ and $S(z)$. The transfer function of the secondary path is given by

$$\frac{S(z)\hat{H}(z)P(z)}{1-\hat{H}(z)F(z)}.$$

Observe that the configuration of Figure 1.6 is considerably more complicated than the standard system identification setting of Figure 1.1 due to the presence of $P(z)$,

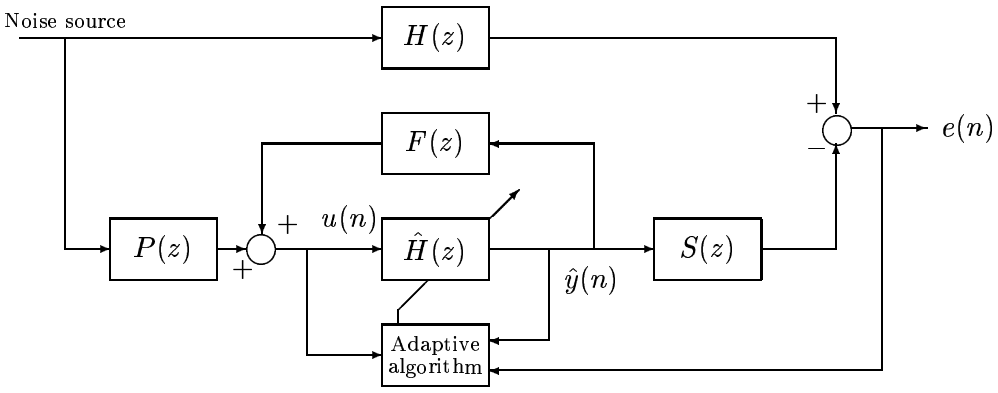

Figure 1.6: Block diagram of an ANC system.

$F(z)$ and $S(z)$. Ideally one would like to have perfect noise cancellation at the error microphone, i.e. $e(n) = 0$. For this, the transfer functions of the primary and secondary paths must equal each other, i.e.

$$H(z) = \frac{S(z)\hat{H}(z)P(z)}{1 - \hat{H}(z)F(z)} \qquad \Rightarrow \qquad \hat{H}(z) = \frac{H(z)}{S(z)P(z) + H(z)F(z)}. \tag{1.3}$$

Note that even if the transfer functions of all the acoustic paths can be regarded as FIR, (1.3) shows that the optimum $\hat{H}(z)$ will in general have both zeros and poles. This has led to consideration of IIR structures for the adaptive filter $\hat{H}(z)$ [16, 15, 24, 86]. Preliminary results obtained with adaptive IIR noise cancellers seem to favor these structures over their FIR counterparts, for the same computational complexity, both in the narrowband [61] and the broadband cases [86]. Thus ANC appears as a very promising area of application of adaptive IIR filters.

1.1.4 Adaptive notch filtering

There are many signal processing applications in which one is faced with the problem of estimating the frequencies in a signal $u(\cdot)$ composed of multiple sinusoids buried in background noise. For example, Dual Tone Multiple Frequency (DTMF) signaling, a technique widely used in telephone dialing and digital answering machines, represents each symbol on a telephone touchtone keypad by the summation of two sinusoids of different frequencies added together. The ITU Q.24 standard [100] requires 100% detection of valid DTMF signals at an SNR of 15 dB. Other examples include narrowband active noise control and vibration control. In other applications, such as interference suppression and synchronization in communication systems, the sinusoidal components (and not just their frequencies) must be retrieved.

Two different approaches to this problem exist. Off-line methods include spectral estimation schemes based on the discrete Fourier transform, and subspace de-

composition techniques such as multiple signal classification (MUSIC); these methods usually have high computational costs. On-line methods tend to be less complex and are better suited for real-time processing and tracking time-varying frequencies. These methods are based on adaptive filtering techniques: the parameters of an adaptive filter $\hat{H}(z)$ driven by the composite signal (sinusoids plus noise) $u(\cdot)$ are tuned so that the resulting transfer function has zeros on the unit circle at the locations of the signal frequencies. Early on-line methods using adaptive FIR filters include the adaptive line enhancer of [128] and the adaptive Pisarenko method [102]. For example, a second-order FIR filter with zeros at $z = \mathrm{e}^{\pm j\omega_0}$ has the transfer function

$$\hat{H}(z) = 1 - 2\cos\omega_0 z^{-1} + z^{-2}. \tag{1.4}$$

The only tunable parameter in (1.4) is ω_0, which controls the position of the zeros; it is not possible to adjust the attenuation bandwidth. In other words, sharp cutoff characteristics cannot be achieved with this structure, which constitutes the main drawback of FIR filters for sinusoidal retrieval. This motivated the consideration of adaptive IIR structures, known as adaptive notch filters (ANFs). A notch filter is one whose magnitude response vanishes at a particular point on the unit circle (the so-called notch frequency) while it remains nearly constant at all other points on the unit circle. Although ideal notch filters are not realizable by rational transfer functions, very good approximations can be obtained using IIR structures. A popular approach is to use a cascade of second-order IIR sections, each of them corresponding with a notch frequency. In this way, and assuming that the notch frequencies match those of the sinusoids, the output of each section in the cascade contains one less sinusoid. Complementary bandpass filters can be implemented by substracting the outputs of each second-order notch section from their inputs, effectively extracting the desired sinusoids.

It is customary to constrain the pole and zero locations of the ANF so that (i) the zeros always lie on the unit circle, and (ii) the poles remain close to the zeros, and inside the unit circle. These constraints on the notch transfer function can be advantageously exploited in adaptive algorithm design. The filter bandwidth is mainly determined by the distance between poles and zeros: the closer they are, the narrower the notch is. Usually a second-order ANF has two tunable parameters: while one is related to the notch frequency and made adaptive, the other controls the attenuation bandwidth and is fixed *a priori*. Many parameterizations are possible, each with its own advantages and problems. We refer the reader to [105, chapter 10] and the references therein.

An interesting feature of ANFs is that there is only one signal available for the adaptation of the filter, namely the composite signal $u(\cdot)$ which constitutes the ANF input. This is in contrast with the applications of the previous sections which also had available a reference signal $d(\cdot)$. Lack of a reference signal is a feature also encountered in other areas amenable for adaptive IIR filtering, such as linear prediction and blind channel equalization, which we proceed to review next.

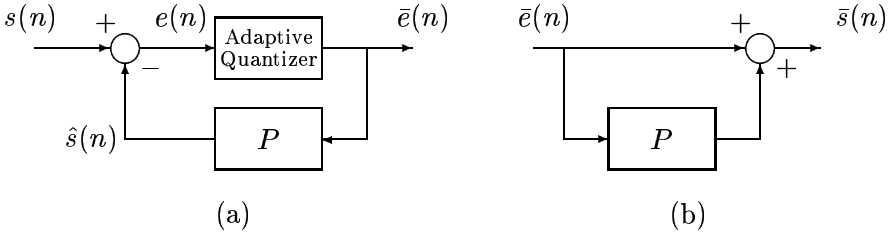

Figure 1.7: An ADPCM system. (a) Encoder; (b) Decoder.

1.1.5 Adaptive linear prediction

One of the many applications of linear predictors is found in the area of speech coding with the technique known as adaptive differential pulse code modulation (ADPCM) [50]. The basic idea is to reduce the dynamic range of the signal to be encoded by substracting a predicted value. The residual signal (the *prediction error*) is then adaptively quantized and transmitted or stored. The receiver performs the inverse operations in order to reconstruct the original signal, up to a quantization error. The ADPCM encoder is is illustrated in Figure 1.7(a), where $s(n)$ is the signal to be encoded, $\hat{s}(n)$ is the predicted value of $s(n)$, $e(n) = s(n) - \hat{s}(n)$ is the prediction error, and $\bar{e}(n)$ denotes the quantized version of $e(n)$. The decoder is depicted in Figure 1.7(b), where $\bar{s}(n)$ is the reconstructed version of the original signal $s(n)$. The quantized error $\bar{e}(n)$ and the predicted value $\hat{s}(n)$ are related via the operator P. Observe that

$$s(n) = e(n) + P\bar{e}(n), \qquad \bar{s}(n) = \bar{e}(n) + P\bar{e}(n),$$

and therefore one has the fundamental relation

$$s(n) - \bar{s}(n) = e(n) - \bar{e}(n), \tag{1.5}$$

showing that the difference between the original and the reconstructed signals equals the error introduced by the quantizer. (Incidentally, note that (1.5) holds regardless of the properties of P, which could even be nonlinear and/or time varying). The advantage of this technique resides in the fact that if $\hat{s}(n)$ is a good estimate of $s(n)$, then the variance of $e(\cdot)$ is much smaller than that of $s(\cdot)$, and therefore $e(\cdot)$ can be encoded with fewer bits for the same distortion level. Ideally, one would like to have a white prediction error process, since in that case all the redundancy is eliminated from the original signal and $e(\cdot)$ has the smallest variance achievable.

One possible approach is to compute $\hat{s}(n)$ as a finite linear combination of past samples of the reconstructed signal $\bar{s}(n)$, i.e. $\hat{s}(n) = N(z)\bar{s}(n)$ where $N(z)$ is a strictly causal FIR filter. This is shown in Figure 1.8(a). With this choice, one has $P = N(z)/[1 - N(z)]$ in Figure 1.7, and $\bar{e}(n)$ is related to $\bar{s}(n)$ via

$$\bar{e}(n) = [1 - N(z)]\bar{s}(n). \tag{1.6}$$

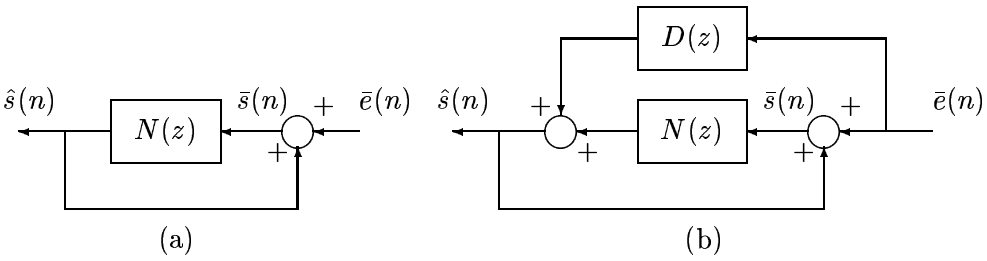

Figure 1.8: Two predictor structures. (a) AR model; (b) ARMA model.

Eq. (1.6) corresponds to an autoregressive (AR) or all-pole model for the power spectrum of the signal to be encoded, which results in an all-zero structure for the prediction error filter $1 - N(z)$.

An alternative scheme shown in Figure 1.8(b) is to compute the predicted value $\hat{s}(n)$ as a finite linear combination of past samples of both the reconstructed signal $\bar{s}(n)$ and the quantized error $\bar{e}(n)$, i.e. $\hat{s}(n) = N(z)\bar{s}(n) + D(z)\bar{e}(n)$. Now both $N(z)$ and $D(z)$ are strictly causal FIR filters. This corresponds to $P = [D(z) + N(z)]/[1 - N(z)]$ in Figure 1.7. Now the relation between $\bar{e}(n)$ and $\bar{s}(n)$ can be readily checked to be

$$\bar{e}(n) = \frac{1 - N(z)}{1 + D(z)}\bar{s}(n). \tag{1.7}$$

Eq. (1.7) corresponds to an autoregressive, moving average (ARMA) or pole-zero model for the power spectrum of the signal. This results in a pole-zero (i.e. IIR) structure for the prediction error filter $[1 - N(z)]/[1 + D(z)]$.

The AR model has been widely used in the area of speech processing. It is derived from the acoustic tube modeling of the human vocal tract under the assumption that during pronunciation the velum is closed and the sound wave propagates only through the oral tract. This ignores the existence of the nasal tract, which results in poor modeling of nasal sounds by the resulting all-pole type spectra. The introduction of zeros in the spectral ARMA model offers more flexibility.

In terms of the ADPCM system, adopting the ARMA model should result in further reduction of the prediction error variance once the predictor parameters are properly tuned. Due to the presence of both poles and zeros in (1.7), the predictor becomes an adaptive IIR filter. To see this, substitute the quantizer in Figure 1.7(a) by a summing junction that injects the quantization noise $q(n) = e(n) - \bar{e}(n)$. In that case the external inputs to the system are $s(n)$ and $q(n)$, and the predicted value $\hat{s}(n)$ relates to these via

$$\hat{s}(n) = \frac{N(z) + D(z)}{1 + D(z)}[s(n) + q(n)],$$

which shows the IIR transfer function of the predictor. (if $D(z) = 0$ as in the AR model, then this transfer function becomes FIR). In 1984 a standard (then labeled

CCITT Recommendation G.721 and now covered by the ITU-T Recommendation G.726 [36]) was developed to digitize 64 kb/s PCM speech signals (8-bits/sample with 8 kHz sampling rate) into 32 kb/s ADPCM coded signals (4 bits/sample with 8 kHz sampling rate). The IIR predictor structure of (1.7) was adopted, using 2 coefficients for the filter $N(z)$ and 6 for $D(z)$. It also specified an algorithm for the adaptation of these parameters which was analyzed in [6]. One salient feature of the standard is that the predictor parameters are not transmitted to the decoder, which has to update its own predictor based on the only signal available: the quantized prediction error $\bar{e}(\cdot)$. The adaptation algorithm achieved a tradeoff between the ability to synchronize decoder and encoder without transmitting side information and the reduction of the prediction error variance, since completely whitening $\bar{e}(\cdot)$ would remove from it all information about the predictor parameters, making it impossible for the decoder to recover them. Observe that the decoder implements the inverse of (1.7), i.e.

$$\bar{s}(n) = \frac{1 + D(z)}{1 - N(z)} \bar{e}(n).$$

This algorithm represents another example of an adaptive IIR filter in which the adaptation is conducted without the aid of a reference signal.

1.1.6 Channel equalization

The discrete-time baseband equivalent model of a digital communication system can be expressed as

$$u(n) = C(z)s(n) + \eta(n) \tag{1.8}$$

where $u(\cdot)$ denotes the received signal, $s(\cdot)$ is the sequence of information-bearing transmitted symbols, $C(z)$ is the transfer function of the channel, and $\eta(\cdot)$ represents additive noise. The nonideal characteristics of the channel introduce intersymbol interference (ISI) which is usually combatted through the use of adaptive equalizers [101]. An equalizer $\hat{H}(z)$ filters the received signal $u(n)$ in an attempt to recover $s(n - \delta)$, a delayed version of the transmitted symbol sequence. The equalizer output $\hat{y}(n) = \hat{H}(z)u(n)$ is converted into a member of the source alphabet by a classification device producing the hard decision $\hat{s}(n - \delta)$. The channel-equalizer configuration is shown in Figure 1.9.

There are two approaches to equalizer adaptation. In the first, a training sequence known in advance by the receiver is transmitted. The receiver then adapts the equalizer so that its output closely matches the reference training signal (usually by minimizing the variance of the error $e(n)$ in Figure 1.9). The second approach, known as blind or unsupervised adaptation, attempts to tune the equalizer coefficients without the aid of a training sequence, with the subsequent improvement in channel capacity. In either case the most popular structure for the adaptive equalizer is the FIR tapped delay line. Recently, however, there has been considerable interest in the use of IIR architectures. These were initially proposed by Mulgrew

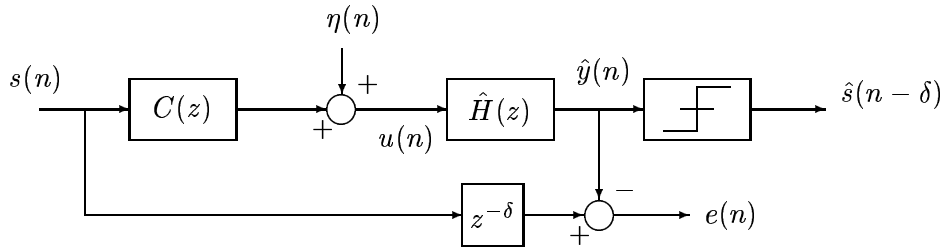

Figure 1.9: Channel-equalizer configuration.

and Cowan [87] based on the observation that under certain conditions, the linear filter that minimizes the mean square error (MSE) $E[|e(n)|^2]$ in Figure 1.9 under the only constraints of causality and stability, has an IIR transfer function *of finite degree.*

Consider the general filtering problem of producing an estimate of a reference signal $d(\cdot)$ by driving a linear filter $\hat{H}(z)$ with an available signal $u(\cdot)$. The goal is to minimize the variance of the estimation error $e(n) = d(n) - \hat{H}(z)u(n)$, and $\hat{H}(z)$ is constrained only to be stable and causal: $\hat{H}(z) = \sum_{k=0}^{\infty} \hat{h}_k z^{-k}$. The solution is given by the Wiener filter which is usually given in terms of the power spectra of the signals $u(\cdot)$ and $d(\cdot)$ [119]. Let the power spectral density (psd) of the observed signal $u(\cdot)$ be

$$S_{uu}(z) = \sum_{n=-\infty}^{\infty} r_{uu}(n) z^{-n} \qquad \text{with} \qquad r_{uu}(n) = E[u(k+n)u^*(k)].$$

$S_{uu}(z)$ can be factorized as $S_{uu}(z) = \gamma^2 F(z) F^*(1/z^*)$, where γ^2 is a constant and $F(z)$ is monic, causal and minimum phase (all poles and zeros inside the unit circle). Define also the cross spectrum

$$S_{du}(z) = \sum_{n=-\infty}^{\infty} r_{du}(n) z^{-n} \qquad \text{with} \qquad r_{du}(n) = E[d(k+n)u^*(k)].$$

The Wiener filter is then given by

$$\hat{H}(z) = \frac{1}{F(z)} \left[\frac{S_{du}(z)}{\gamma^2 F^*(1/z^*)} \right]_{0+} \tag{1.9}$$

where the operator $[\cdot]_{0+}$ extracts the causal part of its argument. Observe that $\hat{H}(z)$ in (1.9) can be seen as the cascade of a whitening filter $1/F(z)$ and a postfilter $[S_{du}(z)/F^*(1/z^*)]_{0+}$.

Mulgrew and Cowan applied in [87] this result to the equalization setting of Figure 1.9, in which the reference signal is $d(n) = s(n-\delta)$. They showed that if:

- The sequence of transmitted symbols $s(\cdot)$ is white;

- The noise process $\eta(\cdot)$ is white and independent of $s(\cdot)$;
- The channel $C(z)$ is FIR with degree L, i.e. $C(z) = \sum_{k=0}^{L} c_k z^{-k}$;

Then $F(z)$ can be taken as a polynomial of degree L, and the transfer function $[S_{du}(z)/\gamma^2 F^*(1/z^*)]_{0+}$ is FIR of degree δ. Therefore under the conditions above the Wiener equalizer has a transfer function that is rational and of finite order (it has L poles and δ zeros), which is somewhat surprising since initially $\hat{H}(z)$ was only assumed to be stable and causal with no restrictions on its degree. Other interesting features of the Wiener equalizer are:

- The positions of the equalizer poles depend only on the psd of the received signal, being independent of the equalization delay δ.
- The recursive part of the equalizer should whiten the received signal. This can be done in principle without the aid of training sequences, and thus the IIR equalizer structure is well suited for unsupervised adaptation.

This last property was exploited in [62] where an unsupervised procedure was presented that decouples the adaptations of the recursive and nonrecursive parts of the IIR equalizer, which are carried out under different criteria. Namely, the received sequence is passed first through an all-pole filter that is adapted in order to whiten its output. This white signal is then fed to an FIR filter which is adapted blindly by means of the Constant Modulus Algorithm (CMA), a popular method for unsupervised adaptation of FIR equalizers [54]. This prewhitening approach was further explored in [89]. Some researchers have also considered the possibility of adapting the recursive part via CMA [22] or some other blind criteria [7].

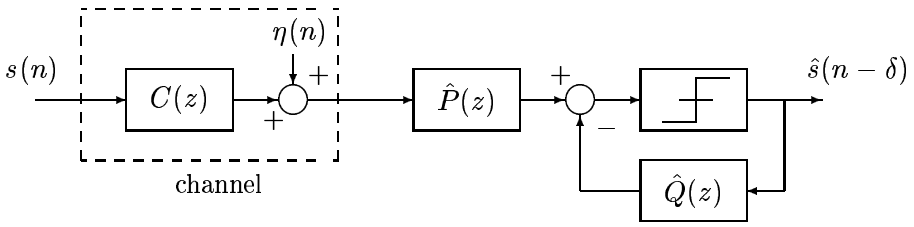

Figure 1.10: Decision-feedback equalization.

The original argument favoring IIR equalizers over traditional FIR architectures of the same complexity was their superior performance in terms of MSE reduction [87]. Also, Labat, Macchi and Laot [62] made an interesting observation relating the Wiener IIR solution to decision feedback equalization. A decision feedback equalizer (DFE) is a nonlinear device in which hard decisions are filtered and fed back in order to additively cancel ISI [66], as depicted in Figure 1.10. DFEs yield very good steady-state performance but their adaptation is usually carried out

using training sequences since successful blind DFE adaptation from a cold start initialization appears to be a very difficult problem [58]. It was noted in [62] that the (linear) Wiener IIR equalizer and the MSE optimum (nonlinear) DFE share similar components and hence the coefficients of the first could be used as starting point for unsupervised DFE adaptation, an approach further investigated in [11, 22]. Labat, Macchi and Laot [62] report good results when testing the algorithm in an underwater acoustic communication system, while Endres *et al.* [22] applied a similar procedure to experimental digital television signals with encouraging results.

Other applications of adaptive IIR filters in digital communications can also be found. For example, implementation of DFEs with IIR structures in the feedback filter (cf. $\hat{Q}(z)$ in Figure 1.10) was suggested in [17, 134] in order to cancel the slowly decaying pulse tails of digital subscriber loop (DSL) channel responses; [68] presented a multichannel adaptive IIR filter for multiple access interference suppression in code division multiple access (CDMA) communication systems; and [96] considers adaptive IIR continuous-time equalizers for magnetic recording read channels.

1.2 A review of IIR filter structures

For any given system with a rational transfer function there exists a wide variety of equivalent sets of difference equations, each corresponding to a different filter implementation. Several considerations affect the choice among these different structures. For example, in digital filter design properties such as computational complexity, finite precision effects, and modularity for efficient VLSI implementation are often taken into account. If the filter is to be adaptive, other considerations such as ease of algorithm implementation and stability monitoring play also an important role when choosing a particular structure. In this section we briefly review the most popular implementations for adaptive IIR filtering applications.

1.2.1 Direct form

Most adaptive IIR algorithms were originally derived for a direct form filter implementation. Suppose it has been decided that a filter with N zeros and M poles be used for a particular application. Let the transfer function of this (adaptive) filter be

$$\hat{H}(z) = \frac{B(z)}{A(z)} = \frac{b_0 + b_1 z^{-1} + \cdots + b_N z^{-N}}{1 + a_1 z^{-1} + \cdots + a_M z^{-M}} \tag{1.10}$$

The input-output relation $\hat{y}(n) = \hat{H}(z)u(n)$ leads to the difference equation

$$\hat{y}(n) = \sum_{k=0}^{N} b_k u(n-k) - \sum_{k=1}^{M} a_k \hat{y}(n-k). \tag{1.11}$$

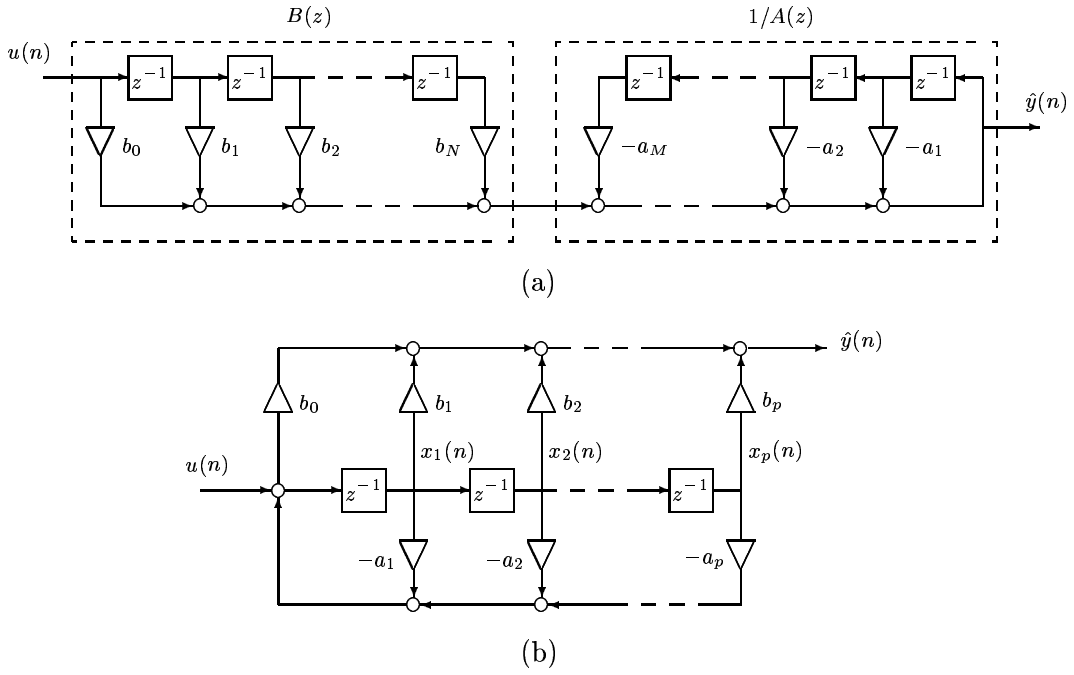

Figure 1.11: Direct form structures. (a) Direct form - I. (b) Direct form - II.

Direct implementation of (1.11) leads to the structure known as *Direct Form - I* which is depicted in Figure 1.11(a). The subfilters $B(z)$ and $1/A(z)$ are cascaded in this implementation, with $B(z)$ preceding $1/A(z)$. If the order of these subfilters is reversed one obtains the *Direct Form - II* structure shown in Figure 1.11(b), where $p = \max\{N, M\}$ (if $N > M$ then the last $N - M$ coefficients a_k are zero, while if $N < M$ then the last $M - N$ coefficients b_k are zero). The difference equations of the Direct Form - II are

$$w(n) = u(n) - \sum_{k=1}^{p} a_k x_k(n), \qquad \hat{y}(n) = b_0 w(n) + \sum_{k=1}^{p} b_k x_k(n), \tag{1.12}$$

$$x_k(n+1) = x_k(n), \qquad k = p, p-1, \ldots, 2; \qquad x_1(n+1) = w(n). \tag{1.13}$$

The Direct Form - II implementation of $\hat{H}(z)$ is minimal in the sense that it requires the smallest possible number of delay elements z^{-1}. This is not true for the Direct Form - I structure.

When either of these structures is chosen for the adaptive filter, the corresponding algorithm updates the coefficients $b_0, \ldots, b_N, a_1, \ldots, a_M$. With adaptation the filter becomes a time-varying system, and due to the presence of feedback in the signal flowgraph it is possible for the filter to become unstable unless some precautions are taken. The direct form, however, is not well suited for efficient stability monitoring unless $M \leq 2$, in which case one usually constrains $|a_2| < 1$ and

$|a_1| < 1 - a_2$ at every iteration (this stability check may fail though unless adaptation is sufficiently slow [10],[105, chap. 6]). Another problem is its sensitivity to quantization effects. Thus although the vast majority of adaptive algorithms were designed with the direct form structure as starting point, practical considerations have led to the investigation of other filter implementations.

1.2.2 Cascade and parallel forms

Cascade and parallel structures tend to be better behaved than direct form implementations in terms of finite precision effects; also, the task of stability monitoring becomes much easier. The cascade form is obtained by factoring the transfer function $\hat{H}(z)$ into first- and second-order sections, each of which is implemented in direct form. Alternatively, the parallel form is obtained from a partial fraction expansion of $\hat{H}(z)$ so that a parallel connection of first- and second-order sections is obtained.

Several researchers have considered the use of cascade and parallel forms for adaptive IIR filtering [91, 114, 131]. However, these structures present several disadvantages that have somewhat stalled research in this direction:

- Parallel forms cannot model transfer functions with repeated complex poles, unless the number of repeated complex poles and their multiplicities are known *a priori* in order to modify the structure of the adaptive filter accordingly. Thus in the general case (no *a priori* information) the space of rational functions of a given degree is not completely reachable using this structure.

- In the cascade form, the output signal of each section depends on the coefficients of that section as well as on those of all previous sections. This considerably increases the computational load of the adaptive algorithms [91], although it can be alleviated by judiciously choosing the implementation of the numerator of the adaptive filter [131].

- For both parallel and cascade forms, the overall transfer function remains unaltered if the coefficients of two different sections are interchanged. This produces manifolds in parameter space along which the convergence rate of the adaptive algorithms may be considerably slower than that of direct form structures [114].

1.2.3 Lattice form

The lattice form of an IIR transfer function $\hat{H}(z)$ as given in (1.10) is based on the parameterization of the denominator $A(z) = 1 + a_1 z^{-1} + \cdots + a_M z^{-M}$ in terms of the so-called *reflection coefficients* $\sin\phi_1, \ldots, \sin\phi_M$ (the quantities ϕ_i are

known as *rotation angles*). One can recover the direct form parameters a_i from the reflection coefficients via the following recursion: for $k = 1, \ldots, M$, do

$$a_k^{(k)} = \sin\phi_k, \tag{1.14}$$

$$a_i^{(k)} = a_i^{(k-1)} + \sin\phi_k \cdot a_{k-i}^{(k-1)}, \quad 1 \le i \le k-1, \tag{1.15}$$

$$A_k(z) = 1 + a_1^{(k)} z^{-1} + \cdots + a_k^{(k)} z^{-k}, \tag{1.16}$$

and then one has $A(z) = A_M(z)$. Conversely, the reflection coefficients can be obtained from the direct form parameters through the following reverse recursion: set $a_i^{(M)} = a_i$, $1 \le i \le M$, and for $k = M, M-1, \ldots, 2$, do

$$\sin\phi_k = a_k^{(k)}, \qquad a_i^{(k-1)} = \frac{a_i^{(k)} + \sin\phi_k \cdot a_{k-i}^{(k)}}{1 - \sin^2\phi_k}, \quad 1 \le i \le k-1. \tag{1.17}$$

The lattice parameterization of $A(z)$ has the property that, provided the rotation angles are restricted to the range $\phi_k \in [-\frac{\pi}{2}, \frac{\pi}{2}]$, the roots of $A(z)$ all lie inside the unit circle if and only if $|\phi_k| < \frac{\pi}{2}$ (or equivalently $|\sin\phi_k| < 1$) for $1 \le k \le M$. This is known as the Schur-Cohn stability test [3].

From (1.16), let us define

$$\hat{A}_0(z) = A_0(z) = 1, \qquad \hat{A}_k(z) = z^{-k} A_k(z^{-1}), \quad k \ge 1. \tag{1.18}$$

Note that $A_k(z)$, $\hat{A}_k(z)$ are degree k polynomials in z^{-1}. One can write

$$\begin{bmatrix} \hat{A}_0(z) \\ \hat{A}_1(z) \\ \vdots \\ \hat{A}_k(z) \end{bmatrix} = \mathbf{L}_k \cdot \begin{bmatrix} 1 \\ z^{-1} \\ \vdots \\ z^{-k} \end{bmatrix}, \tag{1.19}$$

where $\mathbf{L}_k$ is a $(k+1) \times (k+1)$ lower triangular matrix formed from the $a_i^{(j)}$ and with ones on its diagonal. It is also useful to introduce the parameters

$$\gamma_k = \begin{cases} \prod_{i=k+1}^{M} \cos\phi_i, & 0 \le k < M \\ 1, & k \ge M \end{cases} \tag{1.20}$$

and the $(k+1) \times (k+1)$ matrices

$$\mathbf{\Gamma}_k = \operatorname{diag}\left(\gamma_0 \;\; \gamma_1 \;\; \cdots \;\; \gamma_k\right). \tag{1.21}$$

In the range $\phi_k \in (-\frac{\pi}{2}, \frac{\pi}{2})$ one has $\cos\phi_k > 0$ and therefore $\gamma_k > 0$, so that $\mathbf{\Gamma}_k$ is positive definite.

Two different lattice implementations of the transfer function $\hat{H}(z) = B(z)/A(z)$ can be found in the literature, depending on how the numerator $B(z)$ is realized: the cascade and the tapped-state lattices. The cascade normalized lattice form

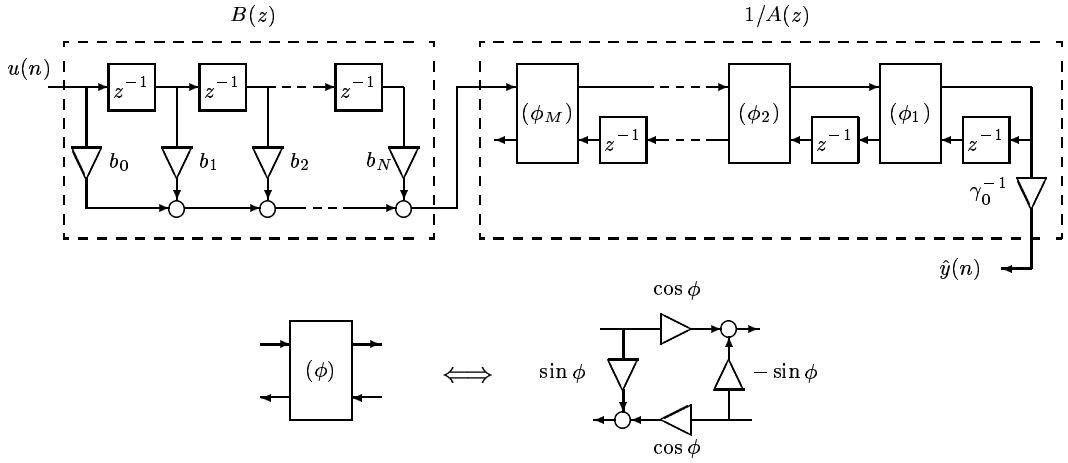

Figure 1.12: Cascade normalized lattice structure.

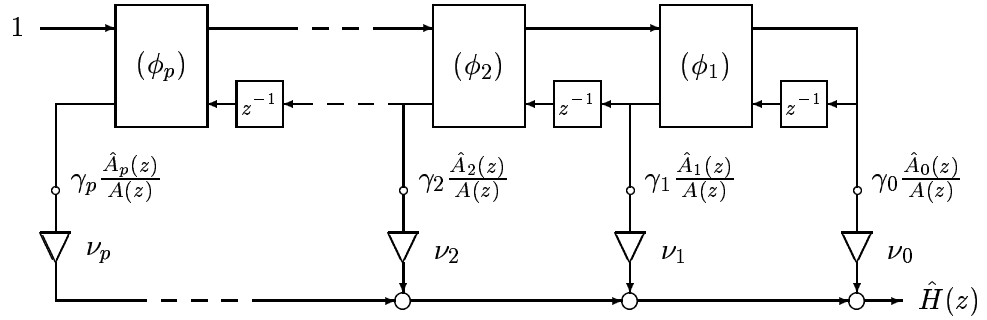

Figure 1.13: Tapped-state normalized lattice structure, indicating the transfer functions to the various nodes of the filter.

is shown in Figure 1.12. Similarly to the Direct Form - I of Figure 1.11(a) this structure is composed of two subfilters, with the numerator $B(z)$ implemented as a tapped delay line and followed by the denominator $1/A(z)$ now implemented in normalized lattice form. Of course it is also possible to reverse the order of these subfilters, i.e. to have first $1/A(z)$ and then $B(z)$, without altering the overall transfer function. The output multiplier γ_0^{-1} in Figure 1.12 is included for clarity purposes only in order to cancel the overall gain of the normalized lattice, but in practical implementations it can be absorbed into the coefficients of the numerator $B(z)$.

The other variant is the tapped-state normalized lattice, shown in Figure 1.13 where again $p = \max\{N, M\}$. In this structure the numerator $B(z)$ is implemented

as a linear combination of the polynomials $\gamma_k \hat{A}_k(z)$:

$$B(z) = \sum_{k=0}^{N} \nu_k [\gamma_k \hat{A}_k(z)]. \tag{1.22}$$

If $N > M$, the last $N - M$ reflection coefficients $\sin \phi_k$ in Figure 1.13 would be set to zero, while the reverse situation $N < M$ is taken care of by setting the last ν_k weights to zero. As indicated in Figure 1.13, the transfer functions from the input to the delay elements are $\gamma_k \hat{A}_k(z)/A(z)$. The numerator parameters $\{b_i\}$ and $\{\nu_i\}$ are related via

$$\begin{bmatrix} b_0 \\ \vdots \\ b_N \end{bmatrix} = \mathbf{L}_N^T \mathbf{\Gamma}_N^T \begin{bmatrix} \nu_0 \\ \vdots \\ \nu_N \end{bmatrix}. \tag{1.23}$$

Eqs. (1.22) and (1.23) show that while the numerator coefficients $\{b_i\}$ are independent of the filter poles, the weights $\{\nu_i\}$ are not: if the poles of $\hat{H}(z)$ change even while its zeros are kept fixed, the corresponding parameters $\{\nu_i\}$ will change as well. Also note that the tapped-state lattice form is minimal while the cascade lattice form is not.

The primary advantage of the normalized lattice structure is that stability monitoring becomes extremely simple, even when the filter becomes time-varying. It was shown in [103] that as long as the rotation angles satisfy $|\phi_k(n)| \leq \pi/2 - \epsilon$ for all k and n, with $0 < \epsilon \leq \pi/2$ a fixed constant, the time-varying normalized lattice structure is exponentially stable. It is worth noting that this nice property need not apply to other lattice structures, such as two-multiplier or one-multiplier forms. Also, there is a unique parameterization of any stable transfer function $\hat{H}(z) = B(z)/A(z)$ in either cascaded or tapped-state lattice form. Therefore the slow convergence problems associated to the nonuniqueness of the cascade or parallel realizations of section 1.2.2 are not present in the lattice implementations. On the other hand, the computational complexity of normalized lattice implementations is greater than that of direct form structures, but if one takes into account the costly stability checks associated with adaptive direct form filters the lattice structures tend to be preferred.

1.3 A review of adaptive IIR filtering algorithms

In this section we present four 'classical' algorithms for adaptive IIR filtering settings in which a reference signal is available. As mentioned before, most adaptive algorithms were originally designed for direct form implementations, although several authors have derived modifications for other structures as well. We start with the direct form versions of the equation error, output error, Steiglitz-McBride, and hyperstability based on-line adaptive algorithms, and then we comment on the lattice versions of these schemes. The cascade and parallel forms will not be further

considered in this thesis due to the inherent problems they present, as explained in section 1.2.2. In addition, we shall focus on constant-gain type algorithms, for which the update takes the form

$$\begin{bmatrix} \text{New} \\ \text{parameter} \\ \text{vector} \end{bmatrix} = \begin{bmatrix} \text{Old} \\ \text{parameter} \\ \text{vector} \end{bmatrix} + \begin{bmatrix} \text{Fixed} \\ \text{stepsize} \end{bmatrix} \cdot \begin{bmatrix} \text{Driving} \\ \text{vector} \end{bmatrix} \cdot \begin{bmatrix} \text{Error} \\ \text{signal} \end{bmatrix}$$

In what follows, $u(\cdot)$, $\hat{y}(\cdot)$ and $d(\cdot)$ designate the adaptive filter input and output and the reference signal respectively. All signals and coefficients are assumed real-valued. We designate the vector of direct form parameters by

$$\theta_d = \left[\, b_0 \, \cdots \, b_N \; a_1 \, \cdots \, a_M \, \right]^T. \tag{1.24}$$

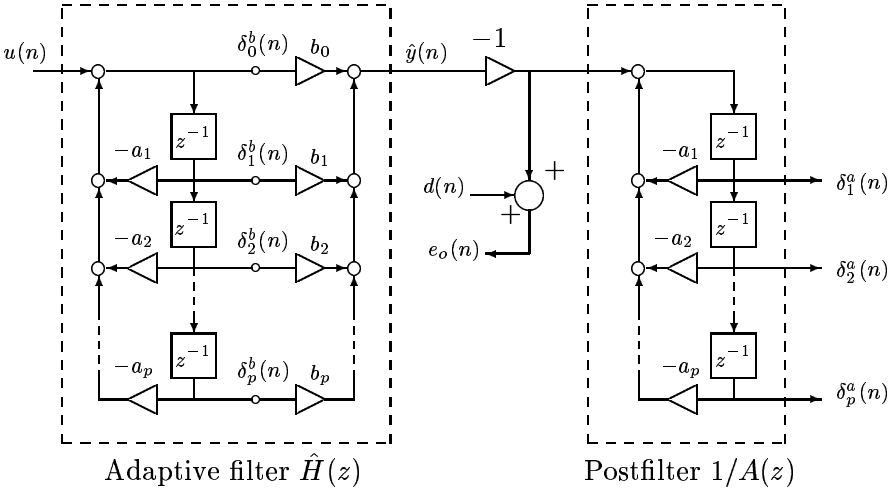

Figure 1.14: Output error configuration.

1.3.1 Output error algorithm

The Output Error (OE) approach attempts to minimize the variance of the output error signal $e_o(n) = d(n) - \hat{y}(n)$. An stochastic gradient descent of the cost function $E[e_o^2(n)]$ takes the form

$$b_k(n+1) = b_k(n) + \mu \frac{\partial \hat{y}(n)}{\partial b_k} e_o(n), \qquad a_k(n+1) = a_k(n) + \mu \frac{\partial \hat{y}(n)}{\partial a_k} e_o(n),$$

where $\mu > 0$ is the stepsize. The gradient signals are readily obtained by taking partial derivatives in (1.11):

$$\delta_k^b(n) = \frac{\partial \hat{y}(n)}{\partial b_k} = \frac{z^{-k}}{A(z)} u(n), \qquad \delta_k^a(n) = \frac{\partial \hat{y}(n)}{\partial a_k} = -\frac{z^{-k}}{A(z)} \hat{y}(n). \tag{1.25}$$

The signals $\delta_k^b(n)$ are readily available from the adaptive filter $\hat{H}(z)$ if the Direct Form - II implementation is chosen. Generation of $\delta_k^a(n)$ requires an additional all-pole postfilter driven by the adaptive filter output $\hat{y}(n)$. The overall configuration is shown in Figure 1.14.

If we define the regressor vector

$$\psi_o(n) = [\, u(n)\ u(n-1)\ \cdots\ u(n-N)\ -\hat{y}(n-1)\ \cdots\ -\hat{y}(n-M)\,]^T \tag{1.26}$$

such that the difference equation (1.11) becomes $\hat{y}(n) = \theta_d^T(n)\psi_o(n)$, then the OE algorithm can be compactly written as

$$\theta_d(n+1) = \theta_d(n) + \mu \left[\frac{1}{A(z)}\psi_o(n)\right] e_o(n). \tag{1.27}$$

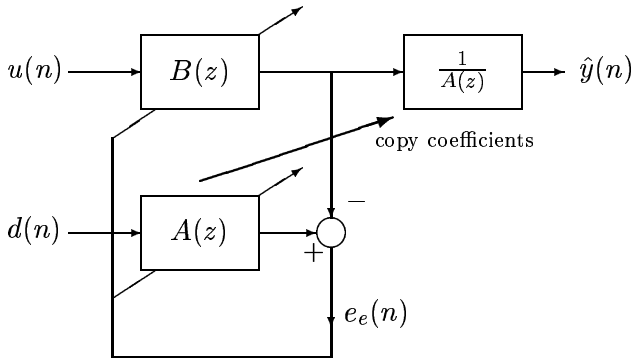

Figure 1.15: Equation-Error configuration.

1.3.2 Equation error algorithm

The equation error (EE) method adjusts the coefficients of two FIR filters $B(z) = \sum_{k=0}^{N} b_k z^{-k}$ and $A(z) = \sum_{k=0}^{M} a_k z^{-k}$ in order to minimize the variance of the equation error signal

$$e_e(n) = A(z)d(n) - B(z)u(n) = \sum_{k=0}^{M} a_k d(n-k) - \sum_{k=0}^{N} b_k u(n-k). \tag{1.28}$$

The coefficients of the FIR filter $A(z)$ are then copied into an all-pole filter $1/A(z)$ to obtain the adaptive pole-zero filter $\hat{H}(z)$. This is represented in Figure 1.15.

In order to avoid the solution $A(z) = B(z) = 0$, some constraint must be placed on the filter coefficients. Traditionally a monic constraint on $A(z)$ has been used: one fixes $a_0 = 1$. Alternatively a quadratic constraint of the type $\sum_{k=0}^{M} a_k^2 = 1$

could be placed [104]. The monic constraint approach leads to a standard two-input one-output FIR filtering problem. Defining the vector

$$\psi_e(n) = [\, u(n)\ u(n-1)\ \cdots\ u(n-N)\ -d(n-1)\ \cdots\ -d(n-M)\,]^T, \tag{1.29}$$

the equation error becomes $e_e(n) = d(n) - \theta_d^T(n)\psi_e(n)$, which is a linear function of the filter coefficients. A stochastic gradient descent on the cost function $E[e_e^2(n)]$ yields the EE algorithm

$$\theta_d(n+1) = \theta_d(n) + \mu\psi_e(n)e_e(n), \tag{1.30}$$

which is just a generalization of the standard LMS algorithm for adaptive FIR filters to the two-channel case. Observe that the equation error and output error signals are related by $e_e(n) = A(z)e_o(n)$.

1.3.3 Steiglitz-McBride algorithm

The Steiglitz-McBride (SM) adaptive algorithm is rooted in an off-line system identification procedure [120] which will be discussed in chapter 3. The on-line direct form algorithm was developed by Fan and Jenkins in [30], and has the form

$$\theta_d(n+1) = \theta_d(n) + \mu\left[\frac{1}{A(z)}\psi_e(n)\right] e_o(n), \tag{1.31}$$

where $e_o(n) = d(n) - \hat{y}(n)$ is the output error and $\psi_e(n)$ is the vector defined in (1.29). Note that the numerator parameters $\{b_i\}$ are adapted in the same way as in the OE algorithm. The update of the denominator coefficients, however, is different, although conceptually similar. Specifically, as shown in Figure 1.14 the signals that drive the adaptation of the coefficients $\{a_i\}$ in the OE algorithm are generated by an all-pole filter driven by the signal $\hat{y}(n)$. In the SM algorithm, these signals are in the same way taken from the states of an all-pole filter but now driven by $d(n)$.

1.3.4 Hyperstability based algorithms

The class of algorithms presented in this section has its origins in the work of Landau [64] in the system identification context of Figure 1.1 and Johnson [51] in the general adaptive filtering setting. The constant gain member of the family is known as SHARF (Simplified hyperstable adaptive recursive filter) and has the following form:

$$\theta_d(n+1) = \theta_d(n) + \mu\psi_o(n)\,[C(z)e_o(n)]\,, \tag{1.32}$$

where the so-called *compensation filter* $C(z)$ is chosen by the designer in order to meet certain *Strictly Positive Real* (SPR) condition that this class of algorithms require for convergence. The role of the SPR condition will be discussed in section 1.4.3. The special case in which $C(z) = 1$ is known as *pseudolinear regression*

(PLR) algorithm and was originally proposed by Feintuch [34]. It can be seen as a simplification of the OE algorithm in which the dependence of the regressor $\psi_o(n)$ with the filter coefficients is ignored when taking the partial derivatives of $\hat{y}(n) = \theta_d^T(n)\psi_o(n)$ with respect to these parameters. From (1.25), this leads to the approximations

$$\delta_k^b(n) \approx u(n-k), \qquad \delta_k^a(n) \approx -\hat{y}(n-k).$$

Due to these simplifications, the convergence properties of the OE and PLR algorithms are quite different.

1.3.5 Lattice algorithms

Due to the difficulty in monitoring stability of the adaptive filter when realized in direct form, there has been considerable effort in translating the host of available adaptive algorithms to the lattice structure. Early attempts in this direction [55, 95] focusing on the Output Error method led to schemes that required heavy computational loads in order to obtain the gradient signals. In particular, each gradient component associated to the reflection coefficients required an additional lattice structure for its computation: the resulting complexity is of order M^2. In contrast, the direct form OE algorithm only requires an additional postfilter, thus its complexity is of order M. For several years this proved a significant obstacle to lattice adaptive IIR filters. Subsequent work showed that the gradient computations can be significantly reduced [110],[105, sec. 7.5], obtaining efficient tapped-state normalized lattice implementations of the OE method with complexity of order M. The resulting algorithms required a single additional postfilter, as the direct form version, with the difference that several internal signals from the lattice adaptive filter are used as inputs to this postfilter (in contrast the postfilter in the direct form version has a single input, namely the adaptive filter output $\hat{y}(\cdot)$).

The algorithms of [110],[105, sec. 7.5] were true stochastic gradient descent methods in the sense that they used the exact sensitivity functions of $\hat{y}(\cdot)$ with respect to the filter coefficients. Further simplifications in the computation of these sensitivity functions led to new lattice algorithms, both in cascade [84] and tapped state forms [105, secs. 7.6 and 7.7]. The driving vectors of these schemes are only approximations to the true gradient and therefore the convergence properties of the simplified algorithms need not be the same as those of the lattice OE method, although similar behavior was observed in simulation experiments.

The driving vectors of the simplified algorithms are generated by a postfilter driven by the adaptive filter output, similarly to the direct form case (with the particularity that the postfilter is now implemented in lattice form). As it could be expected, this opened the door to lattice versions of the Steiglitz-McBride algorithm by simply switching the postfilter input from $\hat{y}(\cdot)$ to the reference signal $d(\cdot)$. This was suggested in [103] for the tapped-state lattice and in [84] for the cascade lattice.

Simplified lattice versions of the EE approach were also developed. Observe

that the driving vector of the direct form EE algorithm, $\psi_e(n)$, is comprised by the state signals of the two FIR filters $B(z)$ and $A(z)$ in Figure 1.15. One can take advantage of the fact that the reflection coefficients of an FIR lattice filter with transfer function $A(z)$ coincide with those of an IIR lattice with transfer function $1/A(z)$ [93], and implement these blocks in lattice form in the setting of Figure 1.15. The state signals of the FIR lattice $A(z)$ were used to generate the driving vector of a lattice EE algorithm proposed in [76]. Another possibility is to use the same driving vector as for the direct form algorithm, as in [92]. As a result of these approximations neither of these schemes is a stochastic gradient descent of the EE cost function $E[e_e^2(n)]$ anymore.

Hyperstability based algorithms in lattice form are also found. By observing that the driving vector of the direct form SHARF algorithm in 1.32 is comprised by the state signals of the Direct Form - I implementation of the adaptive filter, Miao, Fan and Doroslovački [84] proposed the use of a cascade lattice structure, with the corresponding state signals forming now the driving vector. Again, this approach introduced certain approximations so that the convergence analysis of the direct form algorithm does not completely carry over to the lattice variant.

1.4 Issues concerning adaptive IIR filtering algorithms

In previous sections we have described potential applications that could benefit from adaptive recursive filters and presented the most popular criteria for the adaptation of these systems. There is a series of practical obstacles, however, which are not present for traditional adaptive FIR structures and have prevented widespread use of adaptive IIR filters. In this section we describe in some detail the advantages and drawbacks associated to these algorithms, highlighting those issues that have motivated the work that is presented in the subsequent chapters of the thesis.

Consider the general constant-gain adaptive algorithm

$$\theta(n+1) = \theta(n) + \mu \mathbf{x}(n) e(n), \tag{1.33}$$

in which the vector θ comprises the coefficients of the adaptive filter $\hat{H}(z)$ in some parameterization (direct form, lattice, ...). The *stationary points* of the algorithm (1.33) are those values θ_* of the parameter vector for which the update term vanishes on the average, that is,

$$E[\mathbf{x}(n)e(n)]\Big|_{\theta=\theta_*} = 0. \tag{1.34}$$

Observe that if a parameterization θ_* exists for which the error signal $e(n)$ becomes identically zero, then (1.34) is satisfied. For example, in the system identification setting of Figure 1.1 with $\deg \hat{H}(z) \geq \deg H(z)$ and in the absence of noise, $\hat{H}(z) = H(z)$ constitutes a stationary point for any algorithm using the output error $e_o(n)$ or the equation error $e_e(n)$ since these two error signals vanish at such point. In more realistic undermodeled and/or noisy scenarios there is no $\hat{H}(z)$ for which

$e(n) = 0$ identically, although solutions of (1.34) may still exist. Of course different algorithms will exhibit different stationary points in general.

A stationary point θ_* is *locally convergent* or *locally attractive* if once the adaptive algorithm enters a small enough region around θ_*, then it will remain near θ_*. In other words, if the parameter vector is perturbed away from the stationary point, the adaptive algorithm will tend to restore it back to the value that zeroes the expected value of the correction term, provided that the perturbation is small enough. When this property holds irrespective of the magnitude of the perturbation, the stationary point is said to be *globally convergent.* It is worth mentioning that in general the parameter vector will not settle at the well-defined values of a convergent stationary point: convergence takes place only in some mean asymptotic sense, and the parameters will exhibit a random component superimposed on a mean asymptotic value as a result of measurement noise, numerical errors, etc.

We can summarize the main questions arising in the analysis of any adaptive IIR filtering algorithm as follows:

- Does the system remain stable (in a bounded-input bounded-output sense) during adaptation?
- Which are the stationary points of the algorithm?
- Of these, which are locally (or globally) convergent?
- What can be said about the convergence rate of the algorithms?

The answers to these questions strongly depend on the particular configuration and filter structure. In many cases, due to the nonlinear character of the problem, only partial answers are available.

1.4.1 Filter stability

As we mentioned in section 1.2 when discussing adaptive filter structures, in general direct form IIR filters are not well suited for adaptive applications due to their potential instability. The lattice form is much better behaved in this sense since the stability condition for this structure is easily translated in the filter coefficient space. However, as discussed in section 1.3.5, reformulating the original direct form algorithms in lattice form tends to be a complicated task, and the majority of lattice algorithms available in the literature involved some kind of simplification in their development. This immediately raises the question of how the properties of stationary points are affected by these simplifications, which will be the topic of chapter 2. While it is known that the stationary points of the simplified lattice algorithms coincide with those of the original direct form algorithms (in transfer function space), whether this is also true for *convergent* points has remained an open problem. In chapter 2 we answer this question in the negative, by showing

that for several of these simplified lattice schemes one can find system identification settings (with model order matching and in the absence of noise) in which the stationary point corresponding to the unknown system is not convergent, in contrast to the corresponding direct form versions. This constitutes a clear drawback of these methods, which prompts the search for reliable and efficient lattice algorithms. We develop a general approach for the translation of any given direct form adaptive IIR filtering algorithm into lattice form. It is shown that the resulting schemes preserve not only the set of stationary points but also their convergence properties, at least in the sufficient order case. These results have been presented in [80].

1.4.2 Noise induced bias and local minima

Referring again to the system identification setting of Figure 1.1, we observe that the reference signal $d(\cdot)$ includes an additive noise disturbance $\eta(\cdot)$. The physical origin of this noise process depends on the application: it could model sensor measurement noise, or near-end speech in an echo cancellation setting, etc. It is usually assumed that the input signal $u(\cdot)$ and the noise $\eta(\cdot)$ are statistically independent. We say that an adaptive algorithm is *biased* if the locations of its stationary points are affected by the presence and characteristics of the output noise.

The standard example of a biased adaptive algorithm is the monic-constrained EE method (1.30). This scheme shares several nice properties with adaptive FIR algorithms (to which it is closely related) due to the fact that the equation error $e_e(n)$ is a linear function of the filter coefficients, such as a unique stationary point which is globally convergent and relatively fast convergence . On the other hand, if we write the reference signal as $d(n) = y(n) + \eta(n)$ where $y(\cdot)$ is the uncorrupted reference, then $e_e(n)$ becomes

$$e_e(n) = [A(z)y(n) - B(z)u(n)] + A(z)\eta(n).$$

Since $\eta(\cdot)$ is independent of $u(\cdot)$ and $y(\cdot)$, it is seen that minimizing $E[e_e^2(n)]$ involves a tradeoff between reducing the modeling error $A(z)y(n) - B(z)u(n)$ and the noise component $A(z)\eta(n)$: the adaptive filter is trying to minimize the noise power reaching $e_e(n)$ in addition to identifying the unknown system. As a result of these conflicting goals the optimum $A(z)$, $B(z)$ will vary with the signal to noise ratio and the spectral characteristics of $\eta(\cdot)$. When the bias becomes significant, the performance of the adaptive filter may be completely unsatisfactory: the stationary point may even correspond to an unstable transfer function $B(z)/A(z)$ [116]. This stability problem will be addressed in chapter 3, providing a new result which has been reported in [74].

In contrast with the EE approach, the presence of output noise $\eta(\cdot)$ does not bias the OE algorithm (1.27). This is due to the fact that the noise does not appear in the driving vector of the algorithm. On the other hand, although the OE cost function $E[e_o^2(n)]$ is quadratic in the coefficients of the numerator $B(z)$ of the adaptive filter,

this is no longer true for the coefficients of the denominator $A(z)$. As a result, the stochastic gradient descent (1.27) may converge to a local minimum of the cost function depending on the starting point, with the consequent performance loss. Some researchers have isolated sufficient conditions for the absence of local minima in the OE cost function, in a system identification setting like the one in Figure 1.1 and with an adaptive filter whose order matches that of the unknown system. Nayeri [90] shows that the OE cost is unimodal provided that the input signal $u(\cdot)$ is a white process and that $N + 2 \geq M$, where N and M are the number of zeros and poles, respectively, of the adaptive filter as in (1.10). Regalia shows in [105] that in the case $N \geq M$ unimodality follows if $u(\cdot)$ is a first-order autoregressive process, which includes a white input signal as a special case. Whether this is also true regardless of the power spectral density of $u(\cdot)$ remains an open question (to the author's knowledge, no counterexamples have been presented). However, it is widely recognized that in undermodeled cases the presence of local minima in the OE cost function is not the exception but the rule [105].

The EE and OE methods appear to be complementary, in that the former presents a unique, globally convergent stationary point which is biased in the presence of noise, while the latter is unbiased but may converge to a local minimum. There have been several attempts to overcome these problems:

- Instrumental variable methods [117] eliminate the bias problem in the EE algorithm by suitably modifying the driving vector in (1.30), but global convergence is lost in general.
- If the monic constraint in the EE scheme is replaced by a quadratic constraint, the position of the minimum of $E[e_e^2(n)]$ is not altered by the presence of *white* measurement noise [104]. The resulting on-line algorithms tend to be more involved than the standard LMS algorithm (1.30) [20, 37, 48] and sometimes the global convergence property of the monic EE approach may be lost.
- Hybrid algorithms [14, 59, 69] provide a trade-off between the features of the two formulations by using driving vectors and/or error signals that are convex combinations of those of the EE and OE algorithms.
- The Steiglitz-McBride method for off-line system identification [120] transforms the nonquadratic OE minimization problem to a sequence of quadratic, EE-like problems which are iterated until convergence. The presence of output noise does not alter the locations of SM equilibrium points as long as this noise is white. The same is true for the corresponding on-line algorithm (1.31) [30]. In sufficient order system identification settings, $\hat{H}(z) = H(z)$ is the only limit point of the off-line SM iteration and it is locally stable, as long as the disturbance $\eta(\cdot)$ is white [121], irrespective of the spectral characteristics of the input $u(\cdot)$.

A different off-line procedure was presented in [76]. This method, known as

Interpolation Expanded Numerator (IXN), is similar in spirit to the SM scheme in that a sequence of quadratic minimization steps is iteratively performed. IXN is not biased by the presence of output noise (white or otherwise), and has a single equilibrium corresponding to $\hat{H}(z) = H(z)$ in sufficient order system identification settings with white inputs. In chapter 3 this off-line method is further investigated in order to extend the results from [76] to more general input signals. On-line algorithms based on this procedure will be developed and analyzed. In addition, a novel unbiased off-line scheme termed Steiglitz-McBride Expanded Numerator (SMXN) will also be presented together with its on-line version. Part of the results in this chapter can be found in [77].

1.4.3 The SPR condition

The schemes based on hyperstability concepts, such as the SHARF algorithm of (1.32), are not biased by output noise, since the driving vector $\psi_o(n)$ is uncorrelated with the noise component in the error signal $C(z)e_o(n)$. In contrast with the EE and OE approaches, there is no cost function underlying the design of these algorithms. Rather, they were devised from feedback theory concepts applied to the system identification setting in the matching order case, by realizing that the interaction between the unknown system and the adaptive algorithm can be expressed as a feedback loop consisting of a linear block closed by a nonlinear block. The algorithm is then designed in order to meet the conditions of the hyperstability theorem [97] which in turn ensures asymptotic stability of the closed loop, leading to convergence of the output error to zero in the noiseless case [51]. Parameter convergence, i.e. $\hat{H}(z) \to H(z)$, will follow under standard 'persistent excitation' conditions on the input signal $u(\cdot)$ [2]. This convergence is global and still holds in the noisy case, although only in a mean asymptotic sense.

However, in order to invoke the hyperstability theorem a 'Strictly Positive Real' (SPR) condition must be satisfied. A transfer function $F(z)$ is SPR if it is stable and causal and the real part of $F(z)$ evaluated on the unit circle is strictly positive:

$$\mathrm{Re}\left\{F(e^{j\omega})\right\} > 0 \quad \forall\, \omega. \tag{1.35}$$

For the SHARF algorithm (1.32), if the unknown system is written as $H(z) = B_*(z)/A_*(z)$, then the transfer function $C(z)/A_*(z)$ must be SPR in order to ensure global convergence in the matching order case. The designer is free to choose the compensating filter $C(z)$ in order to meet this requirement. However, since $H(z)$ (and therefore $A_*(z)$) is unknown, successful design of $C(z)$ becomes a difficult task. In certain cases some *a priori* knowledge may be available about the poles of the unknown system, e.g. in the form of uncertainty regions, which can be exploited in order to select the compensating filter [86]. Another possibility is to make $C(z)$ adaptive [64], but for this approach global convergence has not been proven yet in the general case of nonwhite output noise.

Another attempt to circumvent the SPR condition was proposed in [112], based on the fact that the transfer function of the unknown system can be written as

$$H(z) = \frac{B_*(z)}{A_*(z)} = \frac{B_*(z)T(z)}{A_*(z)T(z)} \tag{1.36}$$

where $T(z)$ is a minimum phase polynomial which is otherwise arbitrary. The adaptive filter $\hat{H}(z) = B(z)/A(z)$ can be overparameterized correspondingly so that the orders of $B(z)$ and $A(z)$ match those of $B_*(z)T(z)$ and $A_*(z)T(z)$ respectively. The key observation is that, for any given polynomial $A_*(z)$ of order M such that its roots all lie in the region $|z| \leq \rho < 1$, a polynomial $T(z)$ exists such that $A_*(z)T(z)$ is SPR provided that the degree P of $T(z)$ satisfies

$$P \geq M \left(\frac{\log(\sin \frac{\pi}{2M})}{\log \rho} - 1 \right).$$

Thus if a bound ρ on the magnitude of the poles is available, this expression gives the degree of overparameterization that suffices for convergence of the output error to zero (the compensating filter can be set to $C(z) = 1$ in that case). However, due to the nonuniqueness of the polynomial $T(z)$, parameter convergence is not guaranteed as a result of the pole-zero cancellations artificially introduced in the adaptive filter.

A more refined version of this approach appeared in [85], where $T(z)$ is chosen as the *unique* monic polynomial of degree P such that the coefficients of z^{-1} through z^{-P} in $A_*(z)T(z)$ are all zero. In that case one can write

$$A_*(z)T(z) = 1 + z^{-P}G(z) \qquad \text{with} \qquad G(z) = \sum_{k=1}^{M} g_k z^{-k},$$

and the adaptive filter $\hat{H}(z)$ is accordingly overparameterized: the numerator and denominator orders should be $N + P$ and $M + P$ respectively, but now the first P coefficients of the denominator are fixed to zero. The degree of overparameterization should be such that $1 + z^{-P}G(z)$ is SPR, which will be the case provided that

$$P > \frac{\sqrt[M]{\rho}}{1 - \sqrt[M]{\rho}} - 2M,$$

where again ρ is an upper bound on the magnitude of the poles of $A_*(z)$ [85]. Due to the uniqueness of the overparameterization, in this case satisfaction of the SPR condition yields global parameter convergence.

In chapter 4 we present an analysis of hyperstability based algorithms using another class of overparameterized filters. This architecture is known as the *polyphase structure* and also has the property that the polynomial $T(z)$ in (1.36) is uniquely determined from $A_*(z)$. In other words, the artificial pole-zero cancellations are introduced in a structured way in order to ensure parameter convergence once the

SPR condition is satisfied. Burt and Gerken considered in [9] the use of polyphase structures for IIR filters adapted via the Output Error algorithm and observed that the cost function became better conditioned, with the corresponding improvement in convergence speed. Our goal in chapter 4 will be to investigate the SPR and persistent excitation requirements for hyperstable algorithms with polyphase filters; these results have been reported in [75]. A connection with subband adaptive filtering will also be presented.

1.4.4 Existence of stationary points in undermodeled cases

Most adaptive IIR filtering algorithms have been designed in the system identification context of Figure 1.1, and assuming that the adaptive filter is of sufficient order so that identification is achievable. Under these conditions an 'ideal' adaptive algorithm would have $\hat{H}(z) = H(z)$ as (unique) globally convergent stationary point, irrespective of the presence of output noise and the spectral characteristics of the input signal. As we have seen, no known algorithm simultaneously fulfils all these requirements.

In reduced order cases the situation becomes even more problematic: one must first isolate the set of stationary points, then determine the subset of these stationary points that are locally convergent, and then ask whether any of these convergent points provides a useful approximant to the unknown system $H(z)$. In many instances, even determining the *existence* of stationary points becomes a difficult problem of solving a set of nonlinear equations. Next we summarize what is known about the behavior of the four different approaches discussed in section 1.3 in the undermodeled case.

- The Equation Error method is a minimization criterion and therefore the stationary points correspond to the minima of the cost function. Under the monic constraint, this cost is quadratic irrespective of the order of the unknown system, and therefore uniqueness of the stationary point (which will be generally biased in the presence of noise) and local convergence are ensured. The cost function of the quadratically constrained EE approach is not quadratic; rather, it becomes a Rayleigh quotient of the form $(\mathbf{a}^T\mathbf{R}\mathbf{a})/(\mathbf{a}^T\mathbf{a})$ where $\mathbf{a}$ is the vector of coefficients of $A(z)$ and $\mathbf{R}$ is a symmetric positive definite matrix. Thus the stationary points are found to be the eigenvectors of $\mathbf{R}$ associated to the different eigenvalues. There is still a single minimum which corresponds to the smallest eigenvalue, although the remaining eigenvalues are now associated to saddle points.

  Regalia studied in [104] the approximation properties of the EE scheme in the udermodeled case. Let $\hat{H}(z)$ be the transfer function obtained by minimizing the EE cost, and assume the input $u(\cdot)$ is white and that the output noise is absent (or white for the quadratically constrained approach). If we write

$H(z) = \sum_{k=0}^{\infty} h_k z^{-k}$ and $\hat{H}(z) = \sum_{k=0}^{\infty} \hat{h}_k z^{-k}$, then under both the monic and quadratic constraints,

$$\hat{h}_k = h_k, \qquad 0 \leq k \leq N,$$

where N is the number of zeros of $\hat{H}(z)$. In addition, the quadratically constrained solution satisfies

$$\sum_{k=0}^{\infty} h_k h_{m+k} = \sum_{k=0}^{\infty} \hat{h}_k \hat{h}_{m+k}, \qquad 1 \leq m \leq M,$$

with M the number of poles of $\hat{H}(z)$. Thus both solutions interpolate the first $N+1$ coefficients of the unknown system's impulse response; in addition the quadratically constrained solution also matches the autocorrelation coefficients of lags 1 through M. These interpolation properties translate into fairly good approximation of the unknown system [104].

- The Output Error approach is also a minimization procedure, and as such the (locally convergent) stationary points correspond to the minima of the output error variance. The problem is that in general undermodeled cases, no conditions have been found in order to ensure the unimodality of this cost function. In the absence of *a priori* knowledge of the whereabouts of the global optimum, the gradient descent algorithm (1.27) could easily converge to a local minimum providing unacceptable performance.

- Hyperstable algorithms do not seek the minima of a cost function, which difficults the characterization of stationary points. In addition, the set of these points varies with the choice of the compensating filter $C(z)$ unless the input signal is white [105]. Regalia, Mboup and Ashari showed in [109] that the SHARF algorithm (1.32) admits at least a stationary point corresponding to a stable transfer function provided only that the compensating filter $C(z)$ is minimum phase and that the power spectral density of $u(\cdot)$ is nonzero and bounded for all frequencies. This stationary point will be locally convergent provided that $C(z)/A_*(z)$ is SPR, where now $A_*(z)$ is the denominator of the model obtained at the stationary point.

  What can be said about the quality of the approximants obtained at these stationary points? Regalia studied in [105, sec. 9.7] several examples and concluded that these models need not provide any useful approximation to the unknown system in terms of reduction of the output error. On the other hand, Mosquera reports in [86] good results using SHARF with experimental data in the contexts of echo cancellation and active noise control. In view of this, we believe that further research should be conducted along these lines and more experimental evidence should be gathered before discarding the hyperstable family of algorithms in undermodeled situations.

- Although the Steiglitz-McBride method does not attempt to minimize any meaningful functional either, Fan *et al.* [29, 30, 33] early observed that in many reduced order situations, the SM algorithm converged to a point very close to the global minimum of the OE cost function. This striking property was theoretically justified by Regalia and Mboup in [106] for the case of a white input $u(\cdot)$ and $N = M$. They developed an *a priori* bound for the output error variance obtained at any stationary point of the SM iteration, if one exists. This bound is related to the degree of undermodeling in the sense that if the order of the unknown system $H(z)$ is 'close' to that of the model $\hat{H}(z)$ then the resulting output error variance will be small. Existence of stationary points was addressed by Regalia, Mboup and Ashari in [108], where it is shown that for white input $u(\cdot)$ and white measurement noise $\eta(\cdot)$, the SM algorithm admits a stationary point under a mild stability condition on the unknown system $H(z)$. Although these results do not exclude the existence of settings in which the SM scheme presents several locally convergent stationary points, this is not necessarily harmful since the error bound of [106] should apply at each of them. Because of these features, the SM method is regarded as an appealing approach to adaptive IIR filtering.

It is clear that despite the considerable effort dedicated to the undermodeled system identification problem, many questions remain open. This is also the case for the channel equalization configuration of Figure 1.9, for which results are scarce. In chapter 5 the properties of a pseudolinear regression algorithm proposed for this context are examined, and it will be shown how this scheme admits a stationary point in reduced order cases.

1.4.5 Convergence rate

In adaptive FIR filtering it is well known that, for a fixed value of the stepsize, the convergence rate of the LMS algorithm slows down as the eigenvalue spread of the autocorrelation matrix of the input signal increases [46]. For adaptive IIR filters in a system identification setting, convergence speed can still be linked to the eigenvalue spread of the information matrix associated to the particular algorithm [19], but now this depends not only on the spectral characteristics of the input signal but also on the unknown system to be identified. Fan examined the effect of the location of the unknown system poles [27] and finite precision [28] in sufficient order settings, to find that local convergence speed worsens as the poles approach the unit circle. The case of poles close to $z = 1$ in the complex plane was found to be particularly problematic. The analysis also showed that adaptive normalized lattice structures are numerically more robust than direct form implementations, as in the fixed coefficient case, and that they may provide faster convergence rates.

Burt and Gerken presented in [9] a global analysis of the Output Error cost function for direct form filters, concluding that in general this cost exhibits relatively

flat regions as well as steep minima (steeper as the poles approach the unit circle). This steepness of the cost near the minima imposes a small adaptation stepsize to gradient algorithms, which in turn slows down convergence when the algorithm is traversing the flat regions. This is a fundamental limitation of constant-gain algorithms. Gauss-Newton schemes are more robust to these phenomena [27], but the associated computational loads are considerably higher. The use of polyphase structures [9] and δ-operator based filters [32] have been suggested as a means to improve convergence speed of constant-gain gradient descent algorithms. We discuss the application of the polyphase architecture and related concepts to hyperstability based algorithms in chapter 4, where its potential for faster convergence is observed. In general, the issue of convergence speed for algorithms other than gradient descent ones in reduced-order settings remains open.

1.5 Thesis outline

The main purpose of this thesis is the investigation of certain topics concerning the theory of adaptive recursive filtering. Chapter 2 presents a new look at the problem of implementing the available host of algorithms in lattice form. It will be shown that many of the existing lattice algorithms may fail to converge even in ideal scenarios, a phenomenon which will motivate the development of new lattice schemes with improved convergence properties. This new approach is fairly general and allows the translation of virtually any direct form algorithm into lattice form, and most importantly the resulting schemes can be efficiently implemented with complexity linear in the filter order. The material of this chapter can be found in [80].

Chapter 3 investigates the properties of three off-line system identification methods, which share the common feature of being iterative in nature. Each iteration is based on solving a 'distorted' Equation-Error problem, with the parameters obtained at each stage being used to distort the EE cost function in the next. As a consequence, it is of paramount importance that the model obtained at every iteration by solving the EE problem be stable. The chapter begins with a discussion of this problem, which appeared in [74].

The first off-line scheme considered is the Steiglitz-McBride method. The lattice variant of this method [103] overcomes the problem of finding an unstable intermediate transfer function along the iteration, and its fixed points are known to be the same as those of the direct form off-line version. We show, however, that the convergence properties of the two variants may be quite different. This phenomenon was originally reported in [78].

Next, the properties of the Interpolation Expanded Numerator (IXN) method are revised. It will be shown that the uniqueness of the fixed point of this scheme in sufficient order cases, which was known to hold in the white input case, is also preserved for certain colored inputs. The implementation of on-line algorithms

based on the IXN concept is also discussed. This part is based on results originally published in [77].

To close the chapter a third off-line scheme, the Steiglitz-McBride/Expanded Numerator (SM/XN) method, is presented and analyzed in depth. Conditions are given for the uniqueness of the SM/XN stationary point in system identification settings. An on-line implementation of the SM/XN algorithm is presented.

Chapter 4 presents two novel implementations of hyperstability based adaptive algorithms which have the purpose of relaxing the SPR condition underlying these schemes. The first one is a polyphase implementation of the adaptive filter, while the second involves subband filtering and decimation of the input and reference signals. Some of the results in this chapter can be found in [75].

In Chapter 5 we consider in depth the adaptive IIR filtering problem in the context of channel equalization, analyzing the convergence properties of two candidate algorithms which can be related to the Output Error method and the pseudolinear regression approach. The quality of the solutions in the general case is also examined. These results have been reported in [79].

Finally, conclusions are presented in Chapter 6 together with several open research lines that arise from our work.

Chapter 2

STABILIZATION OF ADAPTIVE LATTICE IIR FILTERING ALGORITHMS

In this chapter we examine the convergence properties of several adaptive algorithms for lattice filters that have been proposed in the literature. Because the development of many of these algorithms introduced certain approximations, this convergence analysis is not a trivial extension of the direct form variant. As such, it has remained an open problem despite the fact that simulation evidence led researchers to believe that the set of convergent points of these simplified lattice schemes coincide (in transfer function space) with those of the corresponding direct form versions. Furthermore, in some cases the approximations introduced seemed to yield faster convergence relative to the 'full' (i.e. nonsimplified) versions. In any case, no theoretical analysis of the convergence properties of these lattice algorithms is available to support these empirical observations.

The purpose of this work is twofold: to show that many lattice algorithms may fail to converge, and to devise new schemes to avoid this problem. It is shown that in identification settings (in which the order of the adaptive filter $\hat{H}(z)$ matches that of the unknown system $H(z)$) there exist situations in which the stationary point $\hat{H}(z) = H(z)$ corresponding to the identification of the unknown system is not attractive for the simplified lattice schemes. This constitutes a clear drawback for these methods: if an algorithm does not prove reliable in an identification experiment with an ideal environment (model order matching and absence of noise), it will be very unlikely to perform well under more realistic conditions including model order mismatch and signal disturbances.

We also develop new algorithms based in the cascade lattice structure, which can be implemented with complexity linear in the filter order. The approach is quite general and can be applied to any direct-form adaptive algorithm in order to obtain a useful lattice variant, thus facilitating algorithm design. In addition, and most importantly, sufficient conditions are given that ensure the stability of stationary points in the sufficient order case. Hence the new algorithms provide both theoretical and practical advantages over existing schemes.

The main tool in our analysis is the ordinary differential equation (ODE) method

[26]. The basic idea of this approach is to link the discrete-time adaptive algorithm to a continuous-time ODE in such a way that the convergence behavior of the algorithm can be related in some probabilistic sense to the stability properties of the ODE. Consider the general form (1.33) of constant-gain adaptive algorithms, repeated here for convenience:

$$\theta(n+1) = \theta(n) + \mu \mathbf{x}(n) e(n). \tag{2.1}$$

Under some general conditions, the ODE method ensures convergence in mean to the solution of the following differential equation as the stepsize μ tends to zero:

$$\dot{\theta}(t) = E[\mathbf{x}(n)e(n)]\Big|_{\theta=\theta(t)} \tag{2.2}$$

The expectation in (2.2) is taken assuming that the adaptive filter parameters are fixed at $\theta = \theta(t)$. If the signals $\mathbf{x}(\cdot)$ and $e(\cdot)$ are jointly stationary, this expectation becomes independent of n although it remains a function of θ. Thus for sufficiently slow adaptation, the parameter trajectories of the algorithm approach asymptotically stationary random variables, whose mean values correspond to an attractive equilibrium point of the ODE (2.2).

Direct analysis of (2.2) is usually difficult because this ODE is highly nonlinear, and often one has to resort to local linearization in order to obtain a more tractable problem. Let θ_* be a stationary point of (2.1), which means that θ_* is also an equilibrium of the associated ODE. Then (2.2) can be linearized in a neighborhood of θ_*, yielding

$$\dot{\theta}(t) \approx \left.\frac{\mathrm{d}E[\mathbf{x}(n)e(n)]}{\mathrm{d}\theta}\right|_{\theta=\theta_*} \cdot [\theta(t) - \theta_*] = \mathbf{S}(\theta_*) \cdot [\theta(t) - \theta_*]. \tag{2.3}$$

From this, the stationary point θ_* is seen to be locally attractive if and only if all the eigenvalues of the feedback matrix $\mathbf{S}(\theta_*)$ have negative real parts (in which case we say that $\mathbf{S}(\theta_*)$ is *stable*). In that case, θ_* is a locally convergent stationary point of the adaptive algorithm (2.1).

The ODE approach is valid for any filter parameterizatrion, although in general the differential equations obtained will be different for different structures. We shall exploit a link between the feedback matrices corresponding to the ODEs for the direct-form and lattice schemes in order to derive the new adaptive algorithms.

The rest of the chapter is organized as follows. Section 2.1 provides the machinery needed to set up the problem. The general lattice algorithm structure and its particularizations (EE, OE, SM and SHARF) are presented in section 2.2. The general convergence analysis is developed in section 2.3, while in section 2.4 the new algorithms and their properties are presented. Simulation results are given in section 2.5.

2.1 Preliminaries

Let the transfer function of the adaptive filter be

$$\hat{H}(z) = \frac{B(z)}{A(z)} = \frac{b_0 + b_1 z^{-1} + \cdots + b_N z^{-N}}{1 + a_1 z^{-1} + \cdots + a_M z^{-M}}. \tag{2.4}$$

We designate the vector of direct-form parameters by

$$\theta_d = \left[\, b_0 \ \cdots \ b_N \ a_1 \ \cdots \ a_M \,\right]^T. \tag{2.5}$$

The subscript d in θ_d stands for 'direct form'. Similarly we shall denote the vector of lattice parameters by θ_l, with an additional label depending on whether we refer to the cascade or to the tapped-state lattice architectures respectively (refer to section 1.2.3 for a description of these structures):

$$\theta_{l,c} = [\, b_0 \ \cdots \ b_N \ \sin\phi_1 \ \cdots \ \sin\phi_M \,]^T, \tag{2.6}$$

$$\theta_{l,ts} = [\, \nu_0 \ \cdots \ \nu_N \ \sin\phi_1 \ \cdots \ \sin\phi_M \,]^T. \tag{2.7}$$

When the symbol θ is used without a subscript, it is meant to represent the actual transfer function $\hat{H}(z)$. A matrix which will be of particular interest to us is the Jacobian $\mathbf{D}(\theta)$, whose i, jth element is $\partial a_i / \partial \sin\phi_j$. An efficient algorithm for the computation of this matrix based on the Schur-Cohn recursion is given in appendix A. The matrices $\mathbf{L}_k(\theta)$ and $\mathbf{\Gamma}_k(\theta)$ introduced in (1.19)-(1.21) will also be useful. As a consequence of the one-to-one correspondence between the direct-form parameters a_i and the reflection coefficients $\sin\phi_j$ in the stability region $\{\theta \ : \ |\phi_k| < \frac{\pi}{2}, \ 1 \le k \le M\}$, for θ in this set the matrices $\mathbf{D}(\theta)$, $\mathbf{L}_k(\theta)$, $\mathbf{\Gamma}_k(\theta)$ are nonsingular.

Defining the map from the lattice parameters to the direct form coefficients as $\theta_d = f(\theta_l)$, then the Jacobian matrix $\mathbf{F}(\theta) = \mathrm{d}f(\theta_l)/\mathrm{d}\theta_l$ is given for the cascade and tapped-state structures respectively by

$$\mathbf{F}(\theta) = \begin{bmatrix} \mathbf{I}_{N+1} & \mathbf{0} \\ \mathbf{0} & \mathbf{D}(\theta) \end{bmatrix} = \mathbf{F}_c(\theta), \tag{2.8}$$

$$\mathbf{F}(\theta) = \begin{bmatrix} \mathbf{L}_N^T(\theta)\mathbf{\Gamma}_N^T(\theta) & \mathbf{C}(\theta) \\ \mathbf{0} & \mathbf{D}(\theta) \end{bmatrix} = \mathbf{F}_{ts}(\theta), \tag{2.9}$$

where $\mathbf{C}(\theta)$ is an $(N+1) \times M$ matrix with the i, jth element given by $\partial b_i / \partial \sin\phi_j$, $0 \le i \le N$, $1 \le j \le M$. For example if $N = 0$ then, using $b_0 = \nu_0\gamma_0$, one obtains

$$\mathbf{C}(\theta) = -\nu_0\gamma_0 \left[\frac{\sin\phi_1}{\cos^2\phi_1} \ \cdots \ \frac{\sin\phi_M}{\cos^2\phi_M} \right]. \tag{2.10}$$

2.2 Algorithm formulation

The four direct-form algorithms for updating θ_d discussed in section 1.3 have the form

$$\theta_d(n+1) = \theta_d(n) + \mu \mathbf{x}_d(n) e(n), \tag{2.11}$$

where $e(\cdot)$ is some error signal and $\mathbf{x}_d(\cdot)$ is a driving vector sequence, which can be written as

$$\mathbf{x}_d(n) = \begin{bmatrix} \mathbf{v}_d(n) \\ \mathbf{w}_d(n) \end{bmatrix}$$

where

$$\mathbf{v}_d(n) = \begin{bmatrix} 1 \\ z^{-1} \\ \vdots \\ z^{-N} \end{bmatrix} v(n), \qquad \mathbf{w}_d(n) = \begin{bmatrix} z^{-1} \\ z^{-2} \\ \vdots \\ z^{-M} \end{bmatrix} \frac{1}{A(z)} w(n),$$

for some signals $v(\cdot)$, $w(\cdot)$. Different choices for $v(\cdot)$, $w(\cdot)$ and $e(\cdot)$ give rise to different adaptive algorithms.

Several authors have attempted to reformulate the direct form update (2.11) in terms of the lattice parameters θ_l. The resulting lattice algorithms have a generic structure resembling (2.11), namely

$$\theta_l(n+1) = \theta_l(n) + \mu \mathbf{x}_l(n) e(n). \tag{2.12}$$

While $e(\cdot)$ is usually the same as in (2.11), it is the choice of $\mathbf{x}_l(\cdot)$ that characterizes the transition from (2.11) to (2.12). In most cases the vectors $\mathbf{x}_d$ and $\mathbf{x}_l$ are related via

$$\mathbf{x}_l(n) = \begin{bmatrix} \mathbf{v}_l(n) \\ \mathbf{w}_l(n) \end{bmatrix} = \mathbf{R}(\theta(n)) \mathbf{x}_d(n) \tag{2.13}$$

for some matrix $\mathbf{R}(\theta)$. Next, we briefly review the four direct form algorithms and their lattice counterparts in order to examine the particular values of $v(\cdot)$, $w(\cdot)$, $e(\cdot)$ and $\mathbf{R}(\theta)$. As usual, $u(\cdot)$ and $\hat{y}(\cdot)$ will denote respectively the adaptive filter input and output, so that $\hat{y}(n) = \hat{H}(z)u(n)$, and $d(\cdot)$ will denote the reference signal.

2.2.1 Equation-error algorithms

For the direct-form equation-error algorithm (1.30), one has

$$v(n) = u(n), \qquad w(n) = -A(z)d(n), \tag{2.14}$$

and $e(n) = A(z)d(n) - B(z)u(n) = e_e(n)$, the equation error. Recall that this algorithm is simply a stochastic gradient descent of the cost $E[e_e^2(n)]$.

Two lattice variants of the EE method have been proposed. The first one was suggested in [76] for a cascade lattice structure, so that θ_l is given by (2.6). It

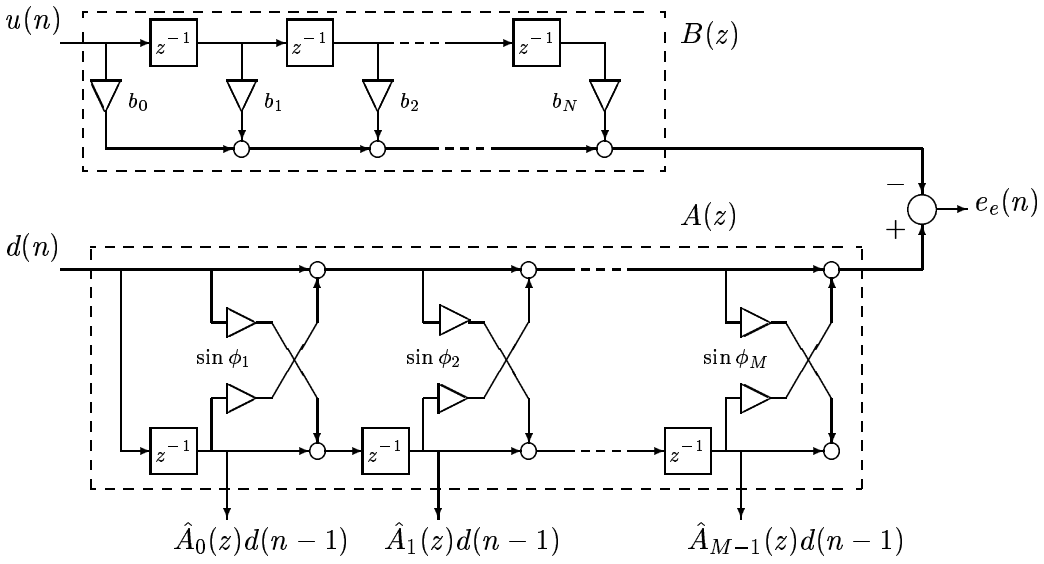

Figure 2.1: Equation-error lattice configuration.

used $\mathbf{v}_l(n) = \mathbf{v}_d(n)$ while $\mathbf{w}_l(\cdot)$ was taken as the state vector of an FIR lattice with transfer function $A(z)$ driven by the reference signal $d(\cdot)$, yielding

$$\mathbf{w}_l(n) = -\begin{bmatrix} \hat{A}_0(z) \\ \vdots \\ \hat{A}_{M-1}(z) \end{bmatrix} z^{-1}d(n).$$

[Recall the definition of the polynomials $\hat{A}_k(z)$ in (1.18)]. This is illustrated in Figure 2.1. Thus for this algorithm, which we term Equation-error Lattice version 1, or EEL-1 for short, the matrix $\mathbf{R}(\theta)$ is given by

$$\mathbf{R}(\theta) = \begin{bmatrix} \mathbf{I}_{N+1} & \mathbf{0} \\ \mathbf{0} & \mathbf{L}_{M-1}(\theta) \end{bmatrix}. \tag{2.15}$$

The second variant, EEL-2, appeared in [92] where it was suggested to use the same driving vector as in the direct form parameter update, i.e. $\mathbf{x}_l(n) = \mathbf{x}_d(n)$. Therefore, for EEL-2, one simply has

$$\mathbf{R}(\theta) = \mathbf{I}_{N+M+1}. \tag{2.16}$$

2.2.2 Output-error algorithms

For the direct form output-error algorithm (1.27), the signals $v(\cdot)$, $w(\cdot)$ are given by

$$v(n) = \frac{1}{A(z)}u(n), \qquad w(n) = -\frac{B(z)}{A(z)}u(n) = -\hat{y}(n), \tag{2.17}$$

and $e(n) = d(n) - \hat{y}(n) = e_o(n)$, the output error. In this way, one has $\mathbf{x}_d(n) = -\nabla_{\theta_d} e_o(n) = -(\mathrm{d}e_o(n)/\mathrm{d}\theta_d)^T$ [113].

Three different schemes for efficient lattice implementation of the output error method can be found in the literature. The first one appeared in [110] and considered a two-multiplier lattice; its extension to the tapped-state normalized form can be found in [105, section 7.5]. The resulting algorithm computes the driving vector by means of

$$\mathbf{x}_l(n) = -\nabla_{\theta_l} e_o(n) = \mathbf{F}_{ts}^T(\theta)\mathbf{x}_d(n), \tag{2.18}$$

with θ_l and $\mathbf{F}_{ts}(\theta)$ given by (2.7) and (2.9) respectively. This algorithm effectively performs a gradient descent of the cost $E[e_o^2(n)]$ in the lattice parameter space, so we refer to it as Gradient Lattice (GL). Thus for GL, $\mathbf{R}(\theta) = \mathbf{F}_{ts}^T(\theta)$.

The second variant (Partial Gradient Lattice or PGL) was presented in [105, section 7.6]. Still using the tapped-state structure, the reflection coefficients $\sin\phi_k$ are adjusted as though the tap parameters ν_k were optimized. This assumption results in the following transformations:

$$\begin{aligned}\mathbf{v}_l(n) &= \begin{bmatrix} \frac{\partial e(n)}{\partial \nu_0} \\ \vdots \\ \frac{\partial e(n)}{\partial \nu_N} \end{bmatrix} = \mathbf{\Gamma}_N(\theta)\mathbf{L}_N(\theta)\mathbf{v}_d(n), \\ \mathbf{w}_l(n) &= \mathbf{D}^T(\theta)\mathbf{w}_d(n).\end{aligned}$$

Consequently the matrix $\mathbf{R}(\theta)$ for PGL is given by

$$\mathbf{R}(\theta) = \begin{bmatrix} \mathbf{\Gamma}_N(\theta)\mathbf{L}_N(\theta) & \mathbf{0} \\ \mathbf{0} & \mathbf{D}^T(\theta) \end{bmatrix}. \tag{2.19}$$

Further approximations in the PGL parameter update led to the Simplified Partial Gradient Lattice (SPGL) algorithm, developed in [103] and [105, section 7.7]. While $\mathbf{v}_l(\cdot)$ is obtained in the same way as for GL and PGL, $\mathbf{w}_l(\cdot)$ is taken as the state vector of an all-pole lattice with transfer function $1/A(z)$ driven by the adaptive filter output $\hat{y}(\cdot)$:

$$\begin{aligned}\mathbf{w}_l(n) &= -\begin{bmatrix} \gamma_0^2 \frac{\hat{A}_0(z)}{A(z)} \\ \vdots \\ \gamma_{M-1}^2 \frac{\hat{A}_{M-1}(z)}{A(z)} \end{bmatrix} z^{-1}\hat{y}(n) \\ &= \mathbf{\Gamma}_{M-1}^2(\theta)\mathbf{L}_{M-1}(\theta)\mathbf{w}_d(n).\end{aligned}$$

Figure 2.2 illustrates the generation of these signals. The corresponding matrix $\mathbf{R}(\theta)$ for the SPGL algorithm is then

$$\mathbf{R}(\theta) = \begin{bmatrix} \mathbf{\Gamma}_N(\theta)\mathbf{L}_N(\theta) & \mathbf{0} \\ \mathbf{0} & \mathbf{\Gamma}_{M-1}^2(\theta)\mathbf{L}_{M-1}(\theta) \end{bmatrix}. \tag{2.20}$$

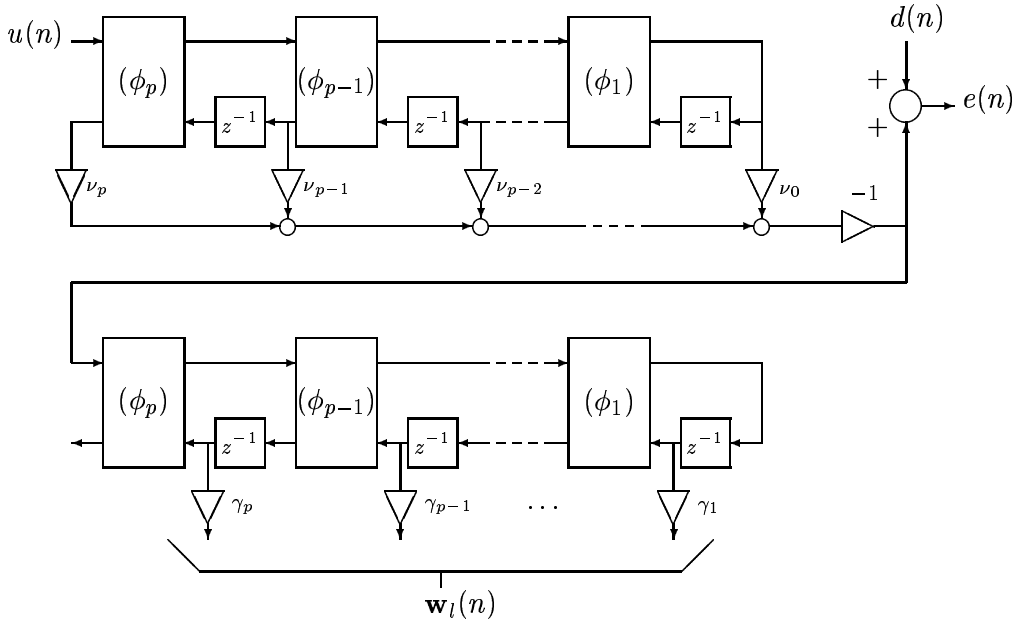

Figure 2.2: Generation of the driving vector in the SPGL algorithm ($p = \max\{N, M\}$).

Finally, an algorithm similar in spirit to SPGL but using the cascade structure was presented in [84]; the corresponding $\mathbf{R}(\theta)$ coincides with that of EEL-1, given in (2.15).

2.2.3 Steiglitz-McBride method

For the direct-form Steiglitz-McBride algorithm (1.31), one has

$$v(n) = \frac{1}{A(z)}u(n), \quad w(n) = -d(n), \quad e(n) = d(n) - \hat{y}(n) = e_o(n).$$

A lattice variant appeared in [103], using the tapped-stated normalized structure. Generation of $\mathbf{w}_l(\cdot)$ is done as shown in Figure 2.2 but driving the postfilter with the reference signal $-d(n)$ rather than the adaptive filter output $-\hat{y}(n)$. The corresponding transformation from $\mathbf{x}_d$ to $\mathbf{x}_l$ is the same as that for SPGL:

$$\begin{aligned}\mathbf{v}_l(n) &= \mathbf{\Gamma}_N(\theta)\mathbf{L}_N(\theta)\mathbf{v}_d(n),\\ \mathbf{w}_l(n) &= \mathbf{\Gamma}^2_{M-1}(\theta)\mathbf{L}_{M-1}(\theta)\mathbf{w}_d(n).\end{aligned}$$

From these, the matrix $\mathbf{R}(\theta)$ is seen to be the same for the Steiglitz-McBride Lattice (SML) and for the SPGL algorithms, and it is given in (2.20). Similarly, [84] considered a cascade structure using $\mathbf{v}_l(n) = \mathbf{v}_d(n)$, $\mathbf{w}_l(n) = \mathbf{L}_{M-1}(\theta)\mathbf{w}_d(n)$, so that the corresponding $\mathbf{R}(\theta)$ is as in (2.15).

2.2.4 Hyperstability based algorithms

For the direct-form SHARF algorithm (1.32), one has

$$v(n) = u(n), \qquad w(n) = -B(z)u(n) = -A(z)\hat{y}(n), \tag{2.21}$$

and $e(n) = C(z)[y(n) - \hat{y}(n)]$, with $C(z)$ the compensating filter. A cascade lattice version of SHARF (LSHARF) appeared in [84]. It uses $\mathbf{v}_l(n) = \mathbf{v}_d(n)$, and $\mathbf{w}_l(n)$ is taken as the (scaled) state vector of the adaptive filter denominator block. This is illustrated in Figure 2.3. The corresponding transformation is given by

$$\mathbf{w}_l(n) = -\begin{bmatrix} \hat{A}_0(z) \\ \vdots \\ \hat{A}_{M-1}(z) \end{bmatrix} z^{-1}\hat{y}(n) = \mathbf{L}_{M-1}(\theta)\mathbf{w}_d(n).$$

Therefore the matrix $\mathbf{R}(\theta)$ for LSHARF is as in (2.15).

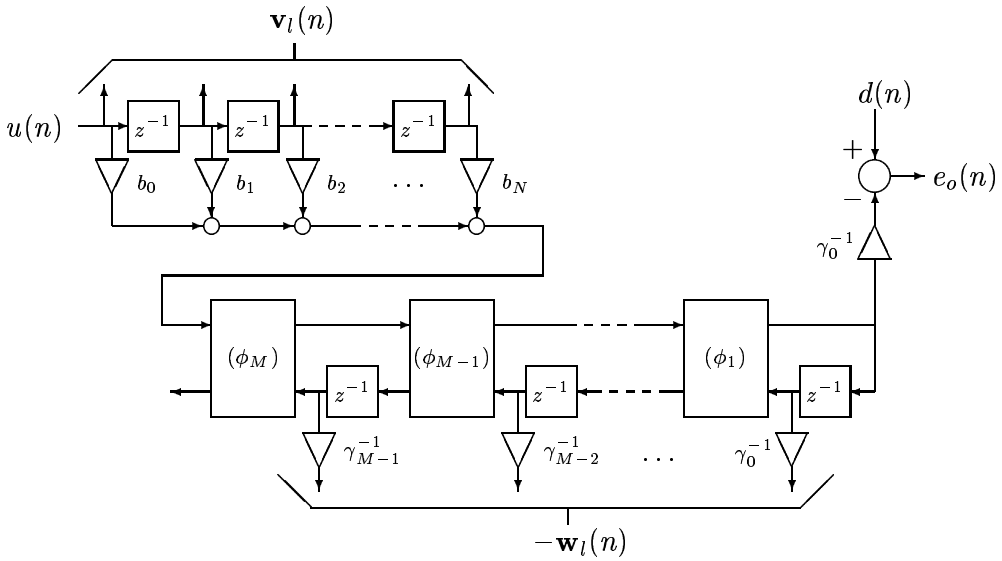

Figure 2.3: Generation of the driving vector in the LSHARF algorithm.

2.3 Analysis of lattice algorithms

In this section we present an analysis of the general lattice algorithm (2.12), in terms of stationary points and local convergence properties. Our approach is based on the relation of these properties to those of the corresponding direct-form algorithm from which the lattice version was derived.

First, consider the set of stationary points of (2.12). These points θ_{l*} are those for which the expectation of the update term vanishes. Using (2.13), one obtains

$$E[\mathbf{x}_l(n)e(n)]\Big|_{\theta_{l*}} = \mathbf{0} \quad \Rightarrow \quad \mathbf{R}(\theta_*)E[\mathbf{x}_d(n)e(n)]\Big|_{\theta_{d*}} = \mathbf{0}, \tag{2.22}$$

where $\theta_{d*} = f(\theta_{l*})$ is the stationary point in direct form parameter space. If $\mathbf{R}(\theta_*)$ is nonsingular, as is the case for all the algorithms presented in section 2.2, then (2.22) shows that θ_{l*} is a stationary point of (2.12) if and only if θ_{d*} is a stationary point of (2.11). Therefore the stationary points of the lattice variants coincide (in transfer function space) with those of their direct-form counterparts, as claimed in [76, 84, 92, 103].

For local convergence analysis, we resort to the ODE method. The stationary point of the lattice algorithm, θ_{l*}, is locally attractive if and only if the feedback matrix

$$\mathbf{S}_l(\theta_*) = \left.\frac{\mathrm{d}E[\mathbf{x}_l(n)e(n)]}{\mathrm{d}\theta_l}\right|_{\theta_{l*}} \tag{2.23}$$

is stable. Similarly, the stationary point of the direct form algorithm, θ_{d*}, is locally attractive if and only if the feedback matrix

$$\mathbf{S}_d(\theta_*) = \left.\frac{\mathrm{d}E[\mathbf{x}_d(n)e(n)]}{\mathrm{d}\theta_d}\right|_{\theta_{d*}} \tag{2.24}$$

is stable. The connection between these matrices is shown in the following result.

Lemma 2.1. *Let θ_* be a stationary point (in transfer function space) of the algorithms (2.11)-(2.12), and let $\mathbf{S}_l(\theta_*)$ and $\mathbf{S}_d(\theta_*)$ be the feedback matrices of the corresponding linearized ODEs as given in (2.23)-(2.24). Then*

$$\mathbf{S}_l(\theta_*) = \mathbf{R}(\theta_*)\mathbf{S}_d(\theta_*)\mathbf{F}(\theta_*), \tag{2.25}$$

where $\mathbf{R}(\theta_*)$ is given by (2.13), and the Jacobian matrix

$$\mathbf{F}(\theta_*) = \left.\frac{\mathrm{d}f(\theta_l)}{\mathrm{d}\theta_l}\right|_{\theta_l=\theta_{l*}}$$

is given by (2.8) or (2.9).

The proof is given in appendix B. Lemma 2.1 provides the crucial link between the convergence properties of the lattice algorithm and those of the corresponding direct-form version. When (2.25) is particularized to the lattice algorithms of section 2.2, one cannot in general conclude anything about the eigenvalue behavior of $\mathbf{S}_l(\theta_*)$. That is, even if it is known that the stationary point θ_{d*} is locally attractive for the direct-form algorithm (2.11), whether the same will be true for the lattice version is not clear since the transformation (2.25) does not necessarily preserve the sign

of the real parts of the eigenvalues. Indeed, examples will be given in section 2.5 showing that the transformation (2.25) may result in an unstable $\mathbf{S}_l(\theta_*)$ starting with a stable $\mathbf{S}_d(\theta_*)$. The only exception is the GL algorithm, for which

$$\mathbf{S}_l(\theta_*) = \mathbf{F}_{ts}^T(\theta_*)\mathbf{S}_d(\theta_*)\mathbf{F}_{ts}(\theta_*). \tag{2.26}$$

Since the direct-form output error and the GL algorithms are just gradient descents of the same cost function, $\mathbf{S}_d(\theta_*)$ and $\mathbf{S}_l(\theta_*)$ are simply the negative Hessian matrices of this cost in terms of θ_d and θ_l respectively. Therefore they are symmetric, and (2.26) shows that $\mathbf{S}_d(\theta_*) < \mathbf{0} \Leftrightarrow \mathbf{S}_l(\theta_*) < \mathbf{0}$, which happens if θ_* is a minimum of the cost function.

Note that should one choose $\mathbf{R}(\theta) = \mathbf{F}^{-1}(\theta)$, then $\mathbf{S}_l(\theta_*)$ and $\mathbf{S}_d(\theta_*)$ would be similar, and therefore they would have the same eigenvalues. Thus, the local convergence properties of stationary points would be the same for the two parameterizations. The main obstacle to such an approach is the transformation $\mathbf{x}_l(n) = \mathbf{F}^{-1}(\theta(n))\mathbf{x}_d(n)$ which requires the computation and inversion of the Jacobian matrix $\mathbf{F}(\theta)$. A lattice algorithm using this scheme would be computationally expensive. In the next section we consider a different approach, which can be thought of as the next best thing to a similarity transformation: a *congruence* transformation.

2.4 New lattice algorithms

The transition from the direct-form algorithms (2.11) to lattice versions (2.12) that we propose is characterized by the following.

1. We use the cascade normalized lattice structure of Figure 1.12. Thus the parameter vector θ_l will be given by (2.6).
2. We have the following choice for the driving vector $\mathbf{x}_l(n)$:

$$\mathbf{x}_l(n) = \mathbf{F}_c^T(\theta(n))\mathbf{x}_d(n). \tag{2.27}$$

This can be applied to any of the approaches in section 2.2. Next, we show how these algorithms can be implemented. A convergence analysis is then presented.

2.4.1 Implementation

Efficient implementation of the new lattice variant is considerably facilitated by the use of the cascade (as opposed to the tapped-state) lattice structure. For this configuration $\mathbf{F}(\theta) = \mathbf{F}_c(\theta)$ is given in (2.8), so that $\mathbf{x}_l(n)$ can be generated as follows. First, one has

$$\mathbf{v}_l(n) = \mathbf{v}_d(n). \tag{2.28}$$

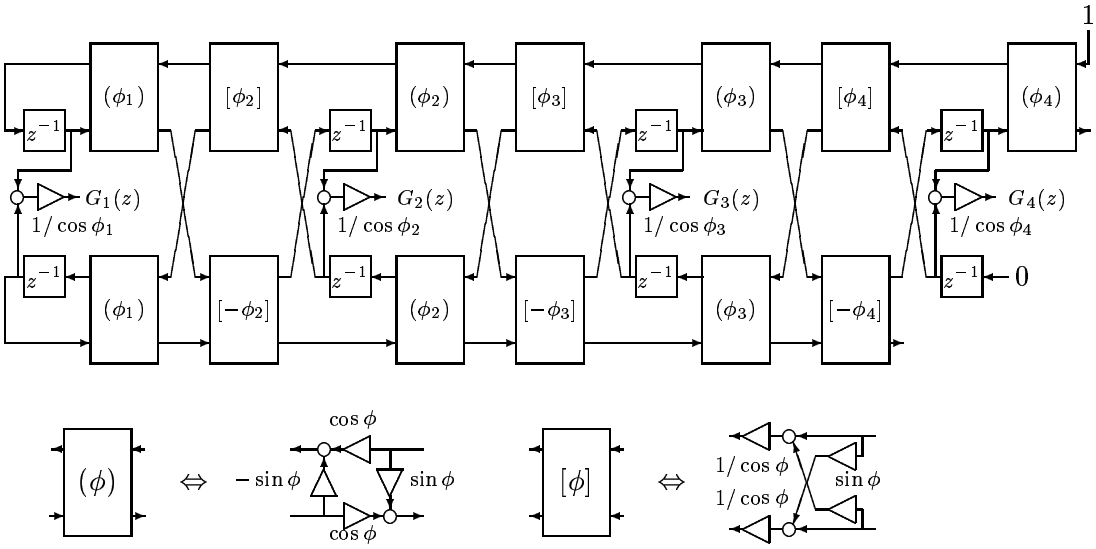

Figure 2.4: Generation of the transfer functions $G_k(z)$ for $M = 4$.

On the other hand, $\mathbf{w}_l(n)$ is computed now by means of

$$\begin{aligned}\mathbf{w}_l(n) &= \mathbf{D}^T(\theta)\mathbf{w}_d(n) \\ &= \begin{bmatrix} \frac{\partial a_1}{\partial \sin\phi_1} & \cdots & \frac{\partial a_M}{\partial \sin\phi_1} \\ \vdots & & \vdots \\ \frac{\partial a_1}{\partial \sin\phi_M} & \cdots & \frac{\partial a_M}{\partial \sin\phi_M} \end{bmatrix} \begin{bmatrix} z^{-1} \\ \vdots \\ z^{-M} \end{bmatrix} \frac{1}{A(z)} w(n) \\ &= \begin{bmatrix} \frac{\partial A(z)}{\partial \sin\phi_1} & \cdots & \frac{\partial A(z)}{\partial \sin\phi_M} \end{bmatrix}^T \frac{1}{A(z)} w(n). \end{aligned} \tag{2.29}$$

Therefore we need an efficient realization of the transfer functions

$$G_k(z) = \frac{1}{A(z)} \frac{\partial A(z)}{\partial \sin\phi_k}, \quad 1 \le k \le M. \tag{2.30}$$

A structure that performs this task with complexity linear in M was developed in [105, section 7.6.2] in order to generate the driving vector of the PGL algorithm. This structure is depicted in Figure 2.4 for the case $M = 4$. In this way, with a secondary lattice $\mathbf{G}(z) = [\, G_1(z) \cdots G_M(z) \,]^T$ fed with the signal $w(\cdot)$ corresponding to the direct-form scheme used as starting point, the new lattice algorithms can be efficiently implemented.

2.4.2 Convergence analysis

As noted before, $\mathbf{F}_c(\theta)$ is nonsingular for all θ corresponding to stable transfer functions. Therefore,

$$E[\mathbf{x}_l(n)e(n)]_{\theta_*} = \mathbf{0} \quad \Leftrightarrow \quad \mathbf{F}_c^T(\theta_*)E[\mathbf{x}_d(n)e(n)]_{\theta_*} = \mathbf{0} \quad \Leftrightarrow \quad E[\mathbf{x}_d(n)e(n)]_{\theta_*} = \mathbf{0}.$$

Thus, the set of stationary points of any of the direct-form algorithms coincides with that of the corresponding lattice version, a feature shared with the variants of section 2.2. On the other hand, by virtue of our choice $\mathbf{R}(\theta) = \mathbf{F}_c^T(\theta)$ and Lemma 2.1, the feedback matrix $\mathbf{S}_l(\theta_*)$ is given now by

$$\mathbf{S}_l(\theta_*) = \mathbf{F}_c^T(\theta_*)\mathbf{S}_d(\theta_*)\mathbf{F}_c(\theta_*), \tag{2.31}$$

so that $\mathbf{S}_l(\theta_*)$ and $\mathbf{S}_d(\theta_*)$ are congruent. Due to this fact, sufficient conditions for local stability can be given.

Lemma 2.2. *Let θ_{l*} be a stationary point of the lattice algorithm (2.12), using the cascade lattice structure and with $\mathbf{x}_l(n)$ generated via (2.27). Also let $\theta_{d*} = f(\theta_{l*})$. If the symmetric matrix $\mathbf{S}_d(\theta_{d*}) + \mathbf{S}_d^T(\theta_{d*})$ is negative definite, then θ_{l*} is locally attractive.*

Proof: Recall that $\mathbf{A} + \mathbf{A}^T < \mathbf{0}$ implies $\mathbf{A}$ stable [63]. As $\mathbf{S}_d(\theta_{d*})$ and $\mathbf{S}_l(\theta_{l*})$ are congruent, $\mathbf{S}_d(\theta_{d*}) + \mathbf{S}_d^T(\theta_{d*}) < \mathbf{0}$ implies $\mathbf{S}_l(\theta_{l*}) + \mathbf{S}_l^T(\theta_{l*}) < \mathbf{0}$ so that $\mathbf{S}_l(\theta_{l*})$ is a stable matrix. ■

Having the symmetric part of $\mathbf{S}_d(\theta_{d*})$ negative definite is a sufficient condition for $\mathbf{S}_d(\theta_{d*})$ to be stable, but by no means necessary. Nevertheless, Lemma 2.2 has immediate application to the new lattice version of the adaptive methods of section 2.2, as summarized next.

1. *Equation-error method:* The direct-form EE algorithm is a gradient descent for the cost $E[e_e^2(n)]$ with $e_e(n)$ the equation error. This cost is quadratic in θ_d, so that there exists a single minimum θ_{d*} which is an attractive stationary point; $\mathbf{S}_d(\theta_*)$ is just the negative of the Hessian of the cost, and in view of Lemma 2.2, the corresponding stationary point θ_{l*} of the new lattice variant is locally stable. Alternatively, this lattice version performs a gradient descent on the cost $E[e_e^2(n)]$ in the space of the cascade lattice parameters.

2. *Output-error method:* Similarly, when applied to the OE scheme, the new lattice variant reduces to a gradient descent on the cost $E[e_o^2(n)]$, where $e_o(n)$ is the output error, in the space of the cascade lattice parameters. The relation (2.31) simply shows how the Hessian matrices relate to each other when moving from the direct-form to the cascade lattice parameter space. Thus, a stationary point θ_{l*} of the lattice algorithm is locally stable if and only if it furnishes an external transfer function corresponding to a (local) minimum of the cost function.

3. *Steiglitz-McBride method:* Consider the sufficient order case, in which the reference signal $d(\cdot)$ is given by

$$d(n) = H(z)u(n) + \eta(n) \tag{2.32}$$

where as usual $\eta(\cdot)$ is the output noise, and $H(z)$ is a transfer function with at most N zeros and M poles. It is known that in that case, the direct-form Steiglitz-McBride algorithm has a single possible stationary point θ_* which is attractive, corresponding to $\hat{H}(z) = H(z)$, provided that the input $u(\cdot)$ is persistently exciting and that $\eta(\cdot)$ is white [121]. The matrix $\mathbf{S}_d(\theta_*)$ is seen to be given by

$$\begin{aligned}\mathbf{S}_d(\theta_*) &= E\left[\frac{\mathrm{d}\mathbf{x}_d(n)}{\mathrm{d}\theta_d}e_o(n)\right]_{\theta_*} + E\left[\mathbf{x}_d(n)\frac{\mathrm{d}e_o(n)}{\mathrm{d}\theta_d}\right]_{\theta_*} \\ &= E\left[\left.\frac{\mathrm{d}\mathbf{x}_d(n)}{\mathrm{d}\theta_d}\right|_{\theta_*}\eta(n)\right] - E\left[\nabla_{\theta_d}e_o(n)\nabla_{\theta_d}^T e_o(n)\right]_{\theta_*}\end{aligned} \tag{2.33}$$

where use has been made of the fact that, at the stationary point θ_*, one has $\hat{y}(n) = H(z)u(n)$, so that the output error and the driving vector reduce to $e_o(n) = \eta(n)$ and $\mathbf{x}_d(n) = -\nabla_{\theta_d}e_o(n)$ respectively. The first term in the right-hand side of (2.33) vanishes if the noise $\eta(\cdot)$ is white, so that $\mathbf{S}_d(\theta_*)$ coincides with the negative of the Hessian of the output-error cost $E[e_o^2(n)]$ at θ_{d*}, which is a minimum. Then applying Lemma 2.2, we conclude that in sufficient order settings with white disturbances, the new lattice variant of the Steiglitz-McBride algorithm has a single stationary point, which is locally attractive, corresponding to $\hat{H}(z) = H(z)$.

On the other hand, it is not possible to establish such a link between the $\mathbf{S}_d$ matrices of the direct-form Steiglitz-McBride and output-error algorithms in undermodeled scenarios. Extensive simulation evidence suggests that even in reduced order cases, a stable $\mathbf{S}_d(\theta_*)$ translates into a stable $\mathbf{S}_l(\theta_*)$, although a formal proof of this statement is not available at this time.

4. *SHARF algorithm:* Consider again a sufficient order setting as in (2.32), and let $A_*(z)$ be the denominator of the system $H(z)$ to be identified. Then the direct-form SHARF algorithm has a single stationary point θ_* corresponding to $\hat{H}(z) = H(z)$, which is stable provided that the input is persistently exciting and that the transfer function $C(z)/A_*(z)$ is SPR. Moreover, the matrix $\mathbf{S}_d(\theta_*)$ at this stationary point is given by

$$\begin{aligned}\mathbf{S}_d(\theta_*) &= E\left[\frac{\mathrm{d}\mathbf{x}_d(n)}{\mathrm{d}\theta_d}e_o(n)\right]_{\theta_*} + E\left[\mathbf{x}_d(n)\frac{\mathrm{d}e_o(n)}{\mathrm{d}\theta_d}\right]_{\theta_*} \\ &= E\left[\left.\frac{\mathrm{d}\mathbf{x}_d(n)}{\mathrm{d}\theta_d}\right|_{\theta_*}\eta(n)\right] - E\left[\mathbf{x}_d(n)\frac{C(z)}{A_*(z)}\mathbf{x}_d^T(n)\right]_{\theta_*}\end{aligned} \tag{2.34}$$

where we have used again the fact that $e_o(n) = \eta(n)$ at the stationary point. Since the noise $\eta(\cdot)$ and the driving vector $\mathbf{x}_d(\cdot)$ are independent, the first term in the right-hand side of (2.34) vanishes. The symmetric part of the second term was shown in [70] to be negative definite provided that $C(z)/A_*(z)$ is SPR. Therefore, for sufficient order settings satisfying the SPR condition, one can apply Lemma 2.2 to conclude that the stationary point of the new lattice variant is locally stable.

2.5 Simulation examples

In order to demonstrate the superior stability properties of the new lattice algorithms with respect to the previously proposed schemes discussed in section 2.2, several computer simulation results are now presented. In all cases the adaptive filter operates in a sufficient order setting, in which, for the sake of simplicity, the unknown system $H(z)$ to be identified is all-pole (i.e. $N = 0$), and the input signal $u(\cdot)$ is a stationary white zero-mean process with unit variance. The white input and all-pole assumptions are useful in order to facilitate the computation of the matrices $\mathbf{S}_l(\theta_*)$ via (2.25) for each algorithm, once $H(z)$ is given. In this way, examples in which the existing algorithms discussed in section 2.2 suffer from instability problems can be relatively easily found.

2.5.1 Equation-error algorithms

It can be shown that for $N = 0$ and white $u(\cdot)$, the matrix $\mathbf{S}_l(\theta_*)$ obtained at the stationary point of EEL-1 and EEL-2 is stable if $M \leq 2$. However, for higher values of M (for which lattice structures provide a real advantage over direct form filters in terms of stability monitoring) this is no longer true. For example, let $H(z)$ be the fifth-order system parameterized in cascade lattice form by

$$\theta_{l,c*} = [\, b_{0*} \;\; \sin\phi_{1*} \;\; \cdots \;\; \sin\phi_{5*} \,]^T = [\, 0.1 \;\; 0.25 \;\; 0.88 \;\; 0.9 \;\; 0.75 \;\; 0.85 \,]^T. \tag{2.35}$$

Then the matrices $\mathbf{S}_l(\theta_*)$ of both EEL-1 and EEL-2 turn out to have a pair of eigenvalues with positive real parts, and hence they are not stable. Figure 2.5 shows the trajectories of the reflection coefficients of the adaptive filter $\hat{H}(z)$ obtained in a computer simulation of this setting. No additive noise was present in the reference signal in order to focus on the convergence properties of the algorithm. The adaptive filter parameters were initialized as

$$\theta_{l,c}(0) = [\, 0.1 \;\; 0.25 \;\; 0.8801 \;\; 0.9 \;\; 0.75 \;\; 0.85 \,]^T, \tag{2.36}$$

which is extremely close to the stationary point. Nevertheless the EEL-1 and EEL-2 algorithms eventually pull the parameter vector away from the stationary point, as could be expected. We should note that this divergence is not the result of a too large stepsize value: Similar behavior was observed if μ was further reduced.

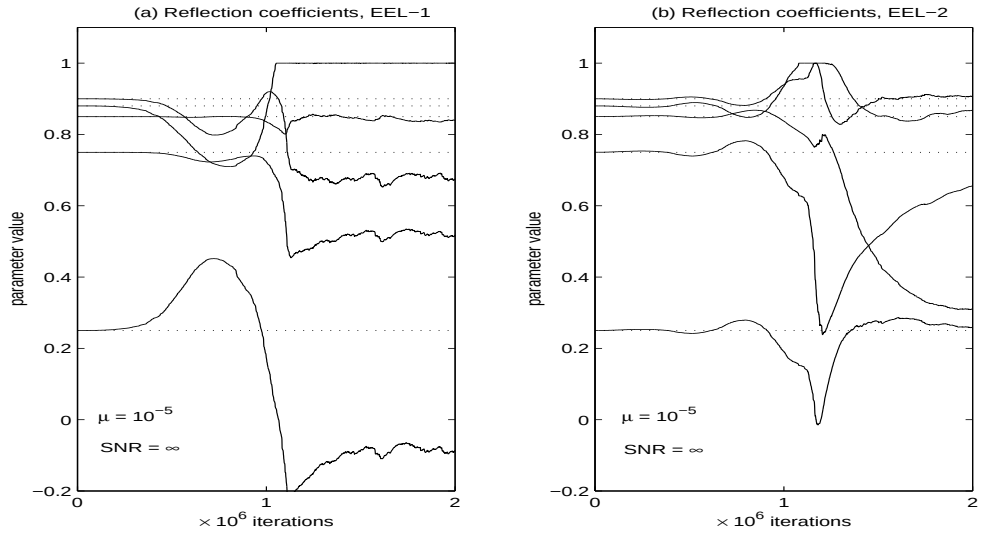

Figure 2.5: Instability of (a) EEL-1 algorithm, and (b) EEL-2 algorithm. Dashed lines show the values of the parameters at the stationary point.

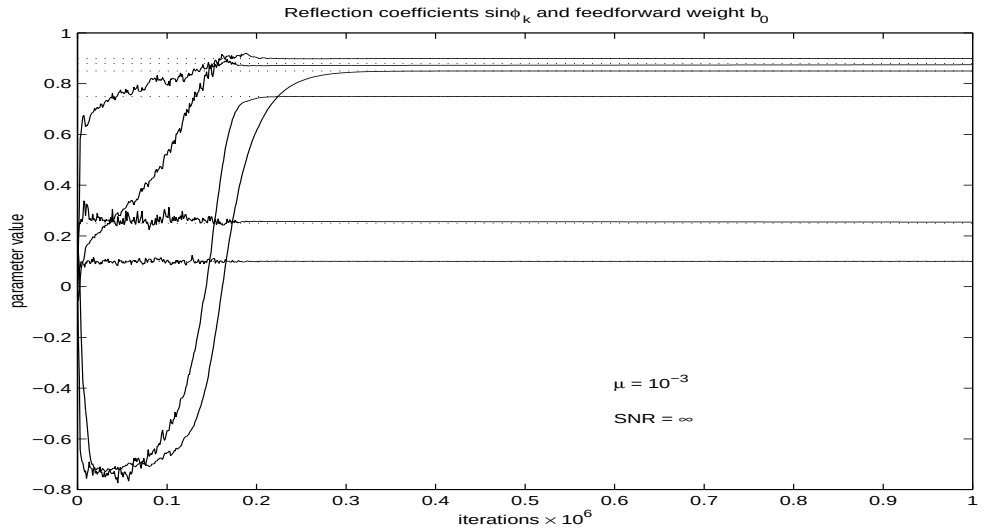

Figure 2.6: Parameter evolution for the new equation-error lattice algorithm.

The new algorithm was also tested in the same environment, with all adaptive parameters initialized to zero. Convergence to the true system parameters was achieved, as predicted by our analysis. This is illustrated in Figure 2.6.

We should note that in the presence of additive noise in the reference signal $d(\cdot)$, the stationary point of the new equation-error lattice algorithm will in general be biased from the true parameter values, since the stationary point is the same (in transfer function space) as that of the direct-form algorithm.

2.5.2 SPGL and SML algorithms

Recall that in sufficient order settings, the matrices $\mathbf{S}_l(\theta_*)$ of SPGL and SML at the point $\hat{H}(z) = H(z)$ are identical if the output noise $\eta(\cdot)$ is white. For low orders this matrix seems to be stable for all $H(z)$, but higher order unstable examples can still be found. Indeed, let $H(z)$ be the sixth-order all-pole system ($N = 0$, $M = 6$) whose cascade lattice parameters are

$$\theta_{l,c*} = [\,0.01\ \ 0.2\ \ 0.85\ \ 0.8\ \ 0.75\ \ 0.7\ \ 0.6\,]^T. \tag{2.37}$$

Then $\mathbf{S}_l(\theta_*)$ turns out to be unstable, for both the tapped-state algorithms of [105] and the cascade algorithms of [84]. Figure 2.7 shows the evolution of the tapped-state algorithms in this setting, initialized within a ball of radius 10^{-4} centered at $\theta_{l,ts*}$. The new algorithm was also tested, initialized at $b_0(0) = 0$, $\sin\phi_k(0) = 0.7$, $1 \leq k \leq 6$. It converges to the true parameter values as shown in Figure 2.8. As predicted by the theory, this stationary point is now attractive.

2.5.3 SHARF algorithm

The LSHARF algorithm of section 2.2.4 can also present stability problems in identification settings, as we show next. In order to ensure that the SPR condition is satisfied, the compensating filter is chosen as $C(z) = A_*(z)$, the denominator of the system to be identified, so that $C(z)/A_*(z) = 1$. With this choice of $C(z)$, it turns out that in the noiseless case the matrices $\mathbf{S}_d(\theta_*)$ for LSHARF and EEL-1 coincide. Since the corresponding matrices $\mathbf{R}(\theta)$ and $\mathbf{F}(\theta)$ are also the same for these algorithms, we conclude from (2.25) that under these conditions the feedback matrices $\mathbf{S}_l(\theta_*)$ for LSHARF and EEL-1 coincide as well. Since (2.35) was shown to be an unstable stationary point for EEL-1, the same must be true for LSHARF.

Figure 2.9 shows the parameter evolution of a single run of LSHARF and the new lattice variant in this scenario. LSHARF was initialized at the point given in (2.36); the unstable character of the stationary point is clear. We must emphasize that this divergence phenomenon is not related to the SPR condition, which is satisfied; its origin resides in the nature of the lattice algorithm itself. The new lattice variant exhibits no convergence problems, as expected. The starting point in this case was $\theta_{l,c}(0) = \mathbf{0}$.

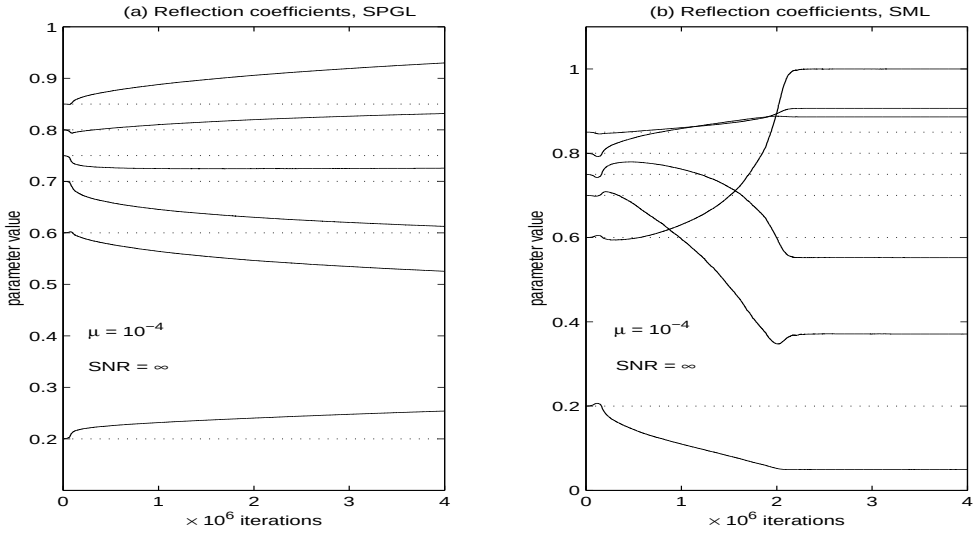

Figure 2.7: Instability of (a) SPGL algorithm, and (b) SML algorithm.

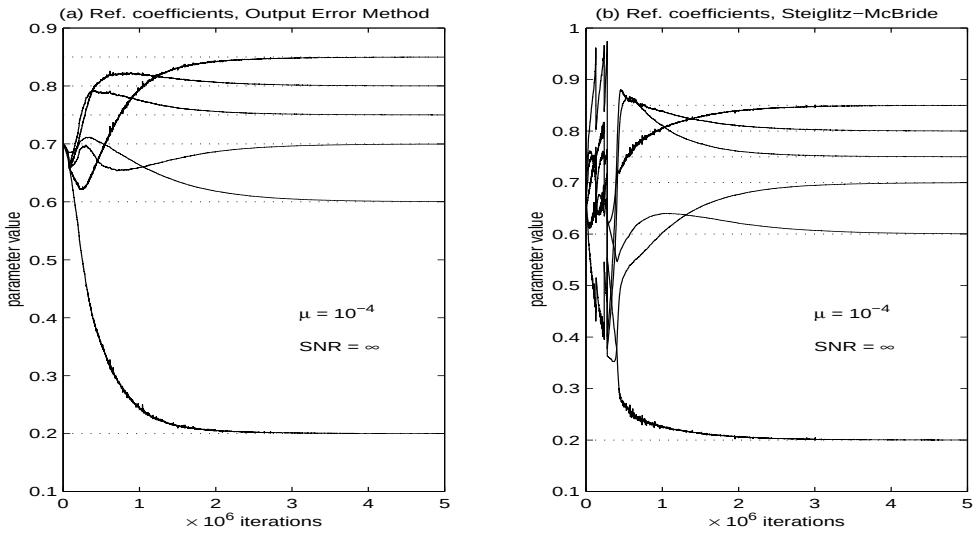

Figure 2.8: Parameter evolution for the new (a) output-error, and (b) Steiglitz-McBride lattice algorithms.

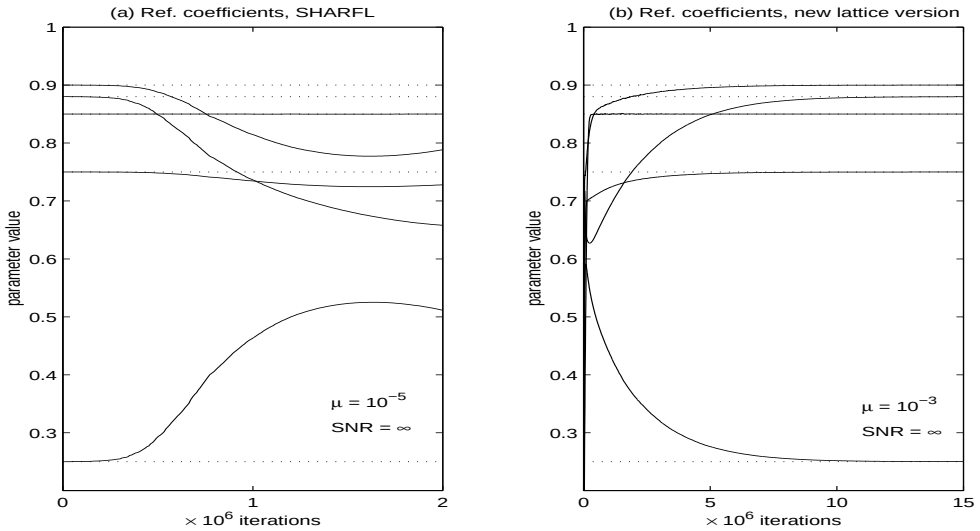

Figure 2.9: Parameter evolution for (a) LSHARF and (b) the new lattice variant of SHARF.

Chapter 3

ITERATIVE OFF-LINE IDENTIFICATION METHODS

In this chapter we explore several off-line procedures for identification of linear systems which share two common features: They are iterative in nature, and each iteration involves an optimization problem which is quadratic in the free parameters. These off-line methods are also interesting for adaptive filtering, since it is possible to derive on-line forms of the algorithms suitable for real-time applications.

The development of the off-line iterative schemes attempted to eliminate the drawbacks associated to the Output Error and the Equation Error approaches. Basically, all of them construct a sequence of EE problems in which the cost function is somehow distorted in order to avoid the bias problem to some extent. This 'distortion' depends on the solution of the EE problem obtained at the previous iteration, and usually involves the inversion of the corresponding estimate of the system denominator. This may break down the iteration if some roots of this estimate happen to be outside the unit circle. Hence, it is important to find conditions guaranteeing the minimum phase character of the EE denominator estimate. This problem is investigated in section 3.1.

The Steiglitz-McBride method was probably the first iterative off-line procedure described in the literature [120]. Recently, there has been renovated interest in the SM approach due to the good approximation properties of the stationary points in reduced order cases. This feature was theoretically justified via a lattice version of the off-line SM procedure [106], whose stationary points coincide with those of the original direct-form off-line SM iteration. Section 3.2 describes the direct-form and lattice variants of the off-line SM method, and comments on the sets of *attractive* points of these two versions.

A different off-line scheme known as the eXpanded Numerator (XN) method was originally proposed (in on-line form) by Gerald, Esteves and Silva in [39] as a modification to a similar procedure, the Master-Slave (MS) method, due to Hall and Hughes [45]. These schemes were analyzed in [73] and [76], where a new off-line iterative procedure termed Interpolation eXpanded Numerator (IXN) was also introduced. It was shown that the MS and XN approaches may present undesirable

stationary points, even in noiseless sufficient-order environments. On the other hand, the stationary point of the IXN method was shown to be unique, in the sufficient order case with a white input signal.

Section 3.3 provides a description of the off-line XN method. Then the IXN approach is further investigated in section 3.4, where we show how the uniqueness result for the IXN method can be extended to allow for a wider class of input signals. On-line implementation will also be discussed. Finally, we present a new iterative off-line scheme and its on-line version in section 3.5. This method incorporates elements from both the SM and the XN methods. Conditions will be given for the uniqueness of this SM/XN procedure.

In this chapter we work with functions of the complex variable z belonging to the space L_2 on the unit circle. In this space, the (weighted) inner product induced by $S_{uu}(z)$, the power spectral density of $u(\cdot)$, is defined as

$$\langle f(z), g(z) \rangle_u = \frac{1}{2\pi j} \oint S_{uu}(z) f(z) g(z^{-1}) \frac{dz}{z},$$

where the path of integration is the unit circle, in the counterclockwise direction. Note that this inner product can be also written as

$$\langle f(z), g(z) \rangle_u = E[f(z)u(n) \cdot g(z)u(n)],$$

that is, as the cross-correlation of the outputs of two filters with transfer functions $f(z)$ and $g(z)$ driven by the same input $u(\cdot)$. When $u(\cdot)$ is white, $S_{uu}(z) = \sigma_u^2$ becomes a constant and the inner product becomes unweighted. We shall denote the unweighted inner product by dropping the subscript u from the $\langle \cdot, \cdot \rangle_u$ notation. Note that

$$\begin{aligned} \langle f(z), g(z) \rangle_u &= \langle f(z), S_{uu}(z) g(z) \rangle, \\ \langle f(z), g(z) q(z) \rangle_u &= \langle f(z) q(z^{-1}), g(z) \rangle_u, \end{aligned}$$

and that

$$f(z) = \sum_{k=-\infty}^{\infty} f_k z^{-k}, \quad g(z) = \sum_{k=-\infty}^{\infty} g_k z^{-k} \quad \Rightarrow \quad \langle f(z), g(z) \rangle = \sum_{k=-\infty}^{\infty} f_k g_k,$$

which is just Parseval's relation.

The Hardy subspace $\mathcal{H}_2$ is the subspace of stable and causal functions of z, whose standard basis is $\{z^{-k}\}_{k=0}^{\infty}$. This basis is orthonormal with respect to the unweighted inner product, but in general this orthonormality is lost once spectral weighting is introduced. This generally complicates the analysis of the off-line methods when the input signal $u(\cdot)$ becomes colored. This problem can be alleviated by introducing the *Szegö polynomials* $\{p_k(z)\}_{k=0}^{\infty}$ associated to $u(\cdot)$, which constitute an orthonormal basis of $\mathcal{H}_2$ with respect to the inner product induced by $S_{uu}(z)$. See appendix C for a review of these polynomials and their properties.

3.1 Stability of Equation-Error models

Assume that the input/output description of the system under study is as follows:

$$d(n) = H(z)u(n) + \eta(n) = y(n) + \eta(n), \tag{3.1}$$

where $H(z)$ is assumed to be stable and causal, the processes $u(\cdot)$ and $y(\cdot)$ are jointly stationary and the noise term $\eta(\cdot)$ is uncorrelated with the input $u(\cdot)$. The EE method fits the rational model

$$\hat{H}(z) = \frac{B(z)}{A(z)} = \frac{b_0 + b_1 z^{-1} + \cdots + b_N z^{-N}}{a_0 + a_1 z^{-1} + \cdots + a_M z^{-M}} \tag{3.2}$$

by minimizing the variance

$$\begin{aligned} E\left[|A(z)d(n) - B(z)u(n)|^2\right] &= \frac{1}{2\pi}\int_{-\pi}^{\pi} S_{uu}(e^{j\omega})|A(e^{j\omega})H(e^{j\omega}) - B(e^{j\omega})|^2 \mathrm{d}\omega \\ &\quad + \frac{1}{2\pi}\int_{-\pi}^{\pi} S_{\eta\eta}(e^{j\omega})|A(e^{j\omega})|^2 \mathrm{d}\omega, \end{aligned} \tag{3.3}$$

where $S_{uu}(e^{j\omega})$, $S_{\eta\eta}(e^{j\omega})$ are the power spectral densities of the input $u(\cdot)$ and the noise $\eta(\cdot)$ respectively, and some constraint must be imposed on $A(z)$ to avoid the zero solution. Usually one fixes $a_0 = 1$ (monic approach) or $\sum_{k=0}^{M} a_k^2 = 1$ (unit norm approach). Let us denote the solution of (3.3) subject to one of these constraints by $A_\star(z)$ and $B_\star(z)$. Then it is desirable that $A_\star(z)$ be minimum phase (i.e., all of its roots lie inside the unit circle) so that $\hat{H}(z) = B_\star(z)/A_\star(z)$ is a stable transfer function. It is known that in certain cases $\hat{H}(z)$ may be unstable: See [116] for an example. Hence, isolating conditions under which $A_\star(z)$ can be ensured to be minimum phase is an important problem.

Regalia [104] has shown that for both monic and unit norm approaches, the EE model $\hat{H}(z)$ is stable provided only that $u(\cdot)$ is an autoregressive (AR) process of degree less than or equal to N, i.e. that its psd satisfies $S_{uu}(z) = 1/[P(z)P(z^{-1})]$ with $P(z)$ a polynomial of degree not exceeding N. In particular, no assumptions were made about the spectral characteristics of the noise $\eta(\cdot)$ or the degree of the unknown system $H(z)$. In this section we show that in fact it suffices to have $u(\cdot)$ AR of degree not exceeding $N+1$.

Introduce the signal vectors

$$\begin{aligned} \mathbf{u}(n) &= [\, u(n)\ u(n-1)\ \cdots\ u(n-N)\,]^T, \\ \mathbf{v}(n) &= [\, \eta(n)\ \eta(n-1)\ \cdots\ \eta(n-M)\,]^T, \\ \mathbf{y}(n) &= [\, y(n)\ y(n-1)\cdots\ y(n-M)\,]^T, \end{aligned}$$

and the coefficient vectors

$$\mathbf{a} = [\, a_0\ a_1\ \cdots\ a_M\,]^T, \qquad \mathbf{b} = [\, b_0\ b_1\ \cdots\ b_N\,]^T.$$

Then the variance (3.3) can be written as

$$E\left[|A(z)d(n) - B(z)u(n)|^2\right] = E\{|\mathbf{a}^T[\mathbf{y}(n) + \mathbf{v}(n)] - \mathbf{b}^T\mathbf{u}(n)|^2\}$$
$$= \mathbf{a}^T(\mathbf{R}_{yy} + \mathbf{R}_{vv})\mathbf{a} + \mathbf{b}^T\mathbf{R}_{uu}\mathbf{b} - 2\mathbf{b}^T\mathbf{R}_{uy}\mathbf{a} \quad (3.4)$$

where

$$\mathbf{R}_{uu} = E[\mathbf{u}(n)\mathbf{u}(n)^T], \qquad \mathbf{R}_{yy} = E[\mathbf{y}(n)\mathbf{y}(n)^T], \qquad \mathbf{R}_{uy} = E[\mathbf{u}(n)\mathbf{y}(n)^T].$$

Now (3.3) is minimized with respect to $B(z)$ if $\mathbf{b} = \mathbf{R}_{uu}^{-1}\mathbf{R}_{uy}\mathbf{a}$. After substituting this in (3.4) one obtains the following reduced cost function:

$$K(\mathbf{a}) = \mathbf{a}^T(\mathbf{R}_{vv} + \mathbf{R}_{y/u})\mathbf{a}, \quad (3.5)$$

where $\mathbf{R}_{y/u} = \mathbf{R}_{yy} - \mathbf{R}_{uy}^T\mathbf{R}_{uu}^{-1}\mathbf{R}_{uy}$. Note that $K(\mathbf{a})$ is a function of $A(z)$ only, through its coefficient vector $\mathbf{a}$.

3.1.1 The monic case

Here we consider the problem of minimizing (3.4) subject to the monic constraint $a_0 = 1$. Let us introduce first the following notation: If $\mathbf{M}$ is an $m \times m$ square matrix, we denote by $\mathbf{M}\rfloor$, $\lceil\mathbf{M}$, $\lfloor\mathbf{M}$ and $\mathbf{M}\rceil$ respectively the northwest, southeast, northeast and southwest matrices of size $(m-1)\times(m-1)$ extracted from $\mathbf{M}$. With this, our main tool will be the following result from [49]:

Lemma 3.1. *Let $\mathbf{R} > \mathbf{0}$, and let $\mathbf{a}_\star$ be the monic vector that minimizes the quadratic cost $J(\mathbf{a}) = \mathbf{a}^T\mathbf{R}\mathbf{a}$. Then the polynomial $A_\star(z)$ constructed from the coefficients of $\mathbf{a}_\star$ has all roots strictly inside the unit circle if $\mathbf{\Delta} \geq \mathbf{0}$, where $\mathbf{\Delta} = \lceil\mathbf{R} - \mathbf{R}\rfloor$ is the displacement matrix of $\mathbf{R}$.*

Hence, in view of Lemma 3.1 and (3.5), it suffices to find conditions on $u(\cdot)$ and $\eta(\cdot)$ to ensure that the displacement matrix of $\mathbf{R}_{vv} + \mathbf{R}_{y/u}$ is positive semidefinite. The following result gives such conditions.

Theorem 3.1. *Assume that $u(\cdot)$ is an autoregressive process of degree not exceeding $N+1$. Then the polynomial constructed from the monic vector that minimizes (3.5) has all roots strictly inside the unit circle.*

The proof is given in Appendix B. Observe that no assumptions are made on the noise properties; this is because the displacement matrix of the noise autocorrelation matrix $\mathbf{R}_{vv}$ is zero, due to the Toeplitz structure of $\mathbf{R}_{vv}$, and therefore automatically positive semidefinite.

3.1.2 The quadratically constrained case

Here we consider the case where a quadratic constraint is placed on the vector $\mathbf{a}$. First we need to recast the result from Lemma 3.1 into this setting.

Lemma 3.2. *Let* $\mathbf{R} \geq \mathbf{0}$ *and* $J(\mathbf{a}) = \mathbf{a}^T\mathbf{R}\mathbf{a}$. *If* $\mathbf{\Delta} = \lceil \mathbf{R} - \mathbf{R} \rfloor \geq \mathbf{0}$, *then there exists a vector* $\mathbf{a}_\star$ *solving*

$$\min_{\mathbf{a}} J(\mathbf{a}) \qquad \textit{subject to } \mathbf{a}^T\mathbf{Q}\mathbf{a} = 1 \tag{3.6}$$

where $\mathbf{Q} > \mathbf{0}$ *is Toeplitz symmetric, such that the polynomial* $A_\star(z)$ *constructed from* $\mathbf{a}_\star$ *has no zeros outside the unit circle. If* $\mathbf{\Delta} > \mathbf{0}$, *then* $A_\star(z)$ *has all zeros strictly inside the unit circle.*

The proof is given in Appendix B. Observe from (3.5) that if $K(\mathbf{a})$ is minimized subject to the constraint $\mathbf{a}^T\mathbf{R}_{vv}\mathbf{a} = 1$, then the minimizing argument $\mathbf{a}_\star$ does not vary with the noise power $E[\eta^2(n)]$, in contrast with the monic approach. In particular, if $\eta(\cdot)$ is white, then the unit norm constraint $||\mathbf{a}||_2^2 = 1$ avoids bias.

We can state now the corresponding stability result for the quadratically constrained EE estimate.

Theorem 3.2. *Assume that* $u(\cdot)$ *is autoregressive of degree not exceeding* $N + 1$. *Then the polynomial constructed from the vector that minimizes (3.5) subject to* $\mathbf{a}^T\mathbf{R}_{vv}\mathbf{a} = 1$ *has no roots outside the unit circle.*

Proof: The result follows immediately in view of Lemma 3.2 by mimicking the proof of Theorem 3.1. ∎

Note that for the monic constraint, $\mathbf{\Delta} \geq \mathbf{0}$ implies strict stability, but not for the unit norm constraint $||\mathbf{a}||_2^2 = 1$. (For example, one can always construct settings for which the matrix $\mathbf{R}_{vv} + \mathbf{R}_{y/u}$ is Toeplitz. If its smallest eigenvalue is simple, then the roots of the corresponding $A_\star(z)$ lie *all on the unit circle* [82]). In the case $N = M$, the results in [107] show that whenever $A_\star(z_0) = 0$ with $|z_0| = 1$, then $B_\star(z_0) = 0$ as well. Therefore all the poles of the approximant $\hat{H}(z) = B_\star(z)/A_\star(z)$ on the unit circle are canceled out, and all of the remaining poles lie strictly inside the unit circle.

3.2 The Steiglitz-McBride method

The off-line Steiglitz-McBride system identification method as originally proposed in [120] constructs the model $\hat{H}(z) = B(z)/A(z)$ from the limit point of a sequence of Equation-Error modeling problems as follows. Let

$$B^{(k)}(z) = b_0^{(k)} + b_1^{(k)}z^{-1} + \cdots + b_N^{(k)}z^{-N}, \qquad A^{(k)}(z) = 1 + a_1^{(k)}z^{-1} + \cdots + a_M^{(k)}z^{-M}$$

be the estimates of the unknown system's numerator and denominator polynomials at iteration k. Assume that the polynomial $A^{(k)}(z)$ has all its roots inside the unit circle. Then with $u(\cdot)$ and $d(\cdot)$ the input and reference signals as usual, we can define the filtered signals

$$u'(n) = \frac{1}{A^{(k)}(z)}u(n), \qquad d'(n) = \frac{1}{A^{(k)}(z)}d(n).$$

The corresponding estimates at the next iteration are then computed in order to minimize the variance of the 'equation-error' signal $e(n) = A^{(k+1)}(z)d'(n) - B^{(k+1)}(z)u'(n)$, i.e.

$$\left\{A^{(k+1)}(z), B^{(k+1)}(z)\right\} = \arg \min_{A(z),B(z)} E\left[\left|A(z)d'(n) - B(z)u'(n)\right|^2\right].$$

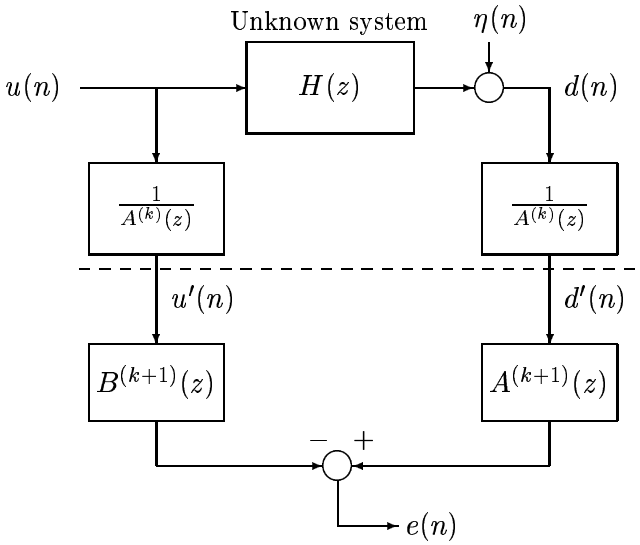

Figure 3.1: Block diagram illustrating the off-line Steiglitz-McBride iteration.

The SM iteration is illustrated in Figure 3.1. Observe that at any SM stationary point, achieved whenever $A^{(k+1)}(z) = A^{(k)}(z)$, the signal $e(n)$ becomes an output error. Also note that it is critical that all the polynomials $A^{(k)}(z)$ constructed along the way be minimum phase; otherwise the corresponding prefilter $1/A^{(k)}(z)$ would become unstable, an event that could stop the iterative process. The following result gives a sufficient condition for this.

Lemma 3.3. *If the input sequence $u(\cdot)$ is an autoregressive process of order not exceeding $N-M+1$, then the monic polynomials $A^{(k)}(z)$ constructed by the Steiglitz-McBride iteration are minimum phase.*

Proof: Observe that if $u(\cdot)$ is AR of order not exceeding $N - M + 1$, then the filtered signal $u'(\cdot)$ is AR of order not exceeding $N + 1$. Then from Theorem 3.1

in the previous section, the equation-error minimization problem yields a minimum phase denominator at every iteration of the SM method. ■

Thus if the input sequence is AR($N - M + 1$), then any limit point of the SM iteration gives a stable transfer function. In addition, it is known [121] that if the order of the model $\hat{H}(z)$ matches that of the unknown system $H(z)$, and if the noise disturbance $\eta(\cdot)$ is white, then the only stationary point of the off-line SM iteration is $\hat{H}(z) = B^{(\infty)}(z)/A^{(\infty)}(z) = H(z)$, which in addition is locally attractive. It is possible, however, that if the process is initialized too far from the stationary point and if the input does not satisfy the AR condition of Lemma 3.3, the iteration could construct an unstable intermediate transfer function.

This problem can be eliminated by introducing a lattice-based variant of the off-line method [103]. This variant presents several advantages with respect to the direct form method:

1. The stability of the intermediate transfer functions and of the approximant obtained at any convergent point (if one exists) is guaranteed since the lattice structure is inherently stable.

2. The iteration is rephrased as a sequence of extremal eigenvalue problems, providing useful error bounds at any stationary point for white inputs [106].

3. It can be used as starting point for developing on-line adaptive algorithms using lattice structures [103].

The key idea behind this lattice reformulation is to implement the prefilters in normalized lattice form, and to obtain the 'equation-error' $e(n)$ as a linear combination of the state signals of the prefilters. This is illustrated in Figure 3.2, where $p = \max\{N, M\}$. It is understood that if $N > M$, then the last $N - M$ rotation angles $\phi_i^{(k)}$ and coefficients q_i are constrained to be zero; and conversely, if $M > N$ then the last $M - N$ tap parameters ν_i are fixed to zero.

The lattice SM iteration is as follows. For simplicity, suppose $p = M = N$. At step k, the rotation angles $\phi_1^{(k)}, \ldots, \phi_p^{(k)}$ are available. Define the orthogonal matrices

$$\mathbf{Q}_i^{(k)} = \begin{bmatrix} \mathbf{I}_{i-1} & & & \\ & -\sin\phi_i^{(k)} & \cos\phi_i^{(k)} & \\ & \cos\phi_i^{(k)} & \sin\phi_i^{(k)} & \\ & & & \mathbf{I}_{p-i} \end{bmatrix}, \qquad \mathbf{Q}^{(k)} = \mathbf{Q}_1^{(k)} \cdots \mathbf{Q}_p^{(k)}, \tag{3.7}$$

and from them the prefilters

$$\begin{bmatrix} \mathbf{x}(n+1) \\ w(n) \end{bmatrix} = \mathbf{Q}^{(k)} \begin{bmatrix} \mathbf{x}(n) \\ u(n) \end{bmatrix}, \qquad \begin{bmatrix} \xi(n+1) \\ s(n) \end{bmatrix} = \mathbf{Q}^{(k)} \begin{bmatrix} \xi(n) \\ y(n) \end{bmatrix}. \tag{3.8}$$

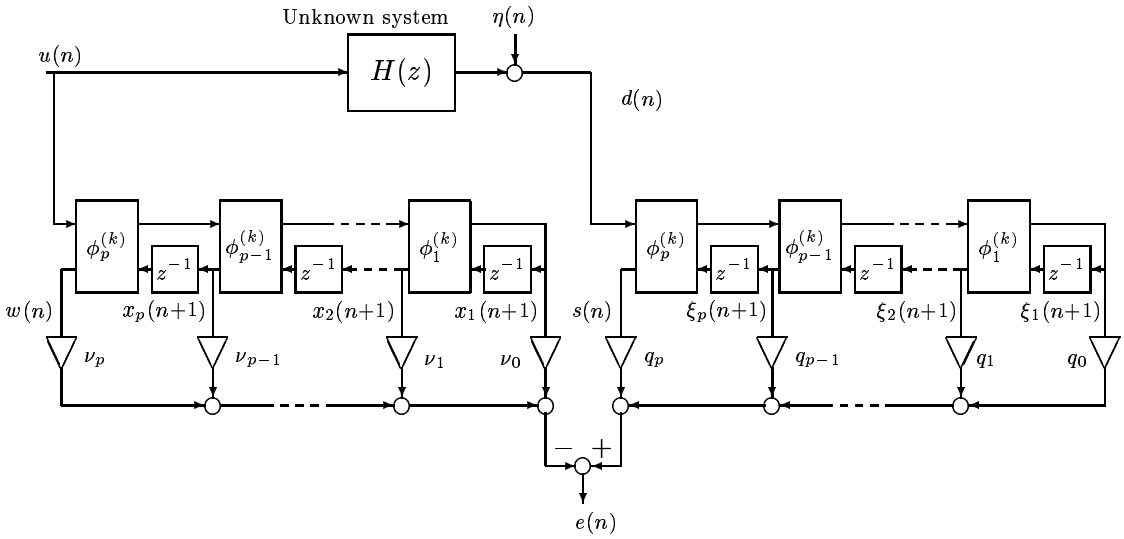

Figure 3.2: Reformulation of the Steiglitz-McBride method in lattice form ($p = \max\{N, M\}$).

Now with $\mathbf{q} = [\, q_0 \cdots q_p \,]^T$ and $\nu = [\, \nu_0 \cdots \nu_M \,]^T$, form the error signal $e(n)$ as follows:

$$e(n) = \mathbf{q}^T \begin{bmatrix} \xi(n+1) \\ s(n) \end{bmatrix} - \nu^T \begin{bmatrix} \mathbf{x}(n+1) \\ w(n) \end{bmatrix} \tag{3.9}$$

and find the coefficients $q_i^{(k+1)}$, $\nu_j^{(k+1)}$ minimizing $E[e^2(n)]$ subject to $\mathbf{q}^T\mathbf{q} = 1$, and taking $q_0^{(k+1)} > 0$. The reflection coefficients for the next iteration are determined from the following relation:

$$\sin \phi_i^{(k+1)} = \frac{q_i^{(k+1)}}{\sqrt{\left[q_0^{(k+1)}\right]^2 + \cdots + \left[q_i^{(k+1)}\right]^2}}, \qquad i = 1, \ldots, p.$$

Upon convergence, $\{\phi_i\}$ and $\{\nu_j\}$ determine the model $\hat{H}(z)$ in tapped normalized lattice form [103]. A fundamental property (and a key advantage) of this reformulation is that the prefilters for the next iteration are automatically stable, due to the inherent stability of the lattice structure.

It is known that the stationary points of the lattice and direct-form versions of the Steiglitz-McBride iteration yield the same set of transfer functions [105], although the convergence properties of these two iterative processes need not be the same. However, it has been suggested [105] that the sets of *convergent* points of both methods may coincide, based on empirical evidence from examination of many examples. In fact, this is not necessarily the case: Next we present an example which shows how the lattice variant of the off-line SM iteration may have stable limit cycles and even to present chaotic behavior in undermodeled cases.

Suppose $u(\cdot)$ is unit-variance white noise and $p = N = M = 1$, and assume $H(z)$ is rational with a minimal state-space description $(\mathbf{A}, \mathbf{b}, \mathbf{c}, d)$ such that $H(z) = \mathbf{c}^t(z\mathbf{I} - A)^{-1}\mathbf{b} + d$. It was shown in [105, p. 429] that in that case the lattice SM variant can be expressed as an iterated eigenproblem:

$$\mathbf{R}\left(\phi_1^{(k)}\right)\begin{bmatrix}\cos\phi_1^{(k+1)}\\ \sin\phi_1^{(k+1)}\end{bmatrix} = \lambda_{\min}\left[\mathbf{R}\left(\phi_1^{(k)}\right)\right]\begin{bmatrix}\cos\phi_1^{(k+1)}\\ \sin\phi_1^{(k+1)}\end{bmatrix}, \tag{3.10}$$

where the matrix $\mathbf{R}(\phi_1)$ is given by

$$\mathbf{R}(\phi_1) = \begin{bmatrix}\mathbf{b}^T(\mathbf{I} + \sin\phi_1\mathbf{A})^{-T}\mathbf{A}^T\cos\phi_1\\ \mathbf{b}^T\end{bmatrix}\mathbf{W}\left[\cos\phi_1\mathbf{A}(\mathbf{I} + \sin\phi_1\mathbf{A})^{-1}\mathbf{b}\ \ \mathbf{b}\right], \tag{3.11}$$

with $\mathbf{W}$ the solution of $\mathbf{W} = \mathbf{A}^T\mathbf{W}\mathbf{A} + \mathbf{c}\mathbf{c}^T$.

Consider the fourth-order system $H(z) = z^{-1} + az^{-4}$ with state-space description $(\mathbf{A}, \mathbf{b}, \mathbf{c}, 0)$ given by

$$\mathbf{A} = \begin{bmatrix}0&0&0&0\\1&0&0&0\\0&1&0&0\\0&0&1&0\end{bmatrix},\quad \mathbf{b} = \begin{bmatrix}1\\0\\0\\0\end{bmatrix},\quad \mathbf{c} = \begin{bmatrix}1\\0\\0\\a\end{bmatrix}\quad\Rightarrow\quad \mathbf{W} = \begin{bmatrix}1+a^2&0&0&a\\0&a^2&0&0\\0&0&a^2&0\\a&0&0&a^2\end{bmatrix}.$$

The corresponding values for $\mathbf{R}(\phi_1)$ and its smallest eigenvalue are

$$\mathbf{R}(\phi_1) = \begin{bmatrix}a^2(1-\sin^6\phi_1) & a\cos\phi_1\sin^2\phi_1\\ a\cos\phi_1\sin^2\phi_1 & 1+a^2\end{bmatrix},$$

$$\lambda_{\min}[\mathbf{R}(\phi_1)] = \frac{1}{2} + a^2 - \frac{1}{2}a^2\sin^6\phi_1 - \frac{1}{2}\sqrt{4a^2\cos^2\phi_1\sin^4\phi_1 + (1 + a^2\sin^6\phi_1)^2},$$

and the explicit SML iteration that results is

$$\sin\phi_1^{(k+1)} = \frac{-a\cos\phi_1^{(k)}\sin^2\phi_1^{(k)}}{\sqrt{a^2\cos^2\phi_1^{(k)}\sin^4\phi_1^{(k)} + \left(1 + a^2 - \lambda_{\min}\left[\mathbf{R}\left(\phi_1^{(k)}\right)\right]\right)^2}}. \tag{3.12}$$

It turns out that for small values of $|a|$, $\sin\phi_1 = 0$ is the only fixed point of (3.12), and it is locally attractive. At $|a| \approx 3.863925$, two new fixed points appear. At $|a| \approx 13.089751$ the first bifurcation occurs, and a stable limit cycle of period 2 appears. The second and third bifurcations take place at $|a| \approx 28.695753$ and $|a| \approx 37.585665$ respectively. Eventually the chaotic regime is reached as $|a|$ is further increased.

In contrast, the direct-form iteration is given in this case by

$$\sin\phi_1^{(k+1)} = \frac{a\sin\phi_1^{(k)}\left[a\left(1-\sin^6\phi_1^{(k)}\right) - \cos^2\phi_1^{(k)}\sin\phi_1^{(k)}\right]}{a^2\sin^2\phi_1^{(k)}\left(1-\sin^6\phi_1^{(k)}\right) + \cos^2\phi_1^{(k)}\left(1 + a^2 - 2a\sin^3\phi_1^{(k)}\right)}, \tag{3.13}$$

which is free of limit cycles for all a. Although the fixed points of the lattice and direct-form iterations are the same, clearly their convergence properties may be quite different. It is relatively easy to find settings in which the lattice variant presents stable limit cycles, but we have been unable to construct any examples with limit cycles for the direct-form method. Figure 3.3 shows the SM maps $\sin\phi_1^{(k)} \rightarrow \sin\phi_1^{(k+1)}$ given by (3.12) and (3.13) for different values of a.

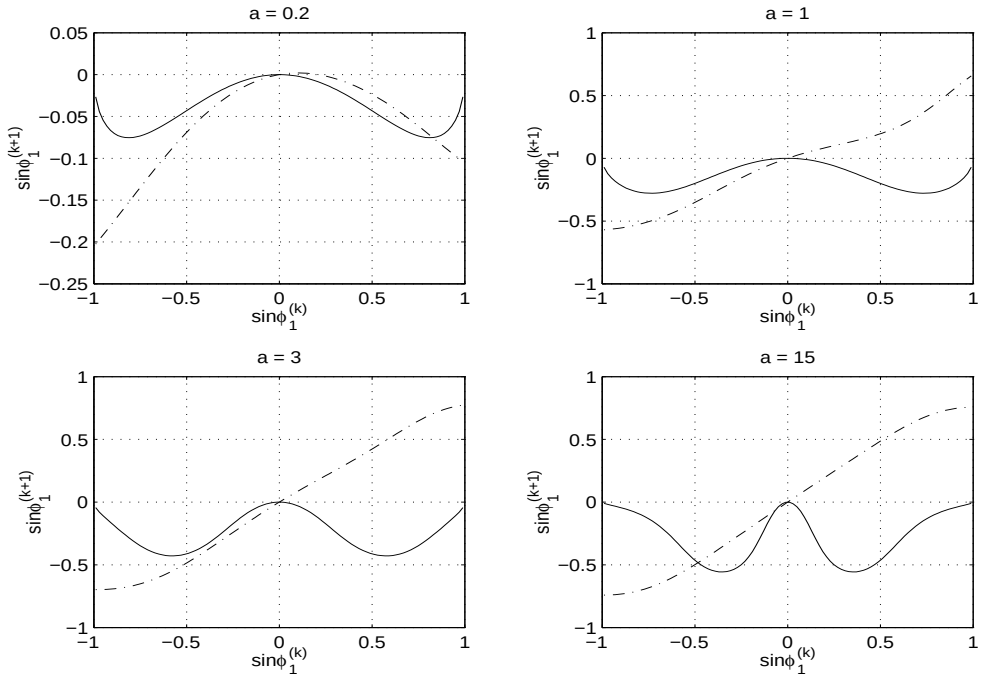

Figure 3.3: The maps obtained from the lattice (solid) and direct-form (dash-dot) Steiglitz-McBride iterations, with $N = M = 1$ and $H(z) = z^{-1} + az^{-4}$.

It is not our purpose to claim superiority of the direct-form variant: Recall that the direct form version may suffer from misconvergence problems as well, as a result of an unstable intermediate transfer function. The problem is most likely attributable to the lack of an optimization criterion underlying the Steiglitz-McBride method, whether it be in direct form, lattice form, or some other variant that someone may devise, since the intermediate transfer functions constructed along the way have no clear interpretation in terms of some distance minimization.

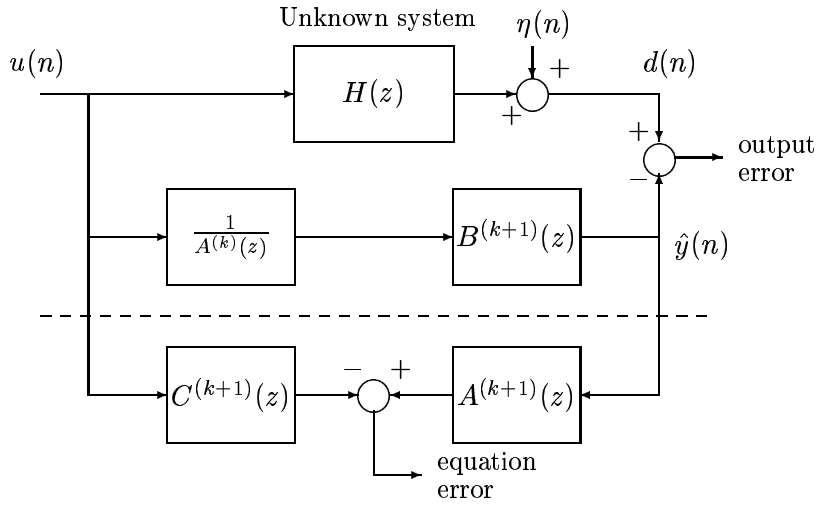

Figure 3.4: Block diagram illustrating the off-line Expanded Numerator iteration.

3.3 The Expanded Numerator method

The Expanded Numerator (XN) method is based on the observation that the output error $d(n) - [B(z)/A(z)]u(n)$ is a linear function of the coefficients of $B(z)$, and therefore its variance can be easily minimized with respect to these parameters. On the other hand, in order to estimate $A(z)$, a series of equation-error problems is iteratively solved. The process, illustrated in Figure 3.4, is summarized next.

1. At iteration k, the estimate $A^{(k)}(z)$ is available. Find $B^{(k+1)}(z)$ as the solution to the following quadratic minimization problem:

$$B^{(k+1)}(z) = \arg\min_{B(z)} E\left[\left|d(n) - \frac{B(z)}{A^{(k)}(z)}u(n)\right|^2\right].$$

2. Let $\hat{y}(n) = [B^{(k+1)}(z)/A^{(k)}(z)]u(n)$, and find the coefficients of the filters $C^{(k+1)}(z)$, $A^{(k+1)}(z)$ by solving the quadratic equation error minimization problem

$$\left\{A^{(k+1)}(z), C^{(k+1)}(z)\right\} = \arg\min_{A(z),C(z)} E\left[|A(z)\hat{y}(n) - C(z)u(n)|^2\right]$$

   subject to a monic constraint on $A(z)$.

3. Discard the filter $C^{(k+1)}(z)$ and repeat the process.

In addition to being quadratic, the minimization problem in Step 1 is not biased regardless of whether the output disturbance $\eta(\cdot)$ is present or not. In addition, the equation error problem in Step 2 uses the signals $\{u(\cdot), \hat{y}(\cdot)\}$ rather than $\{u(\cdot), d(\cdot)\}$. Since the estimate $\hat{y}(\cdot)$ of $d(\cdot)$ is noiseless, the disturbance $\eta(\cdot)$ cannot affect this step either. We conclude that the XN off-line method is unbiased, regardless of the spectral characteristics of the output noise. This is in contrast with the SM method, which is biased in general unless $\eta(\cdot)$ is white.

Observe that in order for the XN method to evolve, the equation error identification problem in Step 2 must face a reduced order setting. Otherwise one would obtain $C^{(k+1)}(z) = B^{(k+1)}(z)$ and $A^{(k+1)}(z) = A^{(k)}(z)$ for all k. This is achieved by overparameterizing the numerator $B(z)$ with respect to the auxiliary filter $C(z)$ (hence the 'Expanded Numerator' label). The analysis of the XN method in [76] for the case in which $u(\cdot)$ is white suggests that the order of $B(z)$ be at least the sum of the orders of $C(z)$ and $A(z)$.

Similarly to the direct-form SM method, the XN iteration may break if the estimate $A^{(k+1)}(z)$ obtained in Step 2 is not minimum phase. In order to find sufficient conditions for stability, we can apply Theorem 3.1 to conclude that if $u(\cdot)$ is autoregressive of order not exceeding $N+1$, where N is the degree of the auxiliary filter $C(z)$, then the polynomials $A^{(k)}(z)$ obtained in the XN iteration are minimum phase.

Although the XN method has the advantage of being unbiased for all kinds of disturbances, simulation results given in [76] show that in sufficient order settings the iteration need not converge to the desired solution $B(z)/A(z) = H(z)$, which constitutes a clear drawback. In the next sections two modifications of the XN method are presented which attempt to sidestep this problem.

3.4 The Interpolation Expanded Numerator method

The Interpolation Expanded Numerator (IXN) method is based on the same configuration as that for the XN procedure, shown in Figure 3.4. The difference from XN resides in the way in which the numerator $B^{(k+1)}(z)$ for the next iteration is computed. The process is as follows:

1. At iteration k, $A^{(k)}(z)$ is available. Let $\hat{y}(n) = [B(z)/A^{(k)}(z)]u(n)$. The numerator $B^{(k+1)}(z)$ is chosen so that $\hat{y}(n)$ satisfies the following interpolation conditions:

$$E[\hat{y}(n)u(n-k)] = E[d(n)u(n-k)], \qquad 0 \leq k \leq L, \tag{3.14}$$

   where L is the degree of $B(z)$.

2. With $\hat{y}(n) = [B^{(k+1)}(z)/A^{(k)}(z)]u(n)$, find the coefficients of the FIR filters $C^{(k+1)}(z)$ (degree N) and $A^{(k+1)}(z)$ (degree M) by solving the quadratic equa-

tion error minimization problem

$$\left\{A^{(k+1)}(z), C^{(k+1)}(z)\right\} = \arg \min_{A(z),C(z)} E\left[|A(z)\hat{y}(n) - C(z)u(n)|^2\right]$$

subject to a monic constraint on $A(z)$.

3. Discard the filter $C^{(k+1)}(z)$ and repeat the process.

Observe that the set of equations (3.14) is linear in the parameters of $B(z)$, and that its solution is not biased by the output disturbance since $u(\cdot)$ and $\eta(\cdot)$ are statistically independent. The equation error step is identical to that in the XN method, and thus the stability of the intermediate transfer functions is guaranteed if $u(\cdot)$ is AR$(N+1)$ where N is the degree of the auxiliary filter $C(z)$.

In this section we present an analysis of the stationary points of the off-line IXN method. Our goal is to extend the result from [76], which showed the uniqueness of this stationary point in sufficient order settings with a white input signal, to a more general class of inputs. On-line implementations will also be presented together with the corresponding convergence analyses.

3.4.1 Minimum length of the expanded numerator $B(z)$

The first point to be addressed about the off-line IXN scheme is what the order L of the numerator $B(z)$ should be. Clearly, L must be greater than N, the order of the auxiliary filter $C(z)$; otherwise the equation error step would face a sufficient order, noiseless scenario, hence preventing the method from evolving ('convergence' would be achieved in the first iteration).

If the input $u(\cdot)$ is white, then the interpolation conditions (3.14) amount to imposing that the first $L+1$ impulse response coefficients of $B^{(k+1)}(z)/A^{(k)}(z)$ match those of the unknown system $H(z)$ at every iteration k [76]. More generally, for nonwhite $u(\cdot)$, the first $L+1$ coefficients of the expansion of $H(z)$ over the Szegö polynomials $\{p_k(z)\}_{k=0}^{\infty}$ associated to $u(\cdot)$ are matched, since (3.14) can be rewritten as

$$\langle H(z), z^{-l}\rangle_u = \left\langle \frac{B^{(k+1)}(z)}{A^{(k)}(z)}, z^{-l}\right\rangle_u, \qquad l = 0, 1 \ldots L,$$

or, since $\text{span}\{z^{-l}\}_{l=0}^{L} = \text{span}\{p_l(z)\}_{l=0}^{L}$,

$$\langle H(z), p_l(z)\rangle_u = \left\langle \frac{B^{(k+1)}(z)}{A^{(k)}(z)}, p_l(z)\right\rangle_u, \qquad l = 0, 1 \ldots L. \tag{3.15}$$

Therefore at every iteration k, the $L+1$ leading coefficients in the expansions of $H(z)$ and $B^{(k+1)}(z)/A^{(k)}(z)$ over the Szegö polynomials associated to $u(\cdot)$ are the same.

Let us denote by $\hat{H}(z)$ the estimate of the unknown system obtained at an IXN stationary point, i.e. $\hat{H}(z) = B^{(\infty)}(z)/A^{(\infty)}(z)$. Then it is one's hope that, in sufficient order scenarios, $\hat{H}(z) = H(z)$. This brings out the question of how many interpolation conditions of the type (3.15) are required in order to ensure that two rational functions of the same degree are equal.

Lemma 3.4. *Let $u(\cdot)$ be an autoregressive process of order not exceeding $N+M+1$. Then any rational function with N zeros and M poles is uniquely specified by the first $N+M+1$ coefficients of its expansion over the Szegö polynomials associated to $u(\cdot)$.*

The proof can be found in Appendix B. Whether this result applies as well to other classes of inputs is left at this stage as a conjecture. It is obviously true for all $u(\cdot)$ if $M = 0$ and N is arbitrary. Also, if $u(\cdot)$ is a first order moving average process, or MA(1), (meaning that $S_{uu}(z) = q(z)q(z^{-1})$ with $q(z)$ a first order polynomial), then it is shown in Appendix B that the result holds for the particular case $N = 0$, $M = 1$.

In view of Lemma 3.4, it is clear that the order of the numerator $B(z)$ should satisfy $L \geq N + M$ in order to impose a sufficient number of interpolation constraints. Incidentally, this is the same lower bound as that obtained in [76] for the white input case. With this result in mind, we can proceed to study the stationary points of the off-line IXN method in the general (non-white input) case.

3.4.2 Analysis of stationary points

At any stationary point of the off-line IXN method, the equation error minimization step produces an estimate $A^{(k+1)}(z) = A^{(k)}(z)$. To characterize the set of these points, let us define the signal vectors

$$\mathbf{u}(n) = [\, u(n)\ u(n-1)\ \cdots\ u(n-N)\,]^T, \tag{3.16}$$

$$\tilde{\mathbf{u}}(n) = [\, u(n-N-1)\ u(n-N-2)\ \cdots\ u(n-L)\,]^T, \tag{3.17}$$

$$\bar{\mathbf{u}}(n) = [\, \mathbf{u}(n)^T\ \tilde{\mathbf{u}}(n)^T\,]^T, \tag{3.18}$$

$$\hat{\mathbf{y}}(n) = [\, \hat{y}(n)\ \hat{y}(n-1)\cdots\ \hat{y}(n-M)\,]^T, \tag{3.19}$$

and let the vectors

$$\mathbf{a} = [\, a_0\ a_1\ \cdots\ a_M\,]^T, \qquad \mathbf{b} = [\, b_0\ b_1\ \cdots\ b_L\,]^T \tag{3.20}$$

comprise the coefficients of the polynomials $A(z)$ and $B(z)$ obtained at a stationary point. It is assumed that the monic constraint $a_0 = 1$ is used. Define also the correlation matrices

$$\mathbf{R}_{uu} = E[\mathbf{u}(n)\mathbf{u}(n)^T], \qquad \mathbf{R}_{\hat{y}\hat{y}} = E[\hat{\mathbf{y}}(n)\hat{\mathbf{y}}(n)^T], \qquad \mathbf{R}_{u\hat{y}} = E[\mathbf{u}(n)\hat{\mathbf{y}}(n)^T],$$

and with these, let

$$\mathbf{R}_{\hat{y}/u} = \mathbf{R}_{\hat{y}\hat{y}} - \mathbf{R}_{u\hat{y}}^T \mathbf{R}_{uu}^{-1} \mathbf{R}_{u\hat{y}}.$$

Then the variance of the equation error $A(z)\hat{y}(n) - C(z)u(n)$, after $C(z)$ has been optimized as a function of $A(z)$, is given by $\mathbf{a}^T \mathbf{R}_{\hat{y}/u} \mathbf{a}$. As shown in [104], the vector $\mathbf{a}$ that minimizes this quadratic cost subject to $a_0 = 1$ is orthogonal to the last M rows of $\mathbf{R}_{\hat{y}/u}$:

$$\mathbf{R}_{\hat{y}/u} \mathbf{a} = \begin{bmatrix} \sigma_e^2 \\ \mathbf{0}_M \end{bmatrix}, \tag{3.21}$$

where σ_e^2 is the resulting equation error variance. On the other hand, observe that $A(z)\hat{y}(n) = B(z)u(n)$, or in vector form, $\hat{\mathbf{y}}(n)^T \mathbf{a} = \bar{\mathbf{u}}(n)^T \mathbf{b}$. This gives

$$E[\mathbf{u}(n)\hat{\mathbf{y}}(n)^T]\mathbf{a} = E[\mathbf{u}(n)\bar{\mathbf{u}}(n)^T]\mathbf{b} \Rightarrow \mathbf{R}_{u\hat{y}} \mathbf{a} = [\, \mathbf{R}_{uu} \;\; \mathbf{P} \,]\mathbf{b} \tag{3.22}$$

$$E[\hat{\mathbf{y}}(n)\hat{\mathbf{y}}(n)^T]\mathbf{a} = E[\hat{\mathbf{y}}(n)\bar{\mathbf{u}}(n)^T]\mathbf{b} \Rightarrow \mathbf{R}_{\hat{y}\hat{y}} \mathbf{a} = [\, \mathbf{R}_{u\hat{y}}^T \;\; \mathbf{S}^T \,]\mathbf{b}, \tag{3.23}$$

where we have introduced the matrices

$$\mathbf{P} = E[\mathbf{u}(n)\tilde{\mathbf{u}}(n)^T], \qquad \mathbf{S} = E[\tilde{\mathbf{u}}(n)\hat{\mathbf{y}}(n)^T].$$

Now if we substitute (3.22) and (3.23) into (3.21), we obtain

$$[\, \mathbf{R}_{u\hat{y}}^T \;\; \mathbf{S}^T \,]\mathbf{b} - \mathbf{R}_{u\hat{y}}^T \mathbf{R}_{uu}^{-1} [\, \mathbf{R}_{uu} \;\; \mathbf{P} \,]\mathbf{b} = \begin{bmatrix} \sigma_e^2 \\ \mathbf{0}_M \end{bmatrix},$$

that is,

$$[\, \mathbf{R}_{u\hat{y}}^T \;\; \mathbf{S}^T \,]\mathbf{b} - [\, \mathbf{R}_{u\hat{y}}^T \;\; \mathbf{R}_{u\hat{y}}^T \mathbf{R}_{uu}^{-1} \mathbf{P} \,]\mathbf{b} = \begin{bmatrix} \sigma_e^2 \\ \mathbf{0}_M \end{bmatrix},$$

or equivalently

$$[\, \mathbf{0} \;\; \mathbf{S}^T - \mathbf{R}_{u\hat{y}}^T \mathbf{R}_{uu}^{-1} \mathbf{P} \,]\mathbf{b} = \begin{bmatrix} \sigma_e^2 \\ \mathbf{0}_M \end{bmatrix}.$$

Thus if we define the vector of the 'extra' coefficients of $B(z)$ as $\tilde{\mathbf{b}} = [\, b_{N+1} \cdots b_L \,]^T$, then we have

$$[\mathbf{S}^T - \mathbf{R}_{u\hat{y}}^T \mathbf{R}_{uu}^{-1} \mathbf{P}]\tilde{\mathbf{b}} = \begin{bmatrix} \sigma_e^2 \\ \mathbf{0}_M \end{bmatrix}. \tag{3.24}$$

It is possible to further reveal the structure of this equation with the aid of the Szegö polynomials $p_k(z)$. Let us introduce the lower triangular matrices $\mathbf{C}_k$ comprising the coefficients of these polynomials:

$$\begin{bmatrix} p_0(z) \\ p_1(z) \\ \vdots \\ p_k(z) \end{bmatrix} = \mathbf{C}_k \begin{bmatrix} 1 \\ z^{-1} \\ \vdots \\ z^{-k} \end{bmatrix}. \tag{3.25}$$

The matrix $\mathbf{C}_L$ can be partitioned as

$$\mathbf{C}_L = \begin{bmatrix} \mathbf{C}_N & \mathbf{0} \\ \mathbf{B} & \mathbf{A} \end{bmatrix} \tag{3.26}$$

where $\mathbf{A}$ is $(L-N)$ square and nonsingular, since the diagonal elements of $\mathbf{C}_L$ are nonzero (see Appendix C). The following result, whose proof is in Appendix B, will be useful.

Lemma 3.5. *With* $\mathbf{R}_{uu}$, $\mathbf{P}$, $\mathbf{A}$ *and* $\mathbf{B}$ *as above,*

$$\mathbf{R}_{uu}^{-1}\mathbf{P} = -\mathbf{B}^T\mathbf{A}^{-T}. \tag{3.27}$$

Now consider the expansion of $B(z)$ over the Szegö polynomials

$$B(z) = \sum_{i=0}^{L} b'_i p_i(z).$$

Then, the vector $\mathbf{b}' = [\, b'_0 \; b'_1 \; \cdots \; b'_L \,]^T$ is related to $\mathbf{b}$ by $\mathbf{b}' = \mathbf{C}_L^{-T}\mathbf{b}$. From this, it follows that $\tilde{\mathbf{b}}' = [\, b'_{N+1} \; \cdots \; b'_L \,]^T$ satisfies

$$\tilde{\mathbf{b}}' = \mathbf{A}^{-T}\tilde{\mathbf{b}} \qquad \Leftrightarrow \qquad \tilde{\mathbf{b}} = \mathbf{A}^T\tilde{\mathbf{b}}'.$$

Substituting this and the result from Lemma 3.5 in (3.24), one obtains

$$[\mathbf{AS} + \mathbf{BR}_{u\hat{y}}]^T\tilde{\mathbf{b}}' = \begin{bmatrix} \sigma_e^2 \\ \mathbf{0}_M \end{bmatrix}. \tag{3.28}$$

The matrix in (3.28) has a crosscorrelation interpretation. Introduce the signals $\bar{\beta}_i(n) = p_i(z)u(n)$, $i \geq 0$, which are the backward prediction errors (normalized to unit variance) associated to the input signal $u(\cdot)$ (see Appendix C), and define the vector

$$\tilde{\beta}(n) = [\, \bar{\beta}_{N+1}(n) \; \cdots \; \bar{\beta}_L(n) \,]^T. \tag{3.29}$$

Then, noting from (3.26) that $\tilde{\beta}(n) = [\, \mathbf{B} \quad \mathbf{A} \,]\bar{\mathbf{u}}(n)$, one has

$$E[\tilde{\beta}(n)\hat{\mathbf{y}}(n)^T] = [\, \mathbf{B} \quad \mathbf{A} \,]E[\bar{\mathbf{u}}(n)\hat{\mathbf{y}}(n)^T] = [\, \mathbf{B} \quad \mathbf{A} \,]\begin{bmatrix} \mathbf{R}_{u\hat{y}} \\ \mathbf{S} \end{bmatrix} = \mathbf{BR}_{u\hat{y}} + \mathbf{AS}.$$

Therefore, at any fixed point of the off-line IXN iteration, the relation

$$E[\hat{\mathbf{y}}(n)\tilde{\beta}(n)^T]\tilde{\mathbf{b}}' = \begin{bmatrix} \sigma_e^2 \\ \mathbf{0}_M \end{bmatrix} \tag{3.30}$$

must hold. The first equation simply gives the equation error variance achieved and is not very informative. The remaining M equations show that at any stationary point, the signal $\tilde{\beta}(n)^T\tilde{\mathbf{b}}'$ is uncorrelated with $\hat{y}(n-1), \ldots, \hat{y}(n-M)$. Note that in principle these M equations are nonlinear in the coefficients of the vector $\tilde{\mathbf{b}}'$, since the signal $\hat{y}(\cdot)$ depends on these parameters. An autoregressive constraint on the input signal suffices to sidestep this problem, as the next result shows (see Appendix B for the proof).

Lemma 3.6. *With $\hat{y}(n) = [B^{(k+1)}(z)/A^{(k)}(z)]u(n)$ the output of the adaptive filter at any iteration k, let $\mathbf{H}$ be the $M \times (L-N)$ matrix obtained after deleting the first row of $E[\hat{\mathbf{y}}(n)\tilde{\beta}(n)^T]$, i.e.*

$$\mathbf{H} = E\left\{ \begin{bmatrix} \hat{y}(n-1) \\ \vdots \\ \hat{y}(n-M) \end{bmatrix} [\, \bar{\beta}_{N+1}(n) \; \cdots \; \bar{\beta}_L(n) \,] \right\}. \tag{3.31}$$

If the input sequence $u(\cdot)$ is an autoregressive process of order not exceeding $L+1$, then the matrix $\mathbf{H}$ is completely specified by the unknown system $H(z)$ and the psd $S_{uu}(z)$.

From this discussion, we find that the IXN fixed points are characterized by the conditions

$$\langle H(z), p_l(z) \rangle_u = \left\langle \frac{B(z)}{A(z)}, p_l(z) \right\rangle_u, \quad l = 0, 1 \ldots L, \qquad \text{and} \qquad \mathbf{H}\tilde{\mathbf{b}}' = \mathbf{0}_M.$$

These constitute $L+M+1$ equations, with the same number of unknowns (the coefficients of $B(z)$ and $A(z)$). Under the conditions of Lemma 3.6, the M equations $\mathbf{H}\tilde{\mathbf{b}}' = \mathbf{0}_M$ are linear in $\tilde{\mathbf{b}}'$. Similarly, the other $L+1$ interpolation conditions are also linear in the coefficients of $B(z)$, although those of $A(z)$ appear in a nonlinear fashion.

Recall from the previous section that we must impose $L \geq N+M$. In that case the matrix $\mathbf{H}$ has at least as many rows as columns, and the following result holds for sufficient order situations.

Theorem 3.3. *Assume $H(z) = B_*(z)/A_*(z)$ with $B_*(z)$, $A_*(z)$ coprime polynomials of orders N and M respectively, and that $L \geq N+M$. If the input signal $u(\cdot)$ is an autoregressive process of order not exceeding $L+1$, then the matrix $\mathbf{H}$ defined in (3.31) has full row rank, i.e.* $\operatorname{rank}\mathbf{H} = M$.

The proof is presented in Appendix B. The full rank character of the matrix $\mathbf{H}$ is the key for establishing the uniqueness of the IXN stationary point in sufficient order settings with autoregressive inputs. The situation in which the numerator and denominator of the model have the same order ($N = M$) is particularly instructive. In that case, Theorem 3.3 can be seen as a spectrally weighted extension of Kronecker's theorem, as discussed at the end of its proof in Appendix B.

We can state the main result of this section as follows.

Theorem 3.4. *If $L \geq N+M$, the input $u(\cdot)$ is an autoregressive process of order not exceeding $L+1$, and the unknown system satisfies $H(z) = B_*(z)/A_*(z)$ with $B_*(z)$, $A_*(z)$ coprime polynomials of orders N and M respectively, then the off-line IXN iteration has a single fixed point given by $B(z)/A(z) = B_*(z)/A_*(z)$.*

See Appendix B for the proof. Next we turn our attention to the problem of devising on-line adaptation algorithms based on the IXN philosophy.

3.4.3 On-line adaptation of the expanded numerator

In contrast with the XN method, in which the adaptive filter's numerator $B(z)$ was updated in order to minimize the output error variance, for IXN there is no minimization objective associated to $B(z)$ but rather the goal is to fulfil the interpolation conditions (3.14). In order to clarify the development to follow, let us assume for the moment that the recursive part of the filter, namely the block $1/A(z)$, is held fixed so that we are to find an update procedure for the coefficients of $B(z)$ in order to have (3.14) at convergence. The original update proposed in [76] was

$$b_k(n+1) = b_k(n) + \mu u(n-k)e_o(n), \qquad 0 \leq k \leq L, \tag{3.32}$$

where $e_o(n) = d(n) - \hat{y}(n)$ is the output error. At any stationary point of this procedure, one must have

$$E[u(n-k)e_o(n)] = 0, \qquad 0 \leq k \leq L, \tag{3.33}$$

which is equivalent to (3.14) as desired.

Let $u_f(n) = [1/A(z)]u(n)$ and

$$\bar{\mathbf{u}}_f(n) = [\, u_f(n) \;\; u_f(n-1) \;\cdots\; u_f(n-L) \,]^T$$

so that, with the definition of $\mathbf{b}$ in (3.20), the adaptive filter output can be written as $\hat{y}(n) = \bar{\mathbf{u}}_f(n)^T\mathbf{b}$. Then (3.33) is equivalent to

$$E[\bar{\mathbf{u}}(n)\bar{\mathbf{u}}_f(n)^T]\mathbf{b} = E[\bar{\mathbf{u}}(n)d(n)]. \tag{3.34}$$

Then the update algorithm (3.32) will have a unique stationary point provided that the matrix $E[\bar{\mathbf{u}}(n)\bar{\mathbf{u}}_f(n)^T]$ is nonsingular. The AR constraint on the input signal guarantees this.

Lemma 3.7. *If $u(\cdot)$ is an autoregressive process of order not exceeding $L+1$, then the matrix*

$$\mathbf{M} = E[\bar{\mathbf{u}}(n)\bar{\mathbf{u}}_f(n)^T] = \left\langle \begin{bmatrix} 1 \\ z^{-1} \\ \vdots \\ z^{-L} \end{bmatrix}, \begin{bmatrix} 1 \\ z^{-1} \\ \vdots \\ z^{-L} \end{bmatrix}^T \frac{1}{A(z)} \right\rangle_u \tag{3.35}$$

is nonsingular, irrespective of the all-pole part $1/A(z)$.

The proof can be found in Appendix B. In order to study the convergence properties of (3.32), we resort to the ODE method. Assume that $\mathbf{M}$ is nonsingular, and let $\mathbf{b}_*$ be the solution of (3.34). Then the ODE associated to (3.32) is

$$\dot{\mathbf{b}}(t) = -\mathbf{M}(\mathbf{b}(t) - \mathbf{b}_*), \tag{3.36}$$

which is linear in $\mathbf{b}$. Thus the stationary point $\mathbf{b}_*$ is seen to be globally convergent provided that the eigenvalues of $\mathbf{M}$ have positive real parts. Observe from (3.35) that for white inputs, $\mathbf{M}$ is lower triangular with ones in the diagonal, so that the ODE (3.36) is globally convergent to $\mathbf{b}_*$. For colored inputs the situation is not so simple. A sufficient condition for global convergence is that $1/A(z)$ be an SPR transfer function. To verify this, define

$$f(z) = [\,1 \;\; z^{-1} \;\; \ldots \;\; z^{-L}\,]^T \mathbf{f},$$

with $\mathbf{f} \neq \mathbf{0}$, and note that

$$\begin{aligned}
\mathbf{f}^T \mathbf{M} \mathbf{f} &= E[f(z)u(n) \cdot \frac{f(z)}{A(z)} u(n)] = \left\langle f(z), \frac{f(z)}{A(z)} \right\rangle_u \\
&= \frac{1}{2\pi} \int_{-\pi}^{\pi} S_{uu}(e^{j\omega}) \frac{|f(e^{j\omega})|^2}{A(e^{j\omega})} d\omega \\
&= \frac{1}{2\pi} \int_{-\pi}^{\pi} S_{uu}(e^{j\omega}) |f(e^{j\omega})|^2 \mathrm{Re}\left\{ \frac{1}{A(e^{j\omega})} \right\} d\omega > 0.
\end{aligned}$$

The third line follows from the second because $S_{uu}(e^{j\omega})|f(e^{j\omega})|^2$ is an even function of ω while $\mathrm{Im}\left\{1/A(e^{j\omega})\right\}$ is an odd function of ω. Positivity of the fourth line follows because the integrand is positive for all ω if $1/A(z)$ is SPR. Now choosing the Lyapunov function $V(\mathbf{b}) = (\mathbf{b} - \mathbf{b}_*)^T (\mathbf{b} - \mathbf{b}_*)$, one has that

$$\begin{aligned}
\frac{dV(\mathbf{b})}{dt} &= \left[\frac{dV(\mathbf{b})}{d\mathbf{b}} \right]^T \cdot \frac{d\mathbf{b}}{dt} \\
&= -2(\mathbf{b} - \mathbf{b}_*)^T \mathbf{M} (\mathbf{b} - \mathbf{b}_*) \quad \begin{cases} = 0, & \mathbf{b} = \mathbf{b}_* \\ < 0, & \mathbf{b} \neq \mathbf{b}_* \end{cases}
\end{aligned}$$

and therefore $\mathbf{b} \to \mathbf{0}$ as $t \to \infty$. Then under the SPR condition on $1/A(z)$ the stationary point of the algorithm (3.32) is stable.

Fortunately, this SPR condition can be sidestepped, because being $A(z)$ part of the adaptive filter, it is known at every time instant. Then the output error $e_o(n)$ in (3.32) can be replaced by a filtered version $\bar{e}_o(n) = A(z)e_o(n)$ to obtain

$$\mathbf{b}(n+1) = \mathbf{b}(n) + \mu \bar{\mathbf{u}}(n) \bar{e}_o(n). \tag{3.37}$$

The stationary points of this algorithm are given by

$$E[\bar{\mathbf{u}}(n)\bar{e}_o(n)] = \mathbf{0}_{L+1}, \tag{3.38}$$

or equivalently

$$E[\bar{\mathbf{u}}(n)\bar{\mathbf{u}}(n)^T]\mathbf{b} = E[\bar{\mathbf{u}}(n) \cdot A(z)d(n)],$$

because $\bar{e}_o(n) = A(z)d(n) - \bar{\mathbf{u}}(n)^T \mathbf{b}$. Note that $\bar{e}_o(\cdot)$ takes the form of an equation error; the algorithm (3.38), however, is still unbiased in the presence of output

noise since the noise component in $\bar{e}_o(\cdot)$ is uncorrelated with the driving vector $\bar{\mathbf{u}}(\cdot)$. The matrix $E[\bar{\mathbf{u}}(n)\bar{\mathbf{u}}(n)^T]$ is positive definite, and therefore the solution of (3.38) is unique. Moreover, the positive definiteness of this matrix implies global convergence of (3.37) for sufficiently small μ.

However, we still have to show that the stationary point of the algorithm does not change after replacing $e_o(n)$ by $\bar{e}_o(n)$ in (3.32). Note that (3.38) is equivalent to

$$\langle A(z)H(z) - B(z), p_k(z)\rangle_u = 0, \quad 0 \leq k \leq L, \tag{3.39}$$

which means that at the stationary point $B(z)$ interpolates the first $L+1$ coefficients of the Szegö expansion of $H(z)A(z)$. One has the following result, whose proof is given in Appendix B:

Lemma 3.8. *If $u(\cdot)$ is an autoregressive process of order not exceeding $L+1$, then the interpolation conditions (3.39) imply $E[\bar{\mathbf{u}}(n)e_o(n)] = \mathbf{0}_{L+1}$.*

Therefore replacing the output error $e_o(n)$ by the filtered error $\bar{e}_o(n)$ in (3.32) leads to global convergence of the algorithm to the same stationary point.

In order to develop the algorithm (3.37) for the update of $B(z)$, we have assumed that $1/A(z)$ remained fixed in the process. This was useful for understanding the problem; however, it is desirable to adapt all the blocks simultaneously. In the next section we present two different forms in which the complete adaptive filtering process can be implemented, with all parameters being updated simultaneously. We will see that these two versions still enjoy a unique stationary point.

3.4.4 On-line adaptation of the remaining blocks

We show two possibilities for the implementation of the adaptive scheme. The first one makes use of an adaptive lattice predictor which serves as a preprocessor, while the second one is readily derived from the off-line IXN block diagram (Figure 3.4).

Consider first the adaptation of the coefficients of $A(z)$. This is done by a standard stochastic gradient descent of the cost $E[e_e^2(n)]$, where $e_e(n)$ is the 'equation error'

$$e_e(n) = A(z)\hat{y}(n) - C(z)u(n).$$

The coefficients of $1/A(z)$ are then updated by means of

$$a_k(n+1) = a_k(n) - \mu\hat{y}(n-k)e_e(n), \qquad 1 \leq k \leq M.$$

However, since $\hat{y}(n) = [B(z)/A(z)]u(n)$, the equation error $e_e(n)$ reduces to

$$e_e(n) = B(z)u(n) - C(z)u(n) = [B(z) - C(z)]u(n), \tag{3.40}$$

which shows that the FIR block labeled $A^{(k+1)}(z)$ in Figure 3.4 need not be implemented in the on-line versions. However, one still needs to implement an FIR block

with transfer function $A(z)$ in order to produce the filtered error $\bar{e}_o(n) = A(z)e_o(n)$ that drives the adaptation of $B(z)$, as discussed in section 3.4.3.

The first structure

The analysis of the previous sections suggests the use of some preprocessing device to decorrelate the input vector $\bar{\mathbf{u}}(n)$. This can be achieved by means of a lattice predictor of order L whose input is $u(\cdot)$. This predictor provides the backward prediction errors $\beta_i(n)$, $i = 0, 1, \ldots L$ associated to $u(\cdot)$, which are (up to a constant) the result of filtering $u(n)$ by the Szegö polynomials $p_i(z)$:

$$\beta_i(n) = \sigma_{\beta_i} p_i(z)u(n), \qquad i = 0, 1, \ldots, L,$$

where $\sigma^2_{\beta_i}$ is the variance of $\beta_i(n)$. Therefore these backward prediction errors are orthogonal: $E[\beta_i(n)\beta_j(n)] = \sigma_{\beta_i}\sigma_{\beta_j}\langle p_i(z), p_j(z)\rangle_u = 0$ if $i \neq j$. See Appendix C for more on the connection between lattice predictors and Szegö polynomials.

The numerator $B(z)$ is implemented as a linear combiner of the backward prediction errors:

$$B(z)u(n) = \sum_{i=0}^{L} w_i\beta_i(n) = \bar{\beta}(n)^T\bar{\mathbf{w}},$$

where $\bar{\beta}(n) = [\,\beta_0(n) \;\cdots\; \beta_L(n)\,]^T$ and $\bar{\mathbf{w}} = [\,w_0 \;\cdots\; w_L\,]^T$. Similarly, the Nth order auxiliary filter $C(z)$ would be implemented as

$$C(z)u(n) = \sum_{i=0}^{N} v_i\beta_i(n).$$

However, since the minimization of $E[e_e^2(n)]$ with $e_e(n)$ computed as in (3.40) would give $v_i = w_i$, $i = 0, 1, \ldots, N$, it makes sense to simplify the computation of $e_e(n)$ into the following form:

$$e_e(n) = \sum_{i=N+1}^{L} w_i\beta_i(n). \tag{3.41}$$

This eliminates the need for the auxiliary filter $C(z)$. The resulting structure is depicted in Figure 3.5. The algorithm can be summarized as

$$w_i(n+1) = w_i(n) + \mu\beta_i(n)\bar{e}_o(n), \qquad 0 \leq i \leq L, \tag{3.42}$$

$$a_k(n+1) = a_k(n) - \mu\hat{y}(n-k)e_e(n), \qquad 1 \leq k \leq M. \tag{3.43}$$

If the statistics of the input signal are known beforehand, the parameters of the lattice predictor can be precomputed so that there is no need to make this block adaptive. Otherwise the predictor coefficients ρ_i can be updated by means of, e.g.,

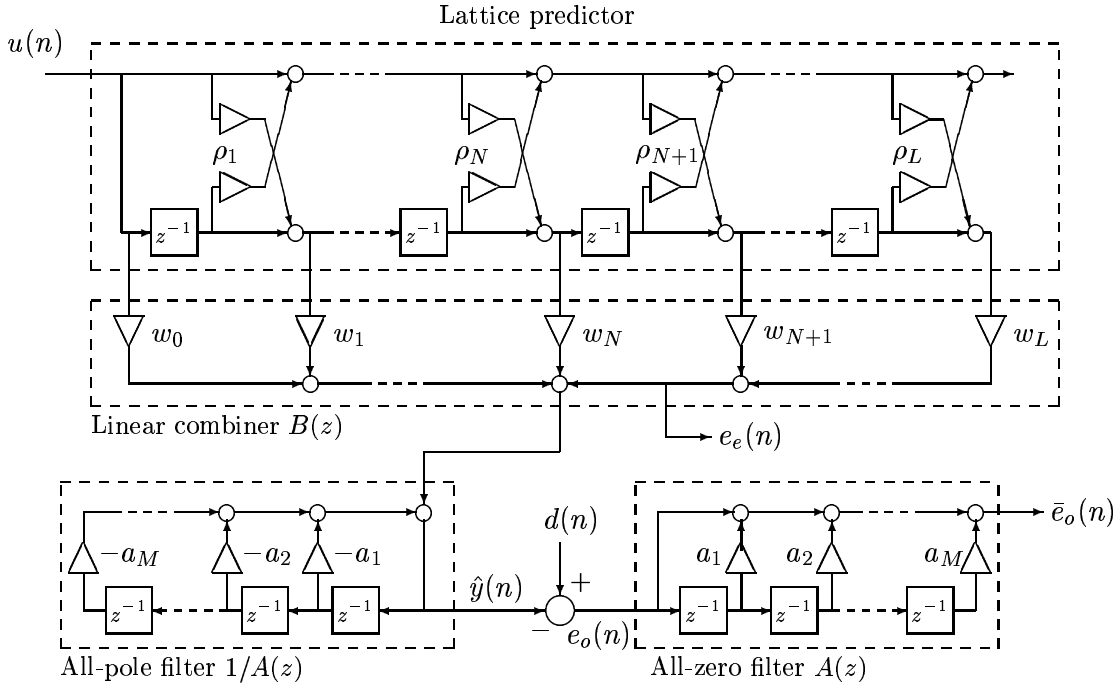

Figure 3.5: Block diagram of the first structure proposed for on-line implementation of the IXN algorithm (IXN-1).

the gradient adaptive lattice (GAL) algorithm [46]. The predictor equations are, for $i = 1, 2, \ldots, L$,

$$\begin{aligned} \alpha_0(n) &= \beta_0(n) = u(n), \\ \alpha_i(n) &= \alpha_{i-1}(n) + \rho_i \beta_{i-1}(n-1), \\ \beta_i(n) &= \beta_{i-1}(n-1) + \rho_i \alpha_i(n), \end{aligned}$$

where $\alpha_i(n)$ is the ith order forward prediction error. The adaptation of the parameters ρ_i according to the GAL algorithm is

$$\rho_i(n+1) = \rho_i(n) - \mu[\alpha_i(n)\beta_{i-1}(n-1) + \beta_i(n)\alpha_{i-1}(n-1)],$$

where each coefficient ρ_i is updated in order to minimize the combined forward-backward prediction error power $E[\alpha_i^2(n) + \beta_i^2(n)]$.

In the following analysis we assume that either the lattice predictor is fixed or it has achieved convergence. Then, the stationary points of the on-line IXN algorithm (3.42)-(3.43), which will be referred to as IXN-1 for convenience, are given by

$$E[\beta_i(n)\bar{e}_o(n)] = 0, \quad 0 \le i \le L, \qquad E[\hat{y}(n-k)e_e(n)] = 0, \quad 1 \le k \le M. \quad (3.44)$$

Observe that

$$\begin{bmatrix} \beta_0(n) \\ \vdots \\ \beta_L(n) \end{bmatrix} = \mathbf{\Lambda}_L \mathbf{C}_L \bar{\mathbf{u}}(n),$$

where

$$\mathbf{\Lambda}_k = \mathrm{diag}(\sigma_{\beta_0}, \cdots, \sigma_{\beta_k})$$

and $\mathbf{C}_L$, $\bar{\mathbf{u}}(n)$ were defined in (3.25) and (3.18) respectively. Therefore the first $L+1$ equations in (3.44) can be written as

$$\mathbf{\Lambda}_L \mathbf{C}_L E[\bar{\mathbf{u}}(n)\bar{e}_o(n)] = \mathbf{0}_{L+1} \qquad \Rightarrow \qquad E[\bar{\mathbf{u}}(n)\bar{e}_o(n)] = \mathbf{0}_{L+1}.$$

On the other hand, $e_e(n)$ is computed by means of (3.41), or alternatively $e_e(n) = \tilde{\beta}(n)^T \tilde{\mathbf{\Lambda}} \tilde{\mathbf{w}}$, where $\tilde{\beta}(n)$ was defined in (3.29), and

$$\tilde{\mathbf{\Lambda}} = \mathrm{diag}(\sigma_{\beta_{N+1}}, \cdots, \sigma_{\beta_L}), \qquad \tilde{\mathbf{w}} = [\, w_{N+1} \ \cdots \ w_L \,]^T.$$

Then the last M conditions in (3.44) can be compactly rewritten as $\mathbf{H}\tilde{\mathbf{\Lambda}}\tilde{\mathbf{w}} = \mathbf{0}_M$, where $\mathbf{H}$ is the matrix defined in (3.31). In view of Theorem 3.4 and Lemma 3.8 it follows that in sufficient order cases, if one takes $L \geq N + M$ and the input signal is AR($L+1$), then the conditions $E[\bar{\mathbf{u}}(n)\bar{e}_o(n)] = \mathbf{0}_{L+1}$, $\mathbf{H}\tilde{\mathbf{\Lambda}}\tilde{\mathbf{w}} = \mathbf{0}_M$ imply that the only stationary point of the IXN-1 algorithm (3.42)-(3.43) corresponds to identification of the unknown system.

What can be said about the convergence properties of this stationary point? If we group the filter parameters in the vector

$$\theta_d = [\, w_0 \ \cdots \ w_L \ a_1 \ \cdots \ a_M \,]^T$$

then the on-line algorithm (3.42)-(3.43) is seen to have the form $\theta_d(n+1) = \theta_d(n) + \mu F_d(\theta_d, u, d)$, where

$$F_d(\theta_d, u, d) = \begin{bmatrix} \beta_0(n)\bar{e}_o(n) \\ \vdots \\ \beta_L(n)\bar{e}_o(n) \\ -\hat{y}(n-1)e_e(n) \\ \vdots \\ -\hat{y}(n-M)e_e(n) \end{bmatrix}.$$

The associated ODE is

$$\dot{\theta_d}(t) = E\left[F_d(\theta_d, u, d)\right]_{\theta_d = \theta_d(t)}.$$

We must then check the eigenvalues of the feedback matrix

$$\mathbf{S}_d(\theta_*) = \left.\frac{\mathrm{d}E\left[F_d(\theta_d, u, d)\right]}{\mathrm{d}\theta_d}\right|_{\theta=\theta_*}$$

where θ_* is the stationary point corresponding to the identification of the unknown system. Taking the corresponding derivatives and noting that $e_e(n)$ vanishes if $\theta = \theta_*$, the matrix $\mathbf{S}_d(\theta_*)$ turns out to be

$$\mathbf{S}_d(\theta_*) = \begin{bmatrix} -\mathbf{\Lambda}_N^2 & \mathbf{0} & \mathbf{\Lambda}_N \mathbf{G}^T \\ \mathbf{0} & -\tilde{\mathbf{\Lambda}}^2 & \tilde{\mathbf{\Lambda}} \mathbf{H}^T \\ \mathbf{0} & -\mathbf{H}\tilde{\mathbf{\Lambda}} & \mathbf{0} \end{bmatrix}, \tag{3.45}$$

where $\mathbf{H}$ is the matrix obtained after substituting $\hat{y}(\cdot)$ by $d(\cdot)$ in (3.31), and

$$\mathbf{G} = E\left\{ \begin{bmatrix} d(n-1) \\ \vdots \\ d(n-M) \end{bmatrix} [\, \bar{\beta}_0(n) \; \cdots \; \bar{\beta}_N(n) \,] \right\}. \tag{3.46}$$

Now we can state:

Lemma 3.9. *Assume that the orders N and M of the model numerator and denominator match those of the unknown system. If $L \geq N + M$ and the input $u(\cdot)$ is an autoregressive process of order not exceeding $L+1$, then all the eigenvalues of the matrix $\mathbf{S}_d(\theta_*)$ given in (3.45) have strictly negative real parts.*

The proof is given in Appendix B. This result ensures local stability of the IXN-1 algorithm (3.42)-(3.43).

The second structure

A different possibility is to implement the numerator $B(z)$ directly as a tapped delay line, therefore disposing of the lattice predictor of the previous section. In that case, however, it becomes necessary to include the auxiliary filter $C(z)$ in order to compute the equation error $e_e(n)$ as in (3.40), i.e.

$$e_e(n) = \sum_{k=0}^{L} b_k u(n-k) - \sum_{k=0}^{N} c_k u(n-k).$$

This second structure, shown in Figure 3.6, is computationally less expensive than the first architecture of Figure 3.5 since the filter $C(z)$ requires $N+1$ multiplications and N additions, in contrast to $2L-1$ multiplications and $2L-1$ additions required by the lattice predictor (recall that $L \geq N + M$). On the other hand the memory requirements of the two versions are identical: Both of them use $L + 2M$ delay elements z^{-1}.

While the adaptive numerator $B(z)$ is updated in order to decorrelate the filtered error $\bar{e}_o(n)$ and the first $L + 1$ lags of the input signal $u(\cdot)$, the coefficients of $A(z)$

and the auxiliary filter $C(z)$ are updated in order to minimize $E[e_e^2(n)]$ using a standard LMS-like algorithm. The procedure can be summarized as follows:

$$b_i(n+1) = b_i(n) + \mu u(n-i)\bar{e}_o(n), \qquad 0 \le i \le L, \tag{3.47}$$

$$c_j(n+1) = c_j(n) + \mu u(n-j)e_e(n), \qquad 0 \le j \le N, \tag{3.48}$$

$$a_k(n+1) = a_k(n) - \mu \hat{y}(n-k)e_e(n), \qquad 1 \le k \le M. \tag{3.49}$$

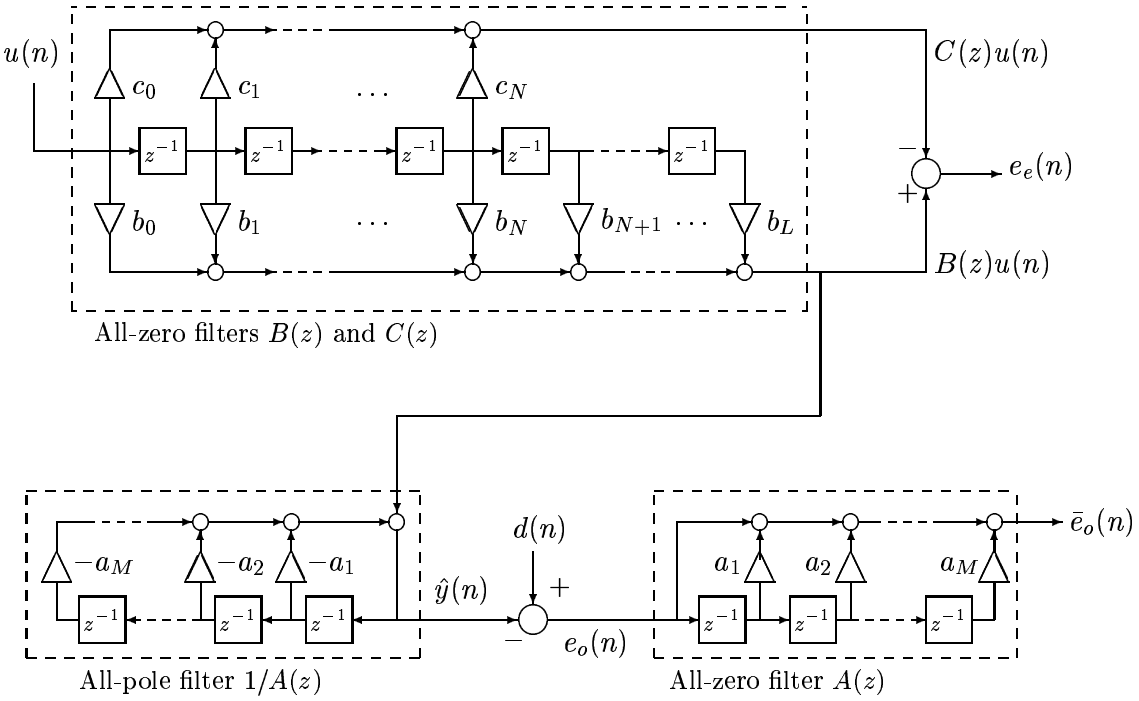

Figure 3.6: Block diagram of the second structure proposed for on-line implementation of the IXN algorithm (IXN-2).

The stationary points of this second on-line version (3.42)-(3.43) of the IXN algorithm, labeled IXN-2, are given by

$$E[u(n-i)\bar{e}_o(n)] = 0, \qquad 0 \le i \le L, \tag{3.50}$$

$$E[u(n-j)e_e(n)] = 0, \qquad 0 \le j \le N, \tag{3.51}$$

$$E[\hat{y}(n-k)e_e(n)] = 0, \quad 1 \le k \le M. \tag{3.52}$$

Eqs. (3.51)-(3.52) indicate that $A(z)$, $C(z)$ minimize the equation error variance $E[e_e^2(n)]$. Straightforward manipulation of these equations paralleling the analysis in section 3.4.2 leads to $\mathbf{H}\tilde{\mathbf{b}}' = \mathbf{0}_M$, which is the same characterization of stationary points found for the off-line IXN method in section 3.4.2. Hence, in sufficient order cases, if $L = N + M$ and $u(\cdot)$ is AR$(N + M + 1)$, then the conditions (3.50) ensure

that $\mathbf{H}$ is nonsingular by Theorem 3.3, which in turn implies that the only stationary point of the on-line IXN-2 algorithm (3.47)-(3.49) corresponds to identification of the unknown system.

It is natural to ask now whether the auxiliary filter $C(z)$ is really necessary in this architecture. That is, the error signal $e_e(n)$ could be computed in a simplified way similar to (3.41), namely

$$e_e(n) = \sum_{i=N+1}^{L} b_i u(n-i).$$

If this is done, then there is no need for $C(z)$. An analysis similar to the one in section 3.4.2 shows that, for $L = N + M$, the uniqueness of the stationary point of such algorithm relies on the invertibility of the matrix

$$E\left\{ \begin{bmatrix} \hat{y}(n-1) \\ \vdots \\ \hat{y}(n-M) \end{bmatrix} [\, u(n-N-1) \cdots u(n-L) \,] \right\}_{B(z)/A(z)=H(z)} . \tag{3.53}$$

However, this matrix can be singular in certain cases. Consider for example the case $N = M = 1$ in which $L = N + M = 2$ is taken. Suppose that the unknown system is FIR of first order, given by $H(z) = 1.01 - 0.25z^{-1}$, and that $u(\cdot)$ is a third-order AR process with $S_{uu}(z) = 1/[q(z)q(z^{-1})]$ and $q(z) = (1 - 0.25z^{-2})(1 - 0.2z^{-1})$. Then the matrix in (3.53) becomes singular, since

$$E[\hat{y}(n-1)u(n-2)]_{B(z)/A(z)=H(z)} = \langle z^{-1}H(z), z^{-2} \rangle_u = 0.$$

The failure of this simplified approach is due to the fact that the functions

$$\{\, z^{-N-1}, \ldots, z^{-L} \,\} \qquad \text{and} \qquad \{\, p_{N+1}(z), \ldots, p_L(z) \,\}$$

need not span the same subspace. Therefore in general the auxiliary filter $C(z)$ is needed for the computation of $e_e(n)$ in the IXN-2 algorithm.

In order to test local convergence of the stationary point θ_* corresponding to identification of the unknown system, one can compute the feedback matrix of the linearized ODE associated to the algorithm (3.47)-(3.49), which turns out to be

$$\mathbf{S}_d(\theta_*) = \begin{bmatrix} -E\left[\bar{\mathbf{u}}(n)\bar{\mathbf{u}}(n)^T\right] & \mathbf{0} & E\left[\bar{\mathbf{u}}(n)\mathbf{d}(n)^T\right] \\ E\left[\mathbf{u}(n)\bar{\mathbf{u}}(n)^T\right] & -E\left[\mathbf{u}(n)\mathbf{u}(n)^T\right] & \mathbf{0} \\ -E\left[\mathbf{d}(n)\bar{\mathbf{u}}(n)^T\right] & E\left[\mathbf{d}(n)\mathbf{u}(n)^T\right] & \mathbf{0} \end{bmatrix}, \tag{3.54}$$

where $\mathbf{d}(n) = [\, d(n-1) \cdots d(n-M) \,]^T$, and $\mathbf{u}(n)$, $\bar{\mathbf{u}}(n)$ have been defined in (3.16) and (3.18). The parameter vector is now given by

$$\theta_d = [\, b_0 \cdots b_L \; c_0 \cdots c_N \; a_1 \cdots a_M \,]^T.$$

Whether the eigenvalues of $\mathbf{S}_d(\theta_*)$ lie in the $\mathrm{Re}\,\lambda < 0$ semiplane remains an open issue. In all the simulations performed with the IXN-2 algorithm, the stationary point turned out to be convergent; the stable character of the matrix $\mathbf{S}_d(\theta_*)$ is therefore advanced as a conjecture.

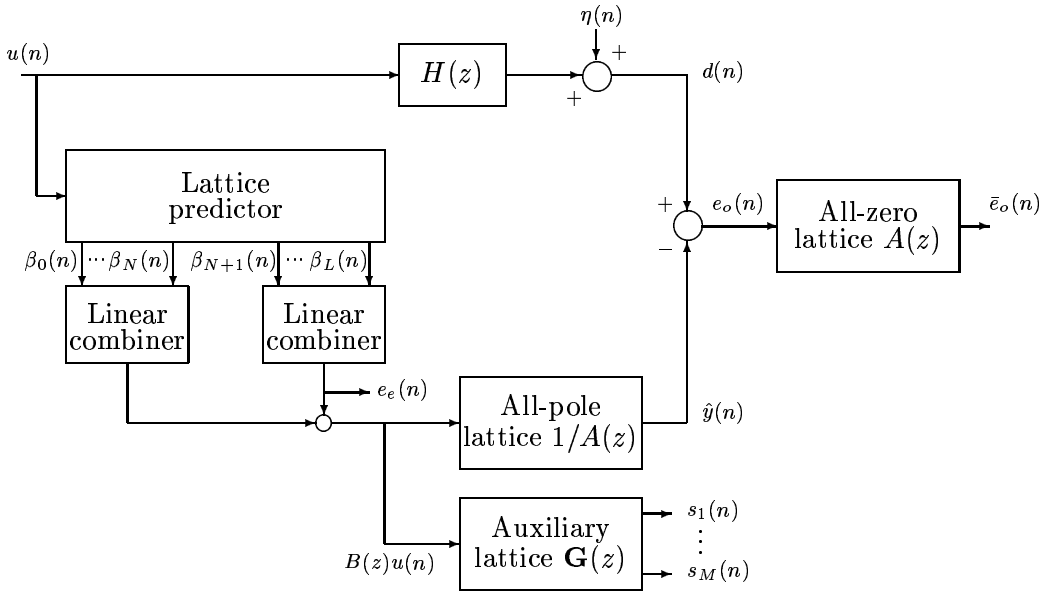

Figure 3.7: Block diagram of the first structure proposed for on-line implementation of the IXN algorithm (IXN-1) in lattice form.

Lattice implementation

So far it has been assumed that the recursive part of the adaptive filter is implemented in direct form, for both the IXN-1 and IXN-2 on-line algorithms. Using the approach of Chapter 2, it is possible to reformulate the adaptive algorithms in terms of the reflection coefficients of a lattice structure. Namely, one just needs to substitute the update formulas for the a_k parameters (3.43) or (3.49) (which are in fact identical) by

$$\sin\phi_k(n+1) = \sin\phi_k(n) - \mu s_k(n) e_e(n), \qquad 1 \le k \le M, \tag{3.55}$$

where the signals

$$s_k(n) = G_k(z)B(z)u(n) = \frac{\partial A(z)}{\partial \sin\phi_k}\frac{B(z)}{A(z)}u(n), \qquad 1 \le k \le M,$$

are generated with the aid of the structure of Figure 2.4. The block $A(z)$ required in order to compute the filtered error $\bar{e}_o(n)$ is implemented as an FIR lattice by taking advantage of the fact that the reflection coefficients for the IIR lattice $1/A(z)$ and the FIR lattice $A(z)$ are the same. The block diagrams of the resulting configurations are shown in Figures 3.7 and 3.8.

Although the stationary points of the lattice variants are the same as those of the direct form versions, it is not possible to apply Lemma 2.2 in these cases since the corresponding direct form feedback matrices do not satisfy in general

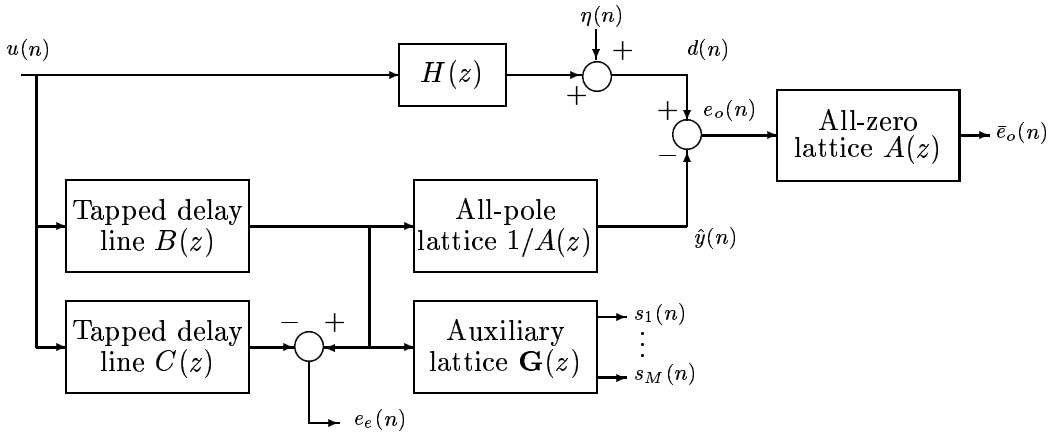

Figure 3.8: Block diagram of the second structure proposed for on-line implementation of the IXN algorithm (IXN-2) in lattice form.

$\mathbf{S}_d(\theta_*) + \mathbf{S}_d^T(\theta_*) < \mathbf{0}$. Nevertheless, as the following result states, it is still possible to show local stability of the IXN-1 lattice algorithm; The proof can be found in Appendix B.

Lemma 3.10. *Assume that the orders N and M of the model numerator and denominator match those of the unknown system $H(z)$. If $L \geq N + M$ and the input $u(\cdot)$ is an autoregressive process of order not exceeding $L + 1$, then the stationary point θ_* corresponding to the identification of $H(z)$ is locally convergent for the on-line IXN-1 lattice algorithm, given by (3.42) and (3.55).*

3.4.5 Simulation examples

In this section we present the results obtained from several computer simulations of the IXN on-line adaptive algorithms. We consider a system identification configuration in which the unknown system is a third-order filter given by

$$H(z) = \frac{1 + 0.8z^{-1} - 0.5z^{-2} + 1.5z^{-3}}{1 - 1.5z^{-1} + 1.3z^{-2} - 0.56z^{-3}}. \tag{3.56}$$

In the first example, the input $u(\cdot)$ is an AR(7) process generated by the all-pole filter $1/q(z)$ with

$$q(z) = (1 + 0.2z^{-1} + 0.6z^{-2})(1 - 0.25z^{-2})(1 - 0.5z^{-1} + 0.5z^{-2})(1 + 0.2z^{-1}) \tag{3.57}$$

when driven with unit variance white noise. The pole-zero plot of $H(z)$ and the plots of $S_{uu}(e^{j\omega})$ and $\mathrm{Re}\left\{1/A(e^{j\omega})\right\}$ are shown in Figure 3.9.

We set $N = M = 3$ and $L = N + M = 6$ in the adaptive filter, whose recursive part was implemented in normalized lattice form and adapted by means of (3.55).

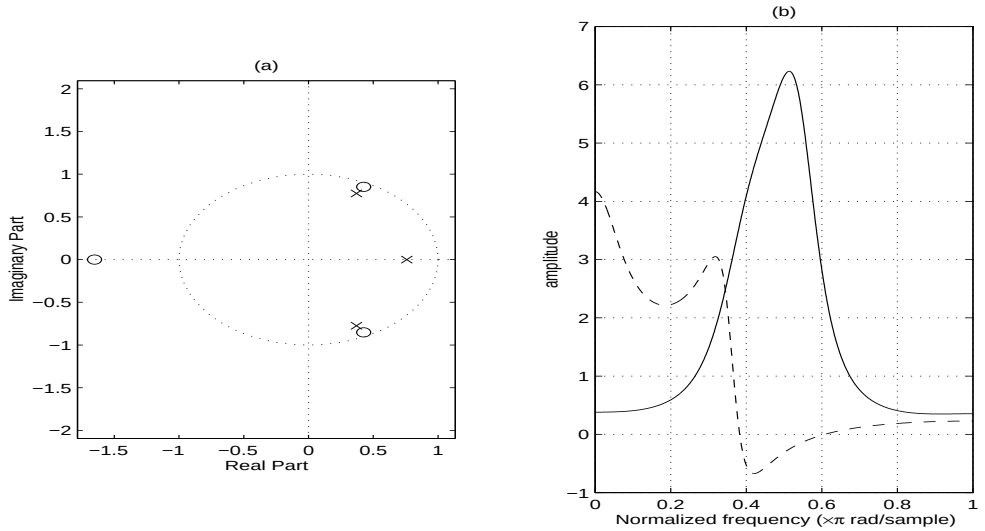

Figure 3.9: (a) Pole-zero plot of the system used in the simulations. (b) Power spectral density of the AR(7) input signal (solid) and real part of $1/A_*(e^{j\omega})$ (dashed).

First we tested the original algorithm from [76] that uses the output error $e_o(n)$ in the update term of the coefficients of $B(z)$. The value of the stepsize μ was 10^{-4}, and the reference signal $d(\cdot)$ was free of additive noise in this case. The numerator $B(z)$ was implemented as a linear combination of the backward prediction errors $\beta_i(n)$, which were generated by a fixed lattice predictor matched to $q(z)$. The reflection coefficients of this predictor are

$$[\,\rho_1 \cdots \rho_6\,] = [\,-0.0577\ 0.6455\ -0.0095\ 0.0782\ 0.0639\ -0.0665\,].$$

Figure 3.10 shows the evolution of the adaptive filter coefficients. Although these migrated initially towards a vicinity of the correct values, they failed to converge. The reason for this is that, as can be seen in Figure 3.9, the denominator $A_*(z)$ of the unknown system does not meet the SPR condition and, in addition, the input power spectral density is significant in the range of frequencies in which $\mathrm{Re}\left\{1/A_*(e^{j\omega})\right\} < 0$. This illustrates a well known fact: that although in general the SPRness of $1/A_*(z)$ is only a sufficient condition for convergence, if it is not satisfied one can usually find input signals that destabilize the corresponding algorithms.

Next we used the filtered error $\bar{e}_o(n)$ in the update of the feedforward parameters, as proposed in section 3.4.3. The reference signal $d(\cdot)$ is now corrupted by additive white noise $\eta(\cdot)$ with variance $\sigma_\eta^2 = 0.2$, which gives an SNR of 17 dB in $d(\cdot)$. Convergence of IXN-1 to the correct parameter values is achieved, supporting the previous analysis. The results are shown in Figure 3.11.

The second structure, which trades the lattice predictor for the auxiliary filter $C(z)$, was also tested in the same scenario. The results are shown in Figure 3.12. It

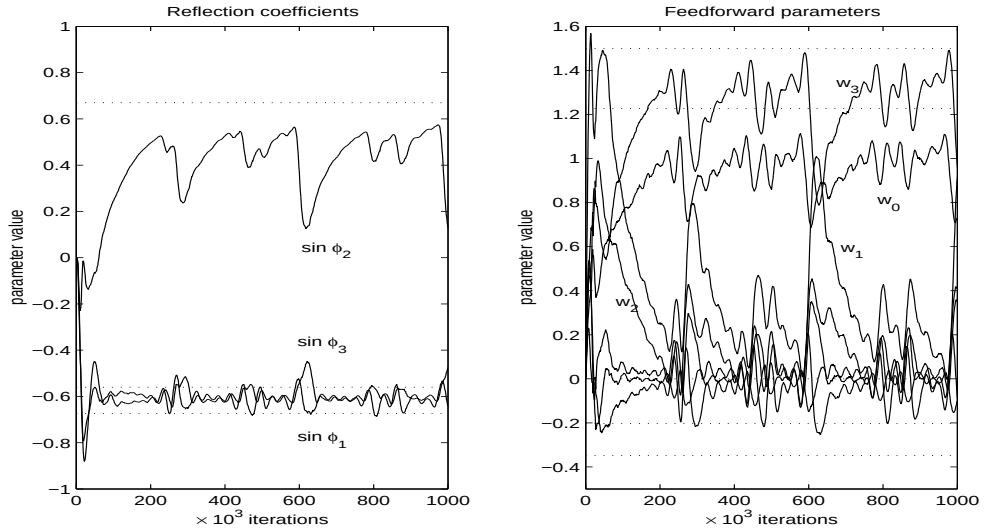

Figure 3.10: Parameter evolution in the original IXN on-line algorithm (output error update term). The dashed lines indicate the correct values. $\mu = 10^{-4}$, SNR $= \infty$, AR(7) input.

is seen that convergence of the lattice version of IXN-2 to the correct values takes place.

Finally, we present a case in which the input signal does not meet the autoregressive constraint. The unknown system $H(z)$ is the same as above, but now the input signal is an ARMA(8) process generated by the filter

$$F(z) = \frac{0.8 + 0.4z^{-6} + 0.4z^{-8}}{1 - 0.4z^{-8}}$$

driven by unit variance white noise. The first reflection coefficients of the lattice predictor matched to this ARMA(8) process are

$$[\,\rho_1 \cdots \rho_6\,] = [\,0 \;\; -0.2368 \;\; 0 \;\; 0.0594 \;\; 0 \;\; -0.3507\,].$$

The additive disturbance was generated by driving a first-order FIR filter with transfer function $0.6 + 0.48z^{-1}$ with unit variance white noise, yielding an SNR of 18 dB. Figures 3.13 and 3.14 show the parameter evolution of the IXN-1 and IXN-2 algorithms respectively. It is seen that, although in this case IXN-2 is considerably slowed down due to the presence of the measurement noise, convergence to the correct values still takes place.

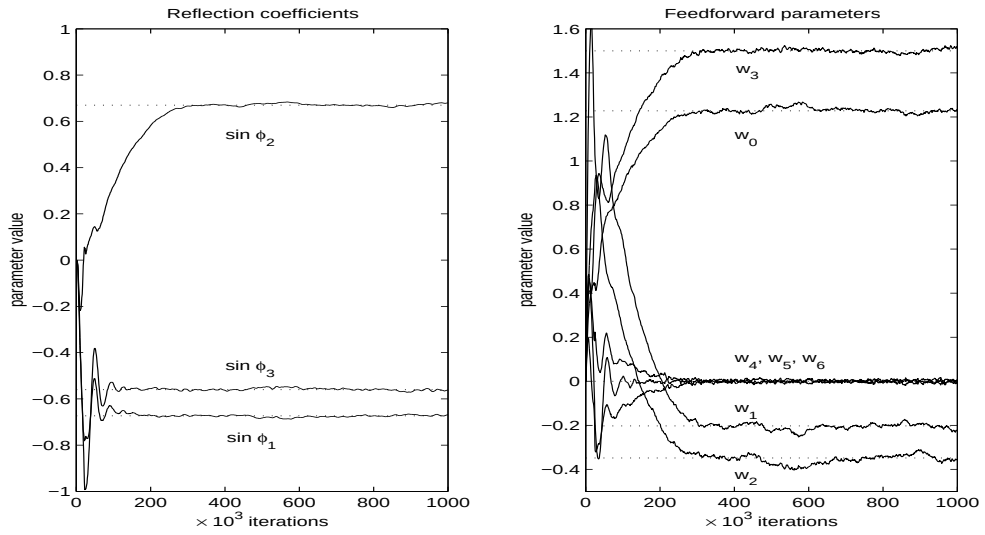

Figure 3.11: Parameter evolution with the on-line IXN-1 algorithm (fixed lattice predictor, filtered error update term). $\mu = 10^{-4}$, SNR = 17 dB, AR(7) input.

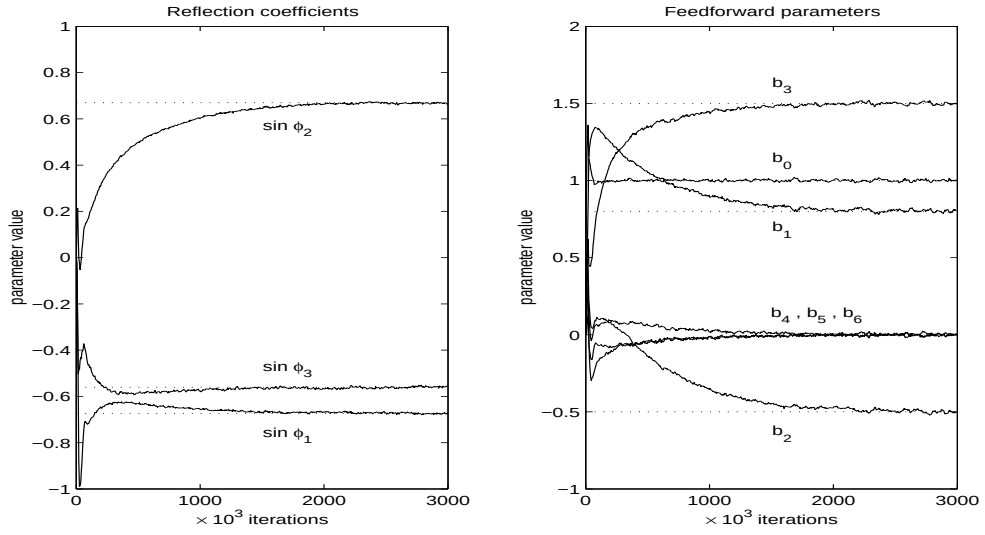

Figure 3.12: Parameter evolution with the on-line IXN-2 algorithm (without predictor, with auxiliary filter $C(z)$, and filtered error update term). $\mu = 10^{-4}$, SNR = 17 dB, AR(7) input.

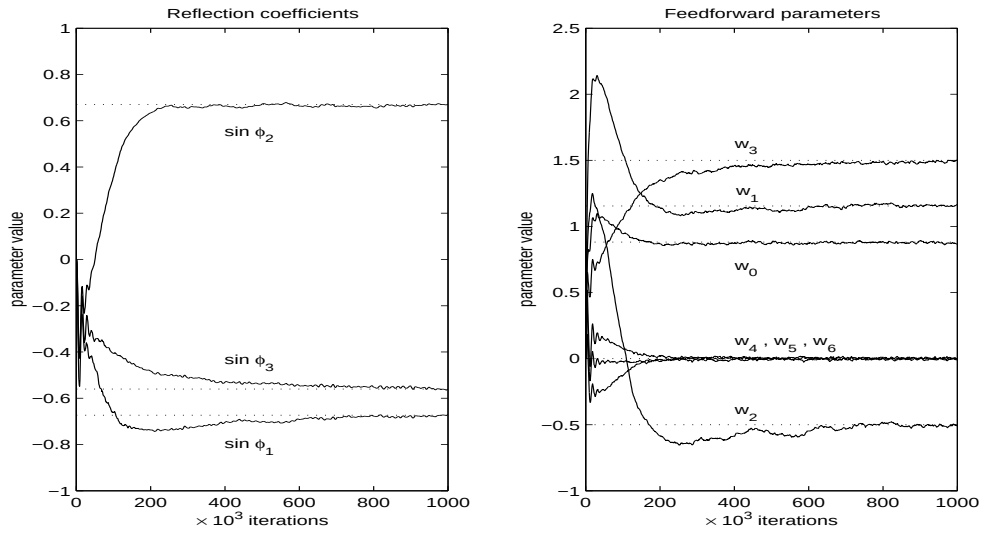

Figure 3.13: Parameter evolution with the on-line IXN-1 algorithm (fixed lattice predictor, filtered error update term). $\mu = 10^{-4}$, SNR = 18 dB, ARMA(8) input.

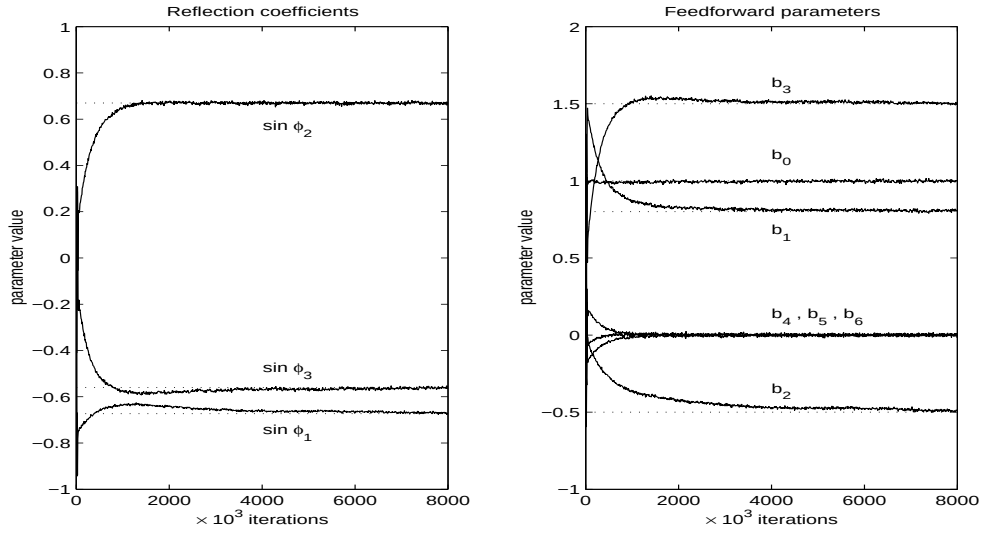

Figure 3.14: Parameter evolution with the on-line IXN-2 algorithm (without predictor, with auxiliary filter $C(z)$, and filtered error update term). $\mu = 10^{-4}$, SNR = 18 dB, ARMA(8) input.

3.4.6 Conclusions

We have presented an analysis of the interpolation expanded numerator (IXN) system identification method for colored input signals. Both off-line and on-line (in direct form and lattice implementations) approaches were discussed. The main advantages of the IXN method can be summarized as follows:

- The presence of measurement noise in the reference signal does not bias the stationary points of the algorithm, irrespectively of the spectral characteristics of the disturbance. This is in contrast with other approaches such as the Equation-Error or the Steiglitz-McBride methods.

- The uniqueness of the stationary point in the sufficient order case provided that the input signal is an autoregressive process of order not exceeding $N + M + 1$ (the number of parameters in the model). In contrast, the Mean-Squared Output Error cost function is known to be unimodal in the sufficient order case only when the input signal is white or a first-order AR process.

Finally we must emphasize that all the results obtained here apply only in the sufficient order case, i.e. it is assumed that the order of the model matches that of the unknown system $H(z)$. When this assumption is not valid, the algorithm suffers from the drawbacks of Padé-like interpolation methods: the reduced-order approximant may not exist (and then the question of convergence becomes irrelevant) or in case it does exist, it may correspond to an unstable transfer function, in which case the on-line algorithm is pushed towards the stability boundary, where it locks up. Different approaches are needed when dealing with the reduced-order case. As discussed in chapter 1, the Steiglitz-McBride method is an attractive alternative since it usually provides good approximations to the unknown system in undermodeled situations. In the next section we present a new scheme which borrows from both the Steiglitz-McBride method and the Expanded Numerator (XN) method of section 3.3.

3.5 The Steiglitz-McBride/Expanded Numerator method

In this section we present a new system identification method which can be seen as a modification of the Expanded Numerator (XN) scheme of section 3.3, in which the equation error step is performed with prefiltering, similarly to what is done in the Steiglitz-McBride method. We refer to this approach as the SM/XN method. The off-line procedure is also iterative in nature, and it is illustrated in Figure 3.15. It can be summarized as follows:

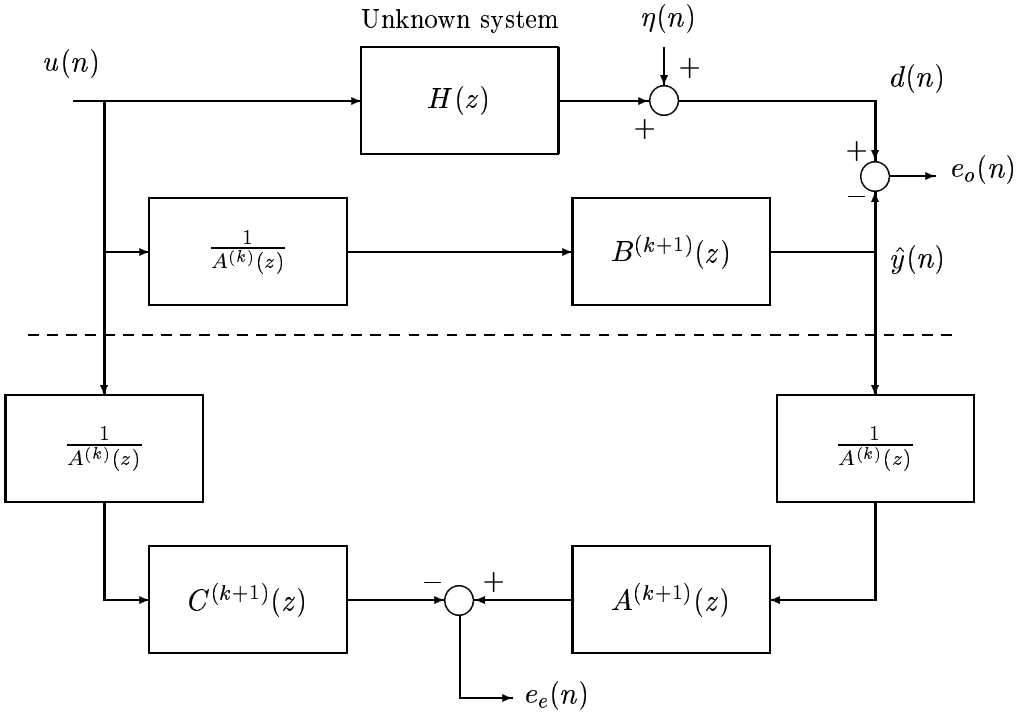

Figure 3.15: Block diagram illustrating the off-line SM/XN iteration.

1. At iteration k, the estimate $A^{(k)}(z)$ is available. Find $B^{(k+1)}(z)$ as the solution to the following minimization problem:

$$B^{(k+1)}(z) = \arg\min_{B(z)} E\left[\left|d(n) - \frac{B(z)}{A^{(k)}(z)}u(n)\right|^2\right].$$

2. Let $\hat{y}(n) = [B^{(k+1)}(z)/A^{(k)}(z)]u(n)$, and find the coefficients of the filters $C^{(k+1)}(z)$ (degree N) and $A^{(k+1)}(z)$ (degree M) by solving the equation error minimization problem

$$\left\{A^{(k+1)}(z), C^{(k+1)}(z)\right\} = \arg\min_{A(z),C(z)} E\left[\left|\frac{A(z)}{A^{(k)}(z)}\hat{y}(n) - \frac{C(z)}{A^{(k)}(z)}u(n)\right|^2\right]$$

   subject to a monic constraint on $A(z)$.

3. Discard the filter $C^{(k+1)}(z)$ and repeat the process.

Observe that the first step is identical to that of the XN off-line iteration, i.e. the adaptive filter numerator is computed at each step in order to minimize the output error variance (a quadratic minimization problem). The disturbance term $\eta(\cdot)$ cannot bias the iteration, a feature in common with the XN and IXN methods.

Also, in order for the method to evolve, the order L of $B(z)$ should again exceed the order N of the auxiliary filter $C(z)$.

In order to guarantee stability of the intermediate transfer functions, one can apply Theorem 3.1 to conclude that if the input signal $u(\cdot)$ is an autoregressive process of order not exceeding $N - M + 1$ (assuming $N \geq M - 1$), then the monic polynomials $A^{(k)}(z)$ constructed by the SM/XN iteration are minimum phase.

The question of what the length of the expanded numerator should be is addressed by the following result, whose proof can be found in Appendix B.

Lemma 3.11. *Assume $H(z) = B_*(z)/A_*(z)$ with $B_*(z)$, $A_*(z)$ coprime polynomials of orders N and M respectively, and that $L \geq N + M$. If the input signal $u(\cdot)$ is an autoregressive process of order not exceeding $N + 1$, then any stationary point $B(z)/A(z)$ of the SM/XN iteration for which $B(z)$ has order N (or less) must satisfy $B(z)/A(z) = H(z)$.*

This suggests that the order of $B(z)$ should be no less than $N + M$, similarly to what was found for the IXN method (see Lemma 3.4).

3.5.1 Stationary points

The analysis of fixed points of SM/XN can be carried out analogously to the corresponding discussion for IXN presented in section 3.4.2. Let $B(z)/A(z)$ be a SM/XN stationary point, and $\hat{y}(n) = [B(z)/A(z)]u(n)$. Define the filtered signals

$$u_f(n) = \frac{1}{A(z)}u(n), \qquad \hat{y}_f(n) = \frac{1}{A(z)}\hat{y}(n), \tag{3.58}$$

and let $\{p_k(z)\}_{k=0}^{\infty}$ be the Szegö polynomials associated to the process $u_f(\cdot)$. Also let $\beta_{f,k}(n) = p_k(z)u_f(n)$ be the kth normalized backward prediction error. One can expand $B(z)$ over the Szegö polynomials:

$$B(z) = \sum_{k=0}^{L} b'_k p_k(z).$$

By analogous computations to those in section 3.4.2, one finds that at any SM/XN fixed point the relation $\mathbf{H}_f \tilde{\mathbf{b}}' = \mathbf{0}_M$ must hold, where $\tilde{\mathbf{b}}' = [\, b'_{N+1} \cdots b'_L \,]^T$ and the matrix $\mathbf{H}_f$ is given by

$$\mathbf{H}_f = E\left\{ \begin{bmatrix} \hat{y}_f(n-1) \\ \vdots \\ \hat{y}_f(n-M) \end{bmatrix} [\, \bar{\beta}_{f,N+1}(n) \cdots \bar{\beta}_{f,L}(n) \,] \right\}. \tag{3.59}$$

Note the structural similarity between $\mathbf{H}_f$ and the matrix $\mathbf{H}$ that appeared in the analysis of the IXN method.

In the case $L = N + M$, $\mathbf{H}_f$ is $M \times M$ square. If it could be guaranteed to be invertible, then $\mathbf{H}_f \tilde{\mathbf{b}}' = \mathbf{0}_M$ would imply $\tilde{\mathbf{b}}' = \mathbf{0}_M$, and then in view of Lemma 3.11 one would have $B(z)/A(z) = H(z)$ provided that the AR$(N+1)$ condition on $u(\cdot)$ holds. This is the outline of the proof of the following result, which is given in Appendix B.

Theorem 3.5. *If $L = N + M$, the input $u(\cdot)$ is an autoregressive process of order not exceeding $N + 1$, and the unknown system satisfies $H(z) = B_*(z)/A_*(z)$ with $B_*(z)$, $A_*(z)$ coprime polynomials of orders N and M respectively, then the off-line SM/XN iteration has a single fixed point given by $B(z)/A(z) = B_*(z)/A_*(z)$.*

Observe that Theorem 3.5 requires $L = N + M$. This is in contrast with the corresponding result for the IXN method (cf. Theorem 3.4) for which $L \geq N + M$ was sufficient. The main difficulty that one encounters when trying to generalize Theorem 3.5 to $L \geq N + M$ is that the matrix $\mathbf{H}_f$ remains a function of the coefficients of the denominator $A(z)$, and hence the resulting equations are nonlinear. We believe that if $L > N+M$, the SM/XN stationary point still remains unique, although we still lack a formal proof at this time.

3.5.2 On-line implementation

In the same way in which the on-line SM, XN, IXN algorithms are derived from their off-line counterparts, we can devise an on-line form of the SM/XN method in order to update the blocks $A(z)$, $B(z)$, $C(z)$ of the adaptive system. The direct form version is given by the following update rules:

$$b_i(n+1) = b_i(n) + \mu u_f(n-i) e_o(n), \qquad 0 \leq i \leq L, \tag{3.60}$$

$$c_j(n+1) = c_j(n) + \mu u_f(n-j) e_e(n), \qquad 0 \leq j \leq N, \tag{3.61}$$

$$a_k(n+1) = a_k(n) - \mu \hat{y}_f(n-k) e_e(n), \qquad 1 \leq k \leq M, \tag{3.62}$$

where the filtered signals $u_f(\cdot)$, $\hat{y}_f(\cdot)$ are generated as in (3.58), and the error signals $e_o(\cdot)$, $e_e(\cdot)$ are given by

$$e_o(n) = d(n) - \hat{y}(n), \qquad e_e(n) = \hat{y}(n) - C(z) u_f(n).$$

The block diagram of this implementation is shown in Figure 3.16.

The stationary points of this on-line SM/XN algorithm (3.60)-(3.62) satisfy

$$E[u_f(n-i) e_o(n)] = 0, \qquad 0 \leq i \leq L, \tag{3.63}$$

$$E[u_f(n-j) e_e(n)] = 0, \qquad 0 \leq j \leq N, \tag{3.64}$$

$$E[\hat{y}_f(n-k) e_e(n)] = 0, \quad 1 \leq k \leq M. \tag{3.65}$$

Eqs. (3.64)-(3.65) indicate that $A(z)$, $C(z)$ minimize the equation error variance $E[e_e^2(n)]$. Straightforward manipulation of these equations leads to $\mathbf{H}_f \tilde{\mathbf{b}}' = \mathbf{0}_M$,

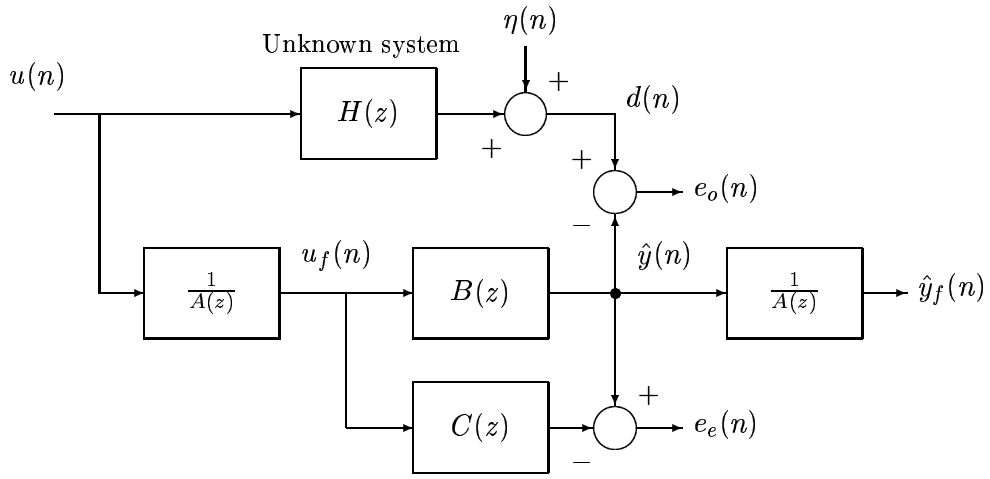

Figure 3.16: Block diagram of the on-line direct form implementation of the SM/XN algorithm.

which is the characterization of stationary points found for the off-line SM/XN method. Thus in sufficient order cases, if $L = N + M$ and $u(\cdot)$ is AR$(N+1)$, then the only stationary point of the on-line SM/XN algorithm (3.60)-(3.62) corresponds to identification of the unknown system. The feedback matrix of the linearized ODE at this stationary point is given by

$$\mathbf{S}_d(\theta_*) = \begin{bmatrix} -E\left[\bar{\mathbf{u}}_f(n)\bar{\mathbf{u}}_f(n)^T\right] & \mathbf{0} & E\left[\bar{\mathbf{u}}_f(n)\mathbf{d}_f(n)^T\right] \\ E\left[\mathbf{u}_f(n)\bar{\mathbf{u}}_f(n)^T\right] & -E\left[\mathbf{u}_f(n)\mathbf{u}_f(n)^T\right] & \mathbf{0} \\ -E\left[\mathbf{d}_f(n)\bar{\mathbf{u}}_f(n)^T\right] & E\left[\mathbf{d}_f(n)\mathbf{u}_f(n)^T\right] & \mathbf{0} \end{bmatrix}, \quad (3.66)$$

where the vectors $\bar{\mathbf{u}}_f(n)$, $\mathbf{u}_f(n)$, $\mathbf{d}_f(n)$ are given by

$$\begin{aligned} \bar{\mathbf{u}}_f(n) &= [\, u_f(n)\ u_f(n-1)\ \cdots\ u_f(n-L)\,]^T, \\ \mathbf{u}_f(n) &= [\, u_f(n)\ u_f(n-1)\ \cdots\ u_f(n-N)\,]^T, \\ \mathbf{d}_f(n) &= [\, d_f(n)\ d_f(n-1)\ \cdots\ d_f(n-M)\,]^T, \end{aligned}$$

with $d_f(n) = [1/A(z)]d(n)$, and $A(z) = A_*(z)$ (the denominator of the 'unknown' system $H(z)$) to be taken everywhere. Observe the similarity in the structures of this matrix and the corresponding feedback matrix for the IXN-2 algorithm given in (3.54). Again, whether the matrix $\mathbf{S}_d(\theta_*)$ is stable in general is left as a conjecture at this stage, although all simulation evidence suggests that this is the case.

The lattice version of the SM/XN on-line algorithm is obtained by implementing the recursive part of the adaptive filter $1/A(z)$ in normalized lattice form, and substituting (3.62) by

$$\sin\phi_k(n+1) = \sin\phi_k(n) - \mu s_k(n)e_e(n), \qquad 1 \le k \le M, \quad (3.67)$$

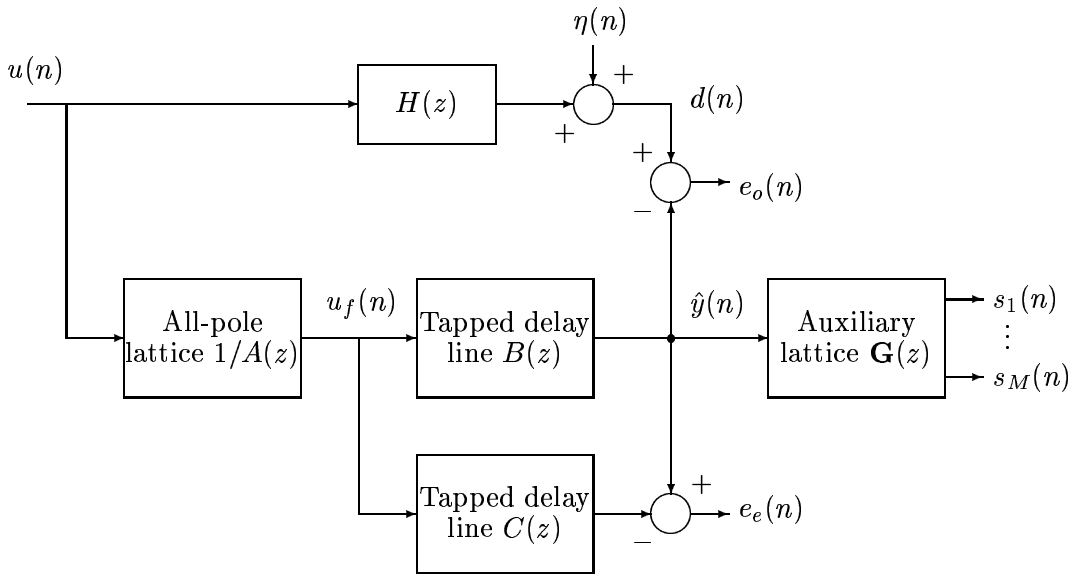

Figure 3.17: Block diagram of the on-line lattice form implementation of the SM/XN algorithm.

where now the signals

$$s_k(n) = G_k(z)\hat{y}(n) = \frac{\partial A(z)}{\partial \sin \phi_k}\hat{y}_f(n), \qquad 1 \leq k \leq M,$$

are again generated by the structure of Figure 2.4, but now driven by $\hat{y}(\cdot)$. The block diagram is shown in Figure 3.17. The feedback matrix of the linearized ODE corresponding to this lattice SM/XN algorithm is $\mathbf{S}_l(\theta_*) = \mathbf{F}^T(\theta_*)\mathbf{S}_d(\theta_*)\mathbf{F}(\theta_*)$, with $\mathbf{F}(\theta_*)$ given by

$$\mathbf{F}(\theta_*) = \begin{bmatrix} \mathbf{I}_{L+1} & \mathbf{0} & \mathbf{0} \\ \mathbf{0} & \mathbf{I}_{N+1} & \mathbf{0} \\ \mathbf{0} & \mathbf{0} & \mathbf{D}(\theta_*) \end{bmatrix}$$

and $\mathbf{D}(\theta_*)$ the Jacobian with i,jth element $\partial a_i/\partial \sin \phi_j$.

3.5.3 Simulation results

We present now several computer simulations of the SM/XN on-line adaptive algorithm. The system to be identified is the third-order $H(z)$ given in (3.56). We took $N = M = 3$ in the adaptive filter, and $L = N + M = 6$. The input signal $u(\cdot)$ was an AR(4) process generated by the all-pole filter $1/q(z)$ with

$$q(z) = (1 - 0.2z^{-1} + 0.6z^{-2})(1 - 0.5z^{-2})$$

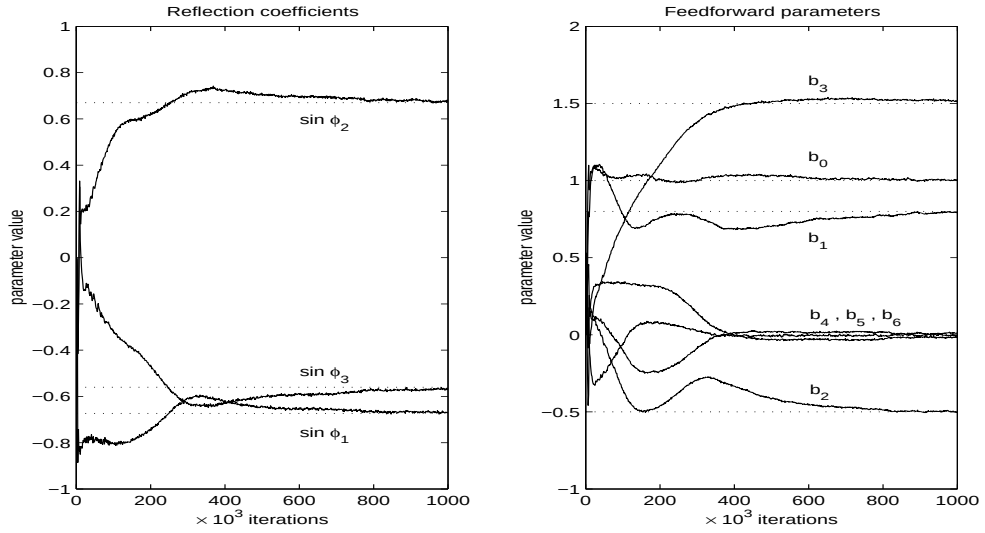

Figure 3.18: Parameter evolution with the on-line SM/XN algorithm. $\mu = 10^{-4}$, SNR = 19 dB, AR(4) input.

when driven with unit variance white noise. This setting is in the hypotheses of Theorem 3.5, so that the uniqueness of the stationary point given by $B(z)/A(z) = H(z)$ is ensured. In the simulation, additive white noise $\eta(\cdot)$ with $\sigma_\eta^2 = 0.3$ was introduced in the reference signal; the resulting SNR is 19 dB. Figure 3.18 shows the parameter evolution of the lattice SM/XN algorithm in this environment. Convergence to the correct parameters is observed.

For comparison purposes, we also include the results obtained with SM/XN in an identification setting with the same $H(z)$ but with an AR(7) input signal whose coloring filter $1/q(z)$ is given by (3.57), and with additive white noise with $\sigma_\eta^2 = 0.2$. Although this setting does not meet the requirements of Theorem 3.5, the algorithm successfully converges to the correct parameter values as shown in Figure 3.19. The results obtained by IXN-1 and IXN-2 in this scenario were shown in Figures 3.11 and 3.12 respectively.

3.5.4 Conclusions

In this section we have presented and analyzed a novel system identification method, termed Steiglitz-McBride/Expanded Numerator since it is inspired from these two schemes. We discussed both off-line and on-line versions of SM/XN. Similarly to the IXN method, the presence of an additive disturbance (white or otherwise) in the reference signal does not bias the stationary points of SM/XN. In sufficient order settings, it was shown that the stationary point is unique provided that the order of the overparameterized numerator is taken as $L = N + M$ and that the input signal is an autoregressive process of order not exceeding $N + 1$, where N

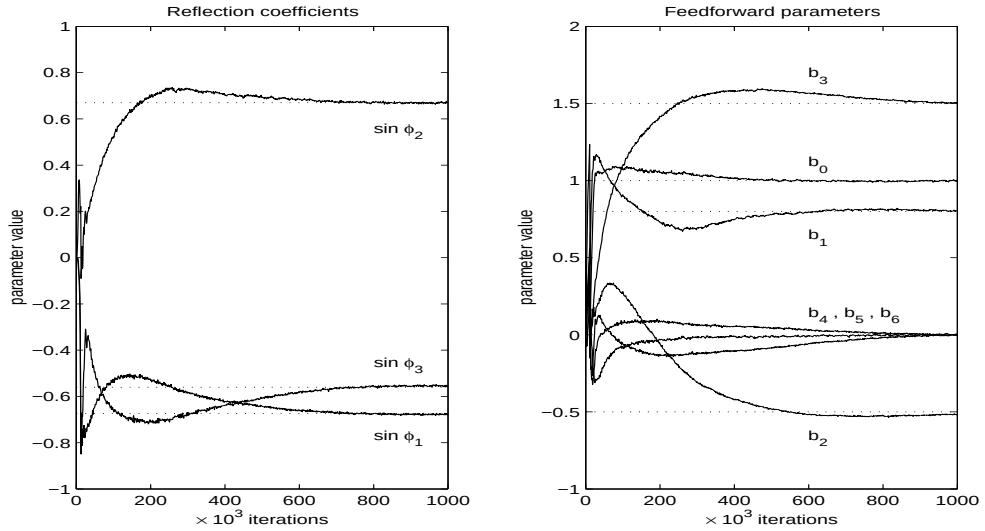

Figure 3.19: Parameter evolution with the on-line SM/XN algorithm. $\mu = 10^{-4}$, SNR = 17 dB, AR(7) input.

and M denote the number of zeros and poles, respectively, of the system to identify.

The convergence properties of the algorithm in reduced order cases strongly depend on the value of L, the order of the 'overparameterized' numerator $B(z)$. Note that at any stationary point, $B(z)$ is optimized (in terms of output error variance) as a function of the denominator $A(z)$. This means that $B(z)$ satisfies

$$\left\langle H(z) - \frac{B(z)}{A(z)}, \frac{z^{-k}}{A(z)} \right\rangle_u = 0, \qquad 0 \leq k \leq L. \tag{3.68}$$

We say then that $B(z)/A(z)$ lies on the 'reduced error surface' $J_{L,M}(\mathbf{a})$ which is defined as the value of the output error variance $E[e_o^2(n)]$ with $e_o(n) = [H(z) - B(z)/A(z)]u(n) + \eta(n)$ when $B(z)$ has order L and satisfies (3.68). Observe that $J_{L,M}(\mathbf{a})$ is a function of the denominator $A(z)$ alone, whose coefficients are comprised in the vector $\mathbf{a} = [\, a_1 \; \cdots \; a_M \,]^T$.

In addition to (3.68), at any stationary point $\mathbf{H}_f \tilde{\mathbf{b}}' = \mathbf{0}_M$ must also hold. Consider the case in which $L = N + M$. Then $\mathbf{H}_f = \mathbf{H}_f(\mathbf{a})$ is $M \times M$ square. Two classes of stationary points appear:

1. Those for which $\mathbf{H}_f(\mathbf{a})$ is invertible. In that case the corresponding vector $\tilde{\mathbf{b}}'$ must be zero.
2. Those for which $\mathbf{H}_f(\mathbf{a})$ is singular. In that case the corresponding vector $\tilde{\mathbf{b}}'$ need not be zero.

Although the possibility of having the SM/XN algorithm converge to a setting for which $\mathbf{H}_f(\mathbf{a})$ becomes singular cannot be discarded, this has never been observed

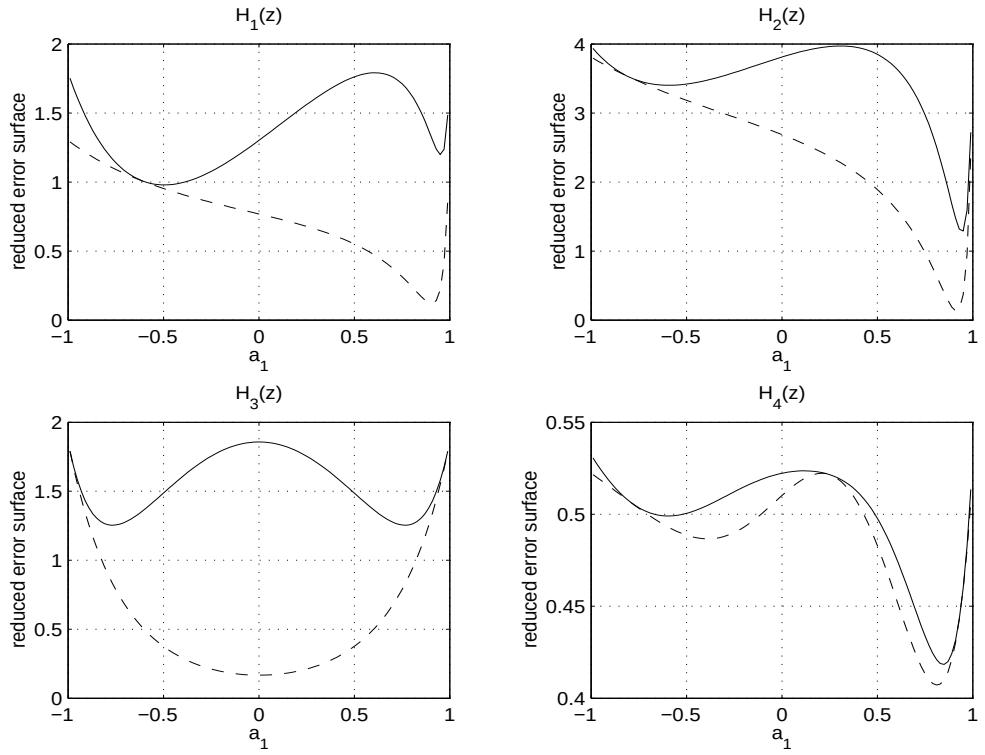

Figure 3.20: Plots of $J_{1,1}(\mathbf{a})$ (solid) and $J_{2,1}(\mathbf{a})$ (dashed) for several reduced-order cases.

in computer simulations. Therefore, let us focus on the solutions satisfying $\tilde{\mathbf{b}}' = \mathbf{0}_M$. This condition means that at the fixed point, the numerator $B(z)$ has degree N and not L. Since it also satisfies the optimality conditions (3.68), it follows that

$$J_{N,M}(\mathbf{a}) = J_{N+M,M}(\mathbf{a}), \tag{3.69}$$

i.e. any candidate stationary point must lie in the set of those points at which the reduced error surfaces computed using numerators of order N and $N+M$ touch each other (note that $J_{N,M}(\mathbf{a}) \geq J_{N+M,M}(\mathbf{a})$ for all $\mathbf{a}$). Figure 3.20 shows several examples, in which the input $u(\cdot)$ was unit-variance white noise, $N = M = 1$, and the system $H(z)$ was successively taken as

$$H_1(z) = \frac{0.5 + z^{-1} + z^{-2}}{1 + 0.6z^{-1} - 0.3z^{-2}}, \qquad H_2(z) = \frac{1 + z^{-1} + z^{-2}}{1 + 0.6z^{-1} - 0.3z^{-2}},$$
$$H_3(z) = \frac{1 + z^{-2}}{1 - 0.3z^{-2}}, \qquad H_4(z) = \frac{1 + z^{-1} + z^{-2} + z^{-3}}{1 + 0.9z^{-1} + 0.8z^{-2} + 0.4z^{-3}}.$$

For $H(z) = H_1(z)$, (3.69) has a single solution at $a_1 = -0.61$, relatively close to the global minimum of $J_{1,1}$ which is located at $a_1 = -0.49$. For $H(z) = H_2(z)$, however, the solution of (3.69), although still unique ($a_1 = -0.81$), is seen to be

near a local minimum and far from the global one. For $H(z) = H_3(z)$, $J_{1,1}$ and $J_{2,1}$ do not intersect in $|a_1| < 1$, and therefore no stationary point exists. Finally, taking $H(z) = H_4(z)$ shows that it is also possible to have several solutions, three in this case. Of these, $a_1 = -0.79$ and $a_1 = 0.9333$ turn out to be locally convergent while $a_1 = 0.25$ is repulsive.

When $L > N + M$, in general the SM/XN algorithm may have fixed points at which the last $L - N$ coefficients of the numerator $B(z)$ are nonzero. However, in view of the preceding examples, it cannot be expected that these stationary points (if any exists) provide any meaningful reduction of the output error variance besides the fact that the zeros of the model are optimized as a function of the poles.

Chapter 4

HYPERSTABLE ALGORITHMS WITH POLYPHASE AND SUBBAND STRUCTURES

We turn our attention in this chapter to adaptive IIR filtering algorithms based on hyperstability concepts, and in particular to two novel implementations that provide a means to relax the Strict Positive Real (SPR) condition that this family of algorithms requires for convergence: The polyphase structure and a decimated subband configuration. The net effect of these implementations is that the roots of the effective polynomial that must be made SPR are pulled towards the interior of the unit circle in the complex plane, by an amount that increases with the polyphase expansion factor or the decimation factor. It is well known that the closer the roots to the origin, the more likely the polynomial is to be SPR. This is the feature that makes the subband and polyphase structures appealing for the implementation of hyperstable adaptive schemes.

4.1 Polyphase structures

Hyperstability based algorithms are usually developed under a model reference approach. Along this line, let the input-output description of the system to be identified be given by

$$y(n) = H(z)u(n) = \frac{B_*(z)}{A_*(z)}u(n) \tag{4.1}$$

where $B_*(z)$ and $A_*(z)$ are coprime polynomials of degree N and M respectively. For simplicity, we shall assume throughout this chapter that $N = M$, as the case $N \neq M$ does not involve any substantial modification of the development to follow and it would only make the notation more involved. Let $\{z_i\}_{i=1}^{M}$ be the roots of the denominator $A_*(z)$, and from these define the polynomial

$$L_*(z) = \prod_{i=1}^{M} \prod_{k=1}^{P-1} (1 - z_i e^{\mathrm{j}\frac{2\pi k}{P}} z^{-1}), \tag{4.2}$$

where P is the so-called polyphase expansion factor. Observe that

$$\begin{aligned} A_*(z)L_*(z) &= \prod_{i=1}^{M}\prod_{k=0}^{P-1}(1 - z_i e^{\mathrm{j}\frac{2\pi k}{P}} z^{-1}) \\ &= \prod_{i=1}^{M}(1 - z_i^P z^{-P}) \\ &= T_*(z^P) \end{aligned} \tag{4.3}$$

only contains powers of z^{-1} which are multiples of the polyphase factor P. The P-fold polyphase form of $H(z)$ is obtained as

$$H(z) = \frac{B_*(z)L_*(z)}{A_*(z)L_*(z)} = \frac{F_*(z)}{T_*(z^P)} = \frac{f_{0*} + f_{1*}z^{-1} + \cdots + f_{MP,*}z^{-MP}}{1 + t_{1*}z^{-P} + \cdots + t_{M*}z^{-MP}}. \tag{4.4}$$

Observe that this polyphase form is unique since $L_*(z)$ is uniquely given by $H(z)$ and P. As a consequence of the overparameterization introduced, the number of parameters of the P-fold polyphase form is $MP + M + 1$, which increases linearly with P.

4.1.1 Polyphase HARF

Based on the considerations above, one can use the polyphase form for the adaptive filter, i.e.,

$$\hat{H}(z) = \frac{F(z)}{T(z^P)} = \frac{f_0 + f_1 z^{-1} + f_2 z^{-2} + \cdots + f_{MP} z^{-MP}}{1 + t_1 z^{-P} + t_2 z^{-2P} + \cdots + t_M z^{-MP}}. \tag{4.5}$$

Now we are in a position to develop the polyphase form of the Hyperstable Adaptive Recursive Filtering (HARF) algorithm. To do so, define the parameter vector $\theta(n)$ and the regressor vector $\psi(n)$ as

$$\theta(n) = \begin{bmatrix} f_0(n) \\ f_1(n) \\ \vdots \\ f_{MP}(n) \\ t_1(n) \\ t_2(n) \\ \vdots \\ t_M(n) \end{bmatrix}, \qquad \psi(n) = \begin{bmatrix} u(n) \\ u(n-1) \\ \vdots \\ u(n-MP) \\ -x(n-P) \\ -x(n-2P) \\ \vdots \\ -x(n-MP) \end{bmatrix}$$

where $x(n)$ is the *a posteriori* estimate given by $x(n) = \theta(n+1)^T\psi(n)$. With $\{c_k\}_{k=1}^m$ suitable constants, the filtered *a posteriori* error is

$$\varepsilon(n) = [y(n) - x(n)] + \sum_{k=1}^{m} c_k[y(n-k) - x(n-k)]. \tag{4.6}$$

The corresponding *a priori* quantities are the estimate $\hat{y}(n) = \theta(n)^T\psi(n)$ and the error

$$e(n) = [y(n) - \hat{y}(n)] + \sum_{k=1}^{m} c_k[y(n-k) - x(n-k)]. \tag{4.7}$$

Note that it is assumed that the unknown system output $y(n)$ is directly available, i.e. the noiseless case. The polyphase form of the HARF algorithm can be written as

$$\theta(n+1) = \theta(n) + \frac{\mu}{1 + \mu\psi(n)^T\psi(n)}\psi(n)e(n). \tag{4.8}$$

The following result applies now.

Lemma 4.1. *Let $C(z) = 1 + \sum_{k=1}^{m} c_k z^{-k}$. If the transfer function $C(z)/T_*(z^P)$ is SPR, i.e. if the system $C(z)/T_*(z^P)$ is stable and causal and*

$$Re\left\{\frac{C(e^{j\omega})}{T_*(e^{j\omega P})}\right\} > 0 \quad \forall\,\omega, \tag{4.9}$$

then the algorithm (4.8) is asymptotically stable, that is, $\varepsilon(n) \to 0$ as $n \to \infty$.

The proof can be found in Appendix B. The choice of the compensating filter $C(z)$ is open to the algorithm designer in order to satisfy the SPR condition (4.9). Note that in principle $C(z)$ could be IIR, i.e. $m = \infty$. On the other hand, if (4.9) is satisfied, then $C(z)$ has no zeros in $|z| \geq 1$ [105]. The problem of the compensating filter design when some *a priori* knowledge about $H(z)$ is available was extensively studied by Mosquera: The interested reader is referred to [86] and the references therein.

The interesting point of Lemma 4.1 is that the transfer function that should be made SPR is $C(z)/T_*(z^P)$. Note that

$$\frac{1}{T_*(z^P)} \quad \text{is SPR} \qquad \Leftrightarrow \qquad \frac{1}{T_*(z)} \quad \text{is SPR}$$

and that the roots of $T_*(z)$ are z_i^P; for stable $H(z)$, $|z_i| < 1$ so that $|z_i^P| \to 0$ as the polyphase expansion factor P increases. For example, if $H(z)$ is the discrete-time transfer function obtained by sampling a continuous-time system with a very small sampling interval, the roots z_i will tend to cluster near the point $z = 1$ in the complex plane, as discussed in section 1.1.1. Under these conditions, $1/A_*(z)$ is very unlikely to be SPR. The transformation $z_i \to z_i^P$ performed by the polyphase implementation tends to pull the roots away from this problematic region.

Figure 4.1 shows how the SPR region in root space for a second-order system varies with P. Observe that this SPR region is stretched and covers more and more of the unit disk as P is increased.

As shown in [86], it is possible to derive a lower bound for the polyphase expansion factor required in order to make $T_*(z^P)$ SPR in terms of an upper bound of

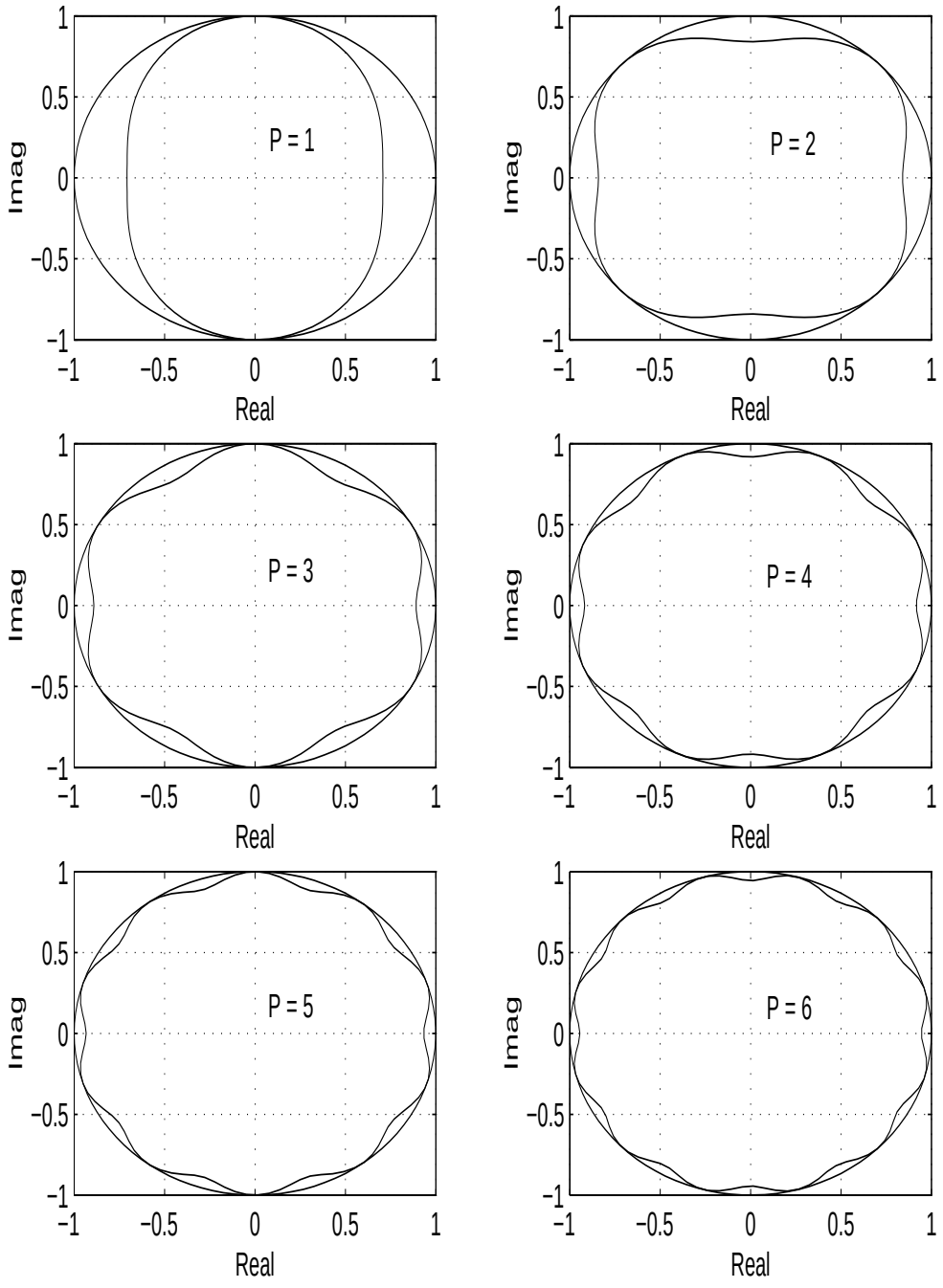

Figure 4.1: Variation of the SPR region with the polyphase expansion factor P for a second-order system.

the magnitude of the poles of the unknown system $H(z)$. If $|z_i| \leq \rho < 1$ for $i = 1, \ldots, M$, then $T_*(z^P)$ will be SPR provided that

$$P > \frac{\log(\sin \frac{\pi}{2M})}{\log \rho}.$$

Therefore, even if the compensating filter is set to $C(z) = 1$, the SPR condition can always be satisfied with a sufficiently high value of P.

Although convergence of the output error $\varepsilon(n)$ to zero is guaranteed if the SPR requirement is met, parameter convergence to the true vector θ_* is not: persistent excitation conditions on the input signal are needed. In particular, one needs that for some S,

$$\mathbf{0} < \alpha_1 \mathbf{I} < \sum_{n=j}^{j+S} \psi(n)\psi(n)^T < \alpha_2 \mathbf{I} < \infty, \qquad \forall\, j. \tag{4.10}$$

This yields convergence of $\theta(n)$ to θ_* and exponential convergence of $\varepsilon(n)$ to zero [2]. In the standard algorithm [i.e. (4.8) with $P = 1$], (4.10) is satisfied provided that the spectrum of the input signal $u(\cdot)$ (or its power spectral density) is nonzero at least at $2M+1$ different frequencies in $[0, 2\pi)$ [2]. For the polyphase form, (4.10) holds if the psd of the input signal $u(\cdot)$ is nonzero at least at $MP + M + 1$ points (the number of parameters). This can be shown using the same arguments as in [2]; loosely speaking, assume that θ has converged to a fixed value, so that we can write $\varepsilon(n) = [H(z) - \hat{H}(z)]u(n) = 0$. Since

$$H(z) - \hat{H}(z) = \frac{B_*(z)}{A_*(z)} - \frac{F(z)}{T(z^P)} = \frac{B_*(z)T(z^P) - F(z)A_*(z)}{A_*(z)T(z^P)},$$

the transfer function $H(z) - \hat{H}(z)$ has at most $(P+1)M$ zeros. If $u(\cdot)$ has nonzero frequency content at least at $MP+M+1$ points, then $\varepsilon(n) = 0$ implies $\hat{H}(z) = H(z)$. The number $MP + M + 1$ increases linearly with P, hence the price to pay for relaxing the SPR condition is a stronger persistent excitation requirement on the input signal. We must also note that the number of coefficients of the adaptive filter, and therefore the computational load associated to the algorithm, is proportional to P as well.

4.1.2 Polyphase SHARF

When noise is present in the reference signal, i.e. only $d(\cdot)$ is available with

$$d(n) = y(n) + \eta(n),$$

the stepsize μ in the HARF algorithm has to be kept small. This leads to 'slow adaptation', under which the algorithm can be simplified [53, 65]:

$$\theta(n+1) = \theta(n) + \mu\psi(n)e(n), \tag{4.11}$$

with $\psi(n)$ now simply given by

$$\psi(n) = [\, u(n)\ u(n-1)\ \cdots\ u(n-MP)\ -\hat{y}(n-M)\ \cdots\ -\hat{y}(n-MP)\,]^T.$$

As before, $\hat{y}(n) = \theta(n)^T\psi(n)$, and now the error signal is simply

$$e(n) = C(z)[d(n) - \hat{y}(n)],$$

a filtered version of the output error. It can be readily verified that

$$e(n) = \frac{C(z)}{T_*(z^P)}s(n) + C(z)\eta(n),$$

with $s(n) = \tilde{\theta}(n)^T\psi(n)$, $\tilde{\theta}(n) = \theta_* - \theta(n)$ and θ_* the vector comprising the parameters of the P-fold polyphase form of $H(z)$. For slow adaptation, we can link the convergence properties (in mean) of the algorithm to those of the associated ordinary differential equation. Following steps similar to those in [105, sec. 9.4], the ODE for (4.11) is found to be given by

$$\dot{\theta} = -\mathbf{M}(\theta)(\theta - \theta_*),$$

with

$$\mathbf{M}(\theta) = E\left[\psi(n)\cdot\frac{C(z)}{T_*(z^P)}\psi(n)^T\right].$$

Observe that the disturbance $\eta(\cdot)$ does not contribute to the ODE. This is because $\eta(\cdot)$ and the input signal $u(\cdot)$ are independent processes, and the vector $\psi(\cdot)$ contains solely filtered versions of $u(\cdot)$.

Note that if $\mathbf{M}(\theta) + \mathbf{M}(\theta)^T$ is positive definite for all θ, then global convergence of the ODE is guaranteed. The following result gives conditions for this.

Lemma 4.2. *If $C(z)/T_*(z^P)$ is SPR, the input signal $u(\cdot)$ is persistently exciting of degree at least $2MP+1$, and $\hat{H}(z)$ has degree MP or M, then $\mathbf{M}(\theta) + \mathbf{M}(\theta)^T$ is positive definite.*

Proof: Let $\mathbf{v} = [\, v_0\ \cdots\ v_{MP}\ w_1\ \cdots\ w_M\,]^T$ be a nonzero vector. Then

$$\mathbf{v}^T[\mathbf{M}(\theta) + \mathbf{M}(\theta)^T]\mathbf{v} = 2\mathbf{v}^T\mathbf{M}(\theta)\mathbf{v} = \frac{1}{\pi}\int_0^{2\pi} S_{\chi\chi}(e^{j\omega})\mathrm{Re}\left\{\frac{C(e^{j\omega})}{T_*(e^{j\omega P})}\right\}d\omega, \quad (4.12)$$

with $S_{\chi\chi}(e^{j\omega})$ the psd of the process $\chi(n) = \mathbf{v}^T\psi(n)$. Therefore, if $C(z)/T_*(z^P)$ is SPR, the quantity in (4.12) is positive provided that $\chi(\cdot)$ does not vanish identically; we must therefore find conditions under which this cannot happen. For fixed θ, $\chi(n)$ is given by

$$\chi(n) = \left[\sum_{k=0}^{PM} v_k z^{-k} + \sum_{k=1}^{M} w_k z^{-kP}\hat{H}(z)\right]u(n). \quad (4.13)$$

Since the psd of $u(\cdot)$ is nonzero at least at $2MP+1$ points, if $\chi(n)=0$ for all n then the transfer function in brackets in (4.13) must be zero. Therefore

$$z^{-P}\hat{H}(z)=\frac{v_0+v_1z^{-1}+\cdots+v_{MP}z^{-MP}}{w_1+w_2z^{-P}+\cdots+w_Mz^{-(M-1)P}}. \tag{4.14}$$

Since $\hat{H}(z)$ is causal, this implies $v_i=0$ for $0\le i\le P-1$. Thus

$$\hat{H}(z)=\frac{v_P+v_{P+1}z^{-1}+\cdots+v_{MP}z^{-(M-1)P}}{w_1+w_2z^{-P}+\cdots+w_Mz^{-(M-1)P}}=\frac{V(z)}{W(z^P)}, \tag{4.15}$$

showing that the degree of $\hat{H}(z)$ is $(M-1)P$ at most. If $\deg\hat{H}(z)=M$, then $\hat{H}(z)=B(z)/A(z)$ with $A(z)$ and $B(z)$ coprime polynomials of degree M; if

$$\frac{B(z)}{A(z)}=\frac{V(z)}{W(z^P)}$$

holds, then every root p_i of $A(z)$ must also be a root of $W(z^P)$. But then $\{p_ie^{j\frac{2\pi k}{P}}\}_{k=1}^{P-1}$ must be roots of $W(z^P)$ as well, since

$$W(z^P)\Big|_{z=p_ie^{j\frac{2\pi k}{P}}}=W(p_i^Pe^{j2\pi k})=W(p_i^P)=0.$$

Since $A(z)$ has M roots, $W(z^P)$ must have MP roots. This is impossible since $\deg W(z^P)\le(M-1)P$. ∎

Some remarks are in order now:

1. The proof required that $\hat{H}(z)$ have degree M or MP. It is reasonable to expect that during adaptation, $\deg\hat{H}(z)=MP$, and upon convergence, $\deg\hat{H}(z)=M=\deg H(z)$. However, $\hat{H}(z)$ may take the form (4.15) at some point along its trajectory, yielding $\mathbf{M}(\theta)$ singular. If by chance $\mathbf{M}(\theta)[\theta-\theta_*]=\mathbf{0}$, then $\dot{\theta}=\mathbf{0}$. Nevertheless any perturbation will destroy the specific structure (4.15), and convergence of θ toward θ_* will continue.

2. The persistent excitation degree required now on the input signal is $2MP+1$ rather than $MP+M+1$. Suppose that the latter is the actual degree. Passing from $\chi(n)=0$ for all n to (4.14) is no longer valid; but even if $\chi(n)=0$ for all n without (4.14) being true, this can cause problems only if θ assumes again a very special structure which will be lost with any small perturbation. Simulations show that persistent excitation degree of $MP+M+1$ yields convergence, as for algorithm (4.8).

3. The SPR condition has been used here to ensure convergence of the ODE, which in turn implies algorithm convergence only in a probabilistic sense. This is in contrast to the algorithm (4.8) for which the SPR condition guarantees asymptotic stability.

4.1.3 Simulation results

It is possible to implement the polyphase structure in lattice form by noting that the reflection coefficients associated to the transfer function (4.5) are all zero except for $\sin\phi_{kP}$, $1 \leq k \leq M$, because the denominator $T(z^P)$ depends only on z^P. Following the guidelines of section 2.4 one obtains the corresponding adaptive algorithm, in which the recursive part $1/T(z^P)$ is implemented in normalized lattice form and the parameter update becomes

$$f_j(n+1) = f_j(n) + \mu u(n-j)e(n), \qquad 0 \leq j \leq MP, \tag{4.16}$$

$$\sin\phi_{kP}(n+1) = \sin\phi_{kP}(n) - \mu s_{kP}(n)e(n), \qquad 1 \leq k \leq M, \tag{4.17}$$

where the signals

$$s_k(n) = G_k(z)[-B(z)u(n)] = -\frac{\partial A(z)}{\partial \sin\phi_k}\hat{y}(n), \qquad 1 \leq k \leq MP,$$

are generated by the structure of Figure 2.4, driven by $-B(z)u(n)$.

Next we show the simulation results obtained with this lattice polyphase version of SHARF in a system identification setting. The input signal was white with unit variance, and the unknown system was third-order and given by

$$H(z) = \frac{1 + 0.5z^{-1} - 0.4z^{-2} + 0.6z^{-3}}{1 - 2.34z^{-1} + 2.097z^{-2} - 0.7z^{-3}} \tag{4.18}$$

Figure 4.2 shows the pole-zero plot as well as $\mathrm{Re}\left\{1/T_*(e^{j\omega})\right\}$ for several values of the polyphase expansion factor P. It is seen that for $P = 1$ the SPR condition is not satisfied. Thus the standard SHARF algorithm with $C(z) = 1$ could be expected to present convergence problems, even in a noiseless environment. This is indeed the case, as can be seen in Figure 4.3.

For $P = 2$, the corresponding denominator is not SPR yet, but the range of frequencies in which the SPR condition is violated is much smaller than in the case $P = 1$, and the algorithm successfully converges to the true parameter values. For $P = 3$ the SPR condition is already satisfied. The evolution of the reflection coefficients is shown in Figure 4.4. Additive unit-variance white noise was included in the reference signal, yielding SNR = 20.6 dB. Observe that convergence is faster in this case using $P = 2$ than $P = 3$. This is likely attributable to the fact that the number of parameters of the adaptive filter increases linearly with P (since the numerator has degree MP). A larger number of adaptive coefficients results in a decrease in convergence speed, similarly to the FIR case [46]. Thus, there seems to be a trade-off in the choice of P between the satisfaction of the SPR condition and convergence speed.

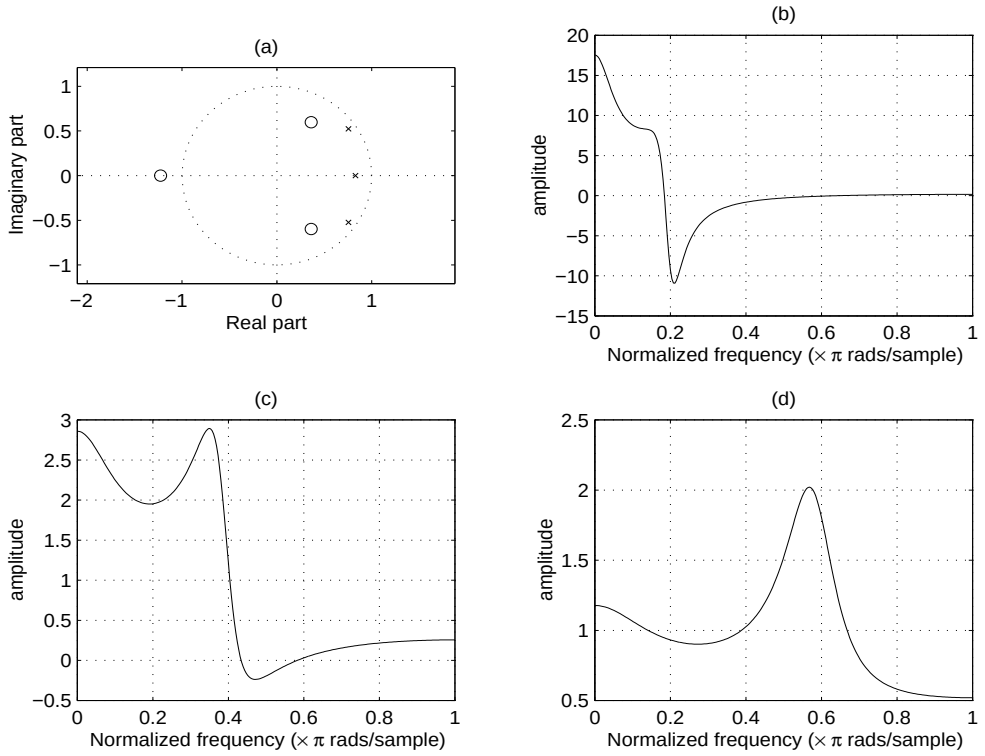

Figure 4.2: (a): Pole-zero plot of the system used in the simulations. (b), (c), (d): Real part of $1/T_*(e^{j\omega})$ for $P = 1, 2, 3$ respectively.

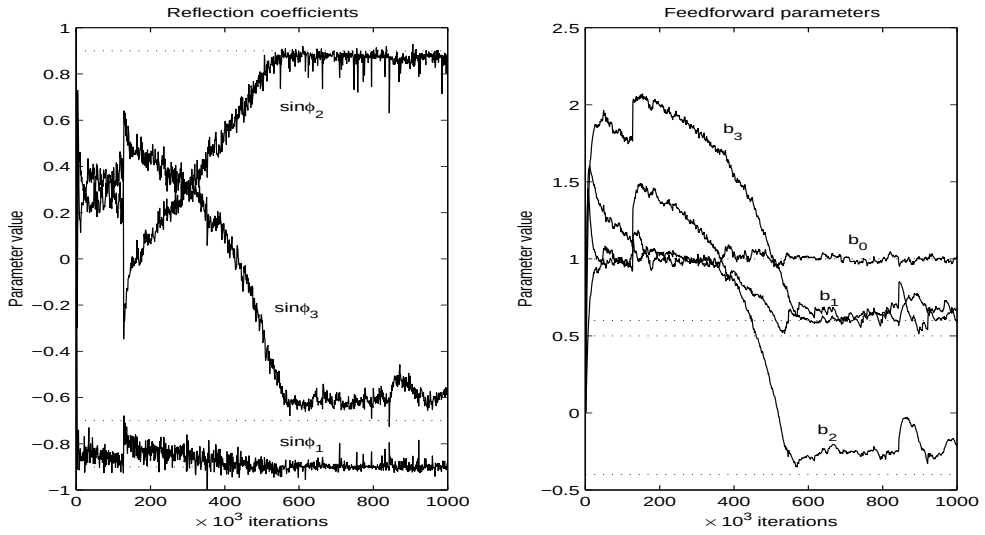

Figure 4.3: Parameter evolution with the standard SHARF algorithm (Polyphase expansion factor $P = 1$, compensating filter $C(z) = 1$). $\mu = 10^{-5}$, SNR $= \infty$.

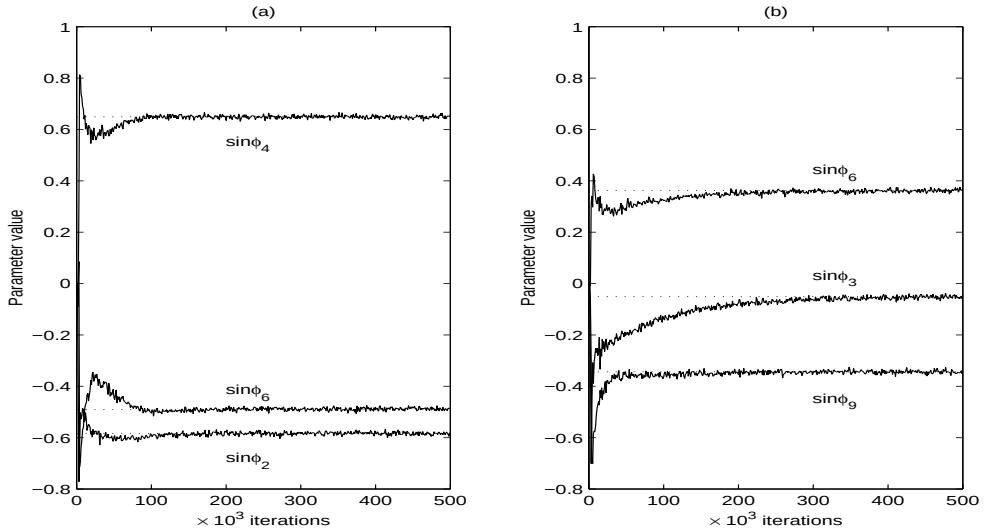

Figure 4.4: Parameter evolution of SHARF. (a) $P = 2$, (b) $P = 3$. Compensating filter $C(z) = 1$, $\mu = 10^{-4}$, SNR = 20.6 dB .

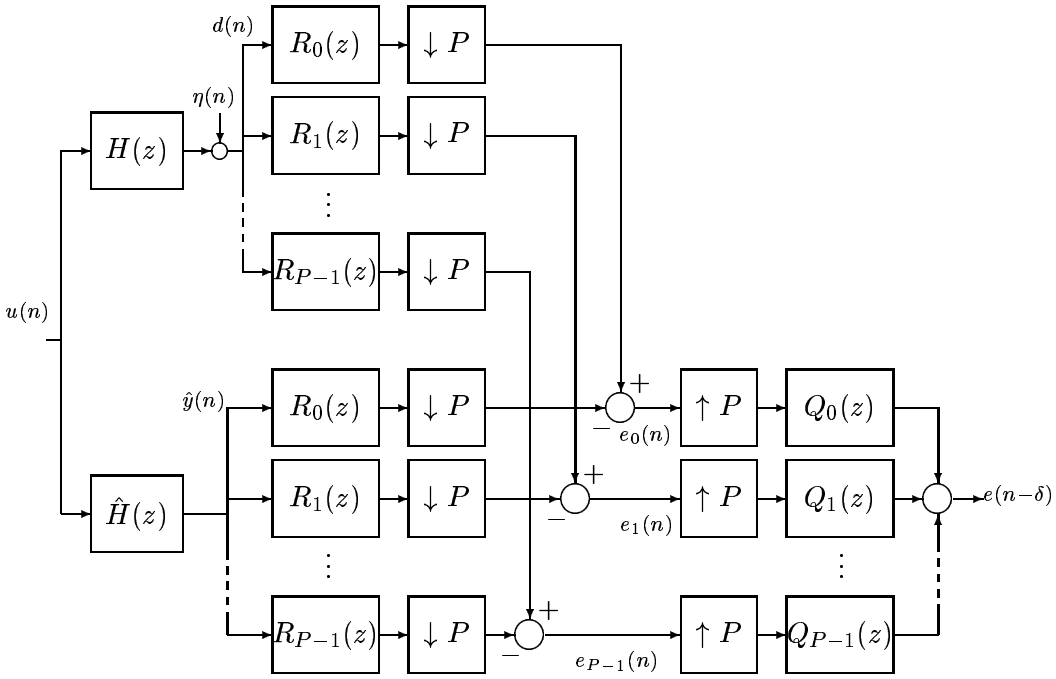

Figure 4.5: Splitting the reference and adaptive filter output signals into subbands.

4.2 Subband structures

Consider the system identification configuration of Figure 1.1 and let $e(n) = d(n) - \hat{y}(n)$ be the output error. It is possible to obtain an equivalent subband configuration, as proposed in [98] for the FIR case. To do so, the reference signal $d(\cdot)$ and the adaptive filter output $\hat{y}(\cdot)$ are split into subbands, decimated, substracted and finally combined using an adequate filterbank to form the error signal $e(\cdot)$. This is shown in Figure 4.5, where now P denotes the number of subbands, and $R_k(z)$, $Q_k(z)$, $0 \leq k \leq P-1$, are the transfer functions of the analysis and synthesis filters respectively. It is assumed that the corresponding filterbanks have the perfect reconstruction property [126], so that they only introduce an overall delay of δ samples. The sequences $e_k(\cdot)$ shown in Figure 4.5 represent the error signals in each subband.

Write $\hat{H}(z) = B(z)/A(z)$ with $A(z)$ and $B(z)$ polynomials of degree M. Similarly to the development in the previous section, one can find a polynomial $L(z)$ such that $A(z)L(z) = T(z^P)$ with $T(z)$ having degree M. This allows us to write

$$\begin{aligned}\hat{H}(z) &= \frac{B(z)L(z)}{A(z)L(z)} \\ &= \frac{F(z)}{T(z^P)} \\ &= \sum_{k=0}^{P-1} z^{-k} \frac{F_k(z^P)}{T(z^P)}\end{aligned}$$

where $F_k(z)$ has degree M for $k = 0$ and $M-1$ otherwise. We can use this representation together with the noble identities [126] to move the block $\hat{H}(z)$ in Figure 4.5 past the decimators. The resulting configuration is shown in Figure 4.6 for the case of $P = 2$ subbands.

This configuration avoids the use of cross filters (a device usually required in subband adaptive filters in order to avoid aliasing [41]) at the expense of having multiple copies of the filters $F_k(z)$ and $1/T(z)$ (one copy per subband).

4.2.1 Subband HARF

In order to derive a HARF-like adaptation algorithm for the two-band configuration, let us write

$$\begin{aligned}F_0(z) &= f_{00} + f_{01}z^{-1} + \cdots + f_{0M}z^{-M}, \\ F_1(z) &= f_{10} + f_{11}z^{-1} + \cdots + f_{1M}z^{-M}, \\ T(z) &= 1 + t_1 z^{-1} + \cdots + t_M z^{-M},\end{aligned}$$

and collect the adaptive filter coefficients in the parameter vector

$$\theta(n) = [\, f_{00}(n)\ f_{01}(n)\ \cdots\ f_{0M}(n)\ f_{10}(n)\ f_{11}(n)\ \cdots\ f_{1M}(n)\ t_1(n)\ \cdots\ t_M(n)\,]^T.$$

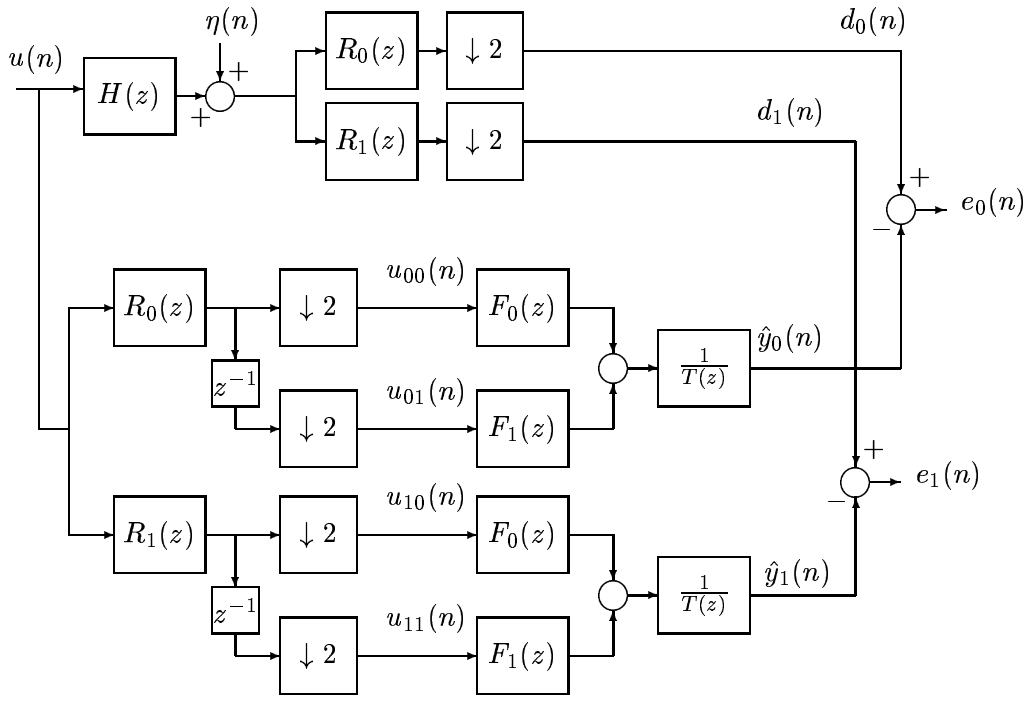

Figure 4.6: Equivalent configuration for the two-band case.

With $u_{00}(\cdot)$, $u_{01}(\cdot)$, $u_{10}(\cdot)$, $u_{11}(\cdot)$ as in Figure 4.6, define also the regressor vectors

$$\psi_0(n) = [\, u_{00}(n) \cdots u_{00}(n-M)\ u_{01}(n) \cdots u_{01}(n-M)\ -x_0(n-1) \cdots -x_0(n-M)\,]^T,$$
$$\psi_1(n) = [\, u_{10}(n) \cdots u_{10}(n-M)\ u_{11}(n) \cdots u_{11}(n-M)\ -x_1(n-1) \cdots -x_1(n-M)\,]^T,$$

where the *a posteriori* estimates $x_0(n)$, $x_1(n)$ are now given by

$$x_0(n) = \theta(n+1)^T \psi_0(n), \qquad x_1(n) = \theta(n+1)^T \psi_1(n).$$

We proceed now to develop and analyze two HARF-like adaptive schemes based on this subband decomposition. For the first algorithm, the filtered *a posteriori* error signals are defined as follows:

$$\varepsilon_i(n) = [d_i(n) - x_i(n)] + \sum_{k=1}^{m} c_k [d_i(n-k) - x_i(n-k)], \qquad i = 0, 1,$$

where $d_0(n)$, $d_1(n)$ are the subband reference signals after decimation, as shown in Figure 4.6. The corresponding *a priori* quantities are the estimates $\hat{y}_i(n) = \theta(n)^T \psi_i(n)$, $i = 0, 1$, and the error signals

$$e_i(n) = [d_i(n) - \hat{y}_i(n)] + \sum_{k=1}^{m} c_k [d_i(n-k) - x_i(n-k)], \qquad i = 0, 1.$$

The first adaptive algorithm is as follows. With α_0, α_1 positive constants, define the signals

$$\begin{aligned}\bar{\psi}(n) &= \alpha_0\psi_0(n) + \alpha_1\psi_1(n),\\ \bar{\varepsilon}(n) &= \alpha_0\varepsilon_0(n) + \alpha_1\varepsilon_1(n),\\ \bar{e}(n) &= \alpha_0 e_0(n) + \alpha_1 e_1(n).\end{aligned}$$

The update formula for the filter coefficients is then

$$\theta(n+1) = \theta(n) + \frac{\mu}{1+\mu\bar{\psi}(n)^T\bar{\psi}(n)}\bar{\psi}(n)\bar{e}(n). \tag{4.19}$$

In the case of having $P > 2$ bands, the update (4.19) remains the same; the only difference is that $\bar{\psi}(n)$, $\bar{\varepsilon}(n)$, $\bar{e}(n)$ are formed as linear combinations of the corresponding signals in the P subbands, with weights $\alpha_0, \ldots, \alpha_{P-1}$. The following result applies to this P-band case.

Lemma 4.3. *Assume that the output disturbance $\eta(\cdot)$ is absent. Let $T_*(z)$ be defined as in (4.3) and $C(z) = 1 + \sum_{k=1}^{m} c_k z^{-k}$. If the transfer function $C(z)/T_*(z)$ is SPR, then the algorithm (4.19) is asymptotically stable, that is, $\bar{\varepsilon}(n) \to 0$ as $n \to \infty$.*

See Appendix B for the proof. Observe that with this subband structure, the SPR condition is on the transfer function $C(z)/T_*(z)$, while for the polyphase architectures of section 4.1, the SPR requirement was on $C(z)/T_*(z^P)$. While having $1/T_*(z)$ SPR is equivalent to $1/T_*(z^P)$ SPR, this difference may affect the design of the compensating filter $C(z)$.

Note that the result of Lemma 4.3 does not guarantee that $\varepsilon_i(n) \to 0$ individually. This drawback can be overcome by redefining the adaptation rule, as we show now. In addition, this second adaptive algorithm offers the possibility of using different compensating filters in different subbands. Thus, let the filtered *a posteriori* error signals be now given by

$$\varepsilon_i(n) = [d_i(n) - x_i(n)] + \sum_{k=1}^{m} c_{ik}[d_i(n-k) - x_i(n-k)], \qquad i = 0, 1, \ldots, P-1,$$

while the *a priori* errors are now

$$e_i(n) = [d_i(n) - \hat{y}_i(n)] + \sum_{k=1}^{m} c_{ik}[d_i(n-k) - x_i(n-k)], \qquad i = 0, 1, \ldots, P-1.$$

Again with α_i positive constants, the update formula of the second algorithm is as follows:

$$\theta(n+1) = \theta(n) + \mu\left[\mathbf{I} + \mu\sum_{i=0}^{P-1}\alpha_i\psi_i(n)\psi_i^T(n)\right]^{-1}\left[\sum_{j=0}^{P-1}\alpha_j\psi_j(n)e_j(n)\right]. \tag{4.20}$$

Matrix inversion in (4.20) can be avoided by defining the matrices

$$\mathbf{A}_0 = \mathbf{I}, \qquad \mathbf{A}_k = \mathbf{A}_{k-1} + \mu\alpha_{k-1}\psi_{k-1}(n)\psi_{k-1}^T(n) \qquad \text{for } k > 0.$$

The matrix appearing in the algorithm (4.20) is then $\mathbf{A}_P^{-1}$. Using the matrix inversion lemma, one finds that this matrix can be recursively computed without inversion as follows:

$$\mathbf{A}_0^{-1} = \mathbf{I}, \qquad \mathbf{A}_{k+1}^{-1} = \mathbf{A}_k^{-1} - \frac{\mu\alpha_k}{1 + \mu\alpha_k\psi_k^T(n)\mathbf{A}_k^{-1}\psi_k(n)}[\mathbf{A}_k^{-1}\psi_k(n)][\mathbf{A}_k^{-1}\psi_k(n)]^T,$$

for $k = 0, \ldots, P-1$.

Application of the multivariable version of the hyperstability theorem to algorithm (4.20) gives the following result, whose proof is given in Appendix B.

Lemma 4.4. *Assume that the output disturbance $\eta(\cdot)$ is absent. Let $T_*(z)$ be defined as in (4.3) and $C_i(z) = 1 + \sum_{k=1}^m c_{ik}z^{-k}$, $0 \le i \le P-1$. If the transfer functions $C_i(z)/T_*(z)$ are SPR for $i = 0, 1, \ldots, P-1$, then the algorithm (4.20) is asymptotically stable, that is, $\varepsilon_i(n) \to 0$ as $n \to \infty$, for $0 \le i \le P-1$.*

Thus, for this second algorithm, each $C_i(z)/T_*(z)$ must be SPR in order to guarantee convergence for all inputs. Hence the ability to have different compensating filters in the different subbands does not seem to be very useful, since it would suffice to find one $C(z)$ such that $C(z)/T_*(z)$ is SPR and take $C_i(z) = C(z)$ for all i. However, this added funcionality could be helpful when one takes into account the frequency domain characteristics of the input signal $u(\cdot)$. As discussed in [1, sec. 2.6], the fullband ($P = 1$) HARF algorithm will be asymptotically stable if the real part of $C(e^{j\omega})/T_*(e^{j\omega})$ is positive just for those frequencies of $\tilde{\theta}(n+1)^T\psi(n)$ with the most energy, where $\tilde{\theta}$ denotes the parameter error vector. For small stepsize values, the frequency content of $\tilde{\theta}(n+1)^T\psi(n)$ is effectively determined by that of $u(\cdot)$. This fact is not taken into account when using the hyperstability theorem, since this only gives sufficient conditions for convergence with all classes of inputs. Similarly, in the P-band case, the real part of $C_i(e^{j\omega})/T_*(e^{j\omega})$ need be positive only for the frequencies of $\tilde{\theta}(n+1)^T\psi_i(n)$ with the most energy. Again, for small stepsize values, the frequency content of this scalar product is effectively determined by that of $u_i(\cdot)$, defined as the signal obtained from $R_i(z)u(n)$ after decimating by a factor of P.

For example, consider an input signal $u(\cdot)$ with psd $S_{uu}(z)$ as shown at the top of Figure 4.7. Also shown are the psd's of the signals $u_0(\cdot)$ and $u_1(\cdot)$ obtained in the two-band case, assuming ideal (brickwall) analysis filters $R_0(z)$ and $R_1(z)$. It is seen that if a single compensating filter $C(z)$ is used for both subbands, it should be designed in order to have $\text{Re}\left\{C(e^{j\omega})/T_*(e^{j\omega})\right\} > 0$ for $|\omega| \le 3\pi/4$. On the other hand, if different filters $C_0(z)$ and $C_1(z)$ are used, it suffices to have

$$\text{Re}\left\{\frac{C_0(e^{j\omega})}{T_*(e^{j\omega})}\right\} > 0 \qquad \text{for } |\omega| \le \tfrac{\pi}{4}, \qquad \text{Re}\left\{\frac{C_1(e^{j\omega})}{T_*(e^{j\omega})}\right\} > 0 \qquad \text{for } \tfrac{\pi}{4} \le |\omega| \le \tfrac{3\pi}{4}.$$

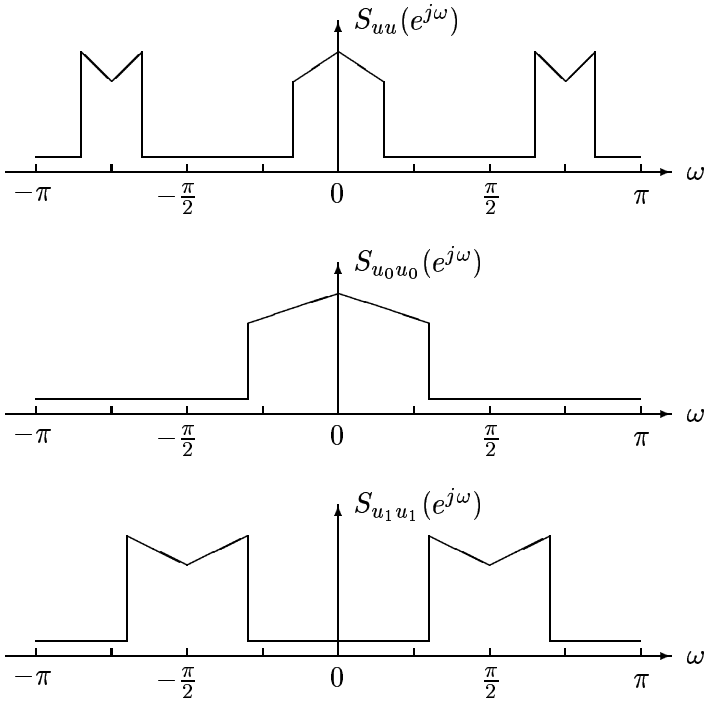

Figure 4.7: Input power spectral density example (two-band case).

Depending on the information that is available about the unknown system, the design of $C_0(z)$, $C_1(z)$ in order to satisfy these requirements could be easier than that of a single $C(z)$.

The subband implementations of the HARF algorithm do not reduce the computational complexity of the scheme with respect to the full-band design, but it has the potential of improving the convergence rate. This is because the choice of the constants α_i adds flexibility in order to emphasize the contribution of the different subbands to the parameter update. In addition, the choice of the number of subbands P provides a means to relax the SPR condition in the same way as for the polyphase structure of section 4.1.

4.2.2 Subband SHARF

Under slow adaptation, the algorithm (4.19) simplifies to the following form:

$$\theta(n+1) = \theta(n) + \mu\bar{\psi}(n)\bar{e}(n), \tag{4.21}$$

where now the regressor vector is defined as follows (in the two-band case):

$$\bar{\psi}(n) = [\,\bar{u}_0(n) \cdots \bar{u}_0(n-M)\ \bar{u}_1(n) \cdots \bar{u}_1(n-M)\ -\bar{y}(n-1) \cdots -\bar{y}(n-M)\,]^T,$$

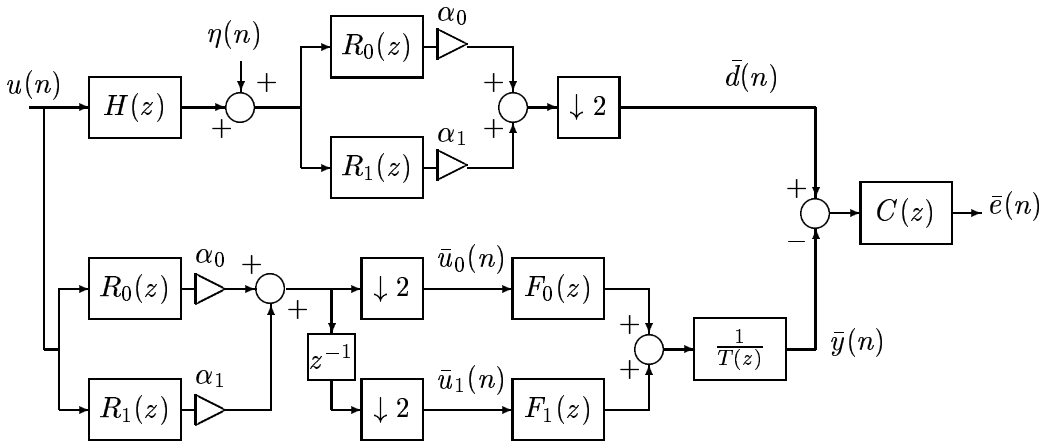

Figure 4.8: SHARF configuration for the two-band case.

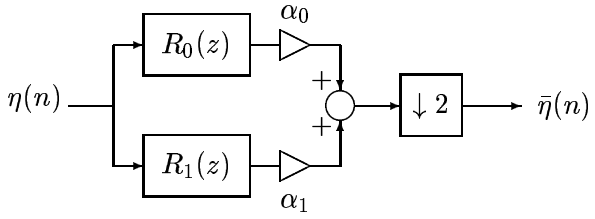

Figure 4.9: Generation of the noise component $\bar{\eta}(\cdot)$.

with $\bar{y}(n) = \theta(n)^T\bar{\psi}(n)$ and $\bar{e}(n) = C(z)[\bar{d}(n) - \bar{y}(n)]$. The signals $\bar{d}(n)$ and $\bar{u}_i(n)$ are generated as shown in Figure 4.8.

It is readily verified that the filtered error $\bar{e}(n)$ satisfies

$$\bar{e}(n) = \frac{C(z)}{T_*(z)}\bar{s}(n) + C(z)\bar{\eta}(n)$$

where $\bar{s}(n) = \tilde{\theta}(n)^T\bar{\psi}(n)$, $\tilde{\theta}(n) = \theta_* - \theta(n)$ as usual is the parameter deviation vector, and $\bar{\eta}(\cdot)$ is generated from the output disturbance $\eta(\cdot)$ as shown in Figure 4.9.

The corresponding ODE for the simplified algorithm (4.21) is found to be

$$\dot{\theta} = -\mathbf{M}(\theta)(\theta - \theta_*),$$

where now the feedback matrix $\mathbf{M}(\theta)$ is given by

$$\mathbf{M}(\theta) = E\left[\bar{\psi}(n) \cdot \frac{C(z)}{T_*(z)}\bar{\psi}(n)^T\right].$$

Again, the disturbance $\bar{\eta}(\cdot)$ does not make any contribution to the ODE, since it still is independent of the input process $u(\cdot)$. Now one would like the matrix

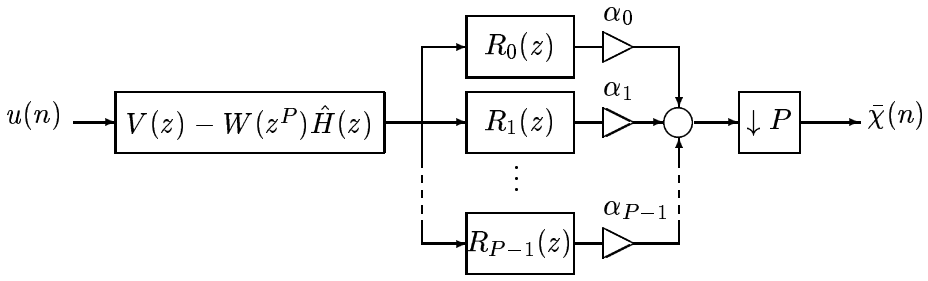

Figure 4.10: Generation of the process $\bar{\chi}(n)$.

$\mathbf{M}(\theta) + \mathbf{M}(\theta)^T$ to be positive definite for global convergence of the ODE. With

$$\mathbf{v} = [\, v_0 \; \cdots \; v_{MP} \; w_1 \; \cdots \; w_M \,]^T \tag{4.22}$$

a nonzero vector, then

$$\mathbf{v}^T[\mathbf{M}(\theta) + \mathbf{M}(\theta)^T]\mathbf{v} = \frac{1}{\pi}\int_0^{2\pi} S_{\bar{\chi}\bar{\chi}}(e^{j\omega})\mathrm{Re}\left\{\frac{C(e^{j\omega})}{T_*(e^{j\omega})}\right\} d\omega, \tag{4.23}$$

where now $S_{\bar{\chi}\bar{\chi}}(e^{j\omega})$ is the psd of $\bar{\chi}(n) = \mathbf{v}^T\bar{\psi}(n)$. Thus, if $C(z)/T_*(z)$ is SPR, then (4.23) will be positive assuming that $\bar{\chi}(\cdot)$ does not identically vanish. If we let

$$V_0(z) = \sum_{i=0}^{M} v_i z^{-i}, \tag{4.24}$$

$$V_k(z) = \sum_{i=kM+1}^{(k+1)M} v_i z^{-i}, \qquad k > 0, \tag{4.25}$$

$$V(z) = \sum_{k=0}^{P-1} z^{-k} V_k(z^P), \tag{4.26}$$

$$W(z) = \sum_{i=1}^{M} w_i z^{-i}, \tag{4.27}$$

then it is readily checked that $\bar{\chi}(n)$ is generated as shown in Figure 4.10. Now if $u(\cdot)$ is persistently exciting of degree $2MP+1$ or higher, the arguments in the proof of Lemma 4.2 show that the process $[V(z) - W(z^P)\hat{H}(z)]u(n)$ cannot be identically zero. Let $\chi(n)$ be the input to the P-fold decimator in Figure 4.10, and note that if $u(\cdot)$ is stationary then so is $\chi(\cdot)$, and therefore if $\chi(\cdot)$ does not vanish identically, neither will $\bar{\chi}(\cdot)$. If the analysis filters $R_k(z)$ are FIR with degree L, then $\chi(\cdot)$ cannot be identically zero provided that $u(\cdot)$ is persistently exciting of degree $2MP+L+1$.

We proceed now to discuss the simplification of the second subband scheme (4.20). For small μ, the term $\mathbf{I} + \mu\sum_{i=0}^{P-1}\alpha_i\psi_i(n)\psi_i^T(n)$ in (4.20) can be approxi-

mated simply by $\mathbf{I}$, so that the resulting algorithm reduces to

$$\theta(n+1) = \theta(n) + \mu \sum_{i=0}^{P-1} \alpha_i \psi_i(n) e_i(n), \tag{4.28}$$

where now the error signals are simply given by $e_i(n) = C_i(z)[d_i(n) - \hat{y}_i(n)]$. The signals $d_i(n)$ and $\hat{y}_i(n) = \theta(n)^T \psi_i(n)$ are generated as shown in Figure 4.6. Observe that the update term for this second subband algorithm can be seen as the 'average of the products' $\psi_i(n)e_i(n)$ across the subbands, while that for the first scheme (4.19) is the 'product of the averages' $\bar{\psi}(n)\bar{e}(n)$.

With $s_i(n) = (\theta_* - \theta(n))^T \psi_i(n)$, it is readily verified that the errors across the subbands satisfy

$$e_i(n) = \frac{C_i(z)}{T_*(z)} s_i(n) + C_i(z)\eta_i(n), \qquad 0 \le i \le P-1,$$

where $\eta_i(n)$ is the signal that results after decimating the filtered noise $R_i(z)\eta(n)$ by a factor of P. These noise signals do not contribute to the associated ODE, which can be written as

$$\dot{\theta} = -\left[\sum_{i=0}^{P-1} \mathbf{M}_i(\theta)\right](\theta - \theta_*),$$

where the matrices $\mathbf{M}_i(\theta)$ are given now by

$$\mathbf{M}_i(\theta) = E\left[\psi_i(n) \cdot \frac{C_i(z)}{T_*(z)} \psi_i(n)^T\right].$$

A sufficient condition for global convergence of the ODE is that $\mathbf{M}_i(\theta) + \mathbf{M}_i(\theta)^T$ be positive definite for all $0 \le i \le P-1$. Again, with $\mathbf{v}$ a nonzero vector as in (4.22), one has

$$\mathbf{v}^T[\mathbf{M}_i(\theta) + \mathbf{M}_i(\theta)^T]\mathbf{v} = \frac{1}{\pi}\int_0^{2\pi} S_{\chi_i\chi_i}(e^{j\omega}) \mathrm{Re}\left\{\frac{C_i(e^{j\omega})}{T_*(e^{j\omega})}\right\} d\omega, \tag{4.29}$$

with $S_{\chi_i\chi_i}(e^{j\omega})$ the psd of $\chi_i(n) = \mathbf{v}^T\psi_i(n)$. Therefore if $C_i(z)/T_*(z)$ is SPR, then (4.29) will be positive assuming that $\chi_i(\cdot)$ does not identically vanish. Defining $V(z)$, $W(z)$ as in (4.24)-(4.27), it is readily seen that $\chi_i(n)$ is obtained by decimating the signal $[V(z) - W(z^P)\hat{H}(z)]R_i(z)u(n)$ by a factor of P. Assuming that the analysis filters are FIR of degree L, it follows that $\chi_i(\cdot)$ cannot be identically zero if the input signal $u(\cdot)$ is persistently exciting of degree $2MP + L + 1$, which is the same requirement as for the first simplified subband scheme.

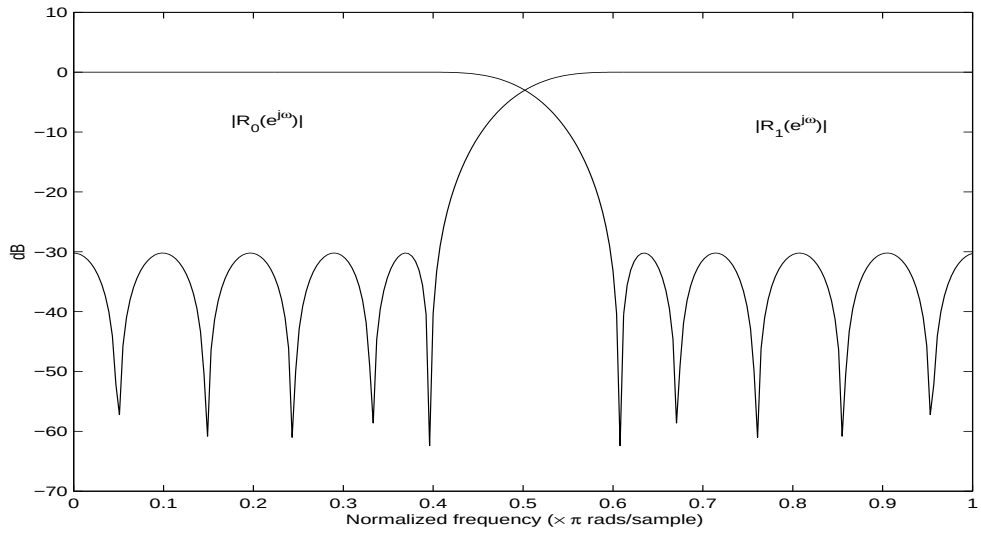

Figure 4.11: Magnitude response of the analysis filter bank used in the simulations.

4.2.3 Simulation results

We tested the two subband implementations of SHARF (4.21) and (4.28) in an identification setting in which the unknown system $H(z)$ is given by (4.18). We considered $P = 2$ subbands, with the analysis filters $R_0(z)$, $R_1(z)$ FIR of degree 19, taken from [126, design example 5.3.2] and shown in Figure 4.11. The adaptive filter denominator $T(z)$ was implemented in normalized lattice form and the adaptation of the reflection coefficients was carried out following the guidelines of section 2.4. The input signal was white with unit variance, and additive white noise was added at the output of $H(z)$ so that the SNR was 20.6 dB. The compensating filters were set at $C(z) = 1$ in all cases. As seen in section 4.1.3, the fullband version of SHARF is not convergent in this setting due to the violation of the SPR requirement. The two-band implementations, on the other hand, successfully identify the system $H(z)$. The evolution of the reflection coefficients for different values of (α_0, α_1) are shown in Figures 4.12 and 4.13. Observe how convergence is sped up if the low frequency band is given more weight than the high frequency band ($\alpha_0 > \alpha_1$), and that the adaptive process slows down in the reverse situation. This could be expected as the system $H(e^{j\omega})$ in (4.18) has most of its energy content located in the lowpass region.

The behavior of the two subband implementations is similar, although the parameter trajectories are not identical. One disadvantage of algorithm (4.28) is that it requires multiple copies of the adaptive filter (one per subband) and therefore is computationally more expensive than algorithm (4.21). Also note from Figure 4.8 that for algorithm (4.21) the analysis filterbank can be collapsed into a single filter with transfer function $\sum_{k=0}^{P-1} \alpha_k R_k(z)$, while this is not the case for algorithm (4.28). On the other hand, algorithm (4.28) offers added flexibility in that it allows

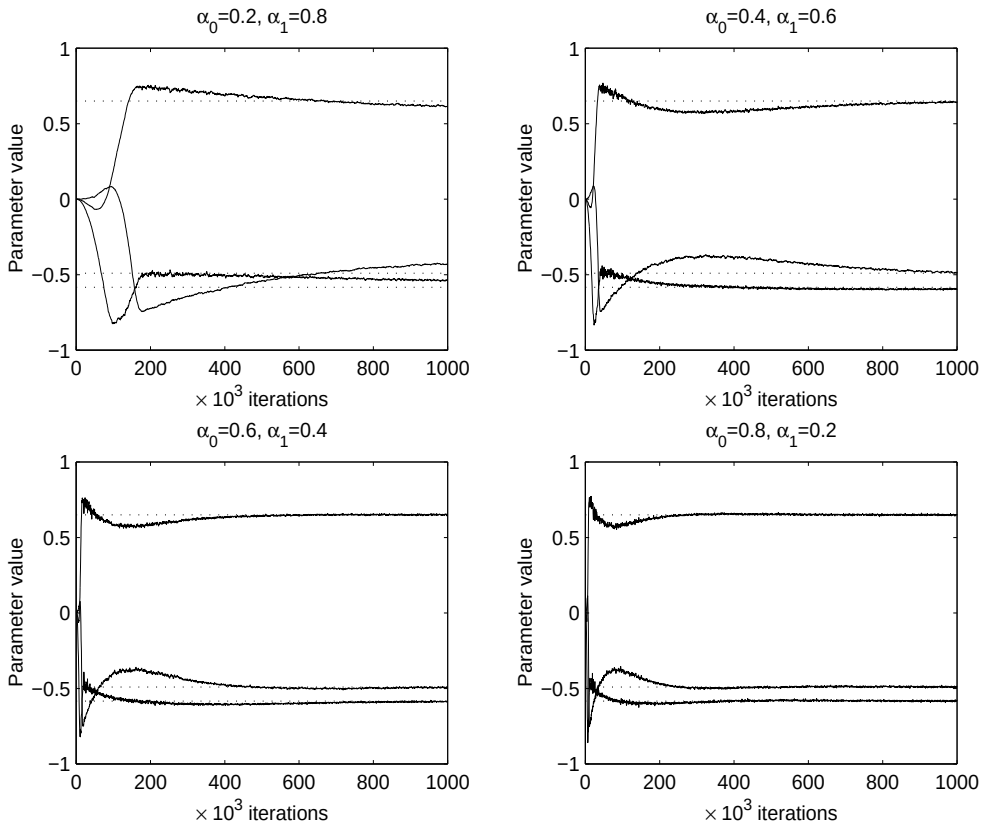

Figure 4.12: Evolution of the reflection coefficients in the two-band SHARF implementation (4.21) for different subband weights. $C(z) = 1$, $\mu = 10^{-4}$, SNR = 20.6 dB.

for different compensating filters in each subband, as discussed in section 4.2.2.

4.3 Conclusions

In this chapter two related schemes have been proposed with the goal of relaxing the SPR condition on hyperstability based adaptive algorithms. The first one is based on overparameterization of the adaptive filter by using a polyphase implementation. The second one uses a subband approach in which the input and reference signals are processed by an analysis bank and then decimated. In both cases the polynomial on which the SPR requirement falls is mapped from $A_*(z)$ (the denominator polynomial of the unknown system) which has roots $\{z_i\}_{i=1}^M$, to another one with roots $\{z_i^P\}_{i=1}^M$, where P is either the polyphase expansion factor (in the first approach) or the decimation factor (in the subband configuration). As P is increased, these roots are pulled towards the interior of the complex plane and the SPR condition is more likely to be satisfied. With the subband implementa-

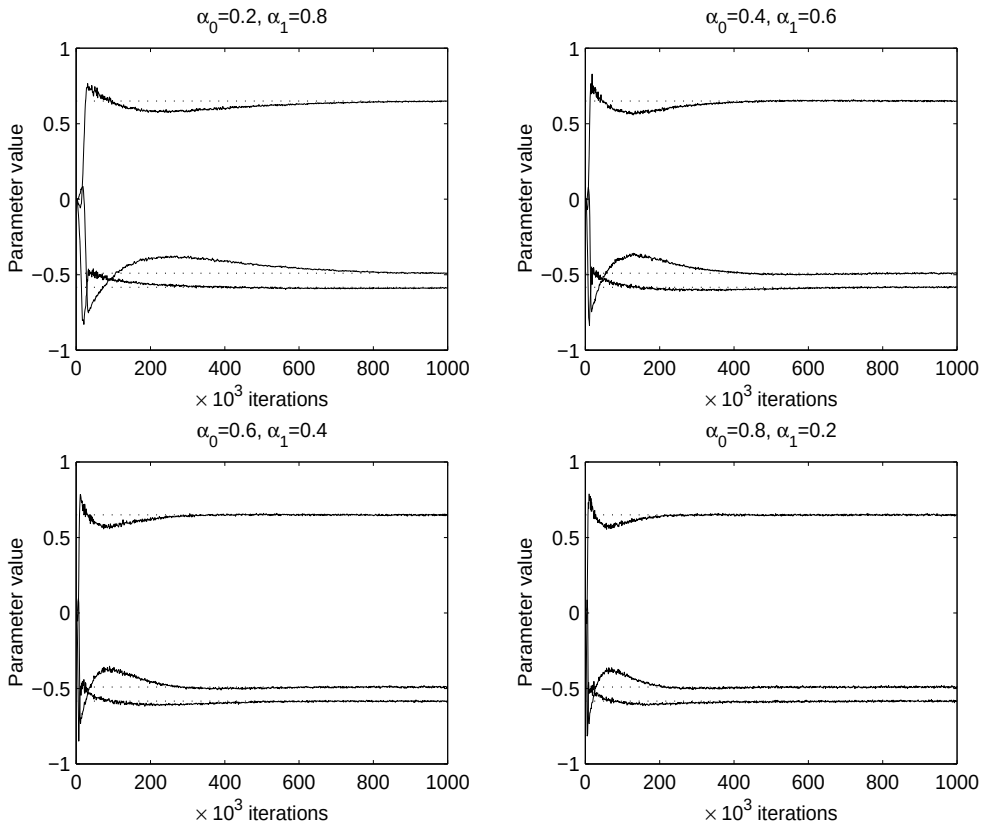

Figure 4.13: Evolution of the reflection coefficients in the two-band SHARF implementation (4.28) for different subband weights. $C(z) = 1$, $\mu = 10^{-4}$, SNR = 20.6 dB.

tion, an additional degree of flexibility is added through the capability of assigning different weights and/or compensating filters to different subbands. This has the potential of speeding up convergence if some kind of knowledge about the frequency response of the unknown system is available *a priori*.

Chapter 5

ADAPTIVE IIR FILTERS FOR CHANNEL EQUALIZATION

Recently there has been considerable interest in the use of adaptive recursive filters for channel equalization purposes, for two reasons: they have the potential to outperform conventional FIR equalizers (in terms of mean squared error), and they provide a means for unsupervised initialization of decision feedback equalizers (DFEs). These conclusions were obtained under certain assumptions (known channel order in one case, and unconstrained equalizer structure in the other) that need not be satisfied in practice. In addition, the channel equalization context is quite different from the more familiar system identification configuration, and there is no systematic approach to the adaptive IIR equalization problem available in the literature. In this chapter we develop such a framework and investigate how imperfect modeling and a constrained equalizer structure affect the conclusions drawn from the ideal case.

Up to this point it has been assumed that the input and reference signals were real valued, and that the adaptive filter had real coefficients. In digital communications it is common to find modulations of the in-phase and quadrature components of the carrier which are usually represented in the baseband discrete-time equivalent model using complex arithmetic. For this reason, in this chapter we allow the signals to take complex values, and the filters to have complex coefficients. The superscripts $(\cdot)^*$ and $(\cdot)^\dagger$ will denote conjugation and conjugate transposition respectively. With this, the weighted inner product induced by a psd $S_{uu}(z)$ is given by

$$\langle f(z), g(z) \rangle_u = \frac{1}{2\pi j} \oint S_{uu}(z) f(z) g^*(1/z^*) \frac{dz}{z},$$

the path of integration still being the unit circle in the counterclockwise direction.

We begin with a review of the minimum mean-squared error (MMSE) unconstrained equalizers, for both the linear and DFE configurations. This will show the connection between the two solutions which motivated the use of an IIR linear equalizer to initialize the DFE structure. Then we examine the situation in the more realistic case of a finitely parameterized equalizer. Two candidate algorithms for the adaptation of the recursive part will be discussed.

Throughout this chapter we consider the discrete-time baseband equivalent model of a digital transmission system sampled at the symbol rate:

$$u(n) = C(z)s(n) + \eta(n),$$

where

- $s(\cdot)$ denotes the sequence of transmitted symbols, which is assumed white with variance $E[|s(n)|^2] = \sigma_s^2$;
- $C(z)$ is the channel transfer function;
- $\eta(\cdot)$ is the channel noise, which is assumed white with variance $E[|\eta(n)|^2] = \sigma_\eta^2$;
- $u(\cdot)$ is the received signal.

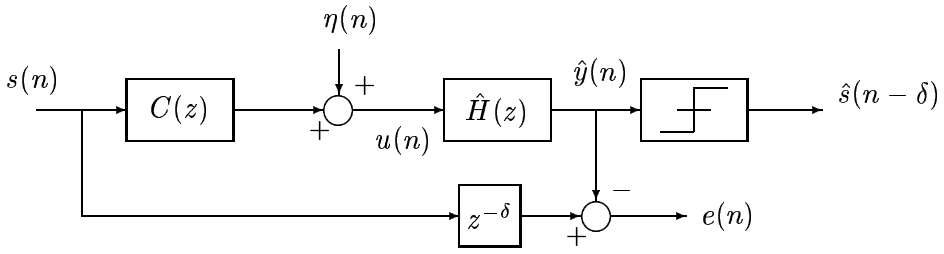

Figure 5.1: Linear equalization.

5.1 Unconstrained MMSE equalizers: a review

5.1.1 Linear equalizer

In a linear equalization configuration, the received signal $u(\cdot)$ is fed to the equalizer, which is a linear filter with transfer function $\hat{H}(z)$. The goal is to minimize the variance of the error $e(n) = s(n-\delta) - \hat{H}(z)u(n)$, where δ is the associated delay. If the filter is assumed to be unconstrained (that is, the impulse response of $\hat{H}(z)$ is allowed to span the whole set of integers from $-\infty$ to $+\infty$), then the optimum linear equalizer (MMSE-LE) is given by (see e.g. [66])

$$\hat{H}_{LE}(z) = \sigma_s^2 z^{-\delta} \frac{C^*(1/z^*)}{S_{uu}(z)}. \tag{5.1}$$

Here $S_{uu}(z)$ is the psd of the observed signal $u(\cdot)$, given by

$$\begin{aligned} S_{uu}(z) &= \sigma_s^2 C(z)C^*(1/z^*) + \sigma_\eta^2 \\ &= \gamma^2 F(z)F^*(1/z^*), \end{aligned} \tag{5.2}$$

with $F(z)$ the monic minimum phase spectral factor. Hence (5.1) can be rewritten as

$$\hat{H}_{LE}(z) = \frac{1}{F(z)}\left[z^{-\delta}\frac{\sigma_s^2 C^*(1/z^*)}{\gamma^2 F(1/z^*)}\right] = \frac{1}{F(z)}\cdot\hat{P}_{LE}(z). \tag{5.3}$$

Observe that $\hat{H}_{LE}(z)$ can be seen as the series interconnection of a whitening filter $1/F(z)$ (since the signal $[1/F(z)]u(n)$ is white) and a block with transfer function

$$\hat{P}_{LE}(z) = z^{-\delta}\frac{\sigma_s^2 C^*(1/z^*)}{\gamma^2 F^*(1/z^*)}, \tag{5.4}$$

which in principle is noncausal. The presence of the whitening filter is a feature that we will encounter as well in the constrained equalizer case.

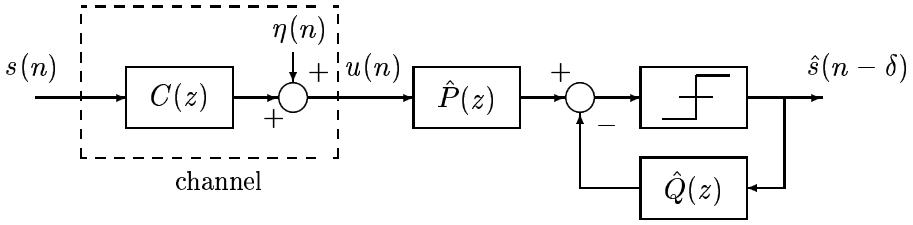

Figure 5.2: Decision-feedback equalization.

5.1.2 Decision feedback equalizer

The DFE architecture, shown in Figure 5.2, includes a forward filter $\hat{P}(z)$ and a strictly causal feedback filter $\hat{Q}(z)$ so that the equalizer output is computed as $\hat{P}(z)u(n) - \hat{Q}(z)\hat{s}(n-\delta)$, where $\hat{s}(n-\delta)$ is the last hard decision produced by the slicer. Due to the presence of the slicer in the feedback loop, the DFE is a nonlinear device. Nevertheless, if it is assumed that the equalizer is working properly so that the decisions are correct ($\hat{s}(n) = s(n)$ for all n), then the DFE output becomes a linear function of the filters' coefficients. Assume that the filters are unconstrained, i.e.

$$\hat{P}(z) = \sum_{k=-\infty}^{\infty} p_k^* z^{-k}, \qquad \hat{Q}(z) = \sum_{k=1}^{\infty} q_k^* z^{-k}.$$

In that case the expression for the MMSE DFE is (see e.g. [66])

$$\hat{P}_{DFE}(z) = z^{-\delta}\frac{\sigma_s^2 C^*(1/z^*)}{\gamma^2 F^*(1/z^*)}, \tag{5.5}$$

$$1 + \hat{Q}_{DFE}(z) = F(z), \tag{5.6}$$

that is, the optimum feedback filter is obtained directly from the spectral factorization of the psd of the received signal. Observe that

$$\hat{P}_{DFE}(z) = \hat{P}_{LE}(z).$$

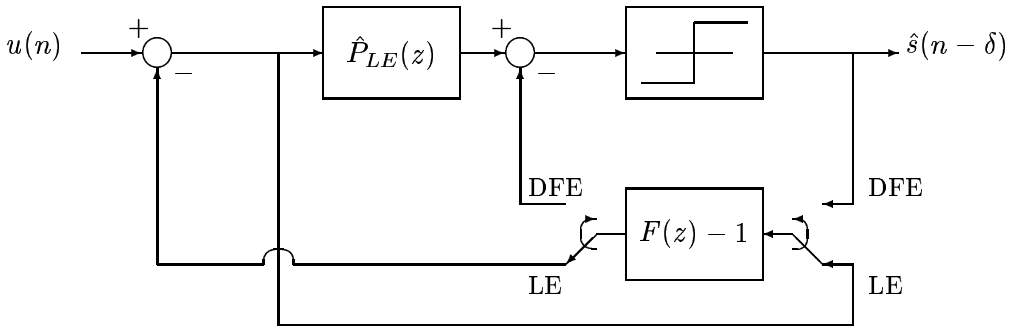

Figure 5.3: Switching from the MMSE LE to the MMSE DFE.

Therefore, if one could approximate the unconstrained MMSE LE and extract its two components $\hat{P}_{LE}(z)$ and $1/F(z)$, then the unconstrained MMSE DFE could also be approximated by merely throwing the switches in Figure 5.3 to DFE mode. The key observation is that the whitening filter $1/F(z)$ appearing in the MMSE LE provides the feedback filter for the MMSE DFE. This fact is the basis of the scheme suggested by Labat, Macchi and Laot in [62] for equalizer adaptation:

- In startup mode, the switches are set in the LE position and the equalizer coefficients are updated blindly. The recursive part is adapted in order to whiten its output, while for the forward part the Constant Modulus Algorithm (CMA) could be used (among other choices).

- An estimate of the MSE is computed during adaptation by smoothing the instantaneous squared error between the input and the output of the slicer. When this MSE estimate falls below a threshold level, it is assumed that the equalizer has achieved a sufficient reduction of the intersymbol interference (ISI) so that the device is switched to DFE operation mode.

- In DFE mode, the equalizer coefficients are updated following a decision directed (DD) MSE minimization criterion, which is based on the assumption that the hard decisions at the slicer output are correct. This adaptation criterion is also unsupervised.

- It could happen that, due to sudden changes in the channel, an error burst takes place at the slicer output. Due to error propagation in the DFE, this could lead the DD algorithm to a local minimum at which the assumption of correct decisions is violated. To avoid this situation, the equalizer is switched back to LE mode whenever the MSE estimate leaps above the selected threshold.

5.2 Finitely parameterized equalizers

The discussion in the previous section assumed that the equalizers had an infinite number of coefficients, and in addition the forward filters could be noncausal. Practical implementation, on the other hand, imposes finitely parameterized causal filters. Thus, the question arises of how the relation between the MMSE LE and the MMSE DFE is affected when one considers equalizers under these constraints.

5.2.1 Linear equalizer

As discussed in section 1.1.6, Mulgrew and Cowan derived in [87] the expression of the MMSE LE with associated delay δ under the only constraint that it be causal. This expression is given by

$$\begin{aligned}\hat{H}_{LE}(z) &= \frac{1}{F(z)}\left[z^{-\delta}\frac{\sigma_s^2 C^*(1/z^*)}{\gamma^2 F^*(1/z^*)}\right]_{0+} \\ &= \frac{1}{F(z)}\cdot[\hat{P}_{LE}(z)]_{0+}, \end{aligned} \tag{5.7}$$

where as before $F(z)$ denotes the monic, minimum phase spectral factor of the input signal psd $S_{uu}(z)$, $[\cdot]_{0+}$ extracts the causal part of its argument, and $\hat{P}_{LE}(z)$ was given in (5.4).

Observe that, as in the unconstrained case, the MMSE LE consists of a whitening filter $1/F(z)$ followed by another block which in this case is causal. A key observation [87] is that if the channel transfer function $C(z)$ is FIR of degree L, i.e.

$$C(z) = c_0^* + c_1^* z^{-1} + \cdots + c_L^* z^{-L},$$

then $F(z)$ can be taken as a polynomial of degree L, and the transfer function $[\hat{P}_{LE}(z)]_{0+}$ is FIR of degree δ. This means that the causal MMSE LE is finitely parameterized since it can be realized by a transfer function with L poles and δ zeros. Note that, despite the apparent similarity, the causal MMSE LE (5.7) does *not* equal the causal projection of the unconstrained MMSE LE (5.3).

5.2.2 Decision feedback equalizer

Let us assume that the channel $C(z)$ is FIR with degree L, and that the forward and backward filters of the DFE have $N+1$ and M coefficients respectively:

$$\hat{P}(z) = \sum_{k=0}^{N} p_k^* z^{-k}, \qquad \hat{Q}(z) = \sum_{k=1}^{M} q_k^* z^{-k}.$$

Collect these coefficients in the vectors

$$\mathbf{p} = [\, p_0 \; p_1 \; \cdots \; p_N \,]^T, \qquad \mathbf{q} = [\, q_1 \; \cdots \; q_M \,]^T.$$

Then, assuming that all past hard decisions are correct, the MMSE DFE with associated delay δ is given by (see e.g. [11])

$$\mathbf{p}_\delta = \left[\mathbf{C}\mathbf{\Lambda}_\delta\mathbf{C}^\dagger + \frac{\sigma_\eta^2}{\sigma_s^2}\mathbf{I}\right]^{-1}\mathbf{C}\mathbf{e}_\delta, \tag{5.8}$$

$$\mathbf{q}_\delta = \mathbf{D}_\delta^\dagger\mathbf{C}^\dagger\mathbf{p}_\delta, \tag{5.9}$$

where $\mathbf{e}_k$ is the kth unit vector (counting from zero), $\mathbf{C}$ is the $(N+1)\times(L+N+1)$ channel matrix, which is Toeplitz and given by

$$\mathbf{C} = \begin{bmatrix} c_0^* & c_1^* & \cdots & c_L^* & & \\ & \ddots & & & \ddots & \\ & & c_0^* & c_1^* & \cdots & c_L^* \end{bmatrix}, \tag{5.10}$$

$\mathbf{D}_\delta$ is an $(L+N+1)\times M$ Toeplitz matrix whose first column is $\mathbf{e}_{\delta+1}$ if $0 \le \delta < L+N$ and $\mathbf{0}$ if $\delta \ge L+N$; and $\mathbf{\Lambda}_\delta = \mathbf{I}-\mathbf{D}_\delta\mathbf{D}_\delta^\dagger$. The MMSE achieved by the DFE (5.8)-(5.9) is

$$\sigma_s^2(1 - \mathbf{p}_\delta^\dagger\mathbf{C}\mathbf{e}_\delta).$$

Observe from (5.9) that the MMSE feedback filter coefficients coincide with a portion of the overall channel-feedforward filter combination. Specifically, if we define this overall system as

$$G(z) = C(z)P(z) = \sum_{k=0}^{L+N} g_k^* z^{-k} \qquad \Rightarrow \qquad \mathbf{g} = [\, g_0 \;\; g_1 \;\; \cdots \;\; g_{L+N} \,]^T,$$

then $\mathbf{C}^\dagger\mathbf{p} = \mathbf{g}$, so that the feedback filter is optimized in terms of $P(z)$ when $q_k = g_{\delta+k}$, $k = 1, \ldots, M$. In other words, the feedback filter is canceling as much postcursor ISI as it can. If $M+\delta \ge L+N$, then all the postcursor ISI is eliminated. Concerning the feedforward filter, we see that the role of the matrix $\mathbf{\Lambda}_\delta$ in (5.8) is to mask the ISI contribution of the channel-feedforward filter combination in the DFE window when finding the optimum $\mathbf{p}$, since the ISI in this window will be taken care of by the feedback filter.

In general, the optimal feedback filter $1 + \hat{Q}_\delta(z)$ parameterized by $\mathbf{q}_\delta$ need not coincide with the minimum phase spectral factor $F(z)$ of the psd $S_{uu}(z)$, unless the forward filter is sufficiently long and the delay δ is sufficiently large (since as $N \to \infty$, then it is reasonable to expect the forward filter to approximate the unconstrained solution). In fact, for finite N, $1 + \hat{Q}_\delta(z)$ need not even be minimum phase. For example, for high values of the SNR so that the noise can be neglected, assuming that $\delta \le N$ and $L \le M$, the choice

$$\hat{P}_\delta(z) = \frac{1}{c_0^*}z^{-\delta}, \qquad \hat{Q}_\delta(z) = \frac{1}{c_0^*}C(z) - 1$$

results in a zero (i.e., minimum) MSE value, since $C(z)\hat{P}_\delta(z) - z^{-\delta}\hat{Q}_\delta(z) = z^{-\delta}$ so that this DFE removes all ISI. However, since

$$1 + \hat{Q}_\delta(z) = \frac{1}{c_0^*}C(z),$$

the roots of the feedback filter coincide with those of the channel. If the channel is nonminimum phase, so will be $1 + \hat{Q}_\delta(z)$. As noted in [11], this could result in two problems for the switching scheme of Labat, Macchi and Laot [62]:

1. It could happen that at the moment of switching from LE to DFE mode, the parameters of the equalizer are not close enough to the desired minimum of the DD cost function so that convergence to a bad minimum could take place.

2. If during DD adaptation in DFE mode the feedback filter becomes nonminimum phase, and due to quick time variations in the channel a switch to LE mode occurs, the resulting recursive equalizer will be unstable.

The first problem appears to be difficult to solve without resorting to training signals, or increasing the length of the forward filter [11]. As for the second, it can be alleviated by the fact that one of the candidate algorithms for the adaptation of the recursive part (the PLR algorithm to be discussed later on) enjoys a so-called 'self-stabilization' property [81] that could push the coefficients back into the stability region. In addition, the observation noise has the effect of pushing the unstable roots of $1 + \hat{Q}_\delta(z)$ towards the stability region. To see this, let $\lambda = \frac{\sigma_\eta^2}{\sigma_s^2}$ and note that for low SNR values (i.e., high λ), we can approximate $\mathbf{C}\mathbf{\Lambda}_\delta\mathbf{C}^\dagger + \lambda\mathbf{I} \approx \lambda\mathbf{I}$, so that (5.8)-(5.9) become

$$\mathbf{p}_\delta \approx \frac{1}{\lambda}\mathbf{C}\mathbf{e}_\delta, \qquad \mathbf{q}_\delta \approx \frac{1}{\lambda}\mathbf{D}_\delta^\dagger\mathbf{C}^\dagger\mathbf{C}\mathbf{e}_\delta,$$

which tend to the zero vectors as the SNR decreases. Hence, by continuity arguments, we have the following:

Lemma 5.1. *If the signal to noise ratio is sufficiently small, then the optimal feedback filter* $1 + \hat{Q}_\delta(z)$ *parameterized by* $\mathbf{q}_\delta$ *in (5.9) is minimum phase.*

To illustrate this discussion, consider a simple first-order channel ($L = 1$) given by $C(z) = \sin\vartheta + e^{j\varphi}\cos\vartheta z^{-1}$. Suppose that $\delta = N = M = 1$. Then one can solve (5.9) in order to find the feedback coefficient q_1:

$$q_1 = \frac{\sin\vartheta\cos\vartheta(\sin^2\vartheta + \lambda)}{(\sin^2\vartheta + \lambda)(1 + \lambda) - \sin^2\vartheta\cos^2\vartheta}e^{-j\varphi}.$$

Figure 5.4 represents the magnitude of q_1 as a function of the channel parameter ϑ and the SNR $1/\lambda$. It is seen that for SNR below a critical value (approximately

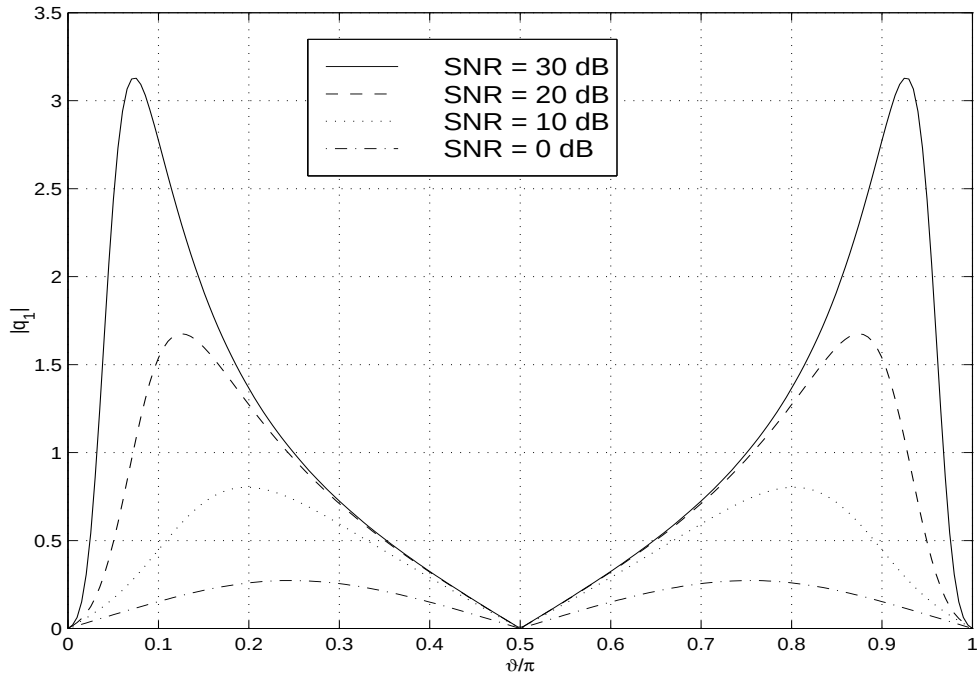

Figure 5.4: Magnitude of the feedback coefficient q_1 as a function of the channel zero and the SNR.

12.7 dB), one has $|q_1| < 1$ for all ϑ so that $1+\hat{Q}_1(z)$ is minimum phase. For λ below this threshold, a nonminimum phase feedback filter can result for some values of ϑ.

An alternative proof of Lemma 5.1 is given in Appendix B for the particular case in which $\delta \geq L$ with L the channel length. One should be aware, however, of the fact that as the SNR decreases, the original assumption of all past decisions being correct is likely to be violated.

5.2.3 Implications

In view of the preceding discussion, it seems that the switching scheme of [62] may fail unless (i) the length of the feedback filter, M, is chosen to be no less than the channel length L, and (ii) the length of the forward filter, N, is 'sufficiently large'. As seen in section 5.2.1, the numerator of the causal MMSE LE has order equal to the associated delay, thus it is reasonable to select $\delta = N$. However, it must be noted that the use of blind algorithms such as CMA for the adaptation of the forward block in the LE does not allow selection of the system delay attained at convergence (in fact, different delays are often associated to different minima of the CM cost [54]). In our opinion, blind initialization of a finitely parameterized DFE in the absence of any kind of knowledge about the channel length remains an open (and difficult) problem. In the remainder of the chapter we focus on the adaptation

of the LE structure.

5.3 Blind algorithms for linear recursive equalizers

Consider the LE configuration shown in Figure 5.1. As discussed in section 5.2.1, if the channel $C(z)$ is FIR of degree L and $\hat{H}(z)$ is only constrained to be causal, then the MMSE solution has δ zeros and L poles. Let the equalizer transfer function be

$$\hat{H}(z) = \frac{B(z)}{A(z)} = \frac{b_0^* + b_1^* z^{-1} + \cdots + b_N^* z^{-N}}{1 + a_1^* z^{-1} + \cdots + a_M^* z^{-M}}.$$

In this section we shall assume that the system delay δ is matched to the order of the numerator N; a procedure to achieve this goal will be presented in section 5.3.7. On the other hand, one would like to have M equal to the channel length, although depending on the situation this may not be realistic. Let

$$x(n) = \frac{1}{A(z)} u(n)$$

be the output of the recursive part (which is assumed to be placed before $B(z)$ for reasons that will become clear soon) when driven by the received signal. If we define the vectors

$$\bar{\mathbf{x}}(n) = [\, x(n)\ x(n-1)\ \cdots\ x(n-N)\,]^T, \qquad \mathbf{b} = [\, b_0\ b_1\ \cdots\ b_N\,]^T, \tag{5.11}$$

then the error can be written as $e(n) = s(n-\delta) - \mathbf{b}^\dagger \bar{\mathbf{x}}(n)$. Thus, the optimal value of $\mathbf{b}$ is $\mathbf{b}_\star = \mathbf{R}_x^{-1}\mathbf{p}_x$, where

$$\mathbf{R}_x = E[\bar{\mathbf{x}}(n)\bar{\mathbf{x}}(n)^\dagger], \qquad \mathbf{p}_x = E[s^*(n-\delta)\bar{\mathbf{x}}(n)]. \tag{5.12}$$

Thus assuming that $N = \delta$ and that $B(z)$ is optimized as a function of $A(z)$, one obtains a 'reduced error surface' of the form

$$J_{\text{red}} = E[|e(n)|^2]_{\mathbf{b}=\mathbf{b}_\star} = \sigma_s^2 - \mathbf{p}_x^\dagger \mathbf{R}_x^{-1} \mathbf{p}_x. \tag{5.13}$$

Observe that for a given delay value δ, J_{red} is a function of $A(z)$ alone, although in a pretty complicated way since both $\mathbf{R}_x$ and $\mathbf{p}_x$ have a nonlinear dependence on the coefficients of $A(z)$. Now, if $C(z)$ is FIR with degree $L \leq M$ (the 'sufficient order case'), it follows from [87] that J_{red} is minimized when $x(\cdot)$ is white, i.e. the optimum $A(z)$ is the minimum phase spectral factor of $S_{uu}(z)$. This observation provides a blind criterion for the adaptation of $1/A(z)$, since no training signal is needed for the whitening of $x(\cdot)$. Note that direct minimization of J_{red} does not lend itself to blind adaptation; however, two unsupervised schemes are available in order to whiten $x(\cdot)$, as described next. As a side benefit, this whitening approach allows one to decouple the adaptation of $A(z)$ from that of $B(z)$.

5.3.1 Two blind algorithms for the recursive part

The first approach is the minimization of $E[|x(n)|^2]$ via a stochastic gradient descent; we refer to this as the Output Variance Minimization (OVM) criterion. Defining the filtered signal

$$x_f(n) = \frac{1}{A(z)}x(n) = \frac{1}{A^2(z)}u(n)$$

and the vectors

$$\mathbf{a} = [\, a_1 \; \cdots \; a_M \,]^T, \qquad \mathbf{x}_f(n) = [\, x_f(n-1) \; \cdots \; x_f(n-M) \,]^T,$$

the OVM algorithm can be written as follows:

$$\mathbf{a}(n+1) = \mathbf{a}(n) + \mu \mathbf{x}_f(n) x^*(n). \tag{5.14}$$

The second possibility is to use the approximation $x_f(n) \approx x(n)$, which leads to the pseudolinear regression (PLR) algorithm proposed in [62]:

$$\mathbf{a}(n+1) = \mathbf{a}(n) + \mu \mathbf{x}(n) x^*(n), \tag{5.15}$$

where

$$\mathbf{x}(n) = [\, x(n-1) \; \cdots \; x(n-M) \,]^T. \tag{5.16}$$

The PLR approach disposes of the additional postfilter $1/A(z)$ that the OVM algorithm requires for the computation of $x_f(\cdot)$, and therefore it is computationally less costly. Also, PLR presents improved stability behavior due to its 'self-stabilization' property [81, ch. 15], so that stability monitoring is usually not necessary. This is not the case for OVM, which may easily become unstable when the optimum filter has poles close to the unit circle. In that case, it is desirable to implement the recursive filter $1/A(z)$ in normalized lattice form. The corresponding adaptive algorithm can be easily obtained following the guidelines of chapter 2.

It is interesting to note that, although the reduced cost J_{red} is a function of the selected system delay δ, neither the OVM nor the PLR criteria are sensitive to the value of δ since they are based on the spectral properties of the received signal $u(\cdot)$ alone. The problem of delay selection is thus transferred to the numerator $B(z)$ of the equalizer, as we shall see in section 5.3.7.

5.3.2 Stationary points

We proceed now to analyze the stationary points of OVM and PLR. Ideally, these stationary points should provide minimization of J_{red}. In general they can be characterized as follows. Let $V(z) = z^{-M}A^*(1/z^*)/A(z)$ be the all-pass function associated with $A(z)$, and for any function $f(z) = \sum_{k=-\infty}^{\infty} f_k z^{-k}$, let $[f(z)]_+ =$

$f_1 z^{-1} + f_2 z^{-2} + \cdots$ denote the operator extracting the strictly causal part. The stationary points of the algorithms are the solutions of

$$E[\mathbf{x}_f(n)x^*(n)] = \mathbf{0}_M \quad \text{(OVM)}, \qquad E[\mathbf{x}(n)x^*(n)] = \mathbf{0}_M \quad \text{(PLR)},$$

or alternatively,

$$\left\langle \begin{bmatrix} z^{-1} \\ \vdots \\ z^{-M} \end{bmatrix} \frac{1}{A(z)}, \frac{S_{uu}(z)}{A(z)A^*(1/z^*)} \right\rangle = \mathbf{0}_M, \tag{5.17}$$

$$\left\langle \begin{bmatrix} z^{-1} \\ \vdots \\ z^{-M} \end{bmatrix} \frac{1}{A(z)}, \frac{S_{uu}(z)}{A(z)} \right\rangle = \mathbf{0}_M. \tag{5.18}$$

With these, one can invoke the Beurling-Lax theorem [105, ch. 3] to conclude that $1/A(z)$ is a stationary point of OVM or PLR if and only if it satisfies, for some causal function $g(z) = \sum_{k=0}^{\infty} g_k z^{-k}$ with $\sum |g_k|^2 < \infty$,

$$\left[\frac{S_{uu}(z)}{A(z)A(z^{-1})}\right]_+ = z^{-1}V(z)g(z) \qquad \text{(OVM)} \tag{5.19}$$

$$\left[\frac{S_{uu}(z)}{A(z)}\right]_+ = z^{-1}V(z)g(z) \qquad \text{(PLR)} \tag{5.20}$$

Observe that

$$\frac{S_{uu}(z)}{A(z)A(z^{-1})} = S_{xx}(z),$$

the psd of the process $x(\cdot)$. Thus (5.19) shows that at any OVM stationary point, the strictly causal part of the resulting psd $S_{xx}(z)$ is causally divisible by the allpass function associated to $A(z)$. On the other hand, (5.20) is the z-domain statement of the conditions

$$E[x(n-k)x^*(n)] = 0, \qquad 1 \le k \le M, \tag{5.21}$$

that must be satisfied at any stationary point of PLR. These can be seen as an approximation to the whiteness conditions $E[x(n-k)x^*(n)] = 0$ for all $k > 0$.

From (5.19) and (5.20) we immediately see that the stationary points of the two algorithms do not necessarily coincide. Recall that our principal concern is the minimization of J_{red} as given in (5.13); let us consider the sufficient order case first.

5.3.3 The sufficient order case

If the channel $C(z)$ is FIR with degree $L \le M$, then $u(\cdot)$ is a moving average process of order L, or MA(L). Then as stated above, J_{red} is minimized if $x(\cdot)$ is white. In this situation, the following result applies:

Theorem 5.1. *If $u(\cdot)$ is an MA process of order $L \leq M$, then both (5.19) and (5.20) have a unique minimum phase solution $A(z)$, which is the minimum phase spectral factor of $S_{uu}(z)$. In addition this $A(z)$ is a locally convergent stationary point of both the OVM algorithm (5.14) and the PLR algorithm (5.15).*

Uniqueness of the stationary point of OVM is a consequence of the results from [4]; local convergence is guaranteed since this stationary point is a minimum of $E[|x(n)|^2]$ and OVM is just a gradient descent of this cost. That the stationary point of PLR is also unique was proven in [72]. Local convergence was shown in [94] by examining the eigenvalues of the feedback matrix of the corresponding linearized ODE.

Thus in sufficient order settings both OVM and PLR present a single stationary point which coincides with the minimum of J_{red}. This is somewhat surprising since the cost $E[|x(n)|^2]$ associated to OVM is not a quadratic function of the coefficients of $A(z)$. Also, Theorem 5.1 shows that it suffices for the all-pole filter $1/A(z)$ to kill the autocorrelation coefficients of $x(\cdot)$ with lags 1 through M (the goal of the PLR approach) to ensure that *all* positive lags are zero.

Theorem 5.1 reveals an additional advantage of the blind criteria over direct (nonblind) minimization of the cost J_{red}, since J_{red} is a highly nonquadratic function of $A(z)$ and could present local minima.

5.3.4 Reduced order case: OVM

When $u(\cdot)$ is not MA(L) with $L \leq M$, no $1/A(z)$ with degree M or less exists that completely whitens $x(\cdot)$. In that case there is no simple description for the global minimum of the reduced cost J_{red} in (5.13). Nevertheless, the cost $E[|x(n)|^2]$ can still be seen as a proxy to J_{red}, as we now discuss.

Consider the case $\delta = 0$ (recall that δ is the system delay). Then $\mathbf{R}_x = E[|x(n)|^2]$, $\mathbf{p}_x = E[x(n)s^*(n)]$ are both scalars. The reduced error surface becomes

$$J_{\text{red}} = \sigma_s^2 - \frac{(E[x(n)s^*(n)])^2}{E[|x(n)|^2]}, \qquad (\delta = 0).$$

Note that, since the sequence of transmitted symbols $s(\cdot)$ is white, the term $E[x(n)s^*(n)]$ does not depend on $A(z)$ at all:

$$E[x(n)s^*(n)] = \sigma_s^2 \left\langle \frac{1}{A(z)}, 1 \right\rangle = \sigma_s^2.$$

Thus

$$J_{\text{red}} = \sigma_s^2 \left(1 - \frac{\sigma_s^2}{E[|x(n)|^2]}\right), \qquad (\delta = 0)$$

so that minimizing J_{red} is equivalent to minimizing $E[|x(n)|^2]$, which is the OVM criterion.

When $\delta > 0$ this is not strictly true. However, note that

$$J_{\text{red}} = \sigma_s^2 - \mathbf{p}_x^\dagger \mathbf{R}_x^{-1} \mathbf{p}_x \leq \sigma_s^2 - \frac{||\mathbf{p}_x||^2}{\lambda_{\max}}, \tag{5.22}$$

where $\lambda_{\max}$ is the largest eigenvalue of $\mathbf{R}_x$. Thus in order to decrease J_{red}, it makes sense to make $\lambda_{\max}$ as small as possible; and since

$$\lambda_{\max} \geq \frac{\text{trace}(\mathbf{R}_x)}{\delta + 1} = E[|x(n)|^2],$$

by making $E[|x(n)|^2]$ small one could expect to decrease $\lambda_{\max}$. This argument is loose since the vector $\mathbf{p}_x$ depends on $A(z)$ as well for $\delta > 0$. The examples in section 5.3.6 will illustrate this point. We should note that in reduced order cases, unimodality of the OVM cost $E[|x(n)|^2]$ is not guaranteed in general.

5.3.5 Reduced order case: PLR

The first question that arises about the behavior of the PLR algorithm in undermodeled settings is the existence of stationary points. This issue is not trivial since PLR does not correspond to the minimization of any meaningful cost. To this purpose, we present a new approach which reveals the stationary points of PLR as fixed points of an off-line iterative scheme. First observe that for fixed $A(z)$, the signal $x(n)$ satisfies

$$x(n) = u(n) - \mathbf{a}^\dagger \mathbf{x}(n),$$

where $\mathbf{x}(n)$ was defined in (5.16). Therefore the conditions (5.21) can be rewritten as

$$E[\mathbf{x}(n)\mathbf{x}(n)^\dagger]\mathbf{a} = E[\mathbf{x}(n)u^*(n)]. \tag{5.23}$$

Note that this equation is not linear in $\mathbf{a}$ since the vector $\mathbf{x}(n)$ depends on $\mathbf{a}$, though it suggests the following iterative off-line process:

1. At iteration i, let $\mathbf{a} = \mathbf{a}_i = [\, a_1^{(i)} \; \cdots \; a_M^{(i)} \,]^T$ be fixed and let

   $$\mathbf{x}(n) = [\, x(n-1) \; \cdots \; x(n-M) \,]^T$$

   with

   $$x(n) = u(n) - \sum_{j=1}^{M} a_j^{(i)} x(n-j). \tag{5.24}$$

2. Let

   $$\mathbf{a}_{i+1} = E\left[\mathbf{x}(n)\mathbf{x}(n)^\dagger\right]^{-1} E[\mathbf{x}(n)u^*(n)].$$

3. Iterate Steps 1 and 2 until convergence.

Clearly, at any fixed point of this iteration, (5.23) is satisfied, so that these fixed points coincide with the stationary points of the PLR algorithm. This iterative process is reminiscent of the Steiglitz-McBride method for system identification discussed in section 3.2, as Figure 5.5 illustrates. Let $A_i(z)$ be the polynomial associated to the vector $\mathbf{a}_i$ obtained at the ith iteration, and let $x(n)$ be as in (5.24). Define

$$x'(n) = u(n) - \sum_{j=1}^{M} a_j x(n-j),$$

where now the coefficients a_j are variables to be determined. Then the components of the vector $\mathbf{a}_{i+1}$ for the next iteration are given by those a_j that minimize the variance $E[|x'(n)|^2]$. Note that at any stationary point $A_{i+1}(z) = A_i(z) = A_\star(z)$ one has

$$x'(n) = \frac{1}{A_\star(z)} u(n) = x(n),$$

in the same way as the 'distorted' equation error in the Steiglitz-McBride identification method reduces to an output error at any stationary point.

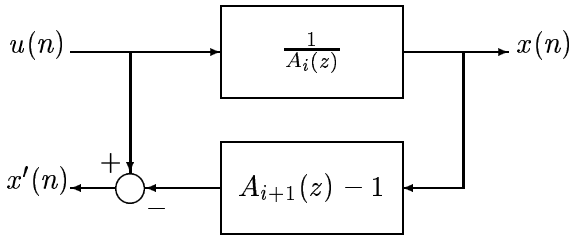

Figure 5.5: Block diagram illustrating the iterative off-line interpretation of the PLR algorithm.

The following result holds now:

Theorem 5.2. *If the psd $S_{uu}(z)$ is bounded and nonzero for all $|z| = 1$, then the iterative method above admits a fixed point $\mathbf{a}_\star$ corresponding to a minimum phase polynomial $A_\star(z)$.*

See Appendix B for the proof. Observe that any small amount of white measurement noise in the received signal $u(\cdot)$ will yield its psd $S_{uu}(z) \neq 0$ for all $|z| = 1$. Theorem (5.2) then shows that under these mild conditions the PLR adaptive algorithm admits at least one stationary point inside the stability region. It does not inform, however, of how many of these points there are, or whether an attractor point always exists among these. Based on simulation evidence, we conjecture that the stationary point of PLR is always unique and attractive even in reduced order cases, although a formal proof is not available at this time.

As an example, consider the undermodeled case in which the length of the channel is $L = M + 1$. In that case the received signal $u(\cdot)$ is an MA$(M+1)$

process, so that we can write $S_{uu}(z) = F(z)F^*(1/z^*)$ where $F(z)$ is a minimum phase polynomial with degree $M+1$. At any minimum phase PLR stationary point, (5.20) must be satisfied; i.e.

$$\left[\frac{F(z)}{A(z)}F^*(1/z^*)\right]_+ = z^{-1}V(z)g(z) \tag{5.25}$$

for some stable and causal $g(z)$. As shown in [105, prob. 8.4], the left-hand side in (5.25) is a rational function of degree not exceeding that of $F(z)/A(z)$, and any pole of this function is a pole of $F(z)/A(z)$. Therefore we can write

$$\left[\frac{F(z)}{A(z)}F^*(1/z^*)\right]_+ = z^{-1}\frac{q(z)}{A(z)}$$

where $q(z)$ is a polynomial of degree not exceeding M. Thus

$$z^{-1}\frac{q(z)}{A(z)} = z^{-1}V(z)g(z) = z^{-1}g(z)\frac{z^{-M}A^*(1/z^*)}{A(z)}.$$

Since all the roots of $z^{-M}A^*(1/z^*)$ lie outside the unit circle, none of them can be canceled out by a pole of $g(z)$ (since $g(z)$ is causal and stable). Therefore every root of $z^{-M}A^*(1/z^*)$ must be a root of $q(z)$, and then $g(z)$ must reduce to a constant: $g(z) = g_0$.

Now note that $S_{uu}(z)/A(z) = S_{xx}(z)A^*(1/z^*)$, and that the psd $S_{xx}(z)$ satisfies

$$S_{xx}(z) = z^{M+1}R^*(1/z^*) + \sigma_x^2 + z^{-(M+1)}R(z),$$

where $R(z) = r_0 + r_1 z^{-1} + \cdots$ is a causal function. This is because at any PLR stationary point the autocorrelation coefficients with lags 1 through M of $x(\cdot)$ are zero. Therefore

$$\begin{aligned}\frac{S_{uu}(z)}{A(z)} &= S_{xx}(z)A^*(1/z^*) \\ &= z^{M+1}R^*(1/z^*)A^*(1/z^*) + \sigma_x^2 A^*(1/z^*) + z^{-(M+1)}R(z)A^*(1/z^*),\end{aligned}$$

so that the strictly causal part reduces to $z^{-(M+1)}R(z)A^*(1/z^*)$. Hence

$$z^{-(M+1)}R(z)A^*(1/z^*) = z^{-1}g_0\frac{z^{-M}A^*(1/z^*)}{A(z)},$$

which shows that

$$g_0 = r_0 = E[x(n)x^*(n-M-1)], \qquad R(z) = \frac{r_0}{A(z)}.$$

Therefore the psd of $x(\cdot)$ must take the form

$$S_{xx}(z) = \frac{r_0^* z^{M+1}}{A^*(1/z^*)} + \sigma_x^2 + \frac{r_0 z^{-(M+1)}}{A(z)}, \tag{5.26}$$

and consequently, since $F(z)F^*(1/z^*) = S_{uu}(z) = S_{xx}(z)A(z)A^*(1/z^*)$, we can write

$$F(z)F^*(1/z^*) = r_0^* z[z^M A(z)] + \sigma_x^2 A(z)A^*(1/z^*) + r_0 z^{-1}[z^{-M}A^*(1/z^*)]. \quad (5.27)$$

Equating the coefficients of z^{-k} in (5.27) for $k = 0$ and $k = M + 1$, we see that

$$r_0 = E[x(n)x^*(n - M - 1)] = E[u(n)u^*(n - M - 1)], \quad (5.28)$$

$$\sigma_x^2 = E[|x(n)|^2] = \frac{E[|u(n)|^2]}{1 + \sum_{i=1}^{M} |a_i|^2} \leq E[|u(n)|^2], \quad (5.29)$$

i.e., the autocorrelation coefficient of lag $M + 1$ of $x(\cdot)$ matches that of $u(\cdot)$. This coefficient can be seen as a measure of the degree of undermodeling. Eq. (5.29) shows the variance reduction from the input to the output of the filter, and it holds in all cases (not only for a channel of length $M + 1$) at any PLR stationary point.

The relation (5.27) shows that $A(z)$ is trying to approximate in some sense $F(z)$ in that $\sigma_x^2 A(z)A^*(1/z^*)$ tries to match $F(z)F^*(1/z^*)$, with the additional 'tails' weighted by r_0. This shows some degree of robustness of the PLR solution, since for small $|r_0|$, $\sigma_x^2 A(z)A^*(1/z^*)$ will be close to $F(z)F^*(1/z^*)$, so that $x(\cdot)$ will be close to white (see also (5.26)). Observe that, because of Theorem 5.2, the polynomial equation (5.27) admits a minimum phase solution $A(z)$ of degree M for any minimum phase $F(z)$ with degree $M + 1$. Whether this solution is unique (as we conjecture) is not immediately obvious from (5.27).

5.3.6 Some examples

We recall that the final assessment of the quality of the filter $1/A(z)$ obtained by either the OVM or the PLR schemes should be the reduction of the cost J_{red} given in (5.13). To this purpose, in this section we present several reduced order examples. In order to ease the visualization of the results, we shall consider the case in which the signals and the filter coefficients are real-valued. In that case, it is possible to show the uniqueness of the PLR stationary point for $M = 1$ in all reduced order cases:

Lemma 5.2. *If the signal $u(\cdot)$ and the coefficients of the filter $A(z)$ are real-valued, and if $M = 1$, i.e. $A(z) = 1 + a_1 z^{-1}$, then the minimum phase stationary point of PLR is unique.*

The proof is included in Appendix B. Again, whether this result also holds true for all orders $M > 1$ in undermodeled scenarios is left as a conjecture at this point.

In all the following examples the variances of the transmitted symbol sequence and of the channel noise were taken as $\sigma_s^2 = 1$ and $\sigma_\eta^2 = 0.1$ respectively.

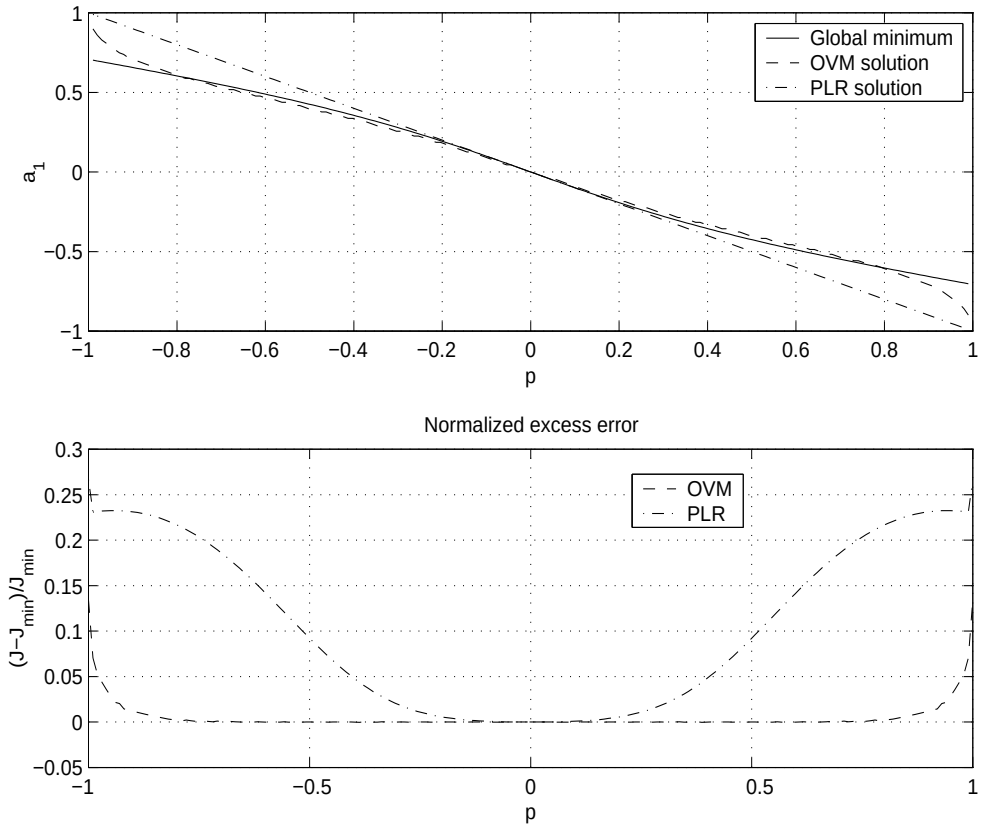

Figure 5.6: Performance of OVM and PLR for Example 1. Top: variation of the global minimum of J_{red} and the OVM and PLR stationary points with the channel pole p. Bottom: Normalized excess error for both methods as a function of p.

Example 1

Let $M = 1$, and consider a channel of the form $C(z) = \frac{1}{1+pz^{-1}}$, with $|p| < 1$. With a value of $\delta = 1$ for the system delay, one has the following:

- J_{red} is unimodal for $|p| < \frac{\sqrt{5}-1}{2}$ and bimodal for $\frac{\sqrt{5}-1}{2} < |p| < 1$.
- The OVM cost function $E[|x(n)|^2]$ presents a single minimum, which is the solution of $a_1^2 p(1 + a_1 p) = a_1 + p$ with $|a_1| < 1$.
- The unique stationary point of PLR is $a_1 = -p$.

Figure 5.6 shows the variation of the global minimum of J_{red} and the OVM and PLR solutions as a function of p, together with the normalized loss

$$\frac{J_{\text{red}} - J_{\min}}{J_{\min}},$$

where $J_{\min}$ is the value of J_{red} at the global minimum. For $p = 0$ we recover the sufficient order case. The degree of undermodeling increases with $|p|$, with a corresponding degradation in performance.

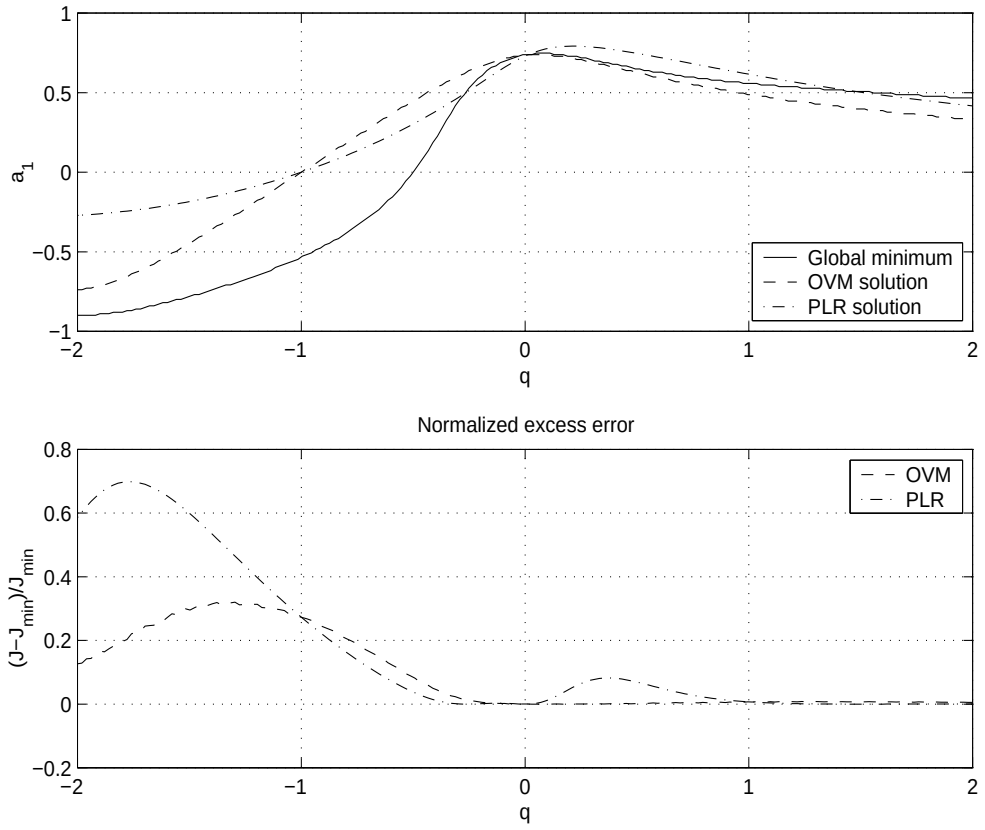

Figure 5.7: Performance of OVM and PLR for Example 2. Top: variation of the global minimum of J_{red} and the OVM and PLR stationary points with the third channel tap q. Bottom: Normalized excess error for both methods as a function of q.

Example 2

Let $M = 1$ again, but now let the channel be second-order FIR given by

$$C(z) = 1 + z^{-1} + qz^{-2}.$$

In that case the reduced cost J_{red} for $\delta = 1$ is unimodal for all values of q, and the same is true for the OVM cost. Figure 5.7 shows the variation of the minimum of J_{red}, the OVM and PLR solutions, and the normalized excess error, for $|q| \leq 2$. In this example both the OVM and PLR stationary points remain close to the global minimum of J_{red} for $q > 0$. For $q < 0$ the performance loss is larger, even though

the OVM and PLR solutions still 'track' the minimum of J_{red}. For $q = 0$, the sufficient order case is recovered.

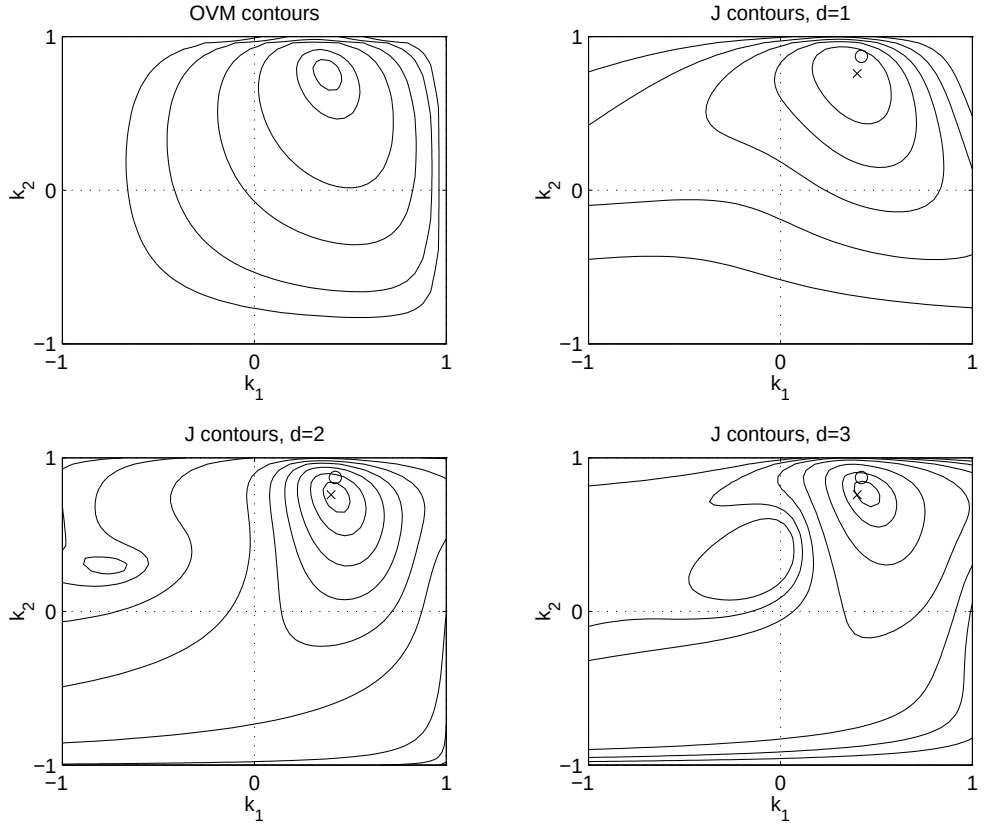

Figure 5.8: Contours of the OVM cost and the reduced error surface J_{red} ($\delta = 1, 2, 3$) for Example 3. '$\circ$' denotes the PLR stationary point, while '$\times$' denotes the OVM minimum.

Example 3

Let now $M = 2$, and consider the fourth order FIR channel

$$C(z) = 1 + z^{-1} + 1.5z^{-2} + 0.5z^{-3} + 0.2z^{-4}.$$

Figure 5.8 shows the contour plots of the reduced error surface J_{red} for $\delta = 1$, 2, 3, (for $\delta = 0$ we know that minimizing J_{red} is equivalent to minimizing the OVM cost), together with those of OVM, which in this case is unimodal, and the PLR stationary point. The plot is made in the stability domain $|k_i| < 1$ where $k_1 = a_1/(1 + a_2)$, $k_2 = a_2$ are the reflection coefficients of the lattice parameterization of $A(z)$. It is seen that for $\delta > 1$, J_{red} becomes multimodal. Even though OVM and PLR do not exactly minimize J_{red}, they lie acceptably close to the global minimum so that they still provide good performance.

These examples suggest that even in reduced order cases, the OVM and PLR approaches might be able to provide an acceptable reduction of the cost J_{red}. In this sense OVM seems to be more robust than PLR which can present a considerable normalized excess loss if the degree of undermodeling is large. Incidentally, it would be very useful if a method to quantify the degree of undermodeling were available. With $C(z) = c_0^* + c_1^* z^{-1} + \cdots$ the channel transfer function, one could think of a criterion of the form

$$\gamma_C = \frac{\sum_{k=M+1}^{\infty} |c_k|^2}{\sum_{k=0}^{\infty} |c_k|^2}.$$

The degree of undermodeling would be small for a value of γ_C close to zero and large for γ_C close to one. However, if one looks at Example 2 above, it is seen that this indicator γ_C is insensitive to the sign of the parameter q, while for some reason the performance of PLR and OVM changes drastically with a sign change in q as can be seen in Figure 5.7.

5.3.7 Adaptation of the numerator $B(z)$

So far we have considered the adaptation of the recursive part of the equalizer, $1/A(z)$, which is located upstream in the receiver configuration. Observe that in the ideal case of a noiseless minimum phase FIR channel with length $L \leq M$, this recursive portion of the equalizer, be it adapted via either the OVM or the PLR algorithms, will completely remove the ISI once it has converged. In less idealistic cases this will not be so, and the numerator $B(z)$ will still be needed in order to achieve an adequate level of performance.

The previous development hinged on the assumption that $B(z)$ had been optimized as a function of $A(z)$ in terms of the MSE

$$J_{\text{MSE}}(\mathbf{b}, \delta) = E[|s(n-\delta) - \hat{y}(n)|^2] \tag{5.30}$$

where $\hat{y}(n) = [B(z)/A(z)]u(n)$ is the equalizer output; we have made explicit the dependence of the MSE with the delay δ for reasons that will become clear soon. In blind equalization the channel input $s(n-\delta)$ is not available, and therefore direct minimization of the MSE is not feasible. Consequently, a different strategy must be adopted.

It has long been recognized that blind adaptation of a symbol spaced transversal equalizer cannot be carried out based on second order statistics alone if the channel is mixed phase (that is, if it contains zeros inside and outside the unit circle), which is the usual situation. This is so because the power spectral density of the received signal, which conveys the second-order information, is insensitive to the phase of the channel frequency response $C(e^{j\omega})$; however, this phase distortion must be corrected since it affects ISI considerably. Observe, however, that the OVM and PLR criteria for blind adaptation of the recursive part of the equalizer use only second order information. This is not a contradiction: the recursive portion $1/A(z)$ compensates

the channel magnitude distortion but does not provide phase correction, which is left to the numerator $B(z)$. Thus any blind criterion for the adaptation of $B(z)$ must be based on statistics of order higher than two. One possibility, suggested by Labat, Macchi and Laot [62] is to use the Godard(2,2) or Constant Modulus Algorithm (CMA) [44, 125], a popular method for blind adaptation of adaptive FIR equalizers. CMA adjusts the coefficients of $B(z)$ in the negative (stochastic) gradient direction of the so-called CM cost function

$$J_{\mathrm{CM}}(\mathbf{b}) = E[(|\hat{y}(n)|^2 - \gamma)^2] \qquad \text{where} \qquad \gamma = \frac{E[|s(n)|^4]}{E[|s(n)|^2]}. \tag{5.31}$$

Hence, with $x(n) = [1/A(z)]u(n)$ the output of the recursive prefilter, and $\hat{y}(n) = \sum_{k=0}^{N} b_k^* x(n-k) = \mathbf{b}^\dagger \bar{\mathbf{x}}(n)$ with the $(N+1)$-dimensional vectors $\mathbf{b}$, $\bar{\mathbf{x}}(n)$ as defined in (5.11), the CMA update rule can be written as

$$\mathbf{b}(n+1) = \mathbf{b}(n) + \mu(\gamma - |\hat{y}(n)|^2)\hat{y}^*(n)\bar{\mathbf{x}}(n). \tag{5.32}$$

We will refer to the stationary points of CMA, which are the minima of the CM cost (5.31), as 'CM receivers'.

Observe from (5.31) that the CM cost J_{CM} does not depend on the phase of the equalizer output $\hat{y}(n)$, and therefore if $\mathbf{b}$ is a CM receiver so is $e^{j\phi}\mathbf{b}$ for any real ϕ. This means that CMA attempts to recover the transmitted symbol sequence up only to a rotation in the complex plane. This issue is usually not a problem if differential encoding of the symbol stream is used prior to transmission [42].

Since different values of the system delay can result in drastic differences in MSE performance, it is convenient to introduce, for fixed $A(z)$, the 'amalgamated' MSE cost function

$$J_{\mathrm{A}}(\mathbf{b}) = \min_{\delta} E[|s(n-\delta) - \hat{y}(n)|^2] \tag{5.33}$$

which is optimized in terms of the delay δ. In general, $J_{\mathrm{A}}(\mathbf{b})$ is a multimodal function of $\mathbf{b}$ with its different minima ('Wiener receivers') being associated to different values of δ [54].

Recent work [135] has shown that under certain conditions, a CM receiver exists in a neighborhood of a Wiener receiver. Thus it can be expected that, by using CMA, the forward block $B(z)$ of the equalizer will converge (in mean) to a setting reasonably close to a minimum of J_{A}. However, since *a priori* selection of the system delay δ is not possible in blind equalization, it is conceivable that this convergent point could yield a high residual MSE or equivalently a small ISI reduction. In other words, convergence to a poor local minimum could take place.

This problem has been addressed, among many others, by Tong *et al.* in [25, 124]. There a reinitialization strategy for transversal equalizers adapted via CMA is proposed, which exploits the aforementioned relation between CM and Wiener receivers. The objective of the scheme is to attain the global minimum of J_{A}. Here we present a procedure which is in the spirit of [25, 124], but assuming that a

recursive whitening prefilter is included in the equalizer and preceding $B(z)$. As will be shown, this results in a much simpler reinitialization mechanism amenable to online implementation.

To begin, observe that the output of the prefilter $1/A(z)$ can be written as

$$\begin{aligned} x(n) &= \frac{1}{A(z)}u(n) \\ &= \frac{C(z)}{A(z)}u(n) + \frac{1}{A(z)}\eta(n) \\ &\approx \frac{C(z)}{A(z)}u(n) \qquad \text{for high SNR.} \end{aligned}$$

If the degree of $A(z)$ is no less than that of the channel, then after convergence of the adaptive algorithm (OVM or PLR) used for the adaptation of $A(z)$, the signal $x(\cdot)$ will be white. If the SNR is high, then

$$V(z) = \frac{C(z)}{A(z)} = \sum_{k=0}^{\infty} v_k^* z^{-k} \tag{5.34}$$

is approximately an allpass system: $A(z)$ will cancel the minimum phase roots of $C(z)$ and will place poles at the conjugate reciprocals of the zeros of $C(z)$ outside the unit circle. Under these conditions, the task of the forward filter $B(z)$ is to equalize an effective allpass channel $V(z)$. Now let us take a look at the expression of the MSE for a given delay δ:

$$\begin{aligned} J_{\text{MSE}}(\mathbf{b}, \delta) &= E[|s(n-\delta) - \mathbf{b}^\dagger \bar{\mathbf{x}}(n)|^2] \\ &= \sigma_s^2 + \mathbf{b}^\dagger E[\bar{\mathbf{x}}(n)\bar{\mathbf{x}}(n)^\dagger]\mathbf{b} - 2\text{Re}\left\{\mathbf{b}^\dagger E[\bar{\mathbf{x}}(n)s^*(n-\delta)]\right\} \\ &= \sigma_s^2 \left(1 + \frac{\sigma_x^2}{\sigma_s^2}\mathbf{b}^\dagger\mathbf{b} - 2\text{Re}\left\{\mathbf{b}^\dagger \mathbf{v}_\delta\right\}\right), \end{aligned} \tag{5.35}$$

where $\mathbf{v}_\delta = E[\bar{\mathbf{x}}(n)s^*(n-\delta)]/\sigma_s^2$ and the last line follows from the fact that $E[\bar{\mathbf{x}}(n)\bar{\mathbf{x}}(n)^\dagger] = \sigma_x^2\mathbf{I}$ since $x(\cdot)$ is white. In addition, whiteness of $s(\cdot)$ also gives

$$E[x(n-i)s^*(n-\delta)] = \sum_{k=0}^{\infty} v_k^* E[s(n-i-k)s^*(n-\delta)] = \sigma_s^2 v_{\delta-i}^*,$$

so that the vector $\mathbf{v}_\delta$ is just

$$\mathbf{v}_\delta = \begin{bmatrix} v_\delta^* \\ v_{\delta-1}^* \\ \vdots \\ v_{\delta-N}^* \end{bmatrix}. \tag{5.36}$$

Since the variance of $x(\cdot)$ is given by $\sigma_x^2 = \sigma_s^2 \sum_{k=0}^{\infty} |v_k|^2 + \sigma_\eta^2 \kappa_A$, where

$$\kappa_A = \frac{1}{2\pi}\int_0^{2\pi} \frac{1}{|A(e^{j\omega})|^2} d\omega,$$

the minimizer of (5.35) is readily found to be

$$\mathbf{b}_\delta = \frac{\sigma_s^2}{\sigma_x^2}\mathbf{v}_\delta = \frac{1}{\lambda\kappa_A + \sum_{k=0}^{\infty}|v_k|^2}\begin{bmatrix} v_\delta^* \\ v_{\delta-1}^* \\ \vdots \\ v_{\delta-N}^* \end{bmatrix}, \tag{5.37}$$

where $\lambda = \sigma_\eta^2/\sigma_s^2$. Thus the Wiener receivers for different values of the system delay δ are related in a fairly simple way to the coefficients of the effective allpass channel $V(z)$, and they are related to each other by simple shift operations. This observation is the key to our reinitialization scheme.

The minimized value of the MSE for the delay δ is

$$J_{\mathrm{MSE}}(\mathbf{b}_\delta, \delta) = \sigma_s^2\left(1 - \frac{\sigma_s^2}{\sigma_x^2}\mathbf{v}_\delta^\dagger\mathbf{v}_\delta\right) = \sigma_s^2\left(1 - \frac{\sum_{k=\delta-N}^{\delta}|v_k|^2}{\lambda\kappa_A + \sum_{k=0}^{\infty}|v_k|^2}\right). \tag{5.38}$$

Therefore, for a given number of coefficients $N+1$ in the forward filter $B(z)$, the optimal delay is the one for which the vector $\mathbf{v}_\delta$ has the largest norm. Observe that if $\delta < N$, then

$$\mathbf{v}_\delta^\dagger\mathbf{v}_\delta = \sum_{k=0}^{\delta}|v_k|^2 \le \sum_{k=0}^{N}|v_k|^2 = \mathbf{v}_N^\dagger\mathbf{v}_N.$$

Therefore the optimal delay satisfies $\delta \ge N$. This is intuitively appealing, since for $\delta < N$ the Wiener receiver $\mathbf{b}_\delta$ has its last $N-\delta$ coefficients equal to zero, an indication of the fact that not all the equalization potential of the filter is being exploited to full extent.

Finding the optimal value of δ amounts to finding the position of a window of size $N+1$ that captures the maximum energy in the impulse response of the effective allpass channel $V(z)$. We propose the following rule of thumb:

> Let M be the order of the recursive prefilter $1/A(z)$, which should be chosen to be no less than the length of the channel $C(z)$. Choose the order of the forward block $B(z)$ to be $N \ge 2M$, and the associated system delay as $\delta = N$.

Of course, N should be as large as possible within design constraints. The guideline above follows from the observation that if $V(z)$ is allpass with degree p and its first coefficient v_0^* has 'significantly large' magnitude, then (5.38) seems to be minimized for $\delta = N$ provided that $N \ge 2p$. (This can be readily verified for $p = 1$, i.e., for $V(z) = (a_1 + z^{-1})/(1 + a_1^* z^{-1})$). Observe that in practice p is not known since pole-zero cancellations will take place in $C(z)/A(z)$ at the minimum phase roots of $C(z)$. Nevertheless, one has $p \le M$, so that taking $p = M$ gives a worst case scenario for the above rule of thumb. On the other hand, note that if $V(z)$ contains a factor of the form z^{-m} then its impulse response is effectively shifted by m samples and

therefore the window $v_0, \ldots, v_N$ may fail to capture most of the energy of $V(z)$; hence the requirement that $|v_0|$ be 'significantly large'. This is not a problem in practice since any factor z^{-m} in the effective channel (or, similarly, having the first m coefficients of its impulse response with very small magnitudes) can be regarded as an overall delay which can be eliminated by redefining the symbol sequence $s(n) \to s(n-m)$.

Now if $B(z)$ is adapted via CMA it is not possible to control the value of the associated system delay to which the algorithm will converge, so that there is no guarantee that this delay will be $\delta = N$ as desired. However, in view of the structure of the Wiener receivers shown in (5.37), it is reasonable to adopt the following reinitialization scheme:

1. Use a 'center spike' initialization for $B(z)$, for example

$$b_k = \begin{cases} 1, \text{ for } k = N/2, \\ 0, \text{ otherwise.} \end{cases}$$

2. Run CMA with this starting point for a given number of iterations. It is likely that $B(z)$ converges to a point near a Wiener receiver with associated delay $\delta < N$:

$$\mathbf{b} \propto [\, v_\delta^* \; v_{\delta-1}^* \; \cdots \; v_0^* \; 0 \; \cdots \; 0 \,]^T.$$

   Then we can shift out the last $N - \delta$ zeros and reinitialize CMA with

$$\mathbf{b} \propto [\, 0 \; \cdots \; 0 \; v_\delta^* \; v_{\delta-1}^* \; \cdots \; v_0^* \,]^T.$$

   This can be done by detecting the coefficient in $\mathbf{b}$ with the highest index whose squared magnitude exceeds a certain percentage of $\mathbf{b}^\dagger\mathbf{b}$.

3. With this reinitialization it is expected that CMA will converge to a CM receiver in the vicinity of the Wiener receiver with delay $\delta = N$. But since in principle this cannot be guaranteed, it may be useful to store a performance measure associated to each CM receiver as a safeguard in order to detect situations in which the MSE actually worsens after reinitialization. In view of (5.38), this measure could be simply the squared equalizer norm $\mathbf{b}^\dagger\mathbf{b}$.

This strategy is efficient and much simpler to implement than that from [25], since it does not require on-line estimation of the autocorrelation matrix of the received signal nor solving a set of equations to find the next starting point. These features are achieved as a result of the input $x(\cdot)$ to the forward block $B(z)$ being white, due to the operation of the recursive prefilter $1/A(z)$.

A simulation experiment

In order to show the validity of the reinitialization strategy described above, we present now a simulation example. A sequence of symbols drawn from a 16-QAM

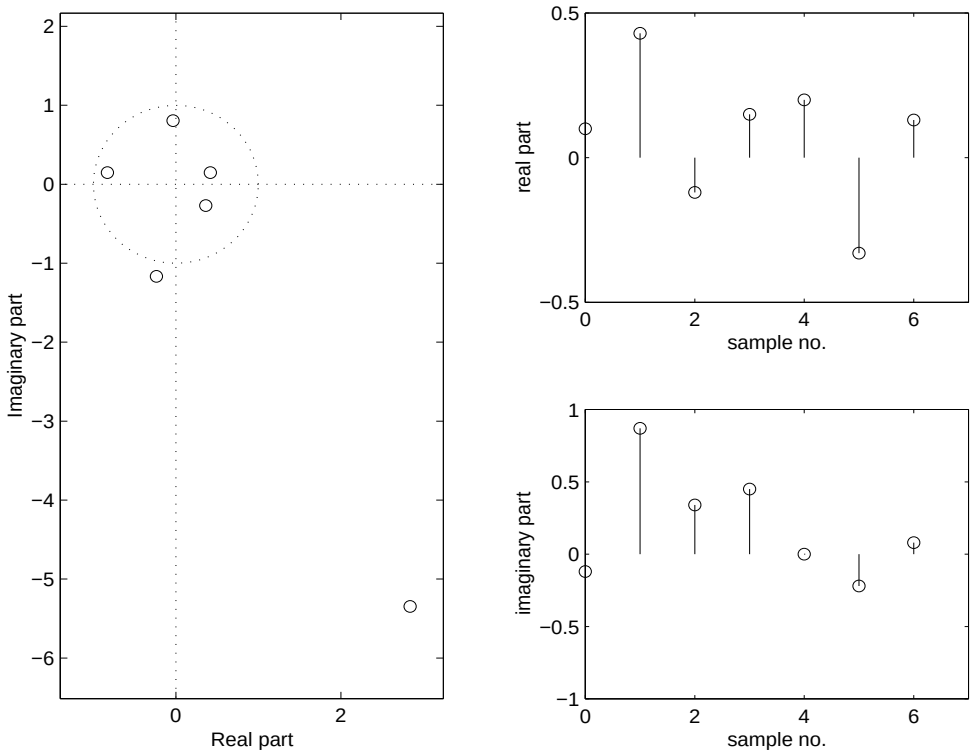

Figure 5.9: Zeros and impulse response of the channel used in the simulations.

constellation is sent through an FIR channel $C(z)$ with impulse response

$$C(z) = (0.1 - j0.12) + (0.43 + j0.87)z^{-1} + (-0.12 + j0.34)z^{-2} + (0.15 + j0.45)z^{-3} + 0.2z^{-4} + (-0.33 - j0.22)z^{-5} + (0.13 + 0.08)z^{-6}.$$

The zero distribution and impulse response of $C(z)$ are plotted in Figure 5.9. This channel is mixed phase since it has roots both inside and outside the unit circle.

White Gaussian noise was added at the channel output so that the SNR was 19 dB. The order of the prefilter $1/A(z)$ was $M = 6$, and the transversal equalizer $B(z)$ had $N + 1 = 16$ taps. The initial setting was $A(z) = 1$ and $B(z) = z^{-7}$, and the stepsize for the PLR and CMA algorithms (which are run simultaneously) was $\mu = 10^{-4}$. The recursive prefilter successfully converges to the inverse of the minimum phase spectral factor of psd of the received signal. The CMA reinitialization subroutine is executed periodically every 10,000 iterations, and it shifts out the last coefficients of $B(z)$ whose squared magnitude is 10% below the average, i.e.

$$|b_i|^2 < 0.1 \times \frac{\sum_{k=0}^{N} |b_k|^2}{N+1}. \tag{5.39}$$

Figure 5.10 illustrates the evolution of the equalizer taps. The reinitialization routine is only executed twice, since beyond that point the last tap b_{15}^* never satisfies

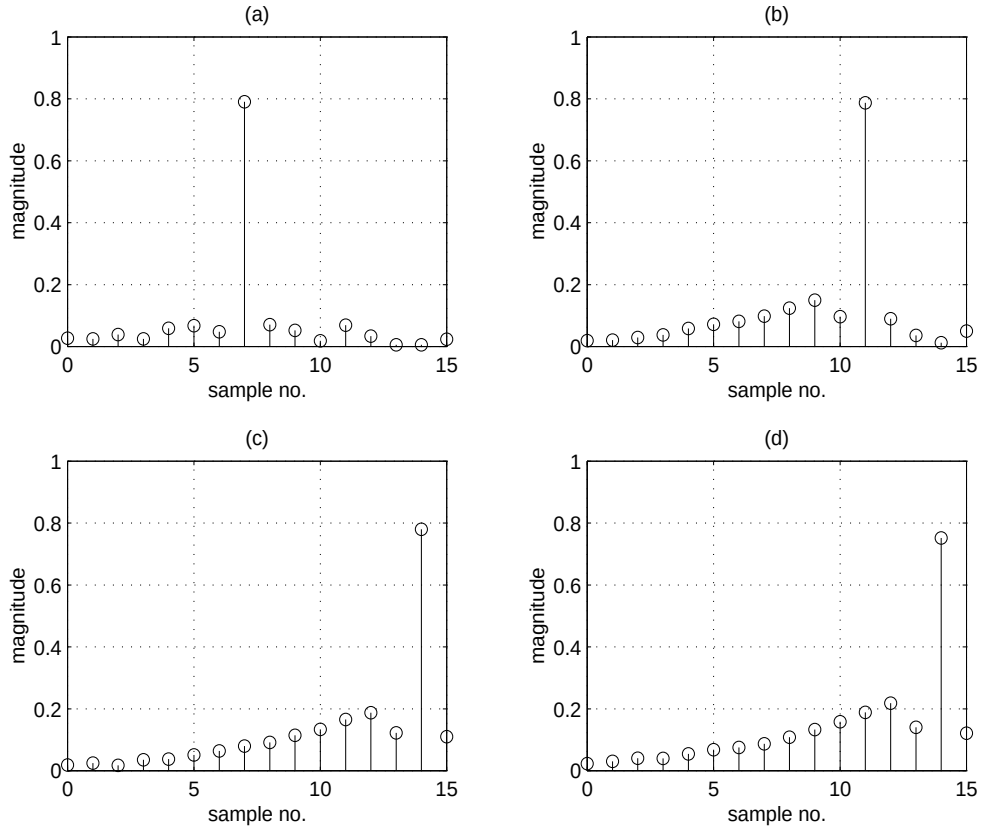

Figure 5.10: Magnitude of the coefficients of the transversal equalizer $B(z)$ adapted with CMA. (a) After 10,000 iterations. (b) After 20,000 iterations. (c) After 30,000 iterations. (d) After 100,000 iterations.

the condition (5.39). At iteration 10,000 the last four coefficients are shifted out, and then after iteration 20,000 three more taps are also shifted out.

It is seen how the shifting strategy successfully leads the equalizer to the optimal system delay. The scatter diagrams of the received and equalized symbols are shown in Figure 5.11 for the iterations 50,000 through 100,000. Clearly the blind equalizer has opened the eye.

Next we reduced the order of the recursive prewhitener from $M = 6$ to $M = 4$ and repeated the experiment with the same channel and an SNR of 32 dB. In that case the order of $A(z)$ is less than that of the channel $C(z)$, so that the signal $x(\cdot)$ fed to the transversal equalizer $B(z)$ will no longer be white. Nevertheless, the PLR algorithm obtains an acceptable setting after convergence, as can be seen from the pole-zero and Bode plots of the cascade $C(z)/A(z)$ shown in Figure 5.12. The maximum peak-to-peak deviation of the magnitude response is seen to be below 5 dB. The reinitialization scheme is also applied to the transversal equalizer $B(z)$, with the results shown in Figure 5.13.

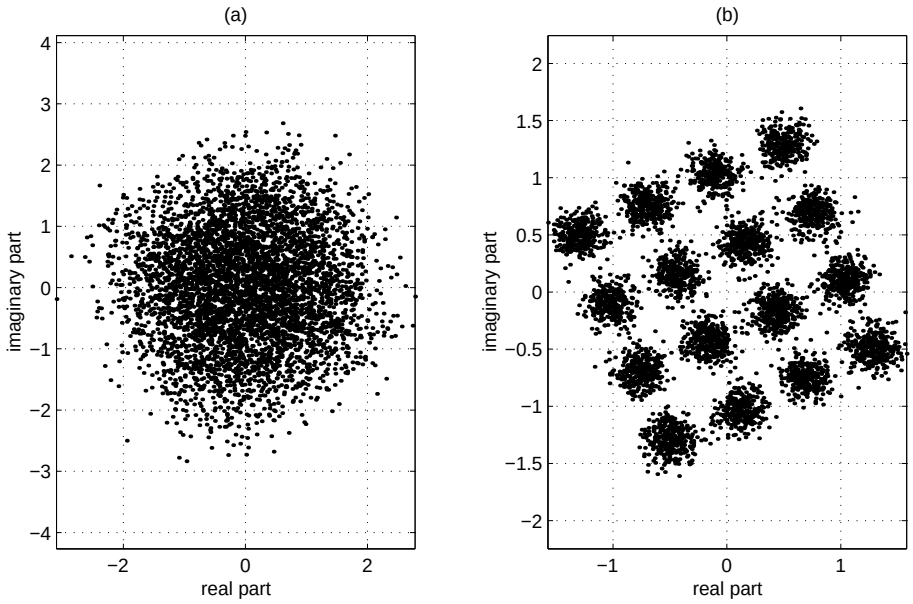

Figure 5.11: Scatter diagrams. (a) Received signal. (b) Equalizer output.

5.4 Conclusions

In this chapter we have analyzed the adaptive IIR filtering problem in the channel equalization context. There are two main reasons to use recursive equalizers: they have the potential to reach a lower MSE than their FIR counterparts, and they could be used in order to blindly initialize a DFE configuration (This strategy, however, may be very sensitive to equalizer length). The recursive part of the equalizer should be placed upstream in the receiver structure, and ideally it should whiten the received signal. This can be achieved by means of two different algorithms: OVM and PLR. These two approaches are blind and based on the second order statistics of the received signal. They seem to provide a certain degree of robustness to channel order mismatch. The existence of stationary points of the PLR algorithm in reduced order cases was shown with the aid of an off-line iterative interpretation of this scheme.

Any blind algorithm for the adaptation of the nonrecursive part of the equalizer has to be based on higher order statistics, like CMA. The relation between CM and Wiener receivers, together with an analysis of the Wiener solutions with different associated system delays for white input signals, provided a computationally simple and efficient procedure for reinitialization of CMA in order to seek the system delay with smallest MSE.

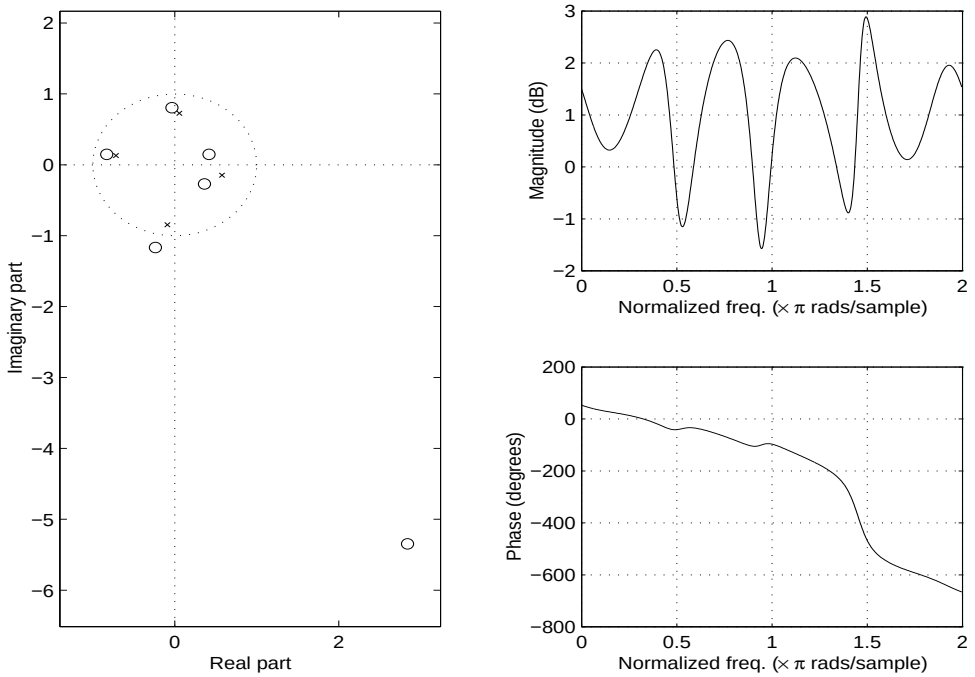

Figure 5.12: Pole-zero and Bode plots of the series $C(z)/A(z)$ after convergence of the PLR algorithm with $M = 4$ and SNR = 32 dB.

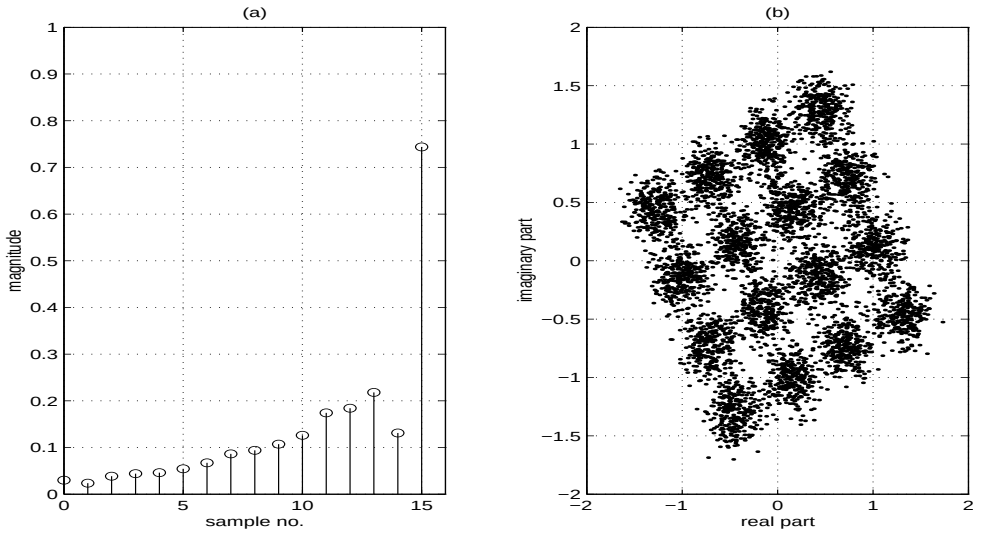

Figure 5.13: Results with a prefilter of order $M = 4$ and SNR = 32 dB. (a) Magnitude of the coefficients of $B(z)$ after 30,000 iterations. (b) Equalizer output.

Chapter 6

CONCLUSIONS AND OPEN PROBLEMS

In this thesis several aspects of the adaptive recursive filtering problem have been discussed in detail. An important issue that must be taken into consideration when implementing an adaptive system of this kind is to guarantee stability of the IIR filter. Because of this, we have focused on normalized lattice realizations since these structures are inherently stable even when they become time-varying. Besides the usual system identification configuration, the adaptive equalization setting using recursive structures has also been considered. The contributions of our work are summarized next.

6.1 Contributions

The derivation of adaptive algorithms for IIR filters in lattice form was considered in Chapter 2. Although several computationally efficient lattice versions of the Equation Error, Output Error, Steiglitz-McBride and hyperstability based algorithms have been previously proposed, it was shown that most of them may present convergence problems even in ideal system identification configurations for which their direct form counterparts do not. In order to overcome this drawback, a systematic approach to the derivation of a lattice variant from a given direct form algorithm was presented, based on the analysis of the associated differential equation. The resulting scheme is fairly general and efficient, and it preserves the local convergence properties of the direct form algorithms in sufficient order settings, in contrast with previous approaches.

Chapter 3 provides an analysis of several off-line system identification schemes which serve as starting points to the development of on-line adaptive algorithms for IIR filters. These methods attempt to circumvent the bias problem of the Equation Error (EE) method and the multimodality of the Output Error (OE) cost function by constructing a sequence of 'distorted' EE problems (which are quadratic and therefore easily solved) which are iterated until convergence. The 'distortion' of each EE problem depends on the solution to the previous one, and typically involves the inversion of the estimate of the denominator polynomial of the unknown system's transfer function. As a consequence, the iteration may break

if this polynomial is not minimum phase. We have provided conditions on the input signal that ensure the minimum phase property of the EE estimate, for both the monic and quadratically constrained approaches.

The standard example of an iterative off-line scheme is the Steiglitz-McBride (SM) method, which has become popular due to the good behavior of the estimates that it provides in reduced order cases. This feature has been analyzed recently with the aid of a lattice off-line variant of the SM iteration, which has the same set of stationary points as the original direct form version. We have shown that, on the other hand, the convergence properties of the two variants can be quite different: a convergent point of the direct form SM iteration need not be convergent for the lattice iteration.

Another iterative off-line procedure is the interpolation expanded numerator (IXN) method, which makes use of an overparameterized numerator in the model. This scheme is not biased in the presence of output measurement noise, and it was known to have a unique stationary point, corresponding to the unknown system, in sufficient order cases with white inputs. It has been shown in Chapter 3 that uniqueness is still preserved for a wider class of inputs (autoregressive processes of certain order), provided that the order of the numerator of the model is above certain threshold value. With colored input signals, the corresponding on-line algorithm was modified in order to preserve local convergence of the stationary points. The approach derived in Chapter 2 can be used to derive a lattice adaptive algorithm based on the IXN method.

Chapter 3 also presented a novel iterative off-line scheme: the Steiglitz-McBride / expanded numerator (SM/XN) method, which is also based on an overparameterized numerator and incorporates elements from the SM method. Uniqueness of the stationary point of the SM/XN iteration in sufficient order cases was shown, again under an autoregressive condition on the input signal and a length condition on the model's numerator. On-line adaptive algorithms based on the SM/XN concepts were also derived for both direct form and lattice implementations.

A new look at the family of hyperstability based adaptive identification algorithms was presented in Chapter 4. Convergence of these schemes requires a strictly positive realness (SPR) condition on the denominator of the transfer function of the system to be identified, which may be hard to determine since this denominator is unknown. In addition, the set of SPR denominators is only a small subset of the set of minimum phase denominators, which places stringent constraints on the applicability of these algorithms. We have presented two related ways to relax the SPR condition. The first one is based on overparameterization of the adaptive filter by using a polyphase realization, while the second is a subband approach in which the input and reference signals are filtered by an analysis bank and then decimated. In both cases the net effect is that the roots of the polynomial on which the SPR requirement falls are pulled toward the interior of the unit circle, by an amount that increases with the polyphase expansion factor or the decimation factor. This makes

the SPR condition more likely to be satisfied. The price to pay is a strongest persistence of excitation requirement on the input signal, which is related to a greater number of adaptive parameters (a consequence of overparameterization).

Motivated by recent interest in the application of adaptive recursive filters to the equalization problem in digital communication systems, this setting was considered in Chapter 5. Two algorithms for the adaptation of the recursive part of the equalizer were discussed in detail. The first one (OVM) attempts to minimize the variance of its output through a stochastic gradient descent. The second (PLR) attempts to decorrelate the output signal up to a lag equal to the filter order. Both approaches have the advantages of being unsupervised (no training signal is needed) and based on second order statistics of the received signal. In addition, in sufficient order cases both algorithms converge to the minimum of the MSE cost, at which the output signal becomes white. In reduced order settings the situation becomes more involved, although OVM and PLR seem to provide a certain degree of robustness to channel order mismatch. It was shown that the PLR approach can be thought of as an off-line iterative scheme, which admits a stationary point in all cases provided the SNR is finite, regardless of the degree of undermodeling.

Assuming that the recursive portion of the equalizer is capable of whitening its output, we considered the issue of blindly adapting the nonrecursive part, which is driven by this white signal, via the constant modulus algorithm (CMA). By examining the structure of the (nonblind) Wiener FIR equalizers for the different system delays when the input signal is white, and exploiting recent results which present conditions for the existence of CMA stationary points in a neighborhood of Wiener equalizers, we developed a procedure to reinitialize CMA in order to find the system delay with smallest MSE. This strategy is computationally much simpler than similar approaches that have been proposed for CMA based FIR equalizers without a prewhitener.

6.2 Open problems

The problem of adaptive recursive filter still poses a challenge to signal processing and control researchers. Application of these devices to practical systems is still impeded by an incomplete understanding of their properties, especially in undermodeled scenarios. In identification settings, an algorithm with global convergence to a valid solution regardless of input coloring, undermodeling, and output measurement noise is simply not known. Although we have provided some results for several issues concerning adaptive IIR filters, many questions still remain unanswered.

For example, our approach to the development of lattice algorithms does not inform of whether the stability properties of stationary points are preserved in reduced order cases, except for stochastic gradient descents such as the Equation Error and the Output Error methods. In this respect, further study of the properties of the associated ODEs and their feedback matrices is clearly needed. This is

also true for the IXN-2 adaptive algorithm, whose local convergence properties in sufficient order cases still have to be determined.

Several results generalizing questions such as stability and uniqueness of the estimates for off-line identification methods to colored inputs were restricted to autoregressive processes. The main reason is that the Szegö polynomials associated to these processes satisfy a nice shift property. It is reasonable to ask whether other orthonormal bases with special properties exist that could allow further results with other kinds of colored signals. Other questions related to Szegö polynomials have also been left open along the thesis. For example, if $H(z)$ is a transfer function with M poles and N zeros, is it completely determined by the first $N + M + 1$ coefficients of its expansion over the Szegö polynomials associated to an arbitrary power spectral density?

In order to relax the SPR condition for hyperstability based algorithms we have considered the use of overparameterization in a structured fashion, in particular through polyphase structures. It could be interesting to investigate different ways to overparameterize the adaptive filter that could result in a more efficient relaxation of the SPR requirement.

Concerning the application of recursive filters to equalization problems, perhaps the most challenging issue is the development of a valid strategy for blind initialization of a DFE under filter length constraints. It is also of interest to develop the structure of the optimal DFE under the only constraint of causality. Based on Kalman filtering ideas, it is expected that this filter be of finite order. This could facilitate the development of new cold start-up schemes based on the corresponding structure.

Although we have provided some evidence for the robustness of the solutions provided by the OVM and PLR algorithms in reduced order cases, theoretical justification of this claim is still lacking. To this end, the first step could be the development of a meaningful measure of the degree of undermodeling for the equalization setting.

An interesting open line of research is the analysis of blind, higher order statistics based adaptive algorithms such as CMA for FIR equalizers, when the input to the filter is white. As we have shown, this property can be exploited in order to devise a simple reinitialization strategy, but it could also provide simplifications in the fairly involved convergence analysis of these algorithms.

Finally, we should note that our focus has been on single input single output (SISO) equalization settings. The applicability of recursive equalizers to communications systems with spatial diversity and/or fractionally sampled, resulting in single input multiple output (SIMO) configurations, surely deserves further consideration.

Appendix A

RECURSIVE COMPUTATION OF THE JACOBIAN $\mathrm{D}(\theta)$

The Jacobian $\mathbf{D}(\theta)$ can be easily obtained by exploiting the structure of the recursions (1.14)-(1.15), as shown by Cruces in [18]. The i, jth element of $\mathbf{D}(\theta)$ is $\partial a_i/\partial \sin\phi_j$. Taking partial derivatives with respect to $\sin\phi_j$ in (1.14-1.15), one obtains:

$$j > k: \quad \frac{\partial a_i^{(k)}}{\partial \sin\phi_j} = 0, \qquad i = 1, \ldots k; \tag{A.1}$$

$$j = k: \quad \frac{\partial a_i^{(k)}}{\partial \sin\phi_k} = \begin{cases} 1, & i = k; \\ a_{k-i}^{(k-1)}, & i < k; \end{cases} \tag{A.2}$$

$$j < k: \quad \frac{\partial a_i^{(k)}}{\partial \sin\phi_j} = \begin{cases} 0, & i = k; \\ \frac{\partial a_i^{(k-1)}}{\partial \sin\phi_j} + \sin\phi_k \frac{\partial a_{k-i}^{(k-1)}}{\partial \sin\phi_j}, & i < k. \end{cases} \tag{A.3}$$

These relations can be expressed in matrix form. Let $\mathbf{D}_k$ be the $k \times k$ matrix with the i, jth element given by $\partial a_i^{(k)}/\partial \sin\phi_j$; then in view of (A.1)-(A.3), for $k = 1$, $\cdots$, $M-1$ one has

$$\mathbf{D}_{k+1} = \begin{bmatrix} & & & a_k^{(k)} \\ \mathbf{D}_k + a_{k+1}^{(k+1)} \mathbf{J}_k \mathbf{D}_k & & & \vdots \\ & & & a_1^{(k)} \\ 0 & \cdots & 0 & 1 \end{bmatrix}, \tag{A.4}$$

where $\mathbf{J}_k$ is the $k \times k$ exchange matrix with ones in the antidiagonal and zeros elsewhere. The recursion starts with $\mathbf{D}_1 = 1$, and it yields $\mathbf{D}(\theta) = \mathbf{D}_M$.

Appendix B

PROOFS

B.1 Proof of Lemma 2.1

Write $\mathbf{S}_l(\theta)$ as the sum of two components $\mathbf{P}(\theta)$, $\mathbf{Q}(\theta)$:

$$\begin{aligned}\mathbf{S}_l(\theta) &= \frac{\mathrm{d}E[\mathbf{x}_l(n)e(n)]}{\mathrm{d}\theta_l} \\ &= \underbrace{E\left[\frac{\mathrm{d}\mathbf{x}_l(n)}{\mathrm{d}\theta_l}\cdot e(n)\right]}_{=\mathbf{P}(\theta)} + \underbrace{E\left[\mathbf{x}_l(n)\frac{\mathrm{d}e(n)}{\mathrm{d}\theta_l}\right]}_{=\mathbf{Q}(\theta)}.\end{aligned}$$

At a stationary point θ_*, the matrix $\mathbf{P}(\theta_*)$ is given by

$$\mathbf{P}(\theta_*) = E\left[\frac{\mathrm{d}\mathbf{x}_l(n)}{\mathrm{d}\theta_l}e(n)\right]_{\theta_*} = E\left\{\frac{\mathrm{d}}{\mathrm{d}\theta_l}\left[\mathbf{R}(\theta)\mathbf{x}_d(n)\right]e(n)\right\}_{\theta_*}$$

Let $\mathbf{R}_k^T(\theta)$ be the kth row of $\mathbf{R}(\theta)$. Then

$$\mathbf{P}(\theta_*) = \mathbf{R}(\theta_*)E\left[\frac{\mathrm{d}\mathbf{x}_d(n)}{\mathrm{d}\theta_l}\cdot e(n)\right]_{\theta_*} + E\left\{\begin{bmatrix}\mathbf{x}_d^T(n)\frac{\mathrm{d}\mathbf{R}_1(\theta)}{\mathrm{d}\theta_l}\\ \vdots \\ \mathbf{x}_d^T(n)\frac{\mathrm{d}\mathbf{R}_{N+M+1}(\theta)}{\mathrm{d}\theta_l}\end{bmatrix}e(n)\right\}_{\theta_*}. \quad \text{(B.1)}$$

Observe that the second term in the right-hand side of (B.1) is zero: Its kth row is

$$E\left[\mathbf{x}_d^T(n)e(n)\right]_{\theta_*}\left.\frac{\mathrm{d}\mathbf{R}_k(\theta)}{\mathrm{d}\theta_l}\right|_{\theta_*}$$

and $E[\mathbf{x}_d(n)e(n)]_{\theta_*} = \mathbf{0}$ since θ_* is a stationary point. Therefore, applying the chain rule,

$$\begin{aligned}\mathbf{P}(\theta_*) &= \mathbf{R}(\theta_*)E\left[\frac{\mathrm{d}\mathbf{x}_d(n)}{\mathrm{d}\theta_d}\cdot e(n)\right]_{\theta_*}\cdot\left.\frac{\mathrm{d}\theta_d}{\mathrm{d}\theta_l}\right|_{\theta_*} \\ &= \mathbf{R}(\theta_*)E\left[\frac{\mathrm{d}\mathbf{x}_d(n)}{\mathrm{d}\theta_d}\cdot e(n)\right]_{\theta_*}\mathbf{F}(\theta_*). \quad \text{(B.2)}\end{aligned}$$

On the other hand, the matrix $\mathbf{Q}(\theta)$ is given by

$$\mathbf{Q}(\theta) = E\left[\mathbf{x}_l(n)\frac{\mathrm{d}e(n)}{\mathrm{d}\theta_l}\right] = \mathbf{R}(\theta)E\left[\mathbf{x}_d(n)\frac{\mathrm{d}e(n)}{\mathrm{d}\theta_d}\right]\mathbf{F}(\theta),$$

where again we have used the chain rule. Hence, the matrix $\mathbf{S}_l(\theta_*) = \mathbf{P}(\theta_*) + \mathbf{Q}(\theta_*)$ reduces to

$$\begin{aligned}\mathbf{S}_l(\theta_*) &= \mathbf{R}(\theta_*)E\left[\frac{\mathrm{d}\mathbf{x}_d(n)}{\mathrm{d}\theta_d}e(n) + \mathbf{x}_d(n)\frac{\mathrm{d}e(n)}{\mathrm{d}\theta_d}\right]_{\theta_*}\mathbf{F}(\theta_*)\\ &= \mathbf{R}(\theta_*)\frac{\mathrm{d}E[\mathbf{x}_d(n)e(n)]}{\mathrm{d}\theta_d}\bigg|_{\theta_*}\mathbf{F}(\theta_*)\\ &= \mathbf{R}(\theta_*)\mathbf{S}_d(\theta_*)\mathbf{F}(\theta_*),\end{aligned}$$

which is (2.25). ∎

B.2 Proof of Theorem 3.1

First note from (3.5) that if $\mathbf{R}_{vv} + \mathbf{R}_{y/u}$ is singular then the smallest achievable error variance is zero. This means that perfect modeling is possible: $\eta(\cdot)$ must be identically zero and the optimum model is $\hat{H}_\star(z) = H(z)$, which is assumed stable. Therefore, assume that $\mathbf{R}_{vv} + \mathbf{R}_{y/u} > \mathbf{0}$. In view of Lemma 3.1, it suffices to show that the displacement matrix of $\mathbf{R}_{vv} + \mathbf{R}_{y/u}$ is positive semidefinite. Note that since $\mathbf{R}_{vv}$ is Toeplitz, this displacement matrix is

$$\mathbf{\Delta} = \underbrace{\lceil \mathbf{R}_{vv} - \mathbf{R}_{vv} \rfloor}_{=\mathbf{0}} + \lceil \mathbf{R}_{y/u} - \mathbf{R}_{y/u} \rfloor.$$

Let $\{p_k(z)\}_{k=0}^{\infty}$ be the Szegö polynomials associated to $u(\cdot)$. Consider shifted versions of $H(z)$ expanded over the Szegö polynomials as

$$z^{-l}H(z) = \sum_{k=0}^{\infty} h_k^{(l)} p_k(z), \qquad h_k^{(l)} = \langle z^{-l}H(z), p_k(z)\rangle,$$

with $l \geq 0$. It is shown in [104] that, with $0 \leq i,\ j \leq M$, the $i,\ j$th element of the matrix $\mathbf{R}_{y/u}$ is

$$(\mathbf{R}_{y/u})_{i,j} = \sum_{k=N+1}^{\infty} h_k^{(i)} h_k^{(j)}. \tag{B.3}$$

If $u(\cdot)$ is AR of degree $N+1$ or less, then $p_{k+1}(z) = z^{-1}p_k(z)$ for all $k \geq N+1$ (see Appendix C for a review of the Szegö polynomials and their properties). As a

consequence, for $k \geq N+1$ one has

$$\begin{aligned} h_k^{(l-1)} &= \langle z^{-l+1}H(z), p_k(z)\rangle \\ &= \langle z^{-l}H(z), z^{-1}p_k(z)\rangle \\ &= \langle z^{-l}H(z), p_{k+1}(z)\rangle \\ &= h_{k+1}^{(l)}. \end{aligned}$$

This together with (B.3) implies that for $1 \leq i,\ j \leq M$,

$$(\mathbf{R}_{y/u})_{i,j} - (\mathbf{R}_{y/u})_{i-1,j-1} = h_{N+1}^{(i)} h_{N+1}^{(j)},$$

and therefore $\mathbf{\Delta} = \mathbf{h}\mathbf{h}^T \geq \mathbf{0}$ where $\mathbf{h} = [\, h_{N+1}^{(1)} \ \cdots \ h_{N+1}^{(M)} \,]^T$. Stability of the minimizer follows from Lemma 3.1. ∎

B.3 Proof of Lemma 3.2

First we shall prove that by reflecting an unstable zero with respect to the unit circle, the cost $J(\mathbf{a})$ cannot increase if $\mathbf{\Delta} \geq \mathbf{0}$. Let $\mathbf{a}_\star$ solve (3.6). Suppose that the corresponding polynomial $A_\star(z)$ has a root at $z = z_0$ with $|z_0| > 1$:

$$A_\star(z) = (1 - z_0 z^{-1})C(z),$$

and let

$$\bar{A}_\star(z) = (z_0^* - z^{-1})C(z)$$

be the polynomial obtained by reflecting z_0 with respect to the unit circle.

Since $\mathbf{Q}$ is symmetric, Toeplitz and positive definite, it can be thought of as the autocorrelation matrix of some process $x(\cdot)$ with psd $S_{xx}(z)$, so that

$$\mathbf{a}_\star^\dagger \mathbf{Q} \mathbf{a}_\star = \frac{1}{2\pi}\int_{-\pi}^{\pi} S_{xx}(e^{j\omega})|A_\star(e^{j\omega})|^2 \mathrm{d}\omega. \tag{B.4}$$

Also observe that

$$A_\star(z) = \bar{A}_\star(z)V(z) \qquad \text{with} \qquad V(z) = \frac{1 - z_0 z^{-1}}{z_0^* - z^{-1}}. \tag{B.5}$$

Since $V(z)$ is all-pass with unit magnitude on the unit circle, we have $|A_\star(e^{j\omega})|^2 = |\bar{A}_\star(e^{j\omega})|^2$. In view of (B.4), this implies that $\mathbf{a}_\star^\dagger \mathbf{Q} \mathbf{a}_\star = \bar{\mathbf{a}}_\star^\dagger \mathbf{Q} \bar{\mathbf{a}}_\star$, where $\bar{\mathbf{a}}_\star$ is the vector of coefficients of $\bar{A}_\star(z)$. Thus $\bar{\mathbf{a}}_\star$ satisfies the original constraint.

Let now $\mathbf{c}$ be the coefficient vector of $C(z)$. Since

$$\mathbf{a}_\star = \begin{bmatrix} \mathbf{c} \\ 0 \end{bmatrix} - z_0 \begin{bmatrix} 0 \\ \mathbf{c} \end{bmatrix}, \qquad \bar{\mathbf{a}}_\star = z_0^* \left(\begin{bmatrix} \mathbf{c} \\ 0 \end{bmatrix} - \frac{1}{z_0^*} \begin{bmatrix} 0 \\ \mathbf{c} \end{bmatrix} \right),$$

one has

$$\begin{aligned} J(\mathbf{a}_\star) &= \mathbf{c}^\dagger \left(\mathbf{R}\rfloor + |z_0|^2 \lceil \mathbf{R} - z_0 \lfloor \mathbf{R} - z_0^* \mathbf{R} \rceil \right) \mathbf{c}, \\ J(\bar{\mathbf{a}}_\star) &= |z_0|^2 \mathbf{c}^\dagger \left(\mathbf{R}\rfloor + \frac{1}{|z_0|^2} \lceil \mathbf{R} - \frac{1}{z_0^*} \lfloor \mathbf{R} - \frac{1}{z_0} \mathbf{R} \rceil \right) \mathbf{c}, \end{aligned}$$

which give $J(\bar{\mathbf{a}}_\star) = J(\mathbf{a}_\star) + (1 - |z_0|^2)\mathbf{c}^\dagger \mathbf{\Delta} \mathbf{c}$.

If $\mathbf{\Delta} \geq \mathbf{0}$, then for $|z_0| > 1$ we have $J(\bar{\mathbf{a}}_\star) \leq J(\mathbf{a}_\star)$. Since $\mathbf{a}_\star$ minimizes J, equality must hold, i.e. $J(\bar{\mathbf{a}}_\star) = J(\mathbf{a}_\star)$.

Let $\lambda = J(\mathbf{a}_*)$, and let $\mathbf{Q} = \mathbf{L}\mathbf{L}^T$ be the Cholesky factorization of $\mathbf{Q}$. Then it can be shown that λ is the smallest eigenvalue of $\mathbf{L}^{-1}\mathbf{R}\mathbf{L}^{-T}$. If λ is simple, then the minimum of the cost J is unique, so we have a contradiction. If λ is multiple then $J(\bar{\mathbf{a}}_\star) = J(\mathbf{a}_\star)$ is possible. However, by reflecting the zero inside the unit circle the cost does not change, which means that a polynomial without roots outside the unit circle can be found in the solution set.

To see that $\mathbf{\Delta} > \mathbf{0}$ gives strict stability, consider the family of polynomials with a zero at $z = re^{j\theta}$, with θ some fixed angle:

$$A_r(z) = g(r)(1 - re^{j\theta} z^{-1}) C(z).$$

The normalization factor

$$\begin{aligned} g(r) &= [(1 + r^2)\alpha - 2r\beta]^{-\frac{1}{2}}, \\ \alpha &= \frac{1}{2\pi} \int_{-\pi}^{\pi} S_{xx}(e^{j\omega}) |C(e^{j\omega})|^2 \mathrm{d}\omega, \\ \beta &= \frac{1}{2\pi} \int_{-\pi}^{\pi} S_{xx}(e^{j\omega}) |C(e^{j\omega})|^2 \cos(\omega - \theta) \mathrm{d}\omega \end{aligned}$$

is chosen so that, with $\mathbf{a}_r$ the coefficient vector of $A_r(z)$, $\mathbf{a}_r^\dagger \mathbf{Q} \mathbf{a}_r = 1$ is satisfied for all $r \geq 0$. The cost J along this radial line can be written as

$$\begin{aligned} J(\mathbf{a}_r) &= \mathbf{a}_r^\dagger \mathbf{R} \mathbf{a}_r \\ &= g^2(r) \left\{ J(\mathbf{a}_1) r + \mathbf{c}^\dagger \left[\mathbf{R}\rfloor - r(\mathbf{R}\rfloor + \lceil \mathbf{R}) + r^2 \lceil \mathbf{R} \right] \mathbf{c} \right\}. \end{aligned}$$

It can be readily verified that

$$\left. \frac{\partial J(\mathbf{a}_r)}{\partial r} \right|_{r=1} = \frac{\mathbf{c}^\dagger \mathbf{\Delta} \mathbf{c}}{2(\alpha - \beta)},$$

which is strictly positive if $\mathbf{\Delta} > \mathbf{0}$, since

$$2(\alpha - \beta) = \frac{\mathbf{a}_1^\dagger \mathbf{Q} \mathbf{a}_1}{g^2(1)} > 0.$$

This precludes the possibility of a root on the unit circle. ∎

B.4 Proof of Lemma 3.4

Let

$$H_1(z) = \frac{B_1(z)}{A_1(z)} \qquad \text{and} \qquad H_2(z) = \frac{B_2(z)}{A_2(z)}$$

be two rational transfer functions, with $B_i(z)$ having order N, and monic $A_i(z)$ having order M, $i = 1, 2$. Assume that

$$\langle H_1(z) - H_2(z), p_k(z) \rangle_u = 0, \qquad k = 0, 1, \ldots N + M, \tag{B.6}$$

where $\{p_k(z)\}_{k=0}^{\infty}$ are the Szegö polynomials associated to $u(\cdot)$. Then

$$H_1(z) - H_2(z) \in \mathcal{K}_{N+M+1} = \text{span}\{p_k(z)\}_{k=N+M+1}^{\infty}.$$

The fact that $u(\cdot)$ is AR$(N + M + 1)$ implies that $\mathcal{K}_{N+M+1}$ is a right shift invariant subspace (see Appendix C). Therefore, the function

$$f(z) = A_1(z)A_2(z)[H_1(z) - H_2(z)]$$

belongs in $\mathcal{K}_{N+M+1}$. But $f(z) = B_1(z)A_2(z) - B_2(z)A_1(z)$ is a polynomial of degree not exceeding $N+M$, and therefore it belongs in the orthogonal complement $\mathcal{K}_{N+M+1}^{\perp} = \text{span}\{p_k(z)\}_{k=0}^{N+M}$. Then

$$f(z) \in \mathcal{K}_{N+M+1}, \quad f(z) \in \mathcal{K}_{N+M+1}^{\perp} \qquad \Rightarrow \qquad f(z) = 0,$$

which implies $H_1(z) = H_2(z)$. ∎

B.5 Proof of the MA(1) case with $N = 0$, $M = 1$

Let $S_{uu}(z) = q(z)q(z^{-1})$ with $q(z) = q_0 + q_1 z^{-1}$. Then $S_{uu}(z) = q_0 q_1 z + (q_0^2 + q_1^2) + q_0 q_1 z^{-1}$. Normalizing $E[u^2(n)] = 1$ gives $q_0^2 + q_1^2 = 1$, so we can equate $q_0 = \sin\vartheta$, $q_1 = \cos\vartheta$. Now if we define $\sin\varphi = \frac{1}{2}\sin 2\vartheta$, we obtain

$$S_{uu}(z) = \sin\varphi z + 1 + \sin\varphi z^{-1}.$$

The Szegö polynomials $p_0(z)$ and $p_1(z)$ associated to this psd are

$$p_0(z) = 1, \qquad p_1(z) = \frac{-\sin\varphi + z^{-1}}{\cos\varphi}.$$

Let $H(z) = b/(1 - az^{-1})$ be a transfer function with $N = 0$ zeros and $M = 1$ pole. Then

$$\begin{aligned} \langle H(z), p_0(z) \rangle_u &= \langle H(z), [p_0(z)S_{uu}(z)]_+ \rangle \\ &= \frac{1}{2\pi j} \oint \frac{b}{z - a}(1 + \sin\varphi z)dz \\ &= b(1 + a\sin\varphi), \end{aligned}$$

and

$$\begin{aligned}\langle H(z), p_1(z)\rangle_u &= \langle H(z), [p_1(z)S_{uu}(z)]_+\rangle \\ &= \frac{1}{2\pi j}\oint \frac{b(\cos^2\varphi z + \sin\varphi z^2)}{\cos\varphi(z-a)}dz \\ &= \frac{ab(\cos^2\varphi + a\sin\varphi)}{\cos\varphi}.\end{aligned}$$

Suppose that $H_1(z) = b_1/(1-a_1z^{-1})$ and $H_2(z) = b_2/(1-a_2z^{-1})$ satisfy

$$\langle H_1(z), p_k(z)\rangle_u = \langle H_2(z), p_k(z)\rangle_u, \qquad k = 0, 1.$$

Then (note that $\cos\varphi \neq 0$ since $|\sin\varphi| = |\sin 2\vartheta|/2 \leq 1/2$),

$$b_1(1 + a_1\sin\varphi) = b_2(1 + a_2\sin\varphi), \tag{B.7}$$

$$a_1b_1(\cos^2\varphi + a_1\sin\varphi) = a_2b_2(\cos^2\varphi + a_2\sin\varphi). \tag{B.8}$$

Define $f(a) = \cos^2\varphi + a\sin\varphi$, and divide (B.8) by (B.7) to obtain

$$\frac{a_1f(a_1)}{f(a_1)+\sin^2\varphi} = \frac{a_2f(a_2)}{f(a_2)+\sin^2\varphi} \qquad \Rightarrow \qquad (f(a_1)f(a_2) + \sin^2\varphi)(a_1 - a_2) = 0.$$

Since $|\sin\varphi| \leq 1/2$, one can check that $f(a) > 0$ for $|a| < 1$. Therefore $f(a_1)f(a_2) + \sin^2\varphi > 0$, so that we must have $a_1 = a_2$. This in turn implies $b_1 = b_2$ in view of (B.7), and therefore $H_1(z) = H_2(z)$. ∎

B.6 Proof of Lemma 3.5

For convenience, let $\mathbf{R}_k$ be the $(k+1)\times(k+1)$ autocorrelation matrix of the process $u(\cdot)$. Then $\mathbf{R}_{uu} = \mathbf{R}_N$, and $\mathbf{R}_L$ can be partitioned as

$$\mathbf{R}_L = \begin{bmatrix}\mathbf{R}_N & \mathbf{P} \\ \mathbf{P}^T & \mathbf{R}_{L-N+1}\end{bmatrix}.$$

As shown in Appendix C, the matrix $\mathbf{C}_L$ in (3.26) satisfies $\mathbf{I} = \mathbf{C}_L\mathbf{R}_L\mathbf{C}_L^T$. On the other hand,

$$\mathbf{C}_L\mathbf{R}_L\mathbf{C}_L^T = \begin{bmatrix}\mathbf{C}_N\mathbf{R}_N\mathbf{C}_N^T & \mathbf{C}_N\mathbf{R}_N\mathbf{B}^T + \mathbf{C}_N\mathbf{P}\mathbf{A}^T \\ \mathbf{B}\mathbf{R}_N\mathbf{C}_N^T + \mathbf{A}\mathbf{P}^T\mathbf{C}_N^T & \mathbf{B}\mathbf{R}_N\mathbf{B}^T + \mathbf{B}\mathbf{P}\mathbf{A}^T + \mathbf{A}\mathbf{P}^T\mathbf{B}^T + \mathbf{A}\mathbf{R}_{L-N+1}\mathbf{A}^T\end{bmatrix},$$

and this must equal the identity matrix. Hence,

$$\mathbf{C}_N\mathbf{R}_N\mathbf{B}^T + \mathbf{C}_N\mathbf{P}\mathbf{A}^T = \mathbf{0} \qquad \Rightarrow \qquad \mathbf{R}_N\mathbf{B}^T + \mathbf{P}\mathbf{A}^T = \mathbf{0}$$

since $\mathbf{C}_N$ is nonsingular. The result of Lemma 3.5 follows immediately. ∎

B.7 Proof of Lemma 3.6

We can write the matrix $\mathbf{H}$ as

$$\mathbf{H} = \left\langle \begin{bmatrix} z^{-1} \\ \vdots \\ z^{-M} \end{bmatrix} \frac{B^{(k+1)}(z)}{A^{(k)}(z)}, \begin{bmatrix} p_{N+1}(z) \\ \vdots \\ p_L(z) \end{bmatrix}^T \right\rangle_u .$$

Since the interpolation conditions (3.15) hold at every iteration k, one has

$$H(z) - \frac{B^{(k+1)}(z)}{A^{(k)}(z)} \in \mathcal{K}_{L+1} = \text{span}\{p_l(z)\}_{l=L+1}^{\infty}.$$

Since $u(\cdot)$ is AR$(L+1)$, the subspace $\mathcal{K}_{L+1}$ is right shift invariant (see Appendix C), so that

$$z^{-i}\left(H(z) - \frac{B^{(k+1)}(z)}{A^{(k)}(z)}\right) \in \mathcal{K}_{L+1} \qquad \text{for all } i \geq 0.$$

Hence for all $i \geq 0$ and for $0 \leq l \leq L$,

$$\langle z^{-i}\frac{B^{(k+1)}(z)}{A^{(k)}(z)}, p_l(z)\rangle_u = \langle z^{-i}H(z), p_l(z)\rangle_u,$$

which shows that

$$\mathbf{H} = \left\langle \begin{bmatrix} z^{-1} \\ \vdots \\ z^{-M} \end{bmatrix} H(z), \begin{bmatrix} p_{N+1}(z) \\ \vdots \\ p_L(z) \end{bmatrix}^T \right\rangle_u ,$$

which depends only on $H(z)$ and the psd of $u(\cdot)$, $S_{uu}(z)$. ∎

B.8 Proof of Theorem 3.3

From the proof of Lemma 3.6, we can write $\mathbf{H}$ as

$$\mathbf{H} = \left\langle \begin{bmatrix} z^{-1} \\ \vdots \\ z^{-M} \end{bmatrix} H(z), \begin{bmatrix} p_{N+1}(z) \\ \vdots \\ p_L(z) \end{bmatrix}^T \right\rangle_u = \begin{bmatrix} t_{1,N+1} & t_{1,N+2} & \cdots & t_{1,L} \\ t_{2,N+1} & t_{2,N+2} & \cdots & t_{2,L} \\ \vdots & \vdots & \ddots & \vdots \\ t_{M,N+1} & t_{M,N+2} & \cdots & t_{M,L} \end{bmatrix} \tag{B.9}$$

where $t_{ij} = \langle z^{-i}H(z), p_j(z)\rangle_u$. Write now $H(z)$ as

$$H(z) = \frac{B_*(z)}{A_*(z)} = \frac{b_{0*} + b_{1*}z^{-1} + \cdots + b_{N*}z^{-N}}{1 + a_{1*}z^{-1} + \cdots + a_{M*}z^{-M}} = \sum_{k=0}^{\infty} h'_k p_k(z).$$

Note that $t_{0k} = h'_k$ for all $k \geq 0$. Expanding $B_*(z)$ over the Szegö polynomials, one can also write

$$H(z) = \frac{b'_{0*}p_0(z) + b'_{1*}p_1(z) + \cdots + b'_{N*}p_N(z)}{1 + a_{1*}z^{-1} + \cdots + a_{M*}z^{-M}}.$$

Since $B_*(z) = H(z)A_*(z)$, one has for all $j \geq 0$

$$\begin{aligned}\langle B_*(z), p_j(z)\rangle_u &= \langle H(z)A_*(z), p_j(z)\rangle_u \\ &= \langle H(z), p_j(z)\rangle_u + \sum_{i=1}^{M} a_{i*}\langle z^{-i}H(z), p_j(z)\rangle_u.\end{aligned}$$

This reads as

$$h'_j + \sum_{i=1}^{M} a_{i*}t_{ij} = \begin{cases} b'_{j*}, & 0 \leq j \leq N, \\ 0, & j > N. \end{cases}$$

For $0 \leq j \leq L$, these equations can be written in matrix form as follows:

$$\begin{bmatrix} b'_{0*} \\ b'_{1*} \\ \vdots \\ b'_{N*} \end{bmatrix} = \begin{bmatrix} t_{1,0} & t_{2,0} & \cdots & t_{M,0} \\ t_{1,1} & t_{2,1} & \cdots & t_{M,1} \\ \vdots & \vdots & \ddots & \vdots \\ t_{1,N} & t_{2,N} & \cdots & t_{M,N} \end{bmatrix} \begin{bmatrix} a_{1*} \\ a_{2*} \\ \vdots \\ a_{M*} \end{bmatrix} + \begin{bmatrix} h'_0 \\ h'_1 \\ \vdots \\ h'_N \end{bmatrix}, \tag{B.10}$$

$$\begin{bmatrix} t_{1,N+1} & t_{2,N+1} & \cdots & t_{M,N+1} \\ t_{1,N+2} & t_{2,N+2} & \cdots & t_{M,N+2} \\ \vdots & \vdots & \ddots & \vdots \\ t_{1,L} & t_{2,L} & \cdots & t_{M,L} \end{bmatrix} \begin{bmatrix} a_{1*} \\ a_{2*} \\ \vdots \\ a_{M*} \end{bmatrix} = - \begin{bmatrix} h'_{N+1} \\ h'_{N+2} \\ \vdots \\ h'_L \end{bmatrix}. \tag{B.11}$$

The matrix in (B.11) is $\mathbf{H}^T$. Now suppose that $\mathbf{H}^T$ does not have full column rank. Then there exists a vector

$$\bar{\mathbf{a}}_* = \begin{bmatrix} \bar{a}_{1*} \\ \bar{a}_{2*} \\ \vdots \\ \bar{a}_{M*} \end{bmatrix} \neq \begin{bmatrix} a_{1*} \\ a_{2*} \\ \vdots \\ a_{M*} \end{bmatrix} = \mathbf{a}_*$$

satisfying (B.11). Let $\bar{\mathbf{b}}'_* = [\,\bar{b}'_{0*} \ \ldots \ \bar{b}'_{N*}\,]^T$ be the vector obtained in the left hand side of (B.10) after substituting $\mathbf{a}_*$ by $\bar{\mathbf{a}}_*$ in the right hand side. Then we can write

$$\begin{bmatrix} \bar{b}'_{0*} \\ \bar{b}'_{1*} \\ \vdots \\ \bar{b}'_{N*} \\ 0 \\ \vdots \\ 0 \\ \times \end{bmatrix} = \begin{bmatrix} t_{0,0} & t_{1,0} & \cdots & t_{M,0} \\ t_{0,1} & t_{1,1} & \cdots & t_{M,1} \\ \vdots & \vdots & \ddots & \vdots \\ t_{0,N} & t_{1,N} & \cdots & t_{M,N} \\ t_{0,N+1} & t_{1,N+1} & \cdots & t_{M,N+1} \\ \vdots & \vdots & \ddots & \vdots \\ t_{0,L} & t_{1,L} & \cdots & t_{M,L} \\ \vdots & \vdots & \ddots & \vdots \end{bmatrix} \begin{bmatrix} 1 \\ \bar{a}_{1*} \\ \vdots \\ \bar{a}_{M*} \end{bmatrix}, \tag{B.12}$$

where the elements from '×' on down are unknown quantities. Since the kth column (counting from zero) of the matrix in (B.12) comprises the coefficients of $z^{-k}H(z)$ in the expansion over the Szegö polynomials, (B.12) can be written in the z-domain as

$$\bar{B}_*(z) + O(z) = H(z)\bar{A}_*(z), \tag{B.13}$$

where

$$\begin{aligned}\bar{B}_*(z) &= \bar{b}'_{0*}p_0(z) + \bar{b}'_{1*}p_1(z) + \cdots + \bar{b}'_{N*}p_N(z),\\ \bar{A}_*(z) &= 1 + \bar{a}_{1*}z^{-1} + \cdots + \bar{a}_{M*}z^{-M},\end{aligned}$$

and $O(z)$ is a function whose Szegö expansion involves only $p_k(z)$ with $k > L$, i. e. $O(z) \in \mathcal{K}_{L+1} = \text{span}\{p_k(z)\}_{k=L+1}^{\infty}$. Substituting $H(z) = B_*(z)/A_*(z)$ in (B.13),

$$\bar{B}_*(z) + O(z) = \frac{B_*(z)\bar{A}_*(z)}{A_*(z)} \qquad \Leftrightarrow \qquad A_*(z)\bar{B}_*(z) + A_*(z)O(z) = B_*(z)\bar{A}_*(z),$$

that is,

$$A_*(z)O(z) = [B_*(z)\bar{A}_*(z) - A_*(z)\bar{B}_*(z)]$$

which is a polynomial of degree not exceeding $N + M \leq L$, and therefore belongs in the orthogonal complement $\mathcal{K}_{L+1}^{\perp} = \text{span}\{p_k(z)\}_{k=0}^{L}$. But since the input signal is autoregressive of order not exceeding $L + 1$, the subspace $\mathcal{K}_{L+1}$ is right shift invariant (see Appendix C), so that

$$O(z) \in \mathcal{K}_{L+1} \qquad \Rightarrow \qquad A_*(z)O(z) \in \mathcal{K}_{L+1}.$$

Therefore

$$A_*(z)O(z) \in \mathcal{K}_{L+1}, \quad A_*(z)O(z) \in \mathcal{K}_{L+1}^{\perp} \qquad \Rightarrow \qquad A_*(z)O(z) = 0,$$

hence $O(z) = 0$ since $A_*(z)$, being a monic polynomial, cannot be identically zero. Thus (B.13) reads as

$$H(z) = \frac{B_*(z)}{A_*(z)} = \frac{\bar{B}_*(z)}{\bar{A}_*(z)},$$

but since $B_*(z)$ and $A_*(z)$ are coprime, this implies $\bar{B}_*(z) = B_*(z)$ and $\bar{A}_*(z) = A_*(z)$, a contradiction since it was assumed that $\bar{\mathbf{a}}_* \neq \mathbf{a}_*$. Therefore the matrix $\mathbf{H}^T$ must have full column rank. ∎

Remark: In the case $N = M$, Theorem 3.3 can be linked to Kronecker's theorem [105], which states that the *Hankel form* of $H(z)$,

$$\Gamma_H = \begin{bmatrix} h_1 & h_2 & h_3 & \cdots \\ h_2 & h_3 & h_4 & \cdots \\ h_3 & h_4 & h_5 & \cdots \\ \vdots & \vdots & \vdots & \ddots \end{bmatrix}, \qquad \text{with} \qquad H(z) = \sum_{k=0}^{\infty} h_k z^{-k},$$

has rank equal to the McMillan degree of $H(z)$, which is M provided that $H(z)$ has no pole-zero cancellations; in that case, $[\Gamma_H]_M$, the $M \times M$ principal submatrix of Γ_H, is nonsingular. Observe that, if $N = M$ and $u(\cdot)$ is a white process, then $\mathbf{H}$ reduces to

$$\mathbf{H} = \begin{bmatrix} h_M & h_{M+1} & \cdots & h_{L-1} \\ h_{M-1} & h_M & \cdots & h_{L-2} \\ \vdots & \vdots & \ddots & \vdots \\ h_1 & h_2 & \cdots & h_{L-M} \end{bmatrix}.$$

Denote by $[\mathbf{A}]_M$ the $M \times M$ principal submatrix of a matrix $\mathbf{A}$. If $L \geq N+M = 2M$, then the determinants of $[\mathbf{H}]_M$ and $[\Gamma_H]_M$ are seen to coincide. By Kronecker's theorem,

$$\begin{aligned} \deg H(z) = M &\Rightarrow [\Gamma_H]_M \text{ nonsingular} \\ &\Rightarrow [\mathbf{H}]_M \text{ nonsingular} \\ &\Rightarrow \mathbf{H} \text{ has full row rank,} \end{aligned}$$

which is the core of the proof of uniqueness of the IXN fixed point for white input signals and $L = N + M = 2M$ given in [76].

Consider now the doubly infinite matrix $\bar{\Gamma}_H$ given by

$$\bar{\Gamma}_H = \begin{bmatrix} t_{M,M+1} & t_{M-1,M+1} & t_{M-2,M+1} & \cdots \\ t_{M,M+2} & t_{M-1,M+2} & t_{M-2,M+2} & \cdots \\ t_{M,M+3} & t_{M-1,M+3} & t_{M-2,M+3} & \cdots \\ \vdots & \vdots & \vdots & \ddots \end{bmatrix} \qquad \text{with } t_{ij} = \langle z^{-i} H(z), p_j(z) \rangle_u.$$

For white $u(\cdot)$, this matrix reduces to the Hankel form Γ_H. Then, it is reasonable to ask whether $\operatorname{rank} \bar{\Gamma}_H = M = \deg H(z)$ also holds.

Suppose $u(\cdot)$ is an AR process of order $L+1$ or less, where now L is an arbitrarily large integer. Then the $M \times L - M$ matrix $\mathbf{H}$ given in (B.9) after taking $N = M$ has full row rank M, in view of Theorem 3.3. Note that after reversing the order of the columns of $\mathbf{H}^T$, one obtains the principal $(L - M) \times M$ block of $\bar{\Gamma}_H$. Therefore the first M columns of $\bar{\Gamma}_H$ are linearly independent, which means that

$$\operatorname{rank} \bar{\Gamma}_H \geq M.$$

This is true for all integers L and therefore for all AR processes $u(\cdot)$ of any order.

On the other hand, writing $A_*(z)H(z) = B_*(z)$ one finds that for all k and all $i \geq 0$,

$$\langle z^k A_*(z) H(z), p_i(z) \rangle_u = \langle z^k B_*(z), p_i(z) \rangle_u$$

that is,

$$\langle z^k H(z), p_i(z) \rangle_u + \sum_{j=1}^{M} a'_{j*} \cdot \langle z^{k-j} H(z), p_i(z) \rangle_u = \sum_{j=0}^{M} b'_{j*} \cdot \langle z^k p_j(z), p_i(z) \rangle_u$$

or equivalently,

$$t_{-k,i} + \sum_{j=1}^{M} a'_{j*} t_{j-k,i} = \sum_{j=0}^{M} b'_{j*} \cdot \langle z^k p_j(z), p_i(z) \rangle_u. \tag{B.14}$$

For $k = 0$ and $i > M$, we have $\langle z^k p_j(z), p_i(z) \rangle_u = 0$ if $0 \leq j \leq M$. Then (B.14) shows that the $M+1$st column of the matrix $\bar{\Gamma}_H$ is a linear combination of the first M columns. What can be said about the remaining columns?

Suppose $u(\cdot)$ is AR of order $M+1$ (*not* $2M+1$), so that $S_{uu}(z) = c^2/[q(z)q(z^{-1})]$ with $q(z)$ a minimum phase polynomial of degree not exceeding $M+1$. Without loss of generality, assume that the constant c is chosen so that $q(z) = z^{-M} p_M(z^{-1})$. Then for all $k \geq 0$, $i > M$ and $0 \leq j \leq M$,

$$\begin{aligned} \langle z^k p_j(z), p_i(z) \rangle_u &= \langle z^k p_j(z), z^{-i} q(z^{-1}) \rangle_u \\ &= \left\langle \frac{z^k p_j(z)}{q(z)}, \frac{z^{-i} q(z^{-1})}{q(z)} \right\rangle \\ &= \left\langle z^k p_j(z), \frac{z^{-i}}{q(z)} \right\rangle = 0, \end{aligned}$$

because the causal part of $z^k p_j(z)$ is a polynomial of degree not exceeding $j-k \leq M$, and the first M coefficients of the impulse response of $z^{-i}/q(z)$ are zero. Hence, for all $k \geq 0$, $i > M$,

$$t_{-k,i} + \sum_{j=1}^{M} a'_{j*} t_{j-k,i} = 0,$$

which shows how all the columns of $\bar{\Gamma}_H$ are linear combinations of the first M columns. To sum up, we have shown that if $u(\cdot)$ is AR of order $M+1$ (or less), then $\operatorname{rank} \bar{\Gamma}_H = \deg H(z)$.

However, this is not necessarily true if $u(\cdot)$ is AR of order m with $m > M+1$. We show a counterexample here. Let $M = 2$, and let $u(\cdot)$ be AR of fourth order, with $q(z) = 1 - \rho z^{-4}$, and let $H(z) = 1/(1 - az^{-2})$. Assuming $|a|, |\rho| < 1$ it is straightforward, although rather tedious, to show that

$$\bar{\Gamma}_H = \alpha \begin{bmatrix} 0 & \beta a & 0 & \beta\gamma & \cdots \\ a & 0 & a^2 & 0 & \cdots \\ 0 & a^2 & 0 & a^3 & \cdots \\ a^2 & 0 & a^3 & 0 & \cdots \\ 0 & a^3 & 0 & a^4 & \cdots \\ \vdots & \vdots & \vdots & \vdots & \ddots \end{bmatrix},$$

with

$$\alpha = \frac{1}{1 - \rho a^2}, \qquad \beta = \frac{1}{\sqrt{1 - \rho^2}}, \qquad \gamma = a^2 + \rho - \rho^2 a^2.$$

Assuming $\rho, a \neq 0$, it is clear that (i) the first two columns are linearly independent; (ii) the third column is a linear combination of the first two; (iii) the fourth column, however, is *not* a linear combination of the first two. Therefore in this case $\operatorname{rank} \bar{\Gamma}_H > M$.

B.9 Proof of Theorem 3.4

Let $\{p_k(z)\}_{k=0}^{\infty}$ be the Szegö polynomials associated to $u(\cdot)$. Let

$$\hat{H}(z) = \frac{B(z)}{A(z)} = \frac{b'_0 p_0(z) + b'_1 p_1(z) + \cdots + b'_L p_L(z)}{1 + a_1 z^{-1} + \cdots + a_M z^{-M}} = \sum_{k=0}^{\infty} \hat{h}'_k p_k(z)$$

be a stationary point of the IXN iteration. The interpolation conditions on the numerator $B(z)$ ensure that

$$\hat{h}'_k = \left\langle \frac{B(z)}{A(z)}, p_k(z) \right\rangle_u = \langle H(z), p_k(z) \rangle_u = h'_k, \qquad 0 \leq k \leq L, \tag{B.15}$$

and, since $u(\cdot)$ is AR$(L+1)$, this implies that

$$\left\langle z^{-i} \frac{B(z)}{A(z)}, p_j(z) \right\rangle_u = \langle z^{-i} H(z), p_j(z) \rangle_u = t_{ij}, \qquad i \geq 0, \quad 0 \leq j \leq L, \tag{B.16}$$

as was shown in the proof of Lemma 3.6. Now since $B(z) = \hat{H}(z) A(z)$, one has that for all $j \geq 0$,

$$\langle B(z), p_j(z) \rangle_u = \langle \hat{H}(z) A(z), p_j(z) \rangle_u.$$

Taking (B.15) and (B.16) into account, this gives

$$b'_j = h'_j + \sum_{i=1}^{M} a_i t_{ij}, \qquad 0 \leq j \leq L. \tag{B.17}$$

This constitutes a linear constraint on the coefficients of $B(z)$ and $A(z)$. In addition we must have

$$\mathbf{H} \begin{bmatrix} b'_{N+1} \\ \vdots \\ b'_L \end{bmatrix} = \mathbf{0}_M, \tag{B.18}$$

as shown in Section 3.4.2, with $\mathbf{H}$ given in (B.9). If we define $\mathbf{h}' = [\, h'_0 \ \cdots \ h'_L \ \mathbf{0}_M^T \,]^T$ and the coefficient vector $\theta = [\, b'_0 \ \cdots \ b'_L \ a_1 \ \cdots \ a_M \,]^T$, we can write (B.17)-(B.18) in matrix-vector form as

$$\begin{bmatrix} \mathbf{I}_{N+1} & \mathbf{0} & -\mathbf{G}^T \\ \mathbf{0} & \mathbf{I}_{L-N} & -\mathbf{H}^T \\ \mathbf{0} & \mathbf{H} & \mathbf{0} \end{bmatrix} \theta = \mathbf{h}', \tag{B.19}$$

where

$$\mathbf{G} = \begin{bmatrix} t_{10} & t_{11} & \cdots & t_{1N} \\ t_{20} & t_{21} & \cdots & t_{2N} \\ \vdots & \vdots & \ddots & \vdots \\ t_{M0} & t_{M1} & \cdots & t_{MN} \end{bmatrix}.$$

Observe that (B.19) is linear in θ. Uniqueness of the stationary point follows if one shows that the matrix in (B.19) is invertible. This we proceed to do. Clearly, it suffices to show that

$$\mathbf{A} = \begin{bmatrix} \mathbf{I}_{L-N} & -\mathbf{H}^T \\ \mathbf{H} & \mathbf{0} \end{bmatrix}$$

is invertible. Let $\mathbf{v}$ be a vector such that $\mathbf{A}\mathbf{v} = \mathbf{0}_{L-N+M}$. Partition $\mathbf{v} = [\,\mathbf{v}_1^T \;\; \mathbf{v}_2^T\,]^T$ where $\mathbf{v}_1$, $\mathbf{v}_2$ have sizes $(L-N)\times 1$ and $M \times 1$ respectively. Then $\mathbf{A}\mathbf{v} = \mathbf{0}_{L-N+M}$ reads as

$$\mathbf{v}_1 = \mathbf{H}^T\mathbf{v}_2, \qquad \mathbf{H}\mathbf{v}_1 = \mathbf{0}_M.$$

These give

$$\mathbf{H}\mathbf{H}^T\mathbf{v}_2 = \mathbf{0}_M,$$

which implies $\mathbf{v}_2 = \mathbf{0}_M$ since $\operatorname{rank}(\mathbf{H}\mathbf{H}^T) = \operatorname{rank}\mathbf{H} = M$ by Theorem 3.3. Then $\mathbf{v}_1 = \mathbf{H}^T\mathbf{v}_2 = \mathbf{0}_{L-N}$ so that $\mathbf{v} = \mathbf{0}_{L-N+M}$, i.e. $\mathbf{A}$ is invertible so that the stationary point of the IXN method is unique. That this point is given by $\hat{H}(z) = H(z)$ follows since $H(z)$ clearly satisfies (B.19). ∎

B.10 Proof of Lemma 3.7

Suppose that $\mathbf{M}$ is singular. Then there exists an $(L+1)\times 1$ vector $\mathbf{b}_\star \neq \mathbf{0}_{L+1}$ such that $\mathbf{M}\mathbf{b}_\star = \mathbf{0}_{L+1}$. Then $E[\bar{\mathbf{u}}(n)\hat{y}_\star(n) = \mathbf{0}_{L+1}$ where $\hat{y}_\star(n) = \hat{H}_\star(z)u(n) = [B_\star(z)/A(z)]u(n)$ with $B_\star(z)$ the polynomial formed from the coefficients of $\mathbf{b}_\star$. We can rewrite this as $\langle \hat{H}_\star(z), z^{-k}\rangle_u = 0$, $0 \le k \le L$ or equivalently,

$$\langle \hat{H}_\star(z), p_k(z)\rangle_u = 0, \qquad 0 \le k \le L$$

where $p_k(z)$ are the Szegö polynomials associated to $u(\cdot)$. Hence $\hat{H}_\star(z) \in \mathcal{K}_{L+1} = \operatorname{span}\{p_k(z)\}_{k=L+1}^{\infty}$, which is a right shift invariant subspace since $u(\cdot)$ is AR$(L+1)$. Thus

$$\hat{H}_\star(z) \in \mathcal{K}_{L+1} \qquad \Rightarrow \qquad B_\star(z) = A(z)\hat{H}_\star(z) \in \mathcal{K}_{L+1}.$$

But since $B_\star(z)$ is a polynomial of order not exceeding L, it belongs in the orthogonal complement $\mathcal{K}_{L+1}^{\perp} = \operatorname{span}\{p_k(z)\}_{k=0}^{L}$. Thus

$$B_\star(z) \in \mathcal{K}_{L+1}, \quad B_\star(z) \in \mathcal{K}_{L+1}^{\perp} \qquad \Rightarrow \qquad B_\star(z) = 0,$$

which implies $\mathbf{b}_\star = \mathbf{0}_{L+1}$, a contradiction. ∎

B.11 Proof of Lemma 3.8

The conditions (3.39) imply that the function $f(z) = A(z)H(z) - B(z)$ belongs to $\mathcal{K}_{L+1}$, which is a right-shift invariant subspace. Therefore $g(z)f(z) \in \mathcal{K}_{L+1}$ for any causal and stable $g(z)$. Taking $g(z) = 1/A(z)$, we see that

$$A(z)f(z) = H(z) - \frac{B(z)}{A(z)} \in \mathcal{K}_{L+1},$$

i. e. $B(z)/A(z)$ matches the first $L+1$ coefficients of the expansion of $H(z)$ over the Szegö polynomials so that $E[\bar{\mathbf{u}}(n)e_o(n)] = \mathbf{0}_{L+1}$. ∎

B.12 Proof of Lemma 3.9

Since $\mathbf{S}(\theta_*)$ in (3.45) is block triangular, we have

$$\text{eig}(\mathbf{S}(\theta_*)) = \text{eig}(-\mathbf{\Lambda}_N^2) \quad \bigcup \quad \text{eig}\left(\begin{bmatrix} -\tilde{\mathbf{\Lambda}}^2 & \tilde{\mathbf{\Lambda}}\mathbf{H}^T \\ -\mathbf{H}\tilde{\mathbf{\Lambda}} & \mathbf{0} \end{bmatrix}\right).$$

One has $\text{eig}(-\mathbf{\Lambda}_N^2) = \{-\sigma_{\beta_0}^2, \ldots, -\sigma_{\beta_N}^2\}$, which are negative. For convenience, let $\tilde{\mathbf{H}} = \mathbf{H}\tilde{\mathbf{\Lambda}}$. Then we just need to show that the eigenvalues of the matrix

$$\mathbf{S}' = \begin{bmatrix} -\tilde{\mathbf{\Lambda}}^2 & \tilde{\mathbf{H}}^T \\ -\tilde{\mathbf{H}} & \mathbf{0} \end{bmatrix}$$

have strictly negative real parts. Note first that, for any $\mathbf{v} = [\,\mathbf{v}_1^T \;\; \mathbf{v}_2^T\,]^T$, one has

$$\mathbf{v}^T\mathbf{S}'\mathbf{v} = [\,\mathbf{v}_1^T \;\; \mathbf{v}_2^T\,] \begin{bmatrix} -\tilde{\mathbf{\Lambda}}^2 & \tilde{\mathbf{H}}^T \\ -\tilde{\mathbf{H}} & \mathbf{0} \end{bmatrix} \begin{bmatrix} \mathbf{v}_1 \\ \mathbf{v}_2 \end{bmatrix} = -\mathbf{v}_1^T\tilde{\mathbf{\Lambda}}^2\mathbf{v}_1 \leq 0,$$

with equality if and only if $\mathbf{v}_1 = \mathbf{0}_{L-N}$. Now let $(\lambda, \mathbf{v}) = (\lambda_r + j\lambda_i, \mathbf{v}_r + j\mathbf{v}_i)$ be an eigenpair of $\mathbf{S}'$. Then

$$\mathbf{S}'\mathbf{v} = \lambda\mathbf{v} \qquad \Rightarrow \qquad \mathbf{v}^\dagger\mathbf{S}'\mathbf{v} = \lambda\mathbf{v}^\dagger\mathbf{v},$$

where the superscript † indicates the conjugate transpose. Since

$$\begin{aligned} \mathbf{v}^\dagger\mathbf{S}'\mathbf{v} &= (\mathbf{v}_r^T - j\mathbf{v}_i^T)\mathbf{S}'(\mathbf{v}_r + j\mathbf{v}_i) \\ &= (\mathbf{v}_r^T\mathbf{S}'\mathbf{v}_r + \mathbf{v}_i^T\mathbf{S}'\mathbf{v}_i) + j(\mathbf{v}_r^T\mathbf{S}'\mathbf{v}_i - \mathbf{v}_i^T\mathbf{S}'\mathbf{v}_r), \end{aligned}$$

and

$$\lambda(\mathbf{v}^\dagger\mathbf{v}) = \lambda_r(\mathbf{v}^\dagger\mathbf{v}) + j\lambda_i(\mathbf{v}^\dagger\mathbf{v}),$$

one has that

$$\lambda_r(\mathbf{v}^\dagger\mathbf{v}) = \mathbf{v}_r^T\mathbf{S}'\mathbf{v}_r + \mathbf{v}_i^T\mathbf{S}'\mathbf{v}_i \leq 0,$$

showing that $\lambda_r \leq 0$. Suppose now that $\lambda_r = 0$. Then

$$\mathbf{v}_r^T \mathbf{S}' \mathbf{v}_r = \mathbf{v}_i^T \mathbf{S}' \mathbf{v}_i = 0,$$

and this implies that the eigenvector $\mathbf{v}$ is of the form

$$\mathbf{v} = \begin{bmatrix} \mathbf{0}_{L-N} \\ \mathbf{v}_2 \end{bmatrix}$$

for some $M \times 1$ vector $\mathbf{v}_2$. Since $\mathbf{S}'\mathbf{v} = \lambda \mathbf{v}$, one has

$$\begin{bmatrix} \tilde{\mathbf{H}}^T \mathbf{v}_2 \\ \mathbf{0}_M \end{bmatrix} = \begin{bmatrix} \mathbf{0}_{L-N} \\ \lambda \mathbf{v}_2 \end{bmatrix},$$

which gives $\mathbf{v}_2 = \mathbf{0}_M$ because in view of Theorem 3.3, $\mathbf{H}^T$ (and therefore $\tilde{\mathbf{H}}^T$) has full column rank. But then $\mathbf{v} = \mathbf{0}$, a contradiction since $\mathbf{v}$ is an eigenvector. This completes the proof. ∎

B.13 Proof of Lemma 3.10

The parameter vector for the lattice structure is

$$\theta_l = [\, w_0 \; \cdots \; w_L \; \sin\phi_1 \; \cdots \; \sin\phi_M \,]^T,$$

and the algorithm given by (3.42) and (3.55) takes now the form $\theta_l(n+1) = \theta_l(n) + \mu F_l(\theta_l, u, d)$, where

$$F_l(\theta_l, u, d) = \begin{bmatrix} \beta_0(n)\bar{e}_o(n) \\ \vdots \\ \beta_L(n)\bar{e}_o(n) \\ -[G_1(z)B(z)u(n)]e_e(n) \\ \vdots \\ -[G_M(z)B(z)u(n)]e_e(n) \end{bmatrix}.$$

For local stability, the eigenvalues of the feedback matrix

$$\mathbf{S}_l(\theta_*) = \left. \frac{\mathrm{d}E\,[F_l(\theta_l, u, d)]}{\mathrm{d}\theta_l} \right|_{\theta=\theta_*}$$

must lie in the $\mathrm{Re}\,\lambda < 0$ semiplane, with θ_* denoting the stationary point corresponding to the identification of $H(z)$. Now $\mathbf{S}_l(\theta_*)$ turns out to be

$$\mathbf{S}_l(\theta_*) = \begin{bmatrix} -\mathbf{\Lambda}_N^2 & \mathbf{0} & \mathbf{\Lambda}_N \mathbf{G}^T \mathbf{D}(\theta_*) \\ \mathbf{0} & -\tilde{\mathbf{\Lambda}}^2 & \tilde{\mathbf{\Lambda}} \mathbf{H}^T \mathbf{D}(\theta_*) \\ \mathbf{0} & -\mathbf{D}(\theta_*)^T \mathbf{H} \tilde{\mathbf{\Lambda}} & \mathbf{0} \end{bmatrix}, \tag{B.20}$$

where $\mathbf{D}(\theta_*)$ is the Jacobian matrix of the lattice to direct form transformation evaluated at the stationary point (refer to Appendix A for more on this matrix), and $\mathbf{H}$, $\mathbf{G}$ are given in (3.31) and (3.46) respectively. Note that the matrix $\mathbf{S}_l(\theta_*)$ in (B.20) has the same structure as $\mathbf{S}_d(\theta_*)$ in (3.45) upon substituting $\mathbf{G}$ and $\mathbf{H}$ by $\mathbf{D}(\theta_*)^T\mathbf{G}$ and $\mathbf{D}(\theta_*)^T\mathbf{H}$ respectively. Therefore, by mimicking the proof of Lemma 3.9, the eigenvalues of $\mathbf{S}_l(\theta_*)$ are seen to have strictly negative real parts since $\mathbf{D}(\theta_*)$ and $\mathbf{H}$ have full row rank under the hypotheses of the lemma. ∎

B.14 Proof of Lemma 3.11

Let $u_f(n) = [1/A(z)]u(n)$. Observe that if $u(\cdot)$ is AR$(N+1)$, then $u_f(\cdot)$ is AR$(N+M+1)$. Let $\{p_k(z)\}_{k=0}^{\infty}$ be the Szegö polynomials associated to the process $u_f(\cdot)$, and define $F(z) = H(z)A(z)$. The output error $e_o(n) = d(n) - \hat{y}(n)$ can be written as

$$\begin{aligned} e_o(n) &= \left[H(z) - \frac{B(z)}{A(z)}\right] u(n) + \eta(n) \\ &= [F(z) - B(z)]u_f(n) + \eta(n). \end{aligned}$$

Therefore, if we expand $F(z)$ and $B(z)$ over the Szegö polynomials as

$$F(z) = \sum_{k=0}^{\infty} f'_k p_k(z), \qquad B(z) = \sum_{k=0}^{L} b'_k p_k(z),$$

we see that

$$E[e_o^2(n)] = \sum_{k=0}^{L}(f'_k - b'_k)^2 + \sum_{k=L+1}^{\infty}(f'_k)^2 + \sigma_\eta^2,$$

so that the optimality conditions on $B(z)$ read as $b'_k = f'_k$, $0 \le k \le L$. Therefore

$$F(z) - B(z) = H(z)A(z) - B(z) \in \mathcal{K}_{L+1} = \text{span}\{p_k(z)\}_{k=L+1}^{\infty}.$$

Since $u_f(\cdot)$ is AR$(N+M+1)$ and $L \ge N+M$, $\mathcal{K}_{L+1}$ is a right shift invariant subspace. Therefore $g(z)[H(z)A(z) - B(z)] \in \mathcal{K}_{L+1}$ for all causal and stable $g(z)$. In particular, if we take $g(z) = A_*(z)$, we obtain

$$B_*(z)A(z) - A_*(z)B(z) \in \mathcal{K}_{L+1}.$$

But this function is a polynomial of degree not exceeding $N+M \le L$ (because by assumption, $B(z)$ has degree N or less). Hence it belongs in the orthogonal complement $\mathcal{K}_{L+1}^{\perp} = \text{span}\{p_k(z)\}_{k=0}^{L}$. Thus

$$B_*(z)A(z) - A_*(z)B(z) \in \mathcal{K}_{L+1} \bigcap \mathcal{K}_{L+1}^{\perp} = \{0\},$$

which implies $B_*(z)A(z) - A_*(z)B(z) = 0$, i.e. $B(z)/A(z) = B_*(z)/A_*(z)$. ∎

B.15 Proof of Theorem 3.5

Since $u(\cdot)$ is AR$(N+1)$, we can write $S_{uu}(z) = 1/[q(z)q(z^{-1})]$ with $q(z)$ a minimum phase polynomial of degree $N+1$ (or less). For convenience, let $\tilde{H}(z) = H(z) - B(z)/A(z)$ be the error transfer function obtained at an SM/XN stationary point. The proof takes three steps.

Step 1: The optimality conditions on the numerator $B(z)$ imply

$$\left\langle \tilde{H}(z), \frac{z^{-k}}{A(z)} \right\rangle_u = \left\langle \frac{\tilde{H}(z)}{q(z)}, \frac{z^{-k}}{A(z)q(z)} \right\rangle = 0, \qquad 0 \le k \le N+M. \tag{B.21}$$

In view of this, we can invoke the Beurling-Lax theorem [105, sec. 3.1] to conclude that $\tilde{H}(z)/q(z)$ must be causally divisible by the all-pass function

$$V(z) = \frac{[z^{-M}A(z^{-1})]}{A(z)} \cdot \frac{[z^{-N-1}q(z^{-1})]}{q(z)},$$

i.e. $\tilde{H}(z)/q(z) = g(z)V(z)$ for some stable and causal $g(z)$. Therefore

$$\tilde{H}(z) = g(z)z^{-(N+M+1)}\frac{A(z^{-1})q(z^{-1})}{A(z)}. \tag{B.22}$$

Now one has that, *for all positive* k,

$$\begin{aligned}
\left\langle \tilde{H}(z), \frac{z^k}{A(z)} \right\rangle_u &= \frac{1}{2\pi j}\oint \frac{\tilde{H}(z^{-1})z^k}{A(z)q(z)q(z^{-1})}\frac{\mathrm{d}z}{z} \\
&= \frac{1}{2\pi j}\oint \frac{g(z^{-1})z^{N+M+k}A(z)q(z)}{A(z^{-1})A(z)q(z)q(z^{-1})}\mathrm{d}z \\
&= \frac{1}{2\pi j}\oint \frac{g(z^{-1})z^{N+M+k}}{A(z^{-1})q(z^{-1})}\mathrm{d}z \\
&= 0.
\end{aligned} \tag{B.23}$$

The second line in (B.23) comes from (B.22), while the last line follows because the integrand is devoid of poles inside the unit circle. Therefore if the conditions (B.21) hold for $0 \le k \le N+M$, then they also hold for all $k \le N+M$.

Step 2: As a consequence, if $f(z) = \sum_{i=0}^{\infty} f_i z^{-i}$ is a causal, stable function, then for all $k \le N+M$ one has

$$\begin{aligned}
\left\langle f(z)\tilde{H}(z), \frac{z^{-k}}{A(z)} \right\rangle_u &= \sum_{i=0}^{\infty} f_i \left\langle z^{-i}\tilde{H}(z), \frac{z^{-k}}{A(z)} \right\rangle_u \\
&= \sum_{i=0}^{\infty} f_i \left\langle \tilde{H}(z), \frac{z^{-k+i}}{A(z)} \right\rangle_u \\
&= 0.
\end{aligned}$$

In particular, for $f(z) = 1/A(z)$, one has

$$\left\langle \frac{\tilde{H}(z)}{A(z)}, \frac{z^{-k}}{A(z)} \right\rangle_u = 0, \qquad k \leq N + M,$$

or equivalently, with $u_f(n) = [1/A(z)]u(n)$,

$$\left\langle \hat{H}(z), z^{-k} \right\rangle_{u_f} = \left\langle \frac{B(z)}{A(z)}, z^{-k} \right\rangle_{u_f}, \qquad k \leq N + M. \tag{B.24}$$

Step 3: Observe that the matrix $\mathbf{H}_f$ given in (3.59) can be written as

$$\mathbf{H}_f = \left\langle \begin{bmatrix} z^{-1} \\ \vdots \\ z^{-M} \end{bmatrix} \frac{B(z)}{A(z)}, \begin{bmatrix} p_{N+1}(z) \\ \vdots \\ p_{N+M}(z) \end{bmatrix}^T \right\rangle_{u_f},$$

where $p_k(z)$ are the Szegö polynomials associated to the process $u_f(\cdot)$. Let $\mathbf{C}$ be the $M \times (N + M + 1)$ matrix of coefficients of $p_{N+1}(z), \ldots p_{N+M}(z)$ such that

$$\begin{bmatrix} p_{N+1}(z) \\ \vdots \\ p_{N+M}(z) \end{bmatrix} = \mathbf{C} \begin{bmatrix} 1 \\ z^{-1} \\ \vdots \\ z^{-(N+M)} \end{bmatrix}.$$

Using this and (B.24), we can write

$$\begin{aligned} \mathbf{H}_f &= \left\langle \begin{bmatrix} z^{-1} \\ \vdots \\ z^{-M} \end{bmatrix} \frac{B(z)}{A(z)}, \begin{bmatrix} 1 \\ z^{-1} \\ \vdots \\ z^{-(N+M)} \end{bmatrix}^T \right\rangle_{u_f} \mathbf{C}^T \\ &= \left\langle \begin{bmatrix} z^{-1} \\ \vdots \\ z^{-M} \end{bmatrix} H(z), \begin{bmatrix} 1 \\ z^{-1} \\ \vdots \\ z^{-(N+M)} \end{bmatrix}^T \right\rangle_{u_f} \mathbf{C}^T \\ &= \left\langle \begin{bmatrix} z^{-1} \\ \vdots \\ z^{-M} \end{bmatrix} H(z), \begin{bmatrix} p_{N+1}(z) \\ \vdots \\ p_{N+M}(z) \end{bmatrix}^T \right\rangle_{u_f}. \end{aligned} \tag{B.25}$$

Since $u_f(\cdot)$ is AR$(N + M + 1)$, we can apply Theorem 3.3 to conclude that the last matrix in (B.25) is nonsingular. Therefore $\mathbf{H}_f$ is nonsingular. Because the stationary point must satisfy $\mathbf{H}_f \tilde{\mathbf{b}}' = \mathbf{0}_M$, it follows that $\tilde{\mathbf{b}}' = \mathbf{0}_M$. By using Lemma 3.11 we conclude that $B(z)/A(z) = H(z)$. ∎

B.16 Proof of Lemma 4.1

To verify the stability of (4.8) we proceed in two steps. First, the relation between the *a posteriori* error $\varepsilon(n)$ and the signal $s(n) = \tilde{\theta}(n+1)^T\psi(n)$ is found. Here $\tilde{\theta}(n) = \theta_* - \theta(n)$ with θ_* the parameter vector of the unknown system $H(z)$. It is shown that $\varepsilon(n)$ and $s(n)$ are related by a linear time-invariant transfer function.

Second, it is shown that $\varepsilon(n)$ and $s(n)$ satisfy a Popov inequality of the form

$$\sum_{n=0}^{S} s(n)\varepsilon(n) \leq c^2, \tag{B.26}$$

for all $S > 0$ and some constant c independent of S. Therefore by virtue of the hyperstability theorem [97, 105], if the transfer function from $s(n)$ to $\varepsilon(n)$ is SPR, the closed-loop system is asymptotically stable, giving $\varepsilon(n) \to 0$.

To begin, let us add and substract the term $\sum_{k=1}^{M} t_{k*}x(n-kP)$ to the quantity

$$\begin{aligned} y(n) - x(n) = &\sum_{k=0}^{MP} f_{k*}u(n-k) - \sum_{k=1}^{M} t_{k*}y(n-kP) \\ &- \sum_{k=0}^{MP} f_k(n+1)u(n-k) + \sum_{k=1}^{M} t_k(n+1)x(n-kP), \end{aligned}$$

in order to obtain

$$\begin{aligned} y(n) - x(n) &= \sum_{k=0}^{MP}[f_{k*} - f_k(n+1)]u(n-k) - \sum_{k=1}^{M}[t_{k*} - t_k(n+1)]x(n-kP) \\ &\quad - \sum_{k=1}^{M} t_{k*}[y(n-kP) - x(n-kP)] \\ &= \tilde{\theta}(n+1)^T\psi(n) - \sum_{k=1}^{M} t_{k*}[y(n-kP) - x(n-kP)]. \end{aligned}$$

Therefore we see that $y(n) - x(n) = [1/T_*(z^P)]s(n)$ or

$$\varepsilon(n) = \frac{C(z)}{T_*(z^P)}s(n). \tag{B.27}$$

It just remains to show the Popov inequality (B.26):

1. Given the definitions of $\varepsilon(n)$ and $e(n)$ in (4.6) and (4.7) respectively, and the update formula (4.8), it is easily verified that

$$\varepsilon(n) = \frac{e(n)}{1 + \mu\psi(n)^T\psi(n)}$$

so that one has

$$\tilde{\theta}(n+1) = \tilde{\theta}(n) - \mu\psi(n)\varepsilon(n),$$

and therefore

$$s(n) = \tilde{\theta}(n+1)^T\psi(n) = \tilde{\theta}(n)^T\psi(n) - \mu\psi(n)^T\psi(n)\varepsilon(n),$$

or

$$s(n)\varepsilon(n) = \tilde{\theta}(n)^T\psi(n)\varepsilon(n) - \mu\psi(n)^T\psi(n)\varepsilon^2(n). \tag{B.28}$$

2. Now express the parameter error vector norm as

$$\tilde{\theta}(n+1)^T\tilde{\theta}(n+1) = \tilde{\theta}(n)^T\tilde{\theta}(n) + \mu^2\psi(n)^T\psi(n)\varepsilon^2(n) - 2\mu\tilde{\theta}(n)^T\psi(n)\varepsilon(n),$$

so that

$$\tilde{\theta}(n)^T\psi(n)\varepsilon(n) = \frac{1}{2\mu}[\tilde{\theta}(n)^T\tilde{\theta}(n) - \tilde{\theta}(n+1)^T\tilde{\theta}(n+1)] + \frac{\mu}{2}\psi(n)^T\psi(n)\varepsilon^2(n). \tag{B.29}$$

3. Putting (B.28) and (B.29) together, one gets

$$s(n)\varepsilon(n) = \frac{1}{2\mu}[\tilde{\theta}(n)^T\tilde{\theta}(n) - \tilde{\theta}(n+1)^T\tilde{\theta}(n+1)] - \frac{\mu}{2}\psi(n)^T\psi(n)\varepsilon^2(n)$$

4. Summing these from 0 to S,

$$\begin{aligned}\sum_{n=0}^{S} s(n)\varepsilon(n) &= \frac{1}{2\mu}[\tilde{\theta}(0)^T\tilde{\theta}(0) - \tilde{\theta}(S+1)^T\tilde{\theta}(S+1)] - \frac{\mu}{2}\sum_{n=0}^{S}\psi(n)^T\psi(n)\varepsilon^2(n) \\ &\leq \frac{1}{2\mu}\tilde{\theta}(0)^T\tilde{\theta}(0) = c^2,\end{aligned}$$

which proves the result. ∎

B.17 Proof of Lemma 4.3

As usual, introduce the parameter error vector $\tilde{\theta}(n) = \theta_* - \theta(n)$, with θ_* the parameter vector of the unknown system $H(z)$. Also let us define the auxiliary signals $s_i(n) = \tilde{\theta}(n+1)^T\psi_i(n)$, $0 \leq i \leq P-1$. Using standard manipulations (see e.g. the proof of Lemma 4.1 above), one can show that these signals are related to the *a posteriori* errors via

$$\varepsilon_i(n) = \frac{C(z)}{T_*(z)}s_i(n), \qquad 0 \leq i \leq P-1.$$

Similarly, the relation between the *a priori* and *a posteriori* errors is

$$\bar{\varepsilon}(n) = \frac{\bar{e}(n)}{1 + \mu\bar{\psi}(n)^T\bar{\psi}(n)},$$

so that one has

$$\tilde{\theta}(n+1) = \tilde{\theta}(n) - \mu\bar{\psi}(n)\bar{\varepsilon}(n).$$

If we define

$$\bar{s}(n) = \alpha_0 s_0(n) + \cdots + \alpha_{P-1}s_{P-1}(n),$$

then

$$\bar{s}(n) = \tilde{\theta}(n+1)^T\bar{\psi}(n) = \tilde{\theta}(n)^T\bar{\psi}(n) - \mu\bar{\psi}(n)^T\bar{\psi}(n)\bar{\varepsilon}(n),$$

or

$$\bar{s}(n)\bar{\varepsilon}(n) = \tilde{\theta}(n)^T\bar{\psi}(n)\bar{\varepsilon}(n) - \mu\bar{\psi}(n)^T\bar{\psi}(n)\bar{\varepsilon}^2(n). \tag{B.30}$$

The relation (B.30) leads to the Popov inequality

$$\sum_{n=0}^{S}\bar{s}(n)\bar{\varepsilon}(n) \leq \frac{1}{2\mu}\tilde{\theta}(0)^T\tilde{\theta}(0) = c^2$$

which holds for all S. Since

$$\bar{\varepsilon}(n) = \frac{C(z)}{T_*(z)}\bar{s}(n),$$

if this transfer function is SPR then the closed-loop system is asymptotically stable by virtue of the hyperstability theorem [97, 105], thus giving $\bar{\varepsilon}(n) \to 0$. ■

B.18 Proof of Lemma 4.4

Let $\tilde{\theta}(n) = \theta_* - \theta(n)$, with θ_* the parameter vector of the unknown system $H(z)$, and define $s_i(n) = \tilde{\theta}(n+1)^T\psi_i(n)$, $0 \leq i \leq P-1$. As in the proofs of Lemmas 4.1 and 4.3 above, one can show that these signals are related to the *a posteriori* errors via

$$\varepsilon_i(n) = \frac{C_i(z)}{T_*(z)}s_i(n), \qquad 0 \leq i \leq P-1.$$

Define now the vector

$$\Phi(n) = \left[\mathbf{I} + \mu\sum_{i=0}^{P-1}\alpha_i\psi_i(n)\psi_i^T(n)\right]^{-1}\left[\sum_{j=0}^{P-1}\alpha_j\psi_j(n)e_j(n)\right], \tag{B.31}$$

so that the algorithm can be written as $\theta(n+1) = \theta(n) + \mu\Phi(n)$. Observe that the difference between the *a priori* and the *a posteriori* errors in the ith subband takes the form

$$\begin{aligned} e_i(n) - \varepsilon_i(n) &= x_i(n) - \hat{y}_i(n) \\ &= [\theta(n+1) - \theta(n)]^T\psi_i(n) \\ &= \mu\Phi^T(n)\psi_i(n). \end{aligned} \tag{B.32}$$

Now note that, from (B.31),

$$\Phi(n) + \mu \sum_{i=0}^{P-1} \alpha_i \psi_i(n) \psi_i^T(n) \Phi(n) = \sum_{j=0}^{P-1} \alpha_j \psi_j(n) e_j(n).$$

Substituting (B.32) in this and simplifying, we obtain the alternative expression of $\Phi(n)$ in terms of the *a posteriori* errors

$$\Phi(n) = \sum_{i=0}^{P-1} \alpha_i \psi_i(n) \varepsilon_i(n),$$

which is useful for the analysis.

In order to obtain a Popov inequality, observe that

$$s_i(n) = \tilde{\theta}(n+1)^T \psi_i(n) = \tilde{\theta}(n)^T \psi_i(n) - \mu \Phi(n)^T \psi_i(n),$$

so that

$$s_i(n)\varepsilon_i(n) = \tilde{\theta}(n)^T \psi_i(n)\varepsilon_i(n) - \mu \Phi(n)^T \psi_i(n)\varepsilon_i(n).$$

Multiplying this by α_i and then summing over the P subbands gives

$$\sum_{i=0}^{P-1} \alpha_i s_i(n)\varepsilon_i(n) = \tilde{\theta}(n)^T \Phi(n) - \mu \Phi(n)^T \Phi(n). \tag{B.33}$$

Now express the parameter error vector norm as

$$\tilde{\theta}(n+1)^T \tilde{\theta}(n+1) = \tilde{\theta}(n)^T \tilde{\theta}(n) + \mu^2 \Phi(n)^T \Phi(n) - 2\mu \tilde{\theta}(n)^T \Phi(n),$$

so that

$$\tilde{\theta}(n)^T \Phi(n) = \frac{1}{2\mu}[\tilde{\theta}(n)^T \tilde{\theta}(n) - \tilde{\theta}(n+1)^T \tilde{\theta}(n+1)] + \frac{\mu}{2} \Phi(n)^T \Phi(n).$$

Substituting this into (B.33), and then summing over n from 0 to S, yields the desired result:

$$\sum_{n=0}^{S} \sum_{i=0}^{P-1} \alpha_i s_i(n)\varepsilon_i(n) \leq c^2, \tag{B.34}$$

where $c^2 = ||\tilde{\theta}(0)||^2/2\mu$ is independent of S. Therefore we can represent the adaptive algorithm by the feedback loop of Figure B.1, where the nonlinear time-varying block satisfies the multivariable Popov inequality (B.34), and $\mathcal{F}(z)$ is a P-input P-output transfer function matrix given by

$$\mathcal{F}(z) = \text{diag}\left(\alpha_0 \frac{C_0(z)}{T_*(z)}, \cdots, \alpha_{P-1} \frac{C_{P-1}(z)}{T_*(z)} \right).$$

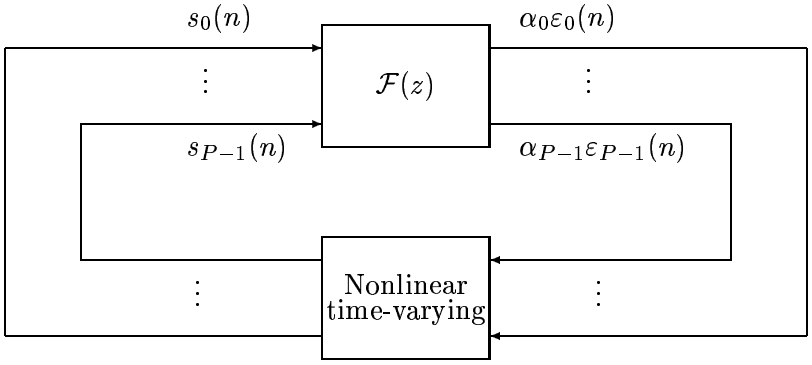

Figure B.1: Feedback loop describing the subband HARF algorithm (4.20).

The multivariable version of the hyperstability theorem states that if $\mathcal{F}(z)$ is SPR, meaning now that it is stable and causal and

$$\mathcal{F}(e^{j\omega}) + \mathcal{F}(e^{j\omega})^\dagger \quad \text{is positive definite for all } \omega,$$

where $(\cdot)^\dagger$ denotes the conjugate transpose, then the vector

$$\mathbf{e}(n) = [\, \alpha_0\varepsilon_0(n) \; \cdots \; \alpha_{P-1}\varepsilon_{P-1}(n) \,]^T$$

satisfies $\mathbf{e}(n)^T\mathbf{e}(n) \to 0$ as $n \to \infty$. This in turn implies that $\varepsilon_i(n) \to 0$ for all i as long as $\alpha_i > 0$. Noting that $\mathcal{F}(z)$ is SPR if and only if $\alpha_i C_i(z)/T_*(z)$ is SPR, the lemma is proved. ∎

B.19 Proof of Lemma 5.1 for $\delta \geq L$

Let the equalizer output (input to the slicer) be

$$\hat{y}(n) = \hat{P}(z)u(n) - \hat{Q}(z)s(n-\delta),$$

where it is assumed that past decisions are correct. The error signal is given by

$$e(n) = s(n-\delta) - \hat{y}(n) = [1 + \hat{Q}(z)]s(n-\delta) - \hat{P}(z)u(n),$$

which closely resembles the expression of the equation error (with a monic constraint) given in (1.28). Let us define the signal vectors

$$\begin{aligned} \mathbf{u}(n) &= [\, u(n) \; u(n-1) \; \cdots \; u(n-N) \,]^T, \\ \mathbf{s}(n) &= [\, s(n-\delta) \; s(n-\delta-1) \; \cdots \; s(n-\delta-M) \,]^T, \end{aligned}$$

so that $e(n) = \bar{\mathbf{q}}^\dagger\mathbf{s}(n) - \mathbf{p}^\dagger\mathbf{u}(n)$, with $\bar{\mathbf{q}} = [\, 1 \; \mathbf{q}^T \,]^T$. Now let

$$\mathbf{R}_{uu} = E[\mathbf{u}(n)\mathbf{u}(n)^\dagger], \qquad \mathbf{R}_{ss} = E[\mathbf{s}(n)\mathbf{s}(n)^\dagger], \qquad \mathbf{R}_{us} = E[\mathbf{u}(n)\mathbf{s}(n)^\dagger].$$

Then $E[|e(n)|^2]$ is minimized with respect to $\mathbf{p}$ if $\mathbf{p} = \mathbf{R}_{uu}^{-1}\mathbf{R}_{us}\bar{\mathbf{q}}$, which gives the reduced cost function

$$E[|e(n)|^2] = J(\bar{\mathbf{q}}) = \bar{\mathbf{q}}^\dagger \mathbf{R}_{s/u}\bar{\mathbf{q}},$$

with the matrix $\mathbf{R}_{s/u}$ given by $\mathbf{R}_{s/u} = \mathbf{R}_{ss} - \mathbf{R}_{us}^\dagger \mathbf{R}_{uu}^{-1}\mathbf{R}_{us}$. In view of Lemma 3.1, it suffices to show that $\mathbf{\Delta}_R = \lceil \mathbf{R}_{s/u} - \mathbf{R}_{s/u} \rfloor$ is positive semidefinite. Note that since $\mathbf{R}_{ss}$ is Toeplitz, one has $\mathbf{\Delta}_R = -\mathbf{\Delta}_M = -(\lceil \mathbf{M} - \mathbf{M} \rfloor)$, where $\mathbf{M} = \mathbf{R}_{us}^\dagger \mathbf{R}_{uu}^{-1}\mathbf{R}_{us}$. Observe that

$$\mathbf{R}_{us} = \sigma_s^2 \begin{bmatrix} c_\delta^* & c_{\delta+1}^* & \cdots & c_{\delta+M}^* \\ c_{\delta-1}^* & c_\delta^* & \cdots & c_{\delta+M-1}^* \\ \vdots & \vdots & \ddots & \vdots \\ c_{\delta-N}^* & c_{\delta-N+1}^* & \cdots & c_{\delta+M-N}^* \end{bmatrix},$$

$$\mathbf{R}_{uu} = \sigma_s^2 \mathbf{C}\mathbf{C}^\dagger + \sigma_\eta^2 \mathbf{I},$$

where $\mathbf{C}$ is the channel matrix defined in (5.10). If the SNR is sufficiently small, then we can approximate $\mathbf{R}_{uu} \approx \sigma_\eta^2 \mathbf{I}$, so that $\mathbf{R}_{uu}^{-1} \approx \sigma_\eta^{-2}\mathbf{I}$. In that case with $0 \leq i,\ j \leq M$ the i,jth element of the matrix $\mathbf{M}$ is

$$(\mathbf{M})_{i,j} \approx \frac{\sigma_s^4}{\sigma_\eta^2} \sum_{k=0}^{N} c_{\delta+i-k} c_{\delta+j-k}^*.$$

Thus for $1 \leq i,\ j \leq M$,

$$(\mathbf{\Delta}_M)_{i,j} = (\mathbf{M})_{i,j} - (\mathbf{M})_{i-1,j-1} \approx \frac{\sigma_s^4}{\sigma_\eta^2}(c_{\delta+i}c_{\delta+j}^* - c_{\delta+i-N-1}c_{\delta+j-N-1}^*).$$

In addition, since $\delta \geq L$ the channel coefficients satisfy $c_{\delta+k} = 0$ for $k > 0$. Thus

$$(\mathbf{\Delta}_M)_{i,j} \approx -\frac{\sigma_s^4}{\sigma_\eta^2} c_{\delta+i-N-1}c_{\delta+j-N-1}^*.$$

This gives $\mathbf{\Delta}_M \approx -\frac{\sigma_s^4}{\sigma_\eta^2}\mathbf{c}\mathbf{c}^\dagger \leq \mathbf{0}$, with $\mathbf{c} = [\, c_{\delta-N}\ c_{\delta-N+1}\ \cdots\ c_{\delta-N+M-1}\,]^T$. ∎

B.20 Proof of Theorem 5.2

Define the function $F : \mathbb{C}^M \to \mathbb{C}^M$ as

$$F(\mathbf{a}) = E[\mathbf{x}(n)\mathbf{x}(n)^\dagger]^{-1} E[\mathbf{x}(n)u^*(n)],$$

with $\mathbf{x}(n) = [\, x(n-1) \cdots x(n-M)\,]^T$ and $x(n) = [1/A(z)]u(n)$, with $A(z)$ the polynomial associated to $\mathbf{a}$. Then the iterative method can be written as $\mathbf{a}_{i+1} = F(\mathbf{a}_i)$. Introduce now the map $\mathbf{k} = L(\mathbf{a})$, where $\mathbf{k} = [\, k_1 \cdots k_M\,]^T$ is the vector of

reflection coefficients (lattice parameters) associated to the polynomial $A(z)$. The stability domain becomes the following convex open subset of $\mathbb{C}^M$:

$$\mathcal{D} = \{ \ \mathbf{k} \ : \ |k_i| < 1 \ \text{ for } i = 1, \ldots, M \ \}.$$

We can define the function $G : \mathcal{D} \to \mathbb{C}^M$ as the composition $G = L \circ F \circ L^{-1}$. Thus the iteration can be reparameterized in lattice coordinates as $\mathbf{k}_{i+1} = G(\mathbf{k}_i)$. Observe that the iteration may break if $\mathbf{k}_i$ is outside $\mathcal{D}$.

Let $\partial\mathcal{D}$ denote the boundary of $\mathcal{D}$. As the vector of lattice parameters $\mathbf{k}$ approaches $\partial\mathcal{D}$, at least one root of the corresponding polynomial $A(z)$ approaches the unit circle. In that case the diagonal entries of the matrix $E[\mathbf{x}(n)\mathbf{x}(n)^\dagger]$ become

$$E[|x(n)|^2] = E\left[\left|\frac{1}{A(z)}u(n)\right|^2\right] \to \infty, \tag{B.35}$$

because $S_{uu}(z) > 0$ on the unit circle is assumed. On the other hand the conjugated components of the vector $E[\mathbf{x}(n)u^*(n)]$ are given by

$$E[u(n)x^*(n-j)] = \left\langle 1, \frac{z^{-j}}{A(z)} \right\rangle_u = \frac{1}{2\pi i}\oint_{|z|=1} S_{uu}(z)\frac{z^{j-1}}{A^*(1/z^*)}dz \tag{B.36}$$

for $1 \le j \le M$. For minimum phase $A(z)$, the only poles of the integrand inside the unit circle are those of $S_{uu}(z)$; therefore, using the residue theorem to evaluate (B.36), we see that these quantities remain finite even as one or more roots of $A(z)$ approach $|z| = 1$.

This implies that as $\mathbf{k} \to \partial\mathcal{D}$ from inside $\mathcal{D}$,

$$F(L^{-1}(\mathbf{k})) \to \mathbf{0},$$

in view of (B.35), (B.36) and the definition of F. Since $L(\mathbf{0}) = \mathbf{0}$, we conclude that the domain of G can be extended in order to include $\partial\mathcal{D}$ by defining $G(\mathbf{k}) = \mathbf{0}$ for all $\mathbf{k} \in \partial\mathcal{D}$, and in this way $G : \mathcal{D} \cup \partial\mathcal{D} \to \mathbb{C}^M$ remains continuous.

We now invoke the following Borsuk fixed point theorem [21, p.46]:

Theorem B.1. *Let $\bar{\mathcal{D}}$ be a closed, bounded, symmetric and convex subset of $\mathbb{C}^M$, and let G be a continuous mapping from $\bar{\mathcal{D}}$ to $\mathbb{C}^M$. If G is odd along the boundary, i.e.*

$$G(-\mathbf{k}) = -G(\mathbf{k}) \quad \textit{for all } \mathbf{k} \in \partial\mathcal{D}, \tag{B.37}$$

then G admits a fixed point in $\bar{\mathcal{D}}$: there exists $\mathbf{k}_\star \in \bar{\mathcal{D}}$ such that $G(\mathbf{k}_\star) = \mathbf{k}_\star$.

We can apply this result with $\bar{\mathcal{D}} = \mathcal{D} \cup \partial\mathcal{D}$: since $G(\mathbf{k}) = \mathbf{0}$ for all $\mathbf{k} \in \partial\mathcal{D}$, (B.37) is clearly satisfied. Thus $G(\mathbf{k}_\star) = \mathbf{k}_\star$ for some $\mathbf{k}_\star \in \bar{\mathcal{D}}$. Moreover $\mathbf{k}_\star$ cannot belong in $\partial\mathcal{D}$ since all $\partial\mathcal{D}$ is mapped onto $\mathbf{0}$ which is not in $\partial\mathcal{D}$. Thus the fixed point lies inside the stability domain $\mathcal{D}$. ∎

B.21 Proof of Lemma 5.2

With $M = 1$, assume that the polynomials $1 + az^{-1}$ and $1 + bz^{-1}$ were both minimum-phase stationary points of PLR. Define the processes

$$x_a(n) = \frac{1}{1 + az^{-1}}u(n), \qquad x_b(n) = \frac{1}{1 + bz^{-1}}u(n),$$

and their autocorrelation coefficients

$$r_a[k] = E[x_a(n)x_a(n-k)], \qquad r_b[k] = E[x_b(n)x_b(n-k)].$$

Then we must have $r_a[1] = r_b[1] = 0$. Define the process $w(\cdot)$ as

$$w(n) = \frac{1}{1 + az^{-1}}x_b(n) = \frac{1}{1 + bz^{-1}}x_a(n),$$

with autocorrelation coefficients $r_w[k] = E[w(n)w(n-k)]$. Noting that $x_a(n) = (1 + bz^{-1})w(n)$, it can be easily shown that

$$r_a[1] = r_w[1] + (r_w[0] + r_w[2])b + r_w[1]b^2. \tag{B.38}$$

Define the cross-correlation coefficients $c[k] = E[x_b(n)w(n-k)]$. Since $w(n) = x_b(n) - aw(n-1)$, they satisfy

$$c[k] = r_b[k] - ac[k+1], \tag{B.39}$$
$$r_w[k] = c[k] - ar_w[k-1]. \tag{B.40}$$

By (B.39), $r_b[1] = 0$ implies $c[1] = -ac[2]$. In view of (B.40), this gives

$$r_w[1] = -a(r_w[0] + c[2]), \tag{B.41}$$
$$\begin{aligned} r_w[2] &= c[2] - ar_w[1] \\ &= c[2] + a^2(r_w[0] + c[2]). \end{aligned} \tag{B.42}$$

Substituting this into (B.38), we obtain

$$\begin{aligned} r_a[1] &= -(a-b)(1-ab)(r_x[0] + c[2]) \\ &= 0 \quad \text{by assumption.} \end{aligned} \tag{B.43}$$

Now note that since

$$r_x[0] + r_x[2] = (1 + a^2)(r_x[0] + c[2])$$

we cannot have $r_x[0] + c[2] = 0$ due to the fact that $|r_x[0]| > |r_x[2]|$. Also, since $|a|, |b| < 1$, one has $1 - ab > 0$. Thus (B.43) implies $a = b$. ∎

Appendix C

A REVIEW OF SZEGÖ POLYNOMIALS

Consider the power spectral density function $S_{uu}(z)$ associated to some zero-mean, real-valued process $u(\cdot)$:

$$S_{uu}(z) = \sum_{n=-\infty}^{\infty} r_{uu}(n) z^{-n} \qquad \text{with} \qquad r_{uu}(n) = E[u(k+n)u(k)].$$

It will be assumed without loss of generality that $u(\cdot)$ is scaled to unit variance, i.e., $r_{uu}(0) = 1$. The weighted inner product induced by $S_{uu}(z)$ of two functions in $\mathcal{H}_2$,

$$f(z) = \sum_{k=0}^{\infty} f_k z^{-k}, \qquad g(z) = \sum_{k=0}^{\infty} g_k z^{-k},$$

is denoted by

$$\begin{aligned} \langle f(z), g(z) \rangle_u &= \frac{1}{2\pi j} \oint S_{uu}(z) f(z^{-1}) g(z) \frac{dz}{z} \\ &= \sum_{i=0}^{\infty} \sum_{j=0}^{\infty} f_i g_j r_{uu}(i-j). \end{aligned}$$

If $u(\cdot)$ is a white process, then one has $r_{uu}(n) = \delta(n)$ (the Kronecker delta), which gives $\langle f(z), g(z) \rangle_u = \sum_{k=0}^{\infty} f_k g_k$. Taking $f(z) = z^{-i}$, $g(z) = z^{-j}$, one finds that these monomials are orthonormal. However, for colored $u(\cdot)$, one has $\langle z^{-i}, z^{-j} \rangle_u = r_{uu}(i-j)$ which need not be zero. Thus the standard basis $\{z^{-k}\}_{k=0}^{\infty}$ of the subspace $\mathcal{H}_2$ is not orthonormal in general with respect to this spectrally weighted inner product.

The Szegö polynomials $\{p_k(z)\}_{k=0}^{\infty}$ associated to $u(\cdot)$ are obtained by applying the Gram-Schmidt orthonormalization procedure to the standard basis: one takes $p_0(z) = 1$, the first element of the original basis $\{z^{-k}\}_{k=0}^{\infty}$; then, $p_1(z)$ is taken as a linear combination of 1 and z^{-1} in order to satisfy

$$\langle p_0(z), p_1(z) \rangle_u = 0, \qquad \langle p_1(z), p_1(z) \rangle_u = 1,$$

and so forth. As a consequence of this procedure, the Szegö polynomials satisfy the following properties:

1. Each polynomial $p_k(z)$ has degree k.

2. The set $\{p_k(z)\}_{k=0}^{P}$ spans the subspace of polynomials of degree not exceeding P.

3. If $f(z) \in \mathcal{H}_2$ is a polynomial of degree not exceeding P, then $\langle f(z), p_k(z)\rangle_u = 0$ for all $k > P$.

Observe that for all $k \geq 0$ one can write

$$\underbrace{\begin{bmatrix} p_0(z) \\ p_1(z) \\ \vdots \\ p_k(z) \end{bmatrix}}_{=\mathbf{p}_k(z)} = \mathbf{C}_k \underbrace{\begin{bmatrix} 1 \\ z^{-1} \\ \vdots \\ z^{-k} \end{bmatrix}}_{=\mathbf{s}_k(z)},$$

where the matrix $\mathbf{C}_k$ is lower triangular and invertible. Note that, by construction,

$$\begin{aligned} \mathbf{I} &= \langle \mathbf{p}_k(z), \mathbf{p}_k^T(z)\rangle_u \\ &= \mathbf{C}_k \langle \mathbf{s}_k(z), \mathbf{s}_k^T(z)\rangle_u \mathbf{C}_k^T \\ &= \mathbf{C}_k \underbrace{\begin{bmatrix} r_{uu}(0) & r_{uu}(1) & \cdots & r_{uu}(k) \\ r_{uu}(1) & r_{uu}(0) & \cdots & r_{uu}(k-1) \\ \vdots & \vdots & \ddots & \vdots \\ r_{uu}(k) & r_{uu}(k-1) & \cdots & r_{uu}(0) \end{bmatrix}}_{=\mathbf{R}_k} \mathbf{C}_k^T, \end{aligned}$$

which reveals the matrix $\mathbf{C}_k^{-1}$ as the Cholesky factor of the $(k+1) \times (k+1)$ autocorrelation matrix of the process $u(\cdot)$, i.e. $\mathbf{R}_k = \mathbf{C}_k^{-1}\mathbf{C}_k^{-T}$.

Note that, due to the orthogonality of the Szegö polynomials, the signals

$$\bar{\beta}_k(n) = p_k(z)u(n)$$

satisfy $E[\bar{\beta}_i(n) \cdot \bar{\beta}_j(n)] = \delta(i-j)$. In fact, $\bar{\beta}_k(n)$ is just the kth backward prediction error (normalized to unit variance) associated with the process $u(\cdot)$, and $p_k(z)$ is just the (normalized) kth order backward prediction error filter. The corresponding (normalized) kth order forward prediction error filter is given by the reverse polynomial $\hat{p}_k(z) = z^{-k}p_k(z^{-1})$. These filters are familiar in the context of linear prediction theory [46], in which it is well known that $p_k(z)$ is maximum phase (all roots lie outside the unit circle), and therefore $\hat{p}_k(z)$ is minimum phase. Moreover, all the prediction error filters up to order k can be implemented together in a lattice structure as shown in Figure C.1. The reflection coefficients $\rho_1, \ldots, \rho_k$ of this lattice filter are known as the *Schur parameters* of the process $u(\cdot)$, and they are uniquely determined by the autocorrelation coefficients $r_{uu}(0), r_{uu}(1), \ldots, r_{uu}(k)$.

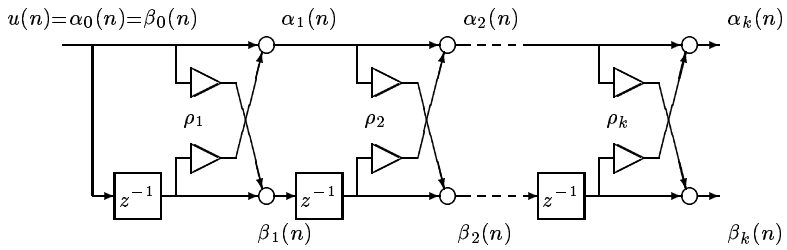

Figure C.1: Lattice implementation of the prediction error filters (unnormalized Szegö polynomials and their reverse counterparts). $\alpha_i(n)$: forward prediction errors; $\beta_i(n)$: backward prediction errors.

The lattice structure of Figure C.1 is an implementation of the recursion

$$\begin{bmatrix} \hat{p}_k(z) \\ p_k(z) \end{bmatrix} = \frac{1}{\sqrt{1-\rho_k^2}} \begin{bmatrix} 1 & \rho_k \\ \rho_k & 1 \end{bmatrix} \begin{bmatrix} \hat{p}_{k-1}(z) \\ z^{-1}p_{k-1}(z) \end{bmatrix} \tag{C.1}$$

in an unnormalized fashion. The variance of the forward and backward prediction errors in Figure C.1 is given by

$$E[\alpha_k^2(n)] = E[\beta_k^2(n)] = E[u^2(n)] \cdot \zeta_k^2, \qquad \text{with} \quad \zeta_k^2 = \prod_{i=1}^{k}(1-\rho_i^2),$$

so that the relation between the normalized and unnormalized signals is just

$$\bar{\beta}_k(n) = \frac{1}{\zeta_k}\beta_k(n)$$

(assuming $E[u^2(n)] = 1$), and similarly for the forward prediction errors.

Although the Szegö polynomials were generated from the natural basis $\{z^{-k}\}_{k=0}^{\infty}$, due to the fact that the dimension of this set is infinite it is not immediately obvious that the Szegö polynomials form a complete basis, i.e. that $\{p_k(z)\}_{k=0}^{\infty}$ spans the whole $\mathcal{H}_2$ subspace. This is the case provided that $S_{uu}(z)$ satisfies

$$\exp\left[\frac{1}{2\pi}\int_{-\pi}^{\pi} \ln S_{uu}(e^{j\omega})\mathrm{d}\omega\right] > 0 \tag{C.2}$$

which is known as the Szegö condition, a technical requirement that will be assumed to hold in the sequel. This condition also ensures $|\rho_k| < 1$ for all k, as well as $\lim_{k\to\infty}\zeta_k > 0$. See [57, 123] for more advanced topics on Szegö polynomials.

If $f(z)$, $g(z) \in \mathcal{H}_2$ and the Szegö polynomials form a complete basis, then we can write

$$f(z) = \sum_{k=0}^{\infty} f_k' p_k(z), \qquad g(z) = \sum_{k=0}^{\infty} g_k' p_k(z),$$

where

$$f'_k = \langle f(z), p_k(z) \rangle_u, \qquad g'_k = \langle g(z), p_k(z) \rangle_u,$$

and the weighted inner product becomes

$$\langle f(z), g(z) \rangle_u = \sum_{k=0}^{\infty} f'_k g'_k$$

due to the orthonormality of the polynomials $\{p_k(z)\}_{k=0}^{\infty}$.

Autoregressive processes

The process $u(\cdot)$ is autoregressive of order m, or AR(m), if its psd can be written as

$$S_{uu}(z) = \frac{c^2}{q(z)q(z^{-1})}$$

with c a constant and $q(z)$ a polynomial of degree m, which can be taken to be minimum phase. This means that $u(\cdot)$ can be seen as the output of an all-pole filter with transfer function $c/q(z)$ driven by unit-variance white noise. Observe that in that case, the optimum forward and backward prediction error filters of order $k \geq m$ are $q(z)$ and $z^{-k}q(z^{-1})$ respectively, since the mth order filters already achieve perfect whitening. Equivalently, the Schur parameters satisfy $\rho_k = 0$, for all $k > m$.

This observation reveals a useful property of the Szegö polynomials associated to an AR(m) process: they satisfy

$$p_k(z) = z^{-(k-m)} p_m(z) \qquad \text{for all } k \geq m, \tag{C.3}$$

and in fact $p_m(z) = z^{-m}q(z^{-1})$ (by suitably scaling $S_{uu}(z)$ if needed).

Observe that, if we define $\mathcal{K}_m = \text{span}\{p_k(z)\}_{k=m}^{\infty}$, then AR($m$) processes satisfy

$$f(z) \in \mathcal{K}_m \quad \Rightarrow \quad z^{-1} f(z) \in \mathcal{K}_m \tag{C.4}$$

so that the subspace $\mathcal{K}_m$ is right shift invariant. In fact, property (C.4) is all that is required of the process $u(\cdot)$ in the proofs of many results in this thesis that invoke an autoregressive condition on $u(\cdot)$. One could think that (C.4) describes a class of processes that is more general than the AR(m) class. Is that the case?

Lemma C.1. *Assume that the Szegö condition (C.2) is satisfied. If the subspace $\mathcal{K}_m$ is right shift invariant, then the process $u(\cdot)$ is autoregressive of order m (or less).*

Proof: It suffices to show that if $\mathcal{K}_m$ is right shift invariant, then the Schur parameters are zero for $k > m$. We proceed by induction in k.

First, we will prove that $z^{-1}p_m(z) \in \mathcal{K}_m$ implies $\rho_{m+1} = 0$. Observe that, if we write

$$p_k(z) = p_{k0} + p_{k1}z^{-1} + \cdots + p_{kk}z^{-k},$$

then the first and last coefficients are given by

$$p_{k0} = \frac{\rho_k}{\zeta_k}, \qquad p_{kk} = \frac{1}{\zeta_k}.$$

Now since $z^{-1}p_m(z) \in \mathcal{K}_m$, it can be written as a linear combination of the Szegö polynomials $p_k(z)$ with $k \geq m$. In addition, $z^{-1}p_m(z)$ is a polynomial of degree $m+1$, and therefore it is orthogonal to $p_k(z)$ for $k > m+1$. Hence we can write

$$z^{-1}p_m(z) = ap_m(z) + bp_{m+1}(z)$$

for some constants a, b. Equating the coefficients of $z^{-(m+1)}$, one obtains

$$\frac{1}{\zeta_m} = \frac{b}{\zeta_{m+1}} \quad \Rightarrow \quad b = \frac{\zeta_{m+1}}{\zeta_m}, \tag{C.5}$$

while equating coefficients of $z^0 = 1$ gives

$$0 = a\frac{\rho_m}{\zeta_m} + b\frac{\rho_{m+1}}{\zeta_{m+1}}. \tag{C.6}$$

Substituting (C.5) into (C.6), we obtain $a\rho_m + \rho_{m+1} = 0$. If $\rho_m = 0$, then it follows that $\rho_{m+1} = 0$ as desired. Hence assume that $\rho_m \neq 0$, in which case $a = -\rho_{m+1}/\rho_m$. Thus

$$z^{-1}p_m(z) = -\frac{\rho_{m+1}}{\rho_m}p_m(z) + \frac{\zeta_{m+1}}{\zeta_m}p_{m+1}(z). \tag{C.7}$$

On the other hand, the recursion (C.1) shows that

$$p_{m+1}(z) = \frac{\rho_{m+1}\hat{p}_m(z) + z^{-1}p_m(z)}{\sqrt{1-\rho_{m+1}^2}} = \frac{\zeta_m}{\zeta_{m+1}}\left[\rho_{m+1}\hat{p}_m(z) + z^{-1}p_m(z)\right]. \tag{C.8}$$

Substituting (C.8) into (C.7) gives

$$z^{-1}p_m(z) = -\frac{\rho_{m+1}}{\rho_m}p_m(z) + \rho_{m+1}\hat{p}_m(z) + z^{-1}p_m(z),$$

that is,

$$\rho_{m+1}\left[\hat{p}_m(z) - \frac{1}{\rho_m}p_m(z)\right] = 0. \tag{C.9}$$

Observe that the coefficient of z^{-m} in $\hat{p}_m(z) - \frac{1}{\rho_m}p_m(z)$ is $\frac{1}{\zeta_m}\left(\rho_m - \frac{1}{\rho_m}\right)$. Thus (C.9) implies

$$\frac{\rho_{m+1}}{\zeta_m}\left(\rho_m - \frac{1}{\rho_m}\right) = 0.$$

For the term in parenthesis to be zero, one must have $|\rho_m| = 1$ which is not possible since the Szegö condition holds. Thus $\rho_{m+1} = 0$.

Now assume that $\rho_{m+1} = \cdots = \rho_{m+k} = 0$, and $z^{-1}p_{m+k}(z) \in \mathcal{K}_m$. Then we will show that $\rho_{m+k+1} = 0$.

Note that $\rho_{m+i} = 0$ for $1 \le i \le k$ implies

$$p_{m+i}(z) = z^{-i}p_m(z), \qquad \hat{p}_{m+i}(z) = \hat{p}_m(z), \qquad \zeta_{m+i} = \zeta_m, \qquad 1 \le i \le k.$$

Therefore

$$\begin{aligned} p_{m+k+1}(z) &= \frac{\rho_{m+k+1}\hat{p}_{m+k}(z) + z^{-1}p_{m+k}(z)}{\sqrt{1-\rho_{m+k+1}^2}} \\ &= \frac{\zeta_m}{\zeta_{m+k+1}}\left[\rho_{m+k+1}\hat{p}_m(z) + z^{-(k+1)}p_m(z)\right]. \end{aligned} \tag{C.10}$$

Now since $z^{-1}p_{m+k}(z)$ belongs in $\mathcal{K}_m$ and it has degree $m+k+1$, it can be written as a linear combination of $p_{m+i}(z)$ with $0 \le i \le k+1$:

$$\begin{aligned} z^{-1}p_{m+k}(z) &= c_0p_m(z) + c_1p_{m+1}(z) + \cdots + c_{k+1}p_{m+k+1}(z) \\ &= (c_0 + c_1z^{-1} + \cdots + c_kz^{-k})p_m(z) + c_{k+1}p_{m+k+1}(z). \end{aligned} \tag{C.11}$$

Equating the coefficients of $z^{-(m+k+1)}$, one sees that

$$c_{k+1} = \frac{\zeta_{m+k+1}}{\zeta_{m+k}} = \frac{\zeta_{m+k+1}}{\zeta_m}.$$

Substituting this and (C.10) in (C.11),

$$z^{-1}p_{m+k}(z) = (c_0 + c_1z^{-1} + \cdots + c_kz^{-k} + z^{-k-1})p_m(z) + \rho_{m+k+1}\hat{p}_m(z). \tag{C.12}$$

Therefore,

$$\frac{1}{\zeta_m}(c_0\rho_m + \rho_{m+k+1}) = 0.$$

Again, if $\rho_m = 0$ then it follows that $\rho_{m+k+1} = 0$ as desired. Otherwise, one has $c_0 = -\rho_{m+k+1}/\rho_m$. With this, and noting that $z^{-1}p_{m+k}(z) = z^{-k-1}p_m(z)$, we obtain from (C.12)

$$0 = \left(-\frac{\rho_{m+k+1}}{\rho_m} + c_1z^{-1} + \cdots + c_kz^{-k}\right)p_m(z) + \rho_{m+k+1}\hat{p}_m(z).$$

Successively equating the coefficients of z^{-m-k}, $\ldots$, z^{-m} in the right-hand side to zero yields $c_k = c_{k-1} = \cdots = c_1 = 0$ and

$$\frac{\rho_{m+k+1}}{\zeta_m}\left(\rho_m - \frac{1}{\rho_m}\right) = 0,$$

which implies $\rho_{m+k+1} = 0$ since $|\rho_m| < 1$. This concludes the proof. ∎

Thus Lemma C.1 shows that the mth order autoregressive condition on a process is completely equivalent to the corresponding subspace $\mathcal{K}_m$ being right shift invariant.

BIBLIOGRAPHY

[1] B. D. O. Anderson, R. R. Bitmead, C. R. Johnson Jr., P. V. Kokotovic, R. L. Kosut, I. M. Y. Mareels, L. Praly, and B. D. Riedle. *Stability of Adaptive Systems: Passivity and Averaging Analysis.* MIT Press, 1986.

[2] B. D. O. Anderson and C. R. Johnson Jr. Exponential convergence of adaptive identification and control algorithms. *Automatica*, 18:1–13, January 1982.

[3] B. D. O. Anderson and E. I. Jury. A simplified Schur-Cohn test. *IEEE Trans. on Automatic Control*, 18:157–163, February 1973.

[4] K. J. Åström and T. Söderström. Uniqueness of the Maximum Likelihood estimates of the parameters of an ARMA model. *IEEE Trans. on Automatic Control*, 19:769–773, December 1974.

[5] K. J. Åström and B. Wittenmark. *Computer-Controlled Systems.* Prentice-Hall, 1997.

[6] M. Bonnet, O. Macchi, and M. Jaidane-Saidane. Theoretical analysis of the ADPCM CCITT algorithm. *IEEE Trans. on Communications*, 38:847–858, June 1990.

[7] A. Bouttier. A truly recursive blind equalization algorithm. In *International Conference on Acoustics, Speech and Signal Processing*, volume 6, pages 3381–3384, May 1998.

[8] C. Breining, P. Dreiscitel, E. Hansler, A. Mader, B. Nitsch, H. Puder, T. Schertler, G. Schmidt, and J. Tilp. Acoustic echo control: an application of very-high-order adaptive filters. *IEEE Signal Processing Magazine*, pages 42–69, July 1999.

[9] P.M.S. Burt and M. Gerken. A polyphase IIR adaptive filter: Error surface analysis and application. In *International Conference on Acoustics, Speech and Signal Processing*, pages 2285–2288, April 1997.

[10] A. Carini, V. J. Mathews, and G. L. Sicuranza. Sufficient stability bounds for slowly varying direct-form recursive linear filters and their applications in adaptive IIR filters. *IEEE Trans. on Signal Processing*, 47:2561–2567, September 1999.

[11] R. A. Casas, C. Richard Johnson Jr., J. Harp, and S. Caffee. On initialization strategies for blind adaptive DFEs. In *IEEE Wireless Communications and Networking Conference*, pages 792–796, September 1999.

[12] J. Chao, S. Kawabe, and S. Tsujii. A new IIR adaptive echo canceler: GIVE. *IEEE Journal on Selected Areas in Communications*, 12:1530–1539, December 1994.

[13] W. Y. Chen, J. L. Dixon, and D. L. Waring. High bit rate digital subscriber line echo cancellation. *IEEE Journal on Selected Areas in Communications*, 9:848–860, August 1991.

[14] J. E. Cousseau and P. S. R. Diniz. A general consistent equation-error algorithm for adaptive IIR filtering. *Signal Processing*, 56(6):121–134, 1997.

[15] D. H. Crawford and R. W. Stewart. Adaptive IIR filtered-v algorithms for active noise control. In *J. Acoust. Soc. Amer.*, pages 2097–2103, April 1997.

[16] D. H. Crawford, R. W. Stewart, and E. Toma. A novel adaptive IIR filter for active noise control. In *International Conference on Acoustics, Speech and Signal Processing*, pages 1629–1632, May 1996.

[17] P. M. Crespo and M. L. Honig. Pole-zero decision feedback equalization with a rapidly converging adaptive IIR algorithm. *IEEE Journal on Selected Areas in Communications*, 9:817–829, August 1991.

[18] S. A. Cruces. Métodos de estabilización óptima para sistemas autorregresivos. Master's thesis, University of Vigo, Spain, 1994.

[19] V. E. DeBrunner and A. A. Beex. An informational approach to the convergence of output error adaptive IIR filter structures. In *International Conference on Acoustics, Speech and Signal Processing*, volume 3, pages 1261–1264, April 1990.

[20] S. C. Douglas and M. Rupp. On bias removal and unit-norm constraints in equation-error adaptive IIR filters. In *30th Asilomar Conference on Signals, Systems and Computers*, pages 1093–1097, November 1996.

[21] J. Dugundji and A. Granas. *Fixed point theory.* PWN-Polish Scientific, 1982.

[22] T.J. Endres, C. H. Strolle, S. N. Hulyalkar, T. A. Schaffer, A. Shah, M. Gittings, C. Hollowell, A. Bhaskaran, J. Roletter, and B. Paratore. Carrier independent blind initialization of a DFE. In *IEEE Workshop on Signal Processing Advances in Wireless Communications*, pages 239–241, May 1999.

[23] N. Erdol and F. Basbug. Wavelet transform based adaptive filters: analysis and new results. *IEEE Trans. on Signal Processing*, 44:2163–2171, September 1996.

[24] L. J. Eriksson, M. C. Allie, and R. A. Greiner. The selection and application of an IIR adaptive filter for use in active sound attenuation. *IEEE Trans. on Acoustics, Speech and Signal Processing*, ASSP-35:433–437, April 1987.

[25] S. Evans and L. Tong. Online adaptive reinitialization of the constant modulus algorithm. *IEEE Transactions on Communications*, 48:537–539, April 2000.

[26] H. Fan. Application of Benveniste's convergence results in the study of adaptive IIR filtering algorithms. *IEEE Trans. on Information Theory*, 34:1692–709, July 1988.

[27] H. Fan. A structural view of asymptotic convergence speed of adaptive IIR filtering algorithms: Part I - infinite precision implementation. *IEEE Transactions on Signal Processing*, 41:1493–1517, April 1993.

[28] H. Fan. A structural view of asymptotic convergence speed of adaptive IIR filtering algorithms: Part II - finite precision implementation. *IEEE Transactions on Signal Processing*, 45:1458–1472, June 1997.

[29] H. Fan and M. Doroslovački. On "global convergence" of the Steiglitz-McBride adaptive algorithm. *IEEE Trans. on Circuits and Systems–part II*, 40:73–87, February 1993.

[30] H. Fan and W. K. Jenkins. A new adaptive IIR filter. *IEEE Trans. on Circuits and Systems*, 33:939–947, October 1986.

[31] H. Fan and W. K. Jenkins. An investigation of an adaptive IIR echo canceller: advantages and problems. *IEEE Trans. on Acoustics, Speech and Signal Processing*, 36:1819–1833, December 1988.

[32] H. Fan and Q. Li. A delta - operator recursive gradient algorithm for adaptive signal processing. In *International Conference on Acoustics, Speech and Signal Processing*, volume 3, pages 492–495, April 1993.

[33] H. Fan and M. Nayeri. On reduced order identification: revisiting "On some system identification techniques for adaptive filtering". *IEEE Trans. on Circuits and Systems*, 37:1144–1151, September 1990.

[34] P. L. Feintuch. An adaptive recursive LMS filter. *Proc. IEEE*, 64:1622–1624, November 1976.

[35] ITU-T Recommendation G.168. *Digital Network Echo Cancellers.* 1997.

[36] ITU-T Recommendation G.726. *40, 32, 24, 16 kbit/s Adaptive Differential Pulse Code Modulation (ADPCM).* 1990.

[37] K. Gao, M. O. Ahmad, and M. N. S. Swamy. A constrained anti-Hebbian learning algorithm for total least-squares estimation with applications to

adaptive FIR and IIR filtering. *IEEE Trans. on Circuits and Systems, part II*, 41:718–729, November 1994.

[38] S. Gee and M. Rupp. A comparison of adaptive IIR echo canceller hybrids. In *International Conference on Acoustics, Speech and Signal Processing*, pages 1541–1544, 1991.

[39] J. A. B. Gerald, N. L. Esteves, and M. M. Silva. An adaptive IIR echo canceller using lattice structures. In *Proc. 5th European Signal Processing Conference, Barcelona, Spain*, pages 265–268, 1990.

[40] J. A. B. Gerald, N. L. Esteves, and M. M. Silva. A new IIR echo canceller structure. *IEEE Transactions on Circuits and Systems II*, 42(12):818–821, 1995.

[41] A. Gilloire and M. Vetterli. Adaptive filtering in subbands with critical sampling: analysis, experiments and application to acoustic echo cancellation. *IEEE Trans. on Signal Processing*, 40:1862–1875, August 1992.

[42] R. D. Gitlin, J. F. Hayes, and S. B. Weinstein. *Data Communication Principles.* Plenum Press, 1992.

[43] G.-O. Glentis, K. Berberidis, and S. Theodoridis. Efficient least squares adaptive algorithms for FIR transversal filtering. *IEEE Signal Processing Magazine*, pages 13–41, July 1999.

[44] D. N. Godard. Self-recovering equalization and carrier tracking in two-dimensional data communication systems. *IEEE Trans. on Communications*, 28:1867–1875, November 1980.

[45] M. C. Hall and P. M. Hughes. The master-slave IIR filter adaptation algorithm. In *IEEE International Symposium on Circuits and Systems*, pages 2145–2148, 1988.

[46] S. Haykin. *Adaptive Filter Theory.* Prentice-Hall, third edition, 1996.

[47] A. Hirano, A. Sugiyama, and S. Ikeda. DSP implementation and performance evaluation of sparse-tap adaptive FIR filters with tap-position control. In *International Conference on Acoustics, Speech and Signal Processing*, pages 1295–1298, 1996.

[48] K. C. Ho and Y. T. Chan. Bias removal in equation-error adaptive IIR filters. *IEEE Trans. on Signal Processing*, 43:51–62, January 1995.

[49] M. Idier and J.-F. Giovannelli. Structural stability of least squares prediction methods. *IEEE Trans. on Signal Processing*, 46:3109–3111, November 1998.

[50] N. S. Jayant and P. Noll. *Digital Coding of Waveforms.* Prentice-Hall, 1984.

[51] C. R. Johnson Jr. A convergence proof for a hyperstable adaptive recursive filter. *IEEE Trans. on Information Theory*, 25:745–759, November 1979.

[52] C. R. Johnson Jr. Adaptive IIR filtering: Current results and open issues. *IEEE Transactions on Information Theory*, 30:237–250, March 1984.

[53] C. R. Johnson Jr. *Lectures on Adaptive Parameter Estimation*. Prentice Hall, 1988.

[54] C. R. Johnson Jr., P. Schniter, T. J. Endres, J. D. Behm, D. R. Brown, and R. A. Casas. Blind equalization using the Constant Modulus criterion: A review. *Proceedings of the IEEE*, 86:1927–1950, October 1998.

[55] S. Horvath Jr. Lattice form adaptive recursive digital filters: algorithms and applications. In *International Symposium on Circuits and Systems*, pages 128–133, May 1980.

[56] A. N. Kaelin, A. G. Lindgren, and G. S. Moschytz. Simplified adaptive IIR filters based on optimized orthogonal prefiltering. *IEEE Trans. on Circuits and Systems, Part II*, 42:326–333, May 1995.

[57] T. Kailath, A. Vieira, and M. Morf. Inverses of Toeplitz operators, innovations and orthogonal polynomials. *SIAM Review*, 20:106–119, January 1978.

[58] R. A. Kennedy, B. D. O. Anderson, and R. R. Bitmead. Blind adaptation of decision feedback equalizers: gross convergence properties. *Intl. J. Adaptive Control and Signal Processing*, 7:497–523, 1993.

[59] J. B. Kenney and C. E. Rohrs. The composite regressor algorithm for IIR adaptive systems. *IEEE Trans. on Signal Processing*, 41:617–628, February 1993.

[60] S. M. Kuo and D. R. Morgan. *Active noise control systems*. John Wiley & Sons, 1996.

[61] S. M. Kuo, I. Panahi, K. M. Chung, T. Horner, M. Nadeski, and J. Chyan. Design of active noise control systems with the TMS320 family. Technical Report SPRA042, Texas Instruments, June 1996.

[62] J. Labat, O. Macchi, and C. Laot. Adaptive decision feedback equalization: Can you skip the training period? *IEEE Transactions on Communications*, 46:921–930, July 1998.

[63] P. Lancaster and M. Tismenetsky. *The theory of matrices*. Academic Press, second edition, 1985.

[64] I. D. Landau. Unbiased recursive identification using model reference adaptive techniques. *IEEE Trans. on Automatic Control*, 21:194–202, April 1976. addendum: 23: 98-99, February 1978.

[65] M. G. Larimore, J. R. Treichler, and C. R. Johnson Jr. SHARF: An algorithm for adapting IIR digital filters. *IEEE Trans. on Acoustics, Speech and Signal Processing*, 28:428–440, August 1980.

[66] E. A. Lee and D. G. Messerschmitt. *Digital Communication.* Kluwer Academic Publishers, 1993.

[67] A. P. Liavas and P. A. Regalia. Acoustic echo cancellation: Do IIR models offer better modeling capabilities than their FIR counterparts? *IEEE Transactions on Signal Processing*, 46:2499–2504, September 1998.

[68] T. J. Lim and S. Y. Wong. Adaptive IIR filtering for asynchronous multiuser CDMA detection. In *33rd Asilomar Conference on Signals, Systems and Computers*, pages 935–939, 1999.

[69] J. Lin and R. Unbenhauen. Bias-remedy least mean square equation error algorithm for IIR parameter recursive estimation. *IEEE Trans. on Signal Processing*, 40:62–69, January 1992.

[70] L. Ljung. On positive real transfer functions and the convergence of some recursive schemes. *IEEE Trans. on Automatic Control*, 22:539–551, August 1977.

[71] L. Ljung and T. Söderström. *Theory and practice of recursive identification.* The MIT Press, 1983.

[72] L. Ljung, T. Söderström, and I. Gustavsson. Counterexamples to general convergence of a commonly used recursive identification method. *IEEE Trans. on Automatic Control*, 20:643–652, October 1975.

[73] R. López-Valcarce. Algoritmos adaptativos para filtros recursivos: esquemas maestro-esclavo. Master's thesis, University of Vigo, Spain, 1995.

[74] R. López-Valcarce and S. Dasgupta. A new proof for the stability of equation-error models. *IEEE Signal Processing Letters*, 6:148–150, June 1999.

[75] R. López-Valcarce, C. Mosquera, and F. Pérez-González. Hyperstable adaptive IIR algorithms with polyphase structures: analysis and design. *IEEE Trans. on Signal Processing*, 47:2043–2046, July 1999.

[76] R. López-Valcarce and F. Pérez-González. New schemes and theoretical analysis of the master-slave family of recursive identification algoritms. *Signal Processing*, 58:79–94, April 1997.

[77] R. López-Valcarce and F. Pérez-González. An adaptive recursive filter for autoregressive inputs. *International Journal of Adaptive Control and Signal Processing*, 12:467–494, September 1998.

[78] R. López-Valcarce and F. Pérez-González. Some remarks on the lattice form of the Steiglitz-McBride iteration. *IEEE Signal Processing Letters*, 6:290–292, November 1999.

[79] R. López-Valcarce and F. Pérez-González. On blind adaptive algorithms for IIR equalizers. In *Ninth Digital Signal Processing Workshop*. Online proceedings in http://spib.ece.rice.edu/SPTM/DSP2000/program.html , October 2000.

[80] R. López-Valcarce and F. Pérez-González. Adaptive lattice IIR filtering revisited: Convergence issues and new algorithms with improved stability properties. *IEEE Trans. on Signal Processing*, 49:811–821, April 2001.

[81] O. Macchi. *The LMS approach with applications in transmission*. Wiley, 1995.

[82] J. Makhoul. On the eigenvectors of symmetric Toeplitz matrices. *IEEE Trans. Acoustics, Speech and Signal Processing*, 29:868–872, August 1981.

[83] M. Mboup and M. Bonnet. On the adequateness of IIR adaptive filtering for acoustic echo cancellation. In *Proc. EUSIPCO, Brussels, Belgium*, pages 111–114, 1992.

[84] K. X. Miao, H. Fan, and M. Doroslovački. Cascade normalized lattice adaptive IIR filters. *IEEE Trans. on Signal Processing*, 42:721–742, April 1994.

[85] J. B. Moore, M. Niedzwiecki, and L. Xia. Identification/prediction algorithms for ARMAX models with relaxed positive real conditions. *International Journal of Adaptive Control and Signal Processing*, 4:49–67, 1990.

[86] C. Mosquera. *Relaxation of the SPR condition with applications to the convergence of adaptive recursive algorithms*. PhD thesis, University of Vigo, Spain, 1998.

[87] B. Mulgrew and C. F. N. Cowan. An adaptive Kalman equalizer: structure and performance. *IEEE Transactions on Signal Processing*, 35:1727–1735, December 1987.

[88] K. Murano, S. Unagami, and F. Amano. Echo cancellation and applications. *IEEE Communications Magazine*, pages 49–55, January 1990.

[89] A. K. Nandi and S. N. Anfinsen. Blind equalisation with recursive filter structures. *Signal Processing*, 80:2151–2167, 2000.

[90] M. Nayeri. A mildly weaker sufficient condition in IIR adaptive filtering. *IEEE Trans. on Signal Processing*, 42:203–206, January 1994.

[91] M. Nayeri and W. K. Jenkins. Alternate realizations to adaptive IIR filters and properties of their performance surfaces. *IEEE Trans. on Circuits and Systems*, 36:485–496, April 1989.

[92] S. L. Netto and P. Agathoklis. Efficient lattice realizations of adaptive iir algorithms. *IEEE Trans. on Signal Processing*, 46:223–227, January 1998.

[93] A. V. Oppenheim and R. W. Schafer. *Discrete-time signal processing.* Prentice-Hall, 1989.

[94] J. Holst P. Stoica and T. Söderström. Eigenvalue location of certain matrices arising in convergence analysis problems. *Automatica*, 18(4):487–489, 1982.

[95] D. Parikh, N. Ahmed, and S. D. Stearns. An adaptive lattice algorithm for recursive filters. *IEEE Trans. Acoustics, Speech and Signal Processing*, 28:110–112, February 1980.

[96] J. C. Park and L. R. Carley. Continuous-time adaptive infinite impulse response (IIR) equalizers for EPR4 channels. In *IEEE Global Telecommunications Conference*, pages 926–931, 1999.

[97] V. M. Popov. The solution of a new stability problem for controlled systems. *Automation and Remote Control*, 24:1–23, January 1963.

[98] S. S. Pradhan and V. U. Reddy. A new approach to subband adaptive filtering. *IEEE Trans. on Signal Processing*, 47:655–664, March 1999.

[99] J. C. Principe, B. de Vries, and P. G. de Oliveira. The gamma filter–A new class of adaptive IIR filter with restricted feedback. *IEEE Trans. on Signal Processing*, 41:649–656, February 1993.

[100] ITU-T Recommendation Q.24. *Multi-Frequency Push-Button Signal Reception.* 1988.

[101] S. U. H. Qureshi. Adaptive equalization. *Proceedings of the IEEE*, 73:1349–1387, September 1985.

[102] V. U. Reddy, B. Egart, and T. Kailath. Least-squares type algorithm for adaptive implementation of Pisarenko's harmonic retrieval method. *IEEE Trans. Acoustics, Speech and Signal Processing*, 30:399–405, June 1982.

[103] P. A. Regalia. Stable and efficient lattice algorithms for adaptive IIR filtering. *IEEE Trans. on Signal Processing*, 40:375–388, February 1992.

[104] P. A. Regalia. An unbiased equation error identifier and reduced order approximations. *IEEE Transactions on Signal Processing*, 42:1397–1412, June 1994.

[105] P. A. Regalia. *Adaptive IIR Filtering in Signal Processing and Control.* Marcel Dekker, 1995.

[106] P. A. Regalia and M. Mboup. Undermodeled adaptive filtering: an *a priori* error bound for the Steiglitz-McBride method. *IEEE Transactions on Circuits and Systems II*, 43:105–116, February 1996.

[107] P. A. Regalia, M. Mboup, and M. Ashari. A class of first- and second-order interpolation problems in model reduction. *Archiv für Elektronik und Übertragungstechnik*, 49:332–343, September 1995.

[108] P. A. Regalia, M. Mboup, and M. Ashari. On the existence of stationary points for the Steiglitz-McBride algorithm. *IEEE Transactions on Automatic Control*, 42:1592–1596, November 1997.

[109] P. A. Regalia, M. Mboup, and M. Ashari. Existence of stationary points for pseudo-linear regression identification algorithms. *IEEE Transactions on Automatic Control*, 44:994–998, May 1999.

[110] J. A. Rodríguez-Fonollosa and E. Masgrau. Simplified gradient calculation in adaptive iir lattice filters. *IEEE Trans. on Signal Processing*, 39:1702–1705, July 1991.

[111] M. Rupp. Adaptive IIR echo cancellers for hybrids using the Motorola 56001. In *Signal Processing V: Theories and Applications*, pages 1487–1490, 1990.

[112] S. Shah and G. F. Franklin. On satisfying strict positive real condition for convergence by overparameterization. *IEEE Trans. on Automatic Control*, 27:715–716, June 1982.

[113] J. J. Shynk. Adaptive IIR filtering. *IEEE ASSP Magazine*, pages 4–21, April 1989.

[114] J. J. Shynk. Adaptive IIR filtering using parallel form realizations. *IEEE Trans. on Signal Processing*, pages 519–533, April 1989.

[115] J. J. Shynk. Frequency domain and multirate adaptive filtering. *IEEE ASSP Magazine*, pages 14–37, January 1992.

[116] T. Söderström and P. Stoica. On the stability of dynamic models obtained by least squares identification. *IEEE Trans. on Automatic Control*, 26:575–577, May 1981.

[117] T. Söderström and P. Stoica. *Instrumental variable methods for system identification.* Springer-Verlag, 1983.

[118] T. Söderström and P. Stoica. *System Identification.* Prentice-Hall, 1989.

[119] M. D. Srinath and P. K. Rajasekaron. *An introduction to statistical processing with applications.* Wiley, 1979.

[120] K. E. Steiglitz and L. E. McBride. A technique for the identification of linear systems. *IEEE Trans. Automat. Contr.*, 10:461–464, October 1965.

[121] P. Stoica and T. Söderström. The Steiglitz-McBride identification algorithm revisited – convergence analysis and accuracy aspects. *IEEE Trans. on Automatic Control*, 26:712–717, June 1981.

[122] A. Sugiyama and G. Homma. A computationally efficient echo canceler algorithm for multiple telephone lines. In *Proc. Ninth IEEE Digital Signal Processing Workshop, Waldemar Ranch, TX*, 2000.

[123] G. Szegö. *Orthogonal polynomials.* American Mathematical Society, fourth edition, 1981.

[124] L. Tong and H. H. Zeng. Channel surfing reinitialization for the constant modulus algorithm. *IEEE Signal Processing Letters*, 4:85–87, March 1997.

[125] J. R. Treichler and B. G. Agee. A new approach to multipath correction of constant modulus signals. *IEEE Trans. on Acoustics, Speech and Signal Processing*, 31:459–472, April 1983.

[126] P. P. Vaidyanathan. *Multirate systems and filter banks.* Prentice-Hall, 1993.

[127] B. Wahlberg. System identification using Laguerre models. *IEEE Trans. on Automatic Control*, 36:551–562, May 1991.

[128] B. Widrow, J. R. Glover Jr., J. M. McCool, J. Kaunitz, C. S. Williams, R. H. Hearn, J. R. Zeidler, E. Dong Jr., and R. C. Goodlin. Adaptive noise cancelling: principles and applications. *Proceedings of the IEEE*, 63:1692–1716, December 1975.

[129] B. Widrow and M. E. Hoff, Jr. Adaptive switching circuits. In *IRE WESCON Convention Record*, pages 96–104, 1960.

[130] B. Widrow and S. D. Stearns. *Adaptive Signal Processing.* Prentice-Hall, 1985.

[131] G. A. Williamson, J. P. Ashley, and M. Nayeri. Structural issues in cascade-form adaptive IIR filters. In *International Conference on Acoustics, Speech and Signal Processing*, volume 2, pages 1436–1439, May 1995.

[132] G. A. Williamson and S. Zimmermann. Globally convergent adaptive IIR filters based on fixed pole locations. *IEEE Trans. on Signal Processing*, 44:1418–1427, June 1996.

[133] S. Wyrsch and A. Kaelin. Adaptive feedback cancelling in subbands for hearing aids. In *International Conference on Acoustics, Speech and Signal Processing*, pages 921–924, 1999.

[134] G. Young. Reduced complexity decision feedback equalization for digital subscriber loops. *IEEE Journal on Selected Areas in Communications*, 9:810–816, August 1991.

[135] H. H. Zeng, L. Tong, and C. R. Johnson Jr. An analysis of constant modulus receivers. *IEEE Transactions on Signal Processing*, 11:2990–2999, November 1999.